



UNIVERSITÀ DELLA CALABRIA



UNIVERSITA' DELLA CALABRIA

Dipartimento di CHIMICA E TECNOLOGIE CHIMICHE

Scuola di Dottorato

Scienza e Tecnica "Bernardino Telesio"

Indirizzo

Metodologie Inorganiche

Con il contributo di

Fondo Sociale Europeo

CICLO

XXVIII

TITOLO TESI

**Theoretical Investigation of Bioinorganic Compounds:
Biomimetic Catalysts and Metal-Mediated mismatched DNA Base-Pairs**

Settore Scientifico Disciplinare CHIM/03

Direttore: Ch.mo Prof. Roberto Bartolino

Firma

Supervisore: Ch.mo Prof. Nino Russo

Firma

Dottorando: Dottessa Mariagrazia Fortino

Firma

La presente tesi è cofinanziata con il sostegno della Commissione Europea, Fondo Sociale Europeo e della Regione Calabria. L'autore è il solo responsabile di questa tesi e la Commissione Europea e la Regione Calabria declinano ogni responsabilità sull'uso che potrà essere fatto delle informazioni in essa contenute.

Abstract

Una delle principali sfide nel mondo scientifico è superare la linea di confine tra la natura e il mondo inanimato. La *Chimica Biomimetica* e la *Biologia Sintetica* collaborano al raggiungimento di questo obiettivo.

Lo sviluppo della Chimica Biomimetica è stato ispirato dall'elevata efficacia catalitica degli enzimi naturali, che giocano un ruolo chiave nella maggior parte delle reazioni chimiche che avvengono nell'organismo. Essa può essere definita come una branca della chimica che cerca di imitare le reazioni naturali e i processi enzimatici allo scopo di accrescere il potere della chimica stessa.

La Biologia Sintetica, invece, è una nuova area di ricerca che rappresenta la convergenza di nuovi sviluppi in chimica, in biologia e in scienza computazionale al fine di progettare e creare nuovi sistemi biologici, partendo da materiale biologico già esistente e modificato mediante l'applicazione di processi chimici, da utilizzare in ambito industriale, energetico, medico e ambientale.

La presente tesi pone l'attenzione sul meccanismo di azione seguito da alcuni catalizzatori biomimetici, per i quali sono state investigate sia la regioselettività, sia l'attività riscontrata sperimentalmente, e sullo studio delle proprietà energetiche e strutturali relative a nuovi sistemi bio-ispirati.

I catalizzatori biomimetici e i nuovi sistemi biologici il cui comportamento è stato studiato e razionalizzato come scopo di questo lavoro di tesi possono essere suddivisi in tre categorie:

- i- Alcuni composti del naftalene caratterizzati dalla presenza di atomi di selenio, zolfo o tellurio, come mimici degli enzimi iodotironine deiodinase (ID), coinvolti nell'attivazione e inattivazione degli ormoni tiroidei.
- ii- Una serie di complessi di monooxomolibdeno(IV) come biomimetici dell'enzima trimetilammina-N-ossidoreduttase (TMAOR).
- iii- Alcuni modelli di DNA duplex, contenenti coppie di nucleobasi non complementari medicate da metalli di transizione.

Lo studio teorico dei sistemi sopra elencati è stato effettuato utilizzando l'approccio quantomeccanici (QM) basato sulla teoria del funzionale della densità (DFT).

Introduction

One of the major challenges for scientists is to overtake the boundaries between nature and artefact and between inanimate world and living matter.

There are two symmetric ways of crossing such borders: using *biomimetic chemistry* that mimics nature's structure and processes, and using *synthetic biology* that imitate synthetic chemistry with biological materials.

The development of biomimetic chemistry has been inspired by the highly effective catalysis of Nature's enzymes, which play a key role in most chemical reactions in the organisms. Biomimetic chemistry can be defined as a branch of chemistry which attempts to imitate natural reactions and enzymatic processes, not only to understand the detailed mechanism of enzymatic catalysis, but also as a way to improve the chemistry power.

On the other hand, the synthetic biology is a new area of research representing a convergence of advances in chemistry, biology, computer science and engineering. Synthetic biology have the aim to design and build novel biological systems for several purposes, at industrial, medicinal, energetic and environmental level, applying chemical modification on existing natural material.

The present thesis has its main focus on the working mechanism followed by some biomimetic catalysts, for which both the regioselectivity factor and the experimental activity have been rationalized, and on the study of energetic and structural properties of novel designed biological systems.

Quantum Mechanical methods (QM) based on density functional theory (DFT) have been used aiming at revealing the main features of each bio-inspired model.

The biomimetic catalysts and the new bio-modified systems that have been investigated can be divided in three categories:

- i- Naphthyl-based compounds characterized by the presence of selenium, sulphur or tellurium atoms, as mimics of iodothyronine deiodinase enzymes (IDs) involved in the activation and inactivation of thyroid hormones (**Paper I and IV**).
- ii- Monooxomolybdenum(IV) complexes as redox biomimetic models of trimethylamine-N-oxide reductase (TMAOR) enzyme (**Paper III**).
- iii- DNA duplex containing metal-mediated mismatched base pairs (**Paper II**).

In this thesis, a brief outline of theoretical background and the used computational methods is given in Chapter 1.

Some features relative to the main aspects of the iodothyronine deiodinase enzymes and their biomimetic naphthyl-based models are discussed in Chapter 2, while the principal characteristics of the trimethylamine-N-oxide reductase enzyme and the corresponding investigated biomimetic systems are described in Chapter 3. In Chapter 4 the most important properties of mismatched DNA base pairs are discussed.

List of Papers included in this thesis

- I. Mechanism of thyroxine deiodination by naphthyl-based iodothyronine deiodinase mimics and halogen bonding role. A DFT investigation.

Mariagrazia Fortino, Tiziana Marino, Nino Russo and Emilia Sicilia
Chem. Eur. J. 2015, 21, 8554-8560

- II. Theoretical Study of Silver-Ion-Mediated Base Pairs: The case of C-Ag-C and C-Ag-A Systems

Mariagrazia Fortino, Tiziana Marino and Nino Russo
J. Phys. Chem. A 2015, 119, 5153-5157.

- III. Mechanistic investigation of the reduction of trimethylamine-N-oxide catalysed by biomimetic molybdenum enzyme models.

Mariagrazia Fortino, Tiziana Marino, Nino Russo and Emilia Sicilia
Submitted to Physical Chemistry Chemical Physics

- IV. Chalcogen Substitution in a series of naphthyl-based iodothyronine deiodinase mimetics. A contribution of theoretical investigations to the elucidation of the role played by halogen bond

Mariagrazia Fortino, Tiziana Marino, Nino Russo and Emilia Sicilia
Manuscript in preparation

Abbreviations and Acronyms

B3LYP	Becke 3 parameter Lee – Yang – Parr functional
bdt	1,2-benzenedithiolato
BE	Binding Energy
BSSE	Basis Set Superposition Error
CC	Coupled Cluster
CI	Configuration Interaction
COSMO	COnductor-like Screening Model
CPCM	Conductor Polarizable Continuum Model
DMSOR	Dimethylsulfoxide reductase
DFT	Density Functional Theory
FES	Free Energy Surface
GGA	Generalized Gradient Approximation
GVB	Generalized Valence Bond
H	Hoogsten
HK	Hohenberg-Kohn
HF	Hartree-Fock
ID	Iodothyronine Deiodinase
IRC	Intrinsic Reaction coordinate
IRD	Inner Ring Deiodination
LSDA	Local Spin Density Approximation
KS	Kohn-Sham
MCSCF	Multi Configurational Self-consistent-Field
MEP	Molecular Electrostatic Potential
MP	Møller-Plesset
NBO	Natural Bond Orbital
ORD	Outer Ring Deiodination
PES	Potential Energy Surface
QM	Quantum Mechanics

rH	reverse Hoogsten
rT3	reverseT3, (3,3',5'-triiodothyronine)
rW-C	reverse Watson-Crick
SCF	Self-Consistent Field
SCRF	Self-Consistent Reaction Field
SMD	Solvatation Model Density
T3	(3,5,3'-triiodothyronine)
T4	Thyroxine, 3,5,3',5'- tetraiodothyronine
TMAOR	Trimethylamine-N-oxide Reductase
TST	Transition State Theory
VWN	Vosko, Wilk and Nusair
WC	Watson-Crick
ZPE	Zero Point Energy

Nitrogenous Bases abbreviations

A Adenine

C Cytosine

G Guanine

T Thymine

U Uracile

Amino acids abbreviations

Ala	Alanine
Cys	Cysteine
Asp	Aspartate
Glu	Glutamate
Phe	Phenylalanine
Gly	Glycine
His	Histidine
Ile	Isoleucine
Lys	Lysine
Leu	Leucine
Met	Methionine
Asn	Asparagine
Pro	Proline
Gln	Glutamine
Arg	Arginine
Ser	Serine
Thr	Threonine
Val	Valine
Trp	Tryptophan
Tyr	Tyrosine

Contents

Introduction.....	i
List of Papers included in this thesis.....	v
Abbreviations and Acronyms.....	vii
Nitrogenous Bases Abbreviations.....	ix
Amino acids Abbreviations.....	x
1 Theoretical Background and Computational Methods.....	1
1.1 The electronic problem.....	1
1.1.1 The Slater Determinant.....	2
1.2 The Hartree-Fock approximation.....	3
1.3 Density Functional Theory (DFT).....	5
1.3.1 The Hohenberg-Kohn theorems.....	5
1.3.2 The Kohn-Sham equations.....	7
1.3.3 Approximate exchange correlation functionals.....	9
1.3.4 The used approximate functionals.....	10
1.4 Solvation and dielectric effects.....	12
Bibliography.....	14
2 Iodothyronine deiodinase enzymes and their biomimetic models.....	17

2.1 Iodothyronine Deiodinases: some features.....	17
2.2 Naphthyl-based iodothyronine deiodinase biomimetics.....	19
2.2.1 The halogen bond and the first hypothesized reaction mechanism....	20
2.2.2 The investigated reaction mechanism and our insights on the experimental order activity of the naphthyl-based ID mimetics (Paper I).	22
2.3 Alteration of reactivity after replacement of Sulphur/Selenium atoms by Tellurium atoms.....	24
2.3.1 The halogen bond role on the alteration of activity after Chalcogen substitution (Paper IV).....	25
2.4 A bulky model for the 5'-outer ring deiodination of thyroxine...	26
Bibliography.....	31
3 Trimethylamine-N-oxide reductase and biomimetic molybdenum enzyme models	35
3.1 Molybdenum enzymes: main features and their classification..	35
3.2 Modeling of molybdoenzymes.....	36
3.2.1 A series of monooxomolybdenum(IV)-dithiolene complexes as mimics of TMAOR.....	37
3.2.2 The proposed reaction mechanisms: Cis and trans attacks.....	38
3.2.3 Our results on the mechanistic aspects of the investigated molybdoenzyme models (Paper III).....	40
Bibliography.....	43

4 Silver ion-mediated mismatched DNA base pairs.....	46
4.1 DNA base pairs and mispairs.....	46
4.2 Metal-modified DNA base pairs: some features and their applications.....	48
4.2.1 Ag(I)-mediated mismatched base pairs.....	49
4.3 A brief overview on our investigation (Paper II).....	50
Bibliography.....	53
Paper I (published).....	I
Paper II (published).....	II
Paper III (submitted)	III
Paper IV (manuscript in preparation).....	IV

1 | Theoretical Background and Computational Methods

(A general view concerning quantum chemistry is traced in this chapter. A more comprehensive description is available in standard textbooks)¹⁻⁷.

1.1 The electronic problem

The central purpose of theoretical chemistry is to explore the electronic structure and properties of molecules.

Electrons are quantum-scale object that show wave-particle duality, so they don't obey classical behaviour and should be treated quantum mechanically¹.

Excluding time-dependent interactions and the relativistic effects due to the mass and the velocity, a system can be described by the *non-relativistic time-independent Schrödinger equation*⁸:

$$\hat{H}\psi = E\psi \tag{1.1}$$

where \hat{H} is the Hamiltonian operator for a system of nuclei and electrons described by position vectors R_A and r_i , respectively.

In atomic units, the Hamiltonian for N electrons and M nuclei is

$$\hat{H} = -\sum_{i=1}^N \frac{1}{2} \nabla_i^2 - \sum_{A=1}^M \frac{1}{2M_A} \nabla_A^2 - \sum_{i=1}^N \sum_{A=1}^M \frac{Z_A}{r_{iA}} + \sum_{i=1}^N \sum_{j>1}^N \frac{1}{r_{ij}} + \sum_{A=1}^M \sum_{B>A}^M \frac{Z_A Z_B}{R_{AB}} \quad (1.2)$$

In Eq. (1.2) the first term is the operator for the kinetic energy of the electron; the second term is the operator for the kinetic energy of nuclei; the third term represents the coulomb attraction between electrons and nuclei; the fourth and fifth terms represent the repulsion between electrons and nuclei, respectively.

Since nuclei are much heavier than electrons and so they move more slowly, the *Born-Oppenheimer* approximation consider the electrons to be moving in the field of fixed nuclei⁹. Within this approximation, the second term of (1.2) can be neglected and the last term can be considered constant.

The remaining terms in (1.2) compose the electronic Hamiltonian or Hamiltonian describing the motion of N electrons in the field of M point charges.

$$\hat{H}_{elec} = -\sum_{i=1}^N \frac{1}{2} \nabla_i^2 - \sum_{i=1}^N \sum_{A=1}^M \frac{Z_A}{r_{iA}} + \sum_{i=1}^N \sum_{j>1}^N \frac{1}{r_{ij}} \quad (1.3)$$

The main aim of quantum chemistry is to find approximate solutions to the electronic Schrödinger equation, since it can be solved exactly only for one-electron system at most, such as hydrogen atom or H₂⁺ molecule.

1.1.1 The Slater Determinant

The appropriate wave function describing a single electron is a *spin orbital*, $\psi(r,s)$, that define both its spatial distribution, $\psi(r)$ and its spin, $\alpha(s)$ or $\beta(s)$.

$$\psi(r,s) = \begin{cases} \psi(r)\alpha(s) \\ \text{or} \\ \psi(r)\beta(s) \end{cases} \quad (1.4)$$

For a collection of electrons, a product of spin orbitals for each electron, known as *Hartree Product*, has been considered as a trial wave function¹.

However there is a basic deficiency in the Hartree product: it doesn't correlate the motion of electrons and it does not satisfy the *antisymmetry principle* (a general statement of the *Pauli exclusion principle*) that requires that electronic wave functions be antisymmetric with respect to the interchange of the space and spin coordinates of any two electrons¹⁰.

Antisymmetrizing the Hartree Product, the *Slater determinant* has been introduced as the simplest antisymmetric wave function which can describe the ground state of an N-electron system:

$$\psi_N^{SD} = \frac{1}{\sqrt{N!}} \begin{vmatrix} \psi_i(r_1, s_1) & \psi_j(r_1, s_1) & \dots & \psi_j(r_1, s_1) \\ \psi_i(r_1, s_1) & \psi_j(r_2, s_2) & \dots & \psi_k(r_2, s_2) \\ \vdots & \vdots & & \vdots \\ \psi_i(r_N, s_N) & \psi_j(r_N, s_N) & \dots & \psi_k(r_N, s_N) \end{vmatrix} \quad (1.5)$$

The Slater determinant incorporated both exchange effects, arising from the requirement that $|\psi|^2$ be invariant to the exchange of the space and spin coordinates of any two electrons, and correlation effect, which means that the motion of two electrons with parallel spins is correlated while the motion of electrons with opposite spins remains uncorrelated¹.

1.2 The Hartree-Fock approximation

A major preoccupation of quantum chemists, as anticipated above, is to find and to describe approximate solutions to the electronic Schrödinger equation.

Central to attempts at solving such problems is the Hartree-Fock (HF) approximation^{11,14}, that is important not only for its own sake but also as a starting point for more accurate approximations.

As explained before, the simplest antisymmetric wave function which can be used to describe the ground state of an N-electron system, is a single Slater determinant.

The variation principle states that the best wave function, of this functional form, is the one which gives the lowest possible energy and, in the Slater Determinant wave function, the variational flexibility is in the choice of spin orbitals.

Minimizing the energy with respect to the choice of spin orbitals lead to the HF equation, that is an eigenvalue equation of the form:

$$f(i)\psi(r_i s_i) = \varepsilon\psi(r_i s_i) \quad (1.6)$$

where $f(i)$ is the Fock operator that includes a one-electron contribute for the kinetic energy of i th electron and for the coulomb attraction between the i th electron and nucleus, and a two-electron contribute that measure the “field” seen by the i th electron due to the presence of the other electrons on the other spin orbitals.

Thus the Hartree-Fock equation depends on its eigenfunctions, so it is a non-linear equation that must be solved iteratively, using the self-consistent-field (SCF) method.

However with the HF approach the motion of the electrons with opposite spins remains not correlated.

Electron correlation can be included explicitly with well-known extensions collectively called post-Hartree-Fock methods¹⁵, like *Moller-Plesset perturbation theory (MP)*, the *generalized valence bond method (GVB)*, *configuration interaction (CI)*, *multiconfigurational self-consistent field (MCSCF)* and *coupled cluster theory (CC)*.

These approaches improve the level of accuracy but become computationally much more demanding and thus are only suitable for relatively small systems. To handle larger systems an alternative approach has been developed.

1.3 Density Functional Theory (DFT)

Density Functional Theory (DFT) allows to deal with large molecular systems, including the electron correlation, with a computational demanding much lower than post-HF methods.

These DFT vantages are due to the use of the *electron density* $\rho(r)$ as basic variable.

$$\rho(r) = N \int \dots \int |\psi(x_1, x_2, \dots x_N)|^2 dx_1 dx_2 \dots dx_N \quad (1.7)$$

In contrast to the wave function, ψ_N , that depends on $3N$ variable excluding the spin variable, the electron density $\rho(r)$ depends on 3 variables only, also for many-electron systems.

In 1964, Hohenberg-Kohn introduced the existence of an unique relationship between $\rho(r)$ and all fundamental properties of a given system¹⁶.

1.3.1 The Hohenberg-Kohn theorems

The *first Hohenberg-Kohn theorem*¹⁶ states that every observable of a stationary quantum mechanical system can be calculated, in principle, exactly from the ground-state electron density $\rho(r)$, meaning that every observable can be written as a functional of the ground-state electron density $\rho(r)$.

For a system defined by an external potential $v(r)$, acting on the electrons due to the nuclear charges, the overall energy E_v can be written as functional of the electron density.

Within the Born Oppenheimer approximation, E_v can be splitted into three terms, which are kinetic energy T , electron-electron repulsion E_{ee} and the nuclei-electron attraction V :

$$E_v[\rho] = T[\rho] + E_{ee}[\rho] + V[\rho] = T[\rho] + E_{ee}[\rho] + \int \rho(r)v(r)dr \quad (1.8)$$

Since the terms T and E_{ee} depend exclusively on the coordinates of the electrons and their forms are the same for all systems, depending only on the number of electrons, they are grouped together into the universal Hohenberg and Kohn functional $F^{HK}[\rho]$.

$$F^{HK}[\rho] = T[\rho] + E_{ee}[\rho] \quad (1.9)$$

F^{HK} contains the functional for the kinetic energy $T[\rho]$ and that for the electron-electron interaction $E_{ee}[\rho]$. The explicit form of both these functionals are unknown.

However from term $E_{ee}[\rho]$ can be extracted at least, analytically, the classical part $J[\rho]$ that measures the coulomb electron-electron interaction, whereas $Vq[\rho]$ is a measure of the non-classical electronic interaction:

$$E_{ee}[\rho] = J[\rho] + Vq[\rho] = \frac{1}{2} \iint \frac{\rho[r]\rho[r']}{|r-r'|} dr dr' + Vq[\rho] \quad (1.10)$$

The complete form of the ground state energy associated with the density $\rho(r)$, is the functional

$$E_v[\rho] = F^{HK}[\rho] + \int \rho(r)v(r)dr = T[\rho] + \frac{1}{2} \iint \frac{\rho[r]\rho[r']}{|r-r'|} dr dr' + Vq[\rho] + \int \rho(r)v(r)dr \quad (1.11)$$

The *second Hohenberg-Kohn theorem*¹⁶, allows to introduce the variational principle into DFT. For a trial electron density $\tilde{\rho}(r)$, the Hohenberg-Kohn variational methods states that:

$$E_0 \leq E_v[\tilde{\rho}] \quad (1.12)$$

where E_0 is the correct energy and $E_v[\tilde{\rho}]$ is the energy, written as functional of trial electron density $\tilde{\rho}(r)$, of a system with an external potential $v(r)$.

The applicability of the variational principle is limited to the ground state. Hence the strategy cannot be easily transferred to the problem of excited states.

1.3.2 The Kohn-Sham Equations

The explicit form of the functional $F^{HK}[\rho]$ is the major challenge of DFT. Since only the $J[\rho]$ term is known, the main problem is to find the expression for $T[\rho]$ and $Vq[\rho]$.

In 1927 Thomas and Fermi provided the first example of density functional theory. However the performance of their model had a deficiency due to the poor approximation of the kinetic energy.

To solve this problem Kohn and Sham proposed, in 1965, a new approach¹⁷. They considered a reference system with non-interacting electrons, having the same density of the real, interacting one.

For the reference system, both the kinetic energy and ground-state electron density can be written using one-electron orbital:

$$T_s[\rho] = \sum_{i=1}^N \langle \psi_i \left| -\frac{1}{2} \nabla_i^2 \right| \psi_i \rangle \quad (1.13)$$

$$\rho[r] = \sum_{i=1}^N \sum_s |\psi_i(r, s)|^2 \quad (1.14)$$

The kinetic energy of the real system can be expressed as sum of two contributes: the kinetic energy of the reference system $T_s[\rho]$ and the kinetic energy that measures the electron correlation $T_c[\rho]$

$$T[\rho] = T_s[\rho] + T_c[\rho] \quad (1.15)$$

Consequently a new redefinition of the universal functional can be introduced:

$$F[\rho] = T_s[\rho] + J[\rho] + E_{xc}[\rho] \quad (1.16)$$

Where $E_{xc}[\rho]$ is the exchange and correlation functional that represents the sum of the terms having an unknown analytically form: i) the difference between the exact kinetic energy and the kinetic energy of the reference system; ii) the non-classical electron-electron interaction; iii) the self-interaction correction.

So the exchange and correlation functional can be defined as

$$E_{xc}[\rho] = (T[\rho] - T_s[\rho]) + (E_{ee}[\rho] - J[\rho]) \quad (1.17)$$

Including all these considerations the expression of energy for the real, interacting system is

$$E_v[\rho] = T_s[\rho] + J[\rho] + E_{xc}[\rho] + \int \rho(r)v(r)dr \quad (1.18)$$

The only term for which no explicit form can be given is E_{xc} .

Applying the variational method, imposing the wave function orthogonality condition and using the Lagrange multipliers method, the Kohn-Sham equations have been obtained:

$$-\frac{1}{2}\nabla_i^2 + v_s(r)\psi_i^{KS} = \varepsilon_i\psi_i^{KS} \quad (1.19)$$

Where v_s is the local potential for the single particle that includes the exchange and correlation potential, v_{xc} , defined as the functional derivative of E_{xc} with respect to $\rho(r)$. So v_s depends on the density and therefore the Kohn-Sham equations have to be solved iteratively.

$$v_{xc} = \frac{\delta E_{xc}[\rho]}{\delta \rho(r)} \quad (1.20)$$

Kohn-Sham equations led to a formalism that is exact and computationally accessible. The only one lack is the fact that the explicit form of the

functional Exc is unknown. The major challenge in DFT is to find an improved approximate model for this unknown functional.

1.3.3 Approximate exchange correlation functionals

The first generation of approximate functional is called *Local (Spin) Density Approximation* (L(S)DA) which is based on assuming that the density ρ varies very slowly and locally with position and can thus be treated as a homogeneous electron gas⁷. Although L(S)DA gives surprisingly accurate predictions for solid-state physics, it is not a useful model for chemistry due to its severe overbinding of chemical bonds and underestimation of barrier heights. The second generation of density functionals is called the *Gradient Corrected or Generalized Gradient Approximation* (GGA) in which functionals depend not only on the density ρ , but also on the gradient $\Delta\rho$. GGA functionals have been shown to give more accurate predictions for thermochemistry than LSDA ones, but they still underestimate barrier heights.

LSDAs, and GGAs are “local” functionals because the electronic energy density at a single spatial point depends only on the behaviour of the electronic density and kinetic energy at and near that point¹⁸.

Local functional can be mixed with non-local HF exchange (calculated via Kohn-Sham orbitals) leading to the hybrid functionals, that are often more accurate than local functional especially for main group thermochemistry. One popular group of hybrid methods is Becke 3 parameter functional ($B3$)^{19,20}, with the three empirical fitted parameters A,B and C:

$$E_{XC}^{B3} = (1 - A)E_x^{\text{Dirac-Slater}} + AE_x^{\text{HF}} + BE_x^{\text{B88}} + E_c^{\text{VWN}} + C\Delta E_C^{\text{GGA}} \quad (1.21)$$

where Δ indicates that $\Delta\rho$ -dependent fractions of corresponding functionals are included. B88 is a widely used gradient correction to exchange by Becke²¹.

LSDA exchange, $E_x^{\text{Dirac-Slater}}$, is given by the Dirac-Slater formula for a uniform electron gas, and LSA correlation energy E_c^{VWN} is the functional by Vosko, Wilk an Nusair (VWN)²².

When ΔE_C^{GGA} gradient correction to correlation in eq (1.21) is Lee, Yang and Parr functional (LYP)²³, the approximate functional is known as B3LYP. So A determines the extent of replacement of the Slater local exchange $E_x^{\text{Dirac-Slater}}$ by the exact HF exchange E_x^{HF} ; B controls the addition of Becke's gradient-correction to the exchange functional E_x^{B88} ; C defines the inclusion weight of the LYP correlation E_C^{LYP} and the VWN correlation E_c^{VWN} functionals.

In the last years, the development of new functional forms and their validation against diverse databases have yielded powerful new density functionals with broad applicability to many areas of chemistry. These new density functionals, belong to the so called M05-class and M06-class functionals (including M05, M052X, M06L, M06, M062X, M06HF)²⁴.

1.3.4 The used approximate functionals

In this thesis, the most popular hybrid functional **B3LYP** is used to investigate the reaction mechanism of the naphtyl-based iodothyronine deiodinase mimics and to determine the electronic and structural properties of the bio-inspired DNA complexes.

Various assessments have been reported in the literature regarding the accuracy of B3LYP with respect to geometries and energies, which are the two crucial properties for this kind of theoretical study. It performs well for the structure determination and for the calculation of thermochemical properties.

A critical deficiency of DFT methods is their well-known inability to accurately model non-covalent interactions (especially dispersion). Several general approaches to improve this aspect have been developed and a very accurate one has been proposed by Stefan Grimme²⁵.

In the investigations performed by using the hybrid B3LYP functional, the Grimme D3 dispersion corrections have been included.

In this case, when **B3LYP-D3** is used, the total energy is given by:

$$E_{B3LYP-D3} = E_{KS-B3LYP} - E_{disp} \quad (1.22)$$

where $E_{KS-B3LYP}$ is the usual self-consistent Kohn-Sham energy obtained with the B3LYP functional and E_{disp} is a dispersion correction given by the sum of two- and three- body energies.

$$E_{disp} = E^{(2)} + E^{(3)} \quad (1.23)$$

With the dominating two-body term

$$E^{(2)} = \sum_{AB} \sum_{n=6,8,10} s_n \frac{c_n^{AB}}{r_{AB}^n} f_{d,n}(r_{AB}) \quad (1.24)$$

s_n is a functional-dependent scaling factor, c_n^{AB} denotes the nth-order dispersion coefficient for atom pair AB, r_{AB} is their interatomic distance, and $f_{d,n}$ is a damping function that avoid near singularities for small distances (r_{AB}).

The hybrid functional B3LYP has some limitations, such as the fact that it is better for main group chemistry than for transition metals.

For this reason, single point calculations on the Ag(I) mediated mismatched DNA base pairs and the entire mechanistic investigation of molybdenum systems, analogues of TMAOR, have been performed using the **M06-L** local functional.

M06-L is a very accurate functional for transition metals, suitable for treating noncovalent interactions, and is the only local functional (no Hartree-Fock exchange) with better across-the-board average performance than B3LYP; this is very important because only local functionals are affordable for many demanding applications on very large systems²⁴.

1.4 Solvation and dielectric effects

One of the factors to be considered in accurate calculations in quantum chemistry is the interaction between solute and solvent. The solute properties depend on the solvent, particularly the polar one.

The common approach is to include the solvent as a continuum with a dielectric permittivity constant ϵ .

In all continuum models the concept of cavity is a basic one²⁶. The model is composed of the solute put into a void cavity within a continuous dielectric medium mimicking the solvent. As a general rule, a cavity should have a physical meaning and not be only a mathematical artifice. In particular, the cavity should exclude the solvent and contain within its boundaries the largest possible part of the solute charge distribution. The shape and size of the cavity are differently defined in the various versions of the continuum models²⁶.

In continuum models much attention has been paid to the interaction between the portion of solute charge distribution outside the boundaries of cavity and the charge distribution of the solvent.

To describe the electrostatic interaction between an arbitrary charge density $\rho(r)$ and a continuum dielectric can be used the Poisson equation:

$$\nabla^2 \phi(r) = \frac{-4\pi\rho(r)}{\epsilon} \quad (1.25)$$

where $\phi(r)$ is the electrostatic potential of charge density.

During a quantum chemical calculation, eq. (1.25) is solved numerically, so the solvent charges distribution is then returned to the SCF procedure which is performed accounting for the solvent charges. This process is called *self-consistent reaction field* (SCRF) method because it is repeated until self-consistency is reached.

Continuum models, based on the assumption that the electrostatic interactions of the solute and the surrounding solvent do not depend on the molecular structure of the solvent, reveal their inadequacy when strong and

specific interactions between a solute and one or more first-shell solvent molecules take place.

The continuum solvation models used in the investigations reported in this thesis are **SMD**, **CPCM** and **COSMO**.

In the CPCM (Conductor Polarizable Continuum Model) and COSMO (COnductor-like Screening MOdel) the cavities are defined as envelopes of spheres centred on atoms with a radii approximately 20% larger than the Van der Waals radius. When the charge distribution of the solute polarizes the dielectric medium, the response of the medium is described by the generation of screening charges (q) on the cavity surface.

In CPCM and COSMO, the dielectric constant of the medium is changed from the specific finite value ϵ , characteristic of each solvent, to infinite. This value corresponds to that of a conductor and this change strongly simplify the electrostatic problem^{26,27}. To take into account the finite permeattivity of real solvents, the charges (q) are scaled by a factor $f(\epsilon)$.

$$q^* = f(\epsilon)q \quad \text{where } f(\epsilon) = \frac{\epsilon - 1}{\epsilon + 0.5} \quad (1.26)$$

The SMD (density-based solvation model) is a universal solvation model , where “universal” denotes its applicability to any charged or uncharged solute in any solvent or liquid medium for which a few key descriptor are known.

The SMD model separates the observable solvation free energy into two main components: i) the first one is the electrostatic contribution; ii) the second component is called the cavity-dispersion-solvent-structure term and it is the contribution arising from short range interactions between the solute and solvent molecules in the first solvation shell²⁸.

Bibliography

1. Szabo, A.; Ostlund, N.S. *Modern Quantum Chemistry*; Dover Publication: New York, **1989**.
2. Cramer, C. J. *Essentials of Computational Chemistry*; John Wiley & Sons Ltd.: New York, **2002**.
3. Lewars, E. *Computational Chemistry*; Kluwer Academic Publishers: New York, **2004**.
4. Piela, L. *Ideas of Quantum Chemistry*; Elsevier B. V.: Oxford, **2007**.
5. Jensen, F. *Introduction to Computational Chemistry*; John Wiley & Sons Ltd.: New York, **2007**.
6. Parr, R. G.; Yang, W. *Density-Functional Theory of Atoms and Molecules*; Oxford University Press: New York, **1989**.
7. Koch, W.; Holthausen, M.C. *A Chemist's Guide to Density Functional Theory*; John Wiley & Sons Ltd.: Weiheim, **2000**.
8. Schrödinger, E. *Ann. Physik.*, **1926**, 79, 361.
9. Born, M.; Oppenheimer, J. *Ann. Physik.*, **1927**, 84, 457.
10. Pauli, W. *Z. Physik.* **1925**, 31, 765.
11. Hartree, D. *Proc. Cambridge Phil. Soc.*, **1928**, 24, 89.
12. Hartree, D. *Proc. Cambridge Phil. Soc.*, **1928**, 24, 111.
13. Hartree, D. *Proc. Cambridge Phil. Soc.*, **1928**, 24, 426.
14. Fock, V. *Z. Physik.*, **1930**, 61, 126.
15. Bartlett, R. J.; Stanton, J. In *Reviews in Computational Chemistry*; Lipkowitz, K. B.; Boyd, D.B.: Eds.; VCH Publishers: New York, **1994**; Vol.V.
16. Hohenberg, P.; Kohn, W. *Phys. Rev. B*, **1964**, 136, 864.
17. Kohn, W.; Sham, L. *J. Phys. Rev. A* **1965**, 136, 1133.
18. a) van Leeuwen, R.; Baerends, E.J.; *Phys. Rev. A*, **1994**, 49, 2421; b) Becke, A. D.; *J. Chem. Phys.*, **1998**, 109, 2092; c) Mori-Sanchez, P.; Cohen, A. J.; Yang, W. *J. Chem. Phys.*, **2006**, 124, 91102/1.
19. Becke, A. D. *J. Phys. Phys.* **1993**, 98, 1372.
20. Becke, A. D. *J. Phys. Phys.* **1993**, 98, 5648.
21. Becke, A. D. *J. Phys. Phys.* **1988**, 38, 3098.
22. Vosko, S.H.; Wilk, L.; Nusair, M. *Can. J. Phys.* **1980**, 58, 1200.

- 23.** Lee, C.; Yang, W.; Parr, R.G. *Phys. Rev. B* **1988**, *37*, 785.
- 24.** Zhao, Y. ; Truhlar, D. G.; *Acc. Chem. Res.*, **2008**, *41* (2) 157.
- 25.** a) Grimme, S. *J. Comput. Chem.*, **2004**, *25*, 1463; b) Grimme, S.; Antony, J.; Ehrlich, S.; Krieg, H. *J. Chem. Phys.*, **2010**, *132*, 154104/1.
- 26.** Tomasi,J.; Mennucci, B.; Cammi, R. *Chem. Soc. Rev.*, **2005**, *105*, 2999.
- 27.** a) Barone, V.; Cossi, M. *J. Phys. Chem. A*, **1998**, *102*, 1995; b) Cossi, M.; Rega, N.; Scalmani, G.; Barone, V. *J. Comp. Chem.*, **2003**, *24*, 669; c) Takano, Y.; Houk, K. N. *J. Chem. Theory Comput.*, **2005**, *1*, 70.
- 28.** Marenich, A. V.; Cramer, C. J.; Truhlar, D. G., *J. Phys. Chem. B*, **2009**, *113*, 6378.

2 | Iodothyronine deiodinase enzymes and their biomimetic models

2.1 Iodothyronine Deiodinases: some features

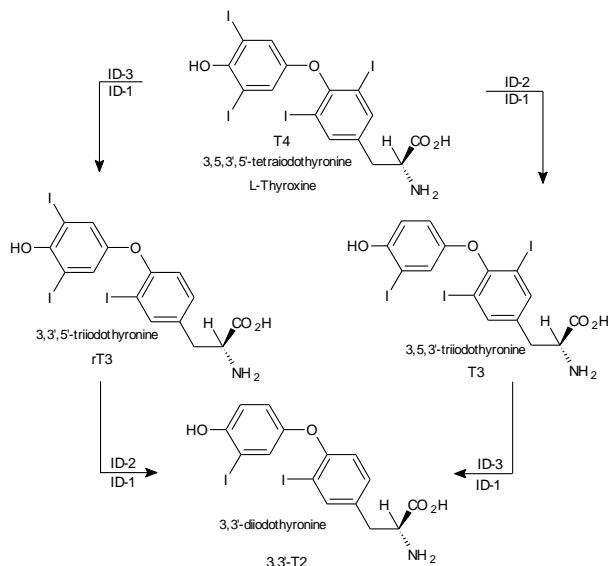
Thyroid hormones are involved in a wide variety of processes in most cells of higher vertebrates, including man. The majority of these actions are mediated by some thyroid hormone receptors, which show a high affinity for 3,5,3'-triiodothyronine (T_3) and a lower affinity for 3,5,3',5'-tetraiodothyronine or thyroxine (T_4), that is the product mainly secreted by thyroid glands¹. T_4 is only a prohormone requiring a (mono-) deiodination process, occurring predominantly in extra-thyroidal tissues, to provide the active hormone T_3 .

Evidence for this type of peripheral conversion was found already in 1950² but it took until 1970 to study the reaction mechanism in more detail.

These studies led to the characterization of three different types of activity and the corresponding enzymes were defined as type 1, type 2 and type 3 iodothyronine deiodinase (ID-1, ID-2 and ID-3)³⁻⁵.

Two of these enzyme types are selective: starting from the prohormone T4, ID-2 only catalyses outer ring (5') deiodination (ORD) to give the active T3, while ID-3 only catalyses inner ring (5) deiodination (IRD) to give the reverse T3 (rT3), an inactive form of the hormone. The ID-1 enzyme is non selective and catalyses both ORD and IRD. Both T3 and rT3 then undergo further mono-deiodination leading to T2 (See **Scheme 1** for the *principal pathways of thyroid hormone deiodination*)³⁻⁵.

The three deiodinase types show a relevant impact on maintenance of serum T₃ levels and they all contribute directly or indirectly to protect the tissues and cells from an excess of thyroid hormones⁴⁻⁶.



Scheme 1. Major pathways of thyroxine, T4, deiodination catalysed by ID-1, ID-2, ID-3.

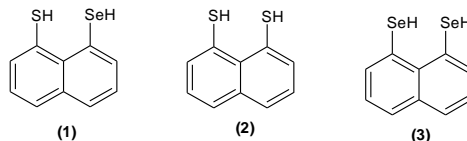
Some structural studies on the three type of deiodinases showed that they belong to the thioredoxin fold superfamily and share a similar structural organization. The IDs are integral membrane proteins that function as

homodimer with hydrophobic transmembrane region of the enzymes located in the N-terminal domain, their active site is oriented towards cytoplasm and their core sequence is very well conserved in all known deiodinases^{7,8}. They all contain a Selenocysteine residue, *Sec*, in the catalytic centre that plays an essential role in the deiodination activity.

Although the deiodinases are involved in basic function of thyroid hormones, information about their three-dimensional conformation and their working mechanism are limited⁹. For such reason in the last decade several selenium containing compounds able to mimic the catalytic functions of IDs, were synthesized and investigated¹⁰⁻¹².

2.2 Naphthyl-based iodothyronine deiodinase biomimetics

The lack of information about the structure and working mechanism of IDs in conjunction with the fascinating regioselectivity characterizing the deiodination reactions of thyroid hormones, performed by different deiodinases, has inspired the development of simple selenium compounds that mimics these enzymes¹⁰⁻¹². At the very beginning, the first attempts to develop such simple selenium compounds have led to only limited success¹². However, in 2010 Manna and Mugesh proposed a series of peri-substituted naphthalenes containing thiol and selenol groups (see **Scheme 2**), able to mimic the ID-3 activity^{11a}.



Scheme 2. Naphtyl-based compounds as mimics of type 3 iodothyronine deiodinase, ID-3.

The naphtyl-based selenol compound bearing a thiol group in the proximity to the selenium atom (compound (1) in **Scheme 2**) has been the first

chemical model that experimentally removed iodine exclusively from inner ring positions of T4 to produce rT3, as the only deiodinated product^{11a}.

Starting from compound **(1)** a long series of other new peri-substituted naphthalene derivatives have been synthesized, in order to chemically and geometrically explain its special selectivity. When the selenol group in compound **(1)** has been replaced by a thiol moiety (compound **(2)** in **Scheme 2**), a reduced deiodinase activity has been experimentally found. Whereas a further substitution of the thiol groups in compound **(1)** with a selenol group (compound **(3)** in **Scheme 2**) exhibited a much higher deiodinase activity^{11b,11c}.

These results agree with Kuiper et al¹³ that have previously demonstrated the importance of the Sec residue in the catalytic centre of ID-3, showing that the substitution of Sec by Cys significantly reduced the catalytic efficiency.

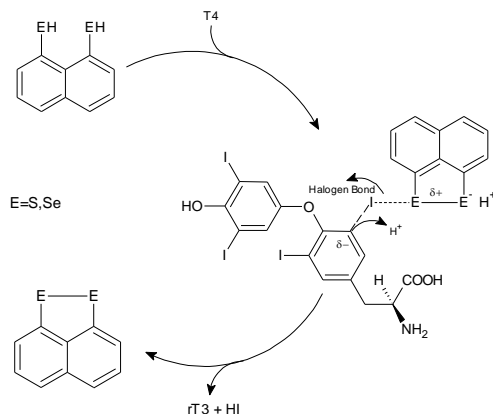
As no 3,3'-T2 formation was observed when pure rT3 was treated with **(1)**, **(2)** or **(3)** compounds, the high selectivity of these compounds was demonstrated^{11b}.

2.2.1 The halogen bond and the first hypothesized reaction mechanism

Halogen bonds play key roles in the recognition of thyroid hormones: it has been shown that T4 forms short I···O interactions with its transport protein transthyretin, and that T4 can bind to RNA sequences through halogen bonds¹⁴. Starting from these evidences, the formation of a halogen bond between a thiol or selenol group and an iodine atom, it has been considered as a key structural motif in mechanism of deiodination of T4^{6c}.

In general, a halogen bond occurs when there is evidence of a net attractive interaction between an electrophilic region associated with a halogen atom in a molecular entity and a nucleophilic region in another, or the same, molecular entity¹⁵.

Analysis of the recent literature reveals that the theoretical studies dedicated to the characterization of the nature of the S···I and Se···I halogen bonds are limited to the investigation of small systems, mimicking Sec residue in the active site of IDs with simple CH₃SeH and CH₃SH molecules, interacting with a truncated model for T4^{10c}. More recently, to understand the nature of iodine atoms present in thyroid hormones, theoretical calculations have been performed using a more extended model, in which the IDs are simulated by naphthyl-based chalcogen compound and the thyroxine substrate is modelled by a simple iodobenzene compound^{6c}. On the basis of these theoretical data obtained on such truncated models, a deiodination mechanism based on halogen bond was proposed^{6c} (see **Scheme 3**).



Scheme 3. The first hypothesized reaction mechanism based on the halogen bond

According to this mechanism, an initial direct interaction of one of the selenol or thiol moieties with an iodine atom leads to the formation of a halogen bond¹⁶. The transfer of electron density from selenium or sulphur to the σ^* orbital of the C-I bond, generates a partial positive charge on the selenium or sulphur atom that should facilitate the chalcogen-chalcogen interaction (chalcogen bond) with a consecutive strengthening of the halogen bond, leading to the heterolytic cleavage of the C-I bond^{6c}.

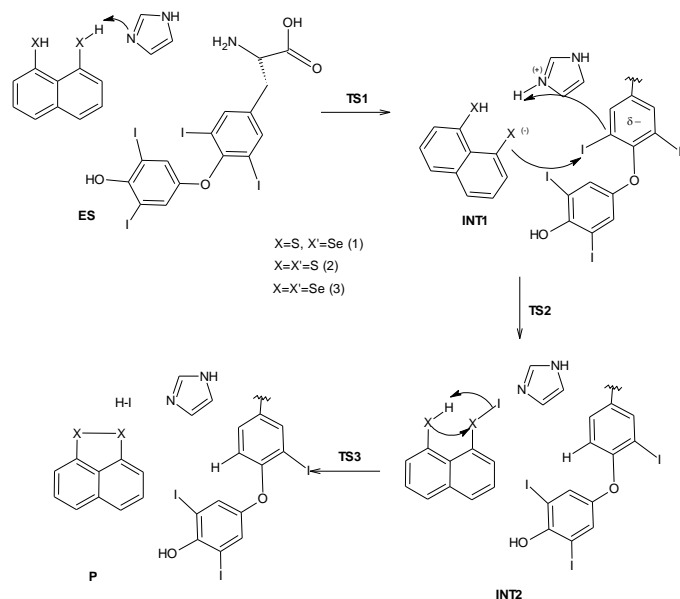
However, at the beginning of our exploration many attempts to simulate the deiodination process according to the hypothesized mechanism, represented in **Scheme 3**, failed.

2.2.2 The investigated reaction mechanism and our insights on the experimental order activity of the naphthyl-based ID mimics (Paper I)

In addition to Sec and Cys residues, one or more histidine residues (His) at the active site of deiodinases appear to play an important role in the deiodination reaction.

Kohrle et al have proposed that one of the His residues at the active site of ID1 may activate the Sec residue toward nucleophilic attack, by forming a selenolate-imidazolium zwitterion¹⁷. It should be highlighted that the His residues corresponding to positions 158 and 174 in human ID-1 are conserved also in ID-2 and ID-3^{15,4a,4b}.

On the basis of these experimental results, a process that occurs in more steps and with a proton-shuttle role played by an imidazole ring has been proposed (see **Scheme 4**).



Scheme 4. The new proposed and investigated reaction mechanism

Indeed in our study we presented a systematic DFT analysis of the IRD process considering the entire thyroxine structure, using different naphthyl-based models as mimics of ID-3 having S-S, S-Se and Se-Se moieties in peri-position (compound **(1)-(3)** in **Scheme 2**) and including a histidine residue simulated by an imidazole ring.

The first step of the whole process is the proton abstraction by the imidazole ring from one of Se-H or S-H groups, to form the selenolate or thiolate anion. The subsequent heterolytic cleavage of the C-I bond and formation of a Se-I or S-I bond occur simultaneously to the proton transfer from the formed imidazolium ion to the carbon atom. The interaction between the two chalcogens induces the proton transfer from the remaining Se-H or S-H group to the iodine atom, followed by the elimination of a HI unit and formation of a chalcogen-chalcogen bond.

The superior deiodinase activity showed by the naphthyl-based compound having two selenol groups in the peri-position, respect to the ones having two thiol moieties or a thiol-selenol pair, was investigated.

For compound **(1)** two alternative pathways were explored, considering that the initial proton transfer can occur from either the selenol, SeH, or thiol, SH, groups.

For all the used complexes, the B3LYP-D3 free energy profiles showed that the reaction proceeds via a first crucial intermediate, INT1, characterized by the presence of the X-I-C (with X= Se, S) halogen bond, that is the key structure for the whole deiodination process.

The directionality of the bond, bond lengths smaller than the corresponding sum of van der Waals radii and the anisotropy in electron density distribution, are the main features that allowed the halogen bond recognition.

The transformation of this first important intermediate into a second one in which the C-I bond is definitively cleaved and the incipient X-I bond is formed represents the rate-determining step of the whole process. The

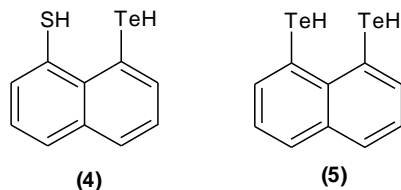
chalcogen interaction forces the proton transfer from the remaining Se/S-H group to iodine atom, with the consequent elimination of HI and formation of a chalcogen–chalcogen bond.

The strongest Se-I interaction for the naphthyl-based compound having two selenol groups corresponds to a lower barrier than those calculated for the other examined compounds and, as a consequence, the deiodination is faster.

2.3 Alteration of reactivity after replacement of Sulphur/Selenium atoms by Tellurium atoms

Compounds **(1)-(3)** in **Scheme 2** have shown a great ability to remove the iodine atom from the (5-) inner ring position of T4 to give the inactive rT3^{10,11}.

Recently Mugesh et al have showed that the replacement of Sulphur/Selenium atoms in this series of deiodinase mimetics by tellurium atoms (see compounds **(4)** and **(5)** respectively in **Scheme 5**) alters the regioselectivity and increases the rate of deiodination under physiological conditions¹⁸.



Scheme 5. Naphtyl-based compounds with tellurium atoms.

Experimental results for the IRD process of T4 by compound **(4)**, having a thiol-tellurol pair in peri-position, indicated that its deiodinase activity is higher than that found of compound **(3)**, having two selenol groups in peri-position.

Similar results were obtained with compound (**5**) having two tellurol groups in peri-position, even if it was found to be less active than (**4**) but more active than (**3**).

2.3.1 The halogen bond role on the alteration of activity after chalcogen substitution (Paper IV)

In order to verify if the observed alteration of activity of thyroxine deiodination process, after chalcogen substitution is controlled by the nucleophilicity and the strength of halogen bond between the iodine atom and the chalcogen atoms, a DFT investigation has been performed on IRD process of T4 by using compounds (**4**) and (**5**). The investigated mechanism is the same one that we have explored in the previous series of naphthyl-based mimetics.

Moreover a comparison with compound (**3**), having two selenol groups in peri-position, that was found to be the most active in the previous series of synthesized naphthyl-based mimic of ID, has been performed.

Our calculations revealed that, also in this case, the proton transfer from the imidazolium ion to the carbon, together with the heterolytic cleavage of C-I bond and the formation of X-I bond represents the rate-determining step of the whole process. The calculated trend in the barrier heights of the corresponding transitions states (TS2) confirms the experimental results, showing that the replacement of sulphur/selenium atoms by tellurium increases the reactivity toward T4. To rationalize this result we have investigated the status of the halogen bond for all INT1 intermediates formed by reaction of compounds (**3**), (**4**) and (**5**) with T4. Our investigations revealed that the geometrical and charge distribution requirements for a halogen bond formation are fulfilled only by compound (**3**). Whereas for compound (**4**) and (**5**) not all the requirements are followed.

These results showed that, when the halogen bond is formed for each napthyl-based compound reacting with T4, the strongest X-I halogen bond interaction corresponds to a lower barrier, and the deiodination process is faster. Whereas, the comparison between species that may not form this non-covalent interaction revealed that, they undergo a minor stabilizing force facilitating the subsequent step of the deiodination process.

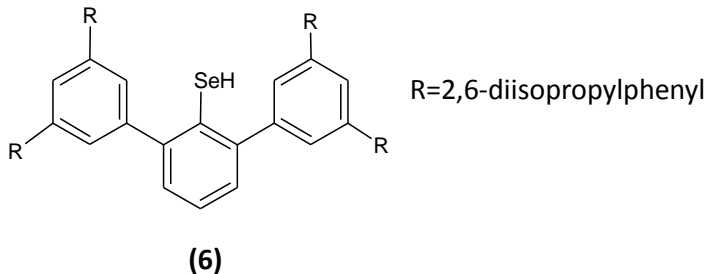
2.4 A bulky model for the 5'-outer ring deiodination of thyroxine

The very first organoselenol compounds showing a good, but non selective, deiodinase activity have been small molecules, such as PhSeH, tested in their deiodinase activity with some T4 derivative¹².

Although the formation of a selenenyl iodide specie (RSeI), in these models, has been widely accepted once the deiodination process occurred, chemical evidences for the formation of a new Se-I bond, have been entirely circumstantial. Indeed the selenenyl iodide specie usually undergoes facile disproportionation to the corresponding diselenide following the bimolecular processes shown in Equation (2.1) and (2.2).



In 2010, Goto et al experimentally showed the formation of a selenenyl iodide specie once the deiodination process of a thyroxine derivative occurred. They generated a nano-sized molecular cavity to avoid the disproportionation process, using a novel steric protection group, a *Bpq* group, that is a cavity-shaped substituent (see **Scheme 6**)^{10b}.



Scheme 6. The steric protection Bpq group

The deiodination of a thyroxine derivative, by using this hindered selenol compound was experimentally investigated and the main emerged aspects are: i) only the iodine atom on the outer ring was removed, probably due to the steric hindrance of compound **(6)**; ii) the reaction took place only in presence of amine, probably as a reminiscence of the histidine role in the active site of the IDs, iii) the new formed Se-I bond is incorporated in the cavity and the bimolecular processes, shown in Equations (2.1) and (2.2) are considered to be effectively prevented by steric repulsion between the periphery of the molecules^{10b}.

On the basis of these experimental evidences, a systematic DFT analysis has been performed on the 5'- outer ring deiodination process considering the entire thyroxine structure, using the steric hindered organoselenol compound **(6)** and including an imidazole group mimicking the histidine residue.

The proposed reaction mechanism for the ORD process of T4 with the compound **(6)**, is the same one that we have investigated for the IRD process of T4 with the naphthyl-based compounds (Paper I).

In this case we have stopped our investigation at the formation of the selenenyl iodide specie, in which the new formed Se-I bond is incorporated in the cavity generated by the Bpq group.

The used computational protocol is the same one performed in the investigation reported in Paper I.

The B3LYP-D3 free energy profile, calculated by including water-solvent effects, for the 5'-deiodination of T4 by compound **(6)** in presence of an imidazole group, is shown in **Figure 1**.

According to the proposed mechanism, the first step of the whole process is the proton abstraction by the imidazole moiety from the Se-H group of compound **(6)**. The proton transfer takes place by overcoming an energy barrier of only 0.9 kcal mol⁻¹ for the TS1 transition state, and leads to the formation of a selenolate-imidazolium zwitterionic species.

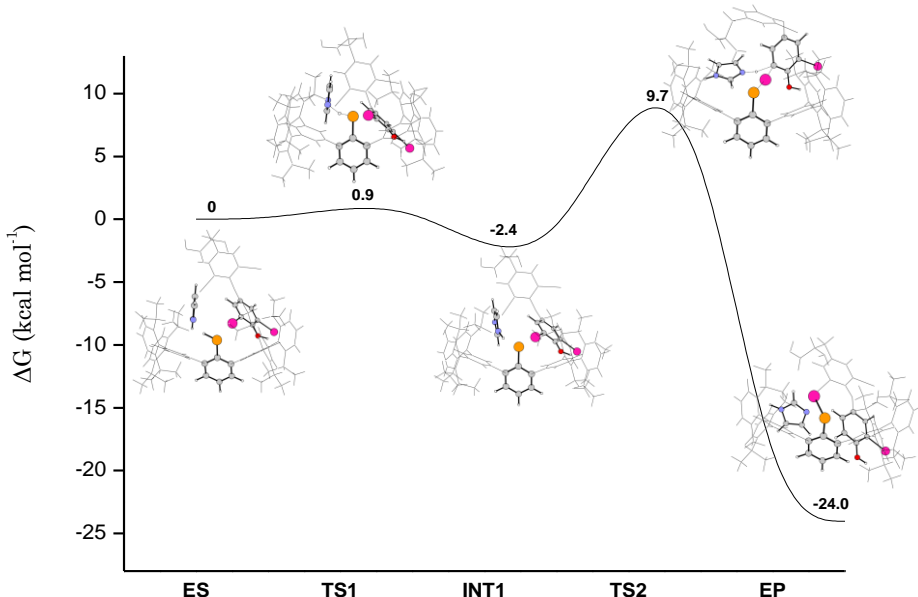


Figure 1. B3LYP-D3 free energy profile for the ORD of T4 by compound **(6)**

The key feature of such intermediate is the formation of the halogen bond, between the selenolate group and the iodine atom.

So also with this model study, the halogen bond is a key structural motif that is involved during the deiodination process.

The increase of the C-I bond length (from 2.132 to 2.169 Å), the almost linear C-I-Se bond angle (170.7°) and the increase in electron density on the

I atom (the NBO positive charge 0.226 become 0.187) are clear indications that a halogen bond is formed. Moreover the Se-I bond length, in INT1, is 3.317 Å and this value is smaller than the corresponding sum of van der Waals radii (that is 3.880 Å)

A comparison between the maps of molecular electrostatic potential (MEP) relative to the complex ES and the first intermediate INT1, reported in **Figure 2**, clearly show a more red area, corresponding to a region of less positive electrostatic potential on the iodine atom in INT1 with respect to ES, confirming, the lone pair donation to the iodine σ -hole and the formation of the halogen bond.

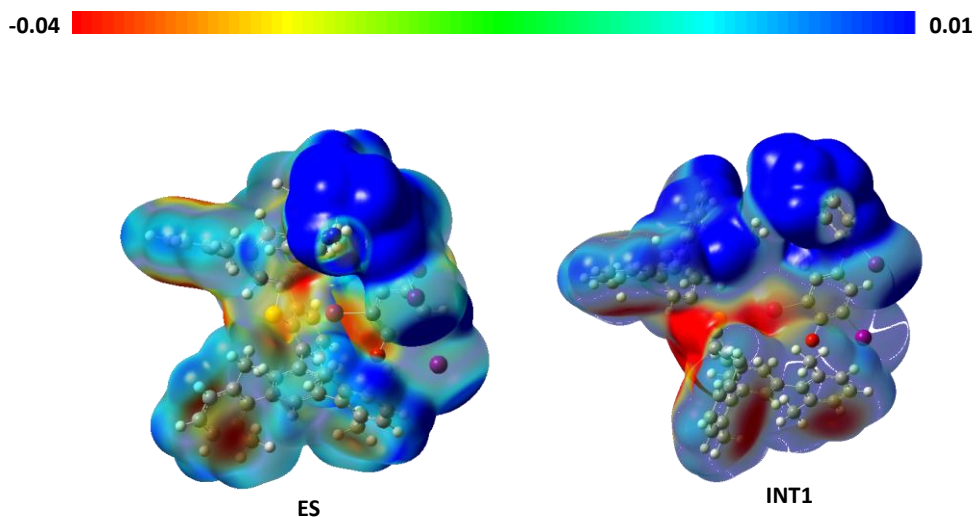


Figure 2. Maps of Electrostatic Potential (MEPs) of ES and INT1.

The reaction is exothermic by 2.4 kcal mol⁻¹ with respect to the reference energy of reactants.

The proton transfer from the formed imidazolium ion to the carbon atom gives rise to the concerted heterolytic cleavage of the C-I bond and the formation of the Se-I bond. The barrier for the corresponding transition state, TS2, is 12.1 kcal mol⁻¹ and it is the rate determining step of the whole

process. The formed product, bearing the Se-I bond in the cavity generated by the Bpq group, lies 24.0 kcal mol⁻¹ below the entrance channel, validating the stabilization effect created by this steric protecting group.

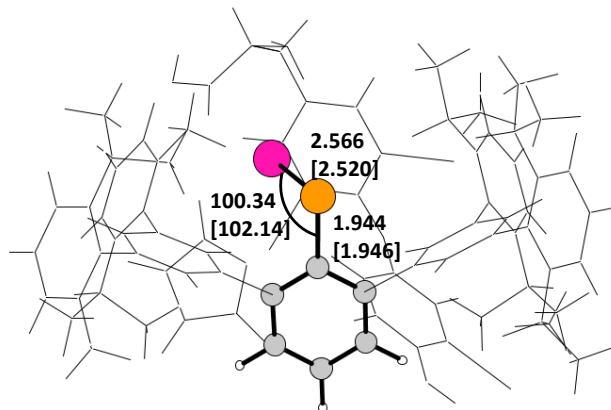


Figure 3. Main geometric parameters of final product compared with the experimental values in square brackets

In **Figure 3** the optimized structure of the final product having the formed Se-I bond is reported, together with the main geometric parameters compared with available experimental values in square brackets.

Bibliography

1. Darras, V. M.; Van Herck, S. L. *J. J. Endocrinology.*, **2012**, *215*, 189.
2. Gross, J.; Leblond, C.P. *J. Bio. Chem.*, **1950**, *184*, 489.
3. a) Leonard, J. L.; Visser, T. J. *Biochemistry of Deiodination in Thyroid Hormone Metabolism*, **1986**, 189, Ed. G. Hennemann, New York & Basel: Marcel Dekker Inc.; b) Behne, D.; Kyriakopoulos, A.; Meinholt, H.; Kohrle, *J. Biochem. Biophys. Res. Commun.*, **1990**, *173*, 1143; c) Berry, M. J.; Banu, L.; Larsen, P.R. *Nature*, **1991**, *349*, 438; d) St. Germain, D. I.; Galton, V. A. *Thyroid*, **1997**, *7*, 665.
4. a) Bianco, A.C., Salvatore, D.; Gereben, B.; Berry, M. J.; Larsen, P. R. *Endocr. Rev.*, **2002**, *23*, 38; b) Kohrle, *J. Methods Enzymol.*, **2002**, *347*, 125; c) Kuiper, J. M.; Kester, M. H. A.; Peeters, R. P.; Visser, T. J. *Thyroid*, **2005**, *15*, 787.
5. a) Visser, T. J.; Schoenmakers, C. H. H. *Acta Med. Austriaca*, **1992**, *19*, 18; b) Kohrle, *J. Mol. Cell. Endocrinol.*, **1999**, *151*, 103.
6. Bianco, A.C.; Kim, B. W. *J. Clin. Invest.*, **2006**, *116*, 2571.
7. Bianco, A. C.; Larse, P. R. *Thyroid*, **2005**, *15*, 777.
8. Gereben, B; Zavacki, A. m.; Ribich, S.; Kim, B. W.; Huang, S. A.; Simonides, W. S; Zeold, A; Bianco, A. C. *Endocr. Rev.*, **2008**, *29*, 898.
9. Schweizer, U.; Schlicker, C.; Braun, D.; Kohrle, J.; Steegborn, C. *Proc. Natl. Acad. Sci. USA*, **2014**, *111*, 10526.
10. a) Beck, C.; Jensen, S. B.; Reglinski, J.; *Bioorg. Med. Chem. Lett.*, **1994**, *4*, 1353; b) Goto, K.; Sonoda, D.; Shimada, K.; Sase, S.; Kawashima, T. *Angew. Chem. Int. Ed.*, **2010**, *49*, 545; c) Bayse, C. A.; Rafferty, E. R. *Inorg. Chem.*, **2010**, *49*, 5365.
11. a) Manna, D.; Mugesh, G. *Angew. Chem. Int. Ed.*, **2010**, *49*, 9246; b) Manna, D; Mugesh, G *J. Am. Chem. Soc.*, **2011**, *133*, 9980; c) Manna, D.; Mugesh, G.; *J. Am. Chem. Soc.*, **2012**, *134*, 4269; d) Metrangolo, P., Resnati, G. *Nat. Chem.*, **2012**, *4*, 437.
12. Vasil'ev A.; Engman, L. *J. Org. Chem*, **1998**, *63*, 3911.
13. Kuiper, G. G. J. M.; Klootwijk, W.; Visser, T. *J. Endocrinology*, **2003**, *144*, 2505.

- 14.** a) Eneqvist, T.; Lundberg, E.; Karlsson, A.; Huang, S.; Santos, C. R. A.; Power, D. M.; Sauer- Eriksson, A. E. *J. Biol. Chem.*, **2004**, *279*, 26411; b) Levesque, D.; Beaudoin, J. -D.; Roy, S.; Perreault, J. -P. *Biochem. J.*, **2007**, *403*, 129; c) Metrangolo, P.; Meyer, F.; Pilati, T.; Resnati, G.; Terraneo, G. *Angew. Chem. Int. Ed.*, **2008**, *47*, 6114.
- 15.** Desiraju, G. R.; Ho, P. S.; Kloo, L.; Legon, A. C.; Marquardt, R.; Metrangolo, P.; Politzer, P.; Resnati, G.; Rissanen, K. *Pure Appl. Chem.*, **2013**, *85*, 1711.
- 16.** a) Guthrie, F. *J. Chem. Soc.*, **1863**, *16*, 239; b) Vonnegut, B.; Warren, B. E. *J. Am. Chem. Soc.*, **1936**, *58*, 2459; c) Hassel, O. *Science*, **1970**, *170*, 497; d) Bent, H. A. *Chem. Rev.*, **1968**, *68*, 587; e) Politzer, P.; Lane, P.; Concha, M. C.; Ma, Y.; Murray, J. S.; *J. Mol. Model.*, **2007**, *13*, 305; f) Politzer, P.; Murray, J. S.; Lane, P. *Int.J. Quantum Chem.*, **2007**, *197*, 3046; g) Awwadi, F. F.; Willett, R.D.; Peterson, K. A.; Twamley, B.; *Chem. Eur. J.*, **2006**, *12*, 8952; h) Tuzuki, S.; Wakisaka, A.; Ono, T.; Sonoda, T.; *Chem. Eur. J.*, **2012**, *18*, 951.
- 17.** a) Kohrle, J.; Hesch, R. D. *Horm. Metab. Res. Suppl. Sr.*, **1984**, *14*, 42; b) Mol, J. A.; Docter, R.; Hennemann, G.; Visser, T. J. *Biochem. Biophys. Res. Commun.*, **1984**, *120*, 28; c) Berry, M. J. *J. Biol. Chem.*, **1992**, *267*, 18055.
- 18.** Raja, K.; Mugesh, G. *Angew. Che. Int. Ed.*, **2015**, *54*, 7674.

3 | Trimethylamine-N-oxide reductase and biomimetic molybdenum enzyme models

3.1 Molybdenum enzymes: main features and their classification

Molybdenum is a widespread metal that plays key roles in the biochemical cycles of nitrogen¹⁻³, sulfur and carbon and it is mainly contained in some classes of enzymes that are called molybdoenzymes.

All molybdoenzymes catalyse redox reactions by taking advantage of the versatile redox chemistry of this element, which is controlled by its geometry in the cofactor and finely tuned by the enzyme environment⁴. In most of the molybdoenzymes, molybdenum shuttles between two oxidation states (IV and VI), thereby catalyzing two-electron redox reaction.

Molybdenum-dependent enzymes can be grouped into two categories: the multinuclear heterometallic bacteria nitrogenase containing Fe-Mo cofactor in the active site⁵⁻⁷, and pterin-based mononuclear molybdenum oxidoreductase enzymes, that are located at the end of respiratory chain, linked to the energy conservation, and mediate the oxo-transfer reaction on small molecules.⁸

The characteristic pterin cofactor of such mononuclear molybdenum enzymes, often known in literature as molybdopterin or Moco (molybdenum cofactor), is an organic dithiolene ligand including phosphate and pterin derivatives¹. It is coordinated, by the sulphur atoms, to the metal centre (see **Scheme 1a**). This class of molybdenum oxidoreductases is further divided into three families: *sulphite oxidase*, *xanthine oxidase* and *dimethylsulphoxide reductase (DMSOR)*, of which each has a distinct active site structure based on the molybdopterin structural motif^{1,4}. Specifically the members of DMSOR family possess a *bis-(dithiolene)* moiety, with two pterin-dithiolenes that coordinate the molybdenum centre. Moreover in the DMSOR family, there is a unique substrate, trimethylamine-N-oxide, (TMAO), which is converted in NMe₃, by a member of DMSOR family, known as *trimethylamine-N-oxide reductase (TMAOR)*⁹.

3.2 Modeling of molybdoenzymes

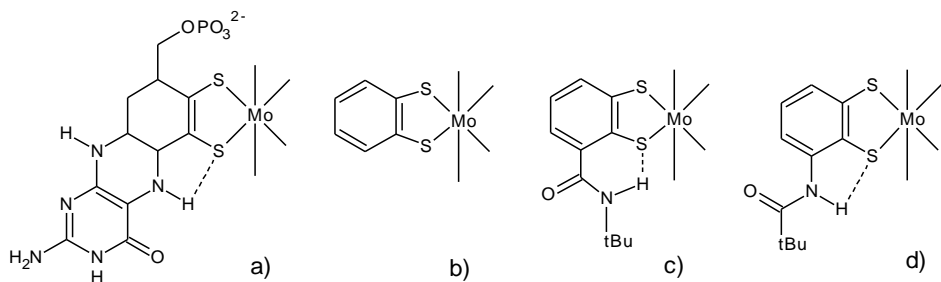
For a biomimetic chemist to replicate such redox reactions using native substrates, is a great challenge for the future. Functional simulations of these natural reactions are already achievements, indeed various molybdenum complexes have been synthesized as models of these oxotransferases, showing a remarkable ability to mimic the reaction of the active site of native proteins⁹.

In order to gain a deeper understanding to explain these experimental results, the reactivity profiles of biomimetic molybdenum complexes have

been addressed by computational studies, that can be complementary to provide insights that cannot be obtained very easily from experiments.

3.2.1 A series of monooxomolybdenum(IV)-dithiolene complexes as mimics of TMAOR

One of the first reported synthetic model of this oxotransferase enzyme was introduced by Boyde et al in 1986, using two 1,2-benzenedithiolato (bdt) moieties (see **Scheme 1b**) simulating the bis-dithiolene chelating effect of pterin cofactor¹⁰, characteristic of this class of enzymes.



Scheme 1. a) molybdopterin moiety b) 1,2-benzenedithiolato moiety; c) 1,2-S₂-3-tBuNHCOCH₃ moiety; d) 1,2-S₂-3-tBuCONHC₆H₃ moiety

The presence of a NH···S hydrogen bond, between amide NH group and the sulphur atom of Cys residue, has been found at most of the active sites of electron transfer proteins, such as iron-sulphur proteins and blue copper proteins, in which this hydrogen bond regulates the metal-thiolate bonding¹¹⁻¹⁴. Also in the active site of molybdenum enzymes, the involvement of the NH···S hydrogen bond has been proposed to be relevant during the oxo-transfer reaction¹⁵.

The important role played by this hydrogen bond can be explained considering that a limit factor during the oxo-transfer process is the possible conproportionation between the monooxomolybdenum(IV) specie

and the oxidized dioxomolybdenum(VI) compound, leading to the formation of the (μ -oxo)dimolybdenum(V)¹⁶.

Experimental data showed that the presence of NH \cdots S hydrogen bond positively shift the Mo(IV/VI) redox potential, preventing the Mo(V) resting state formation and allowing that catalytic cycles in native enzymes smoothly proceed¹⁷.

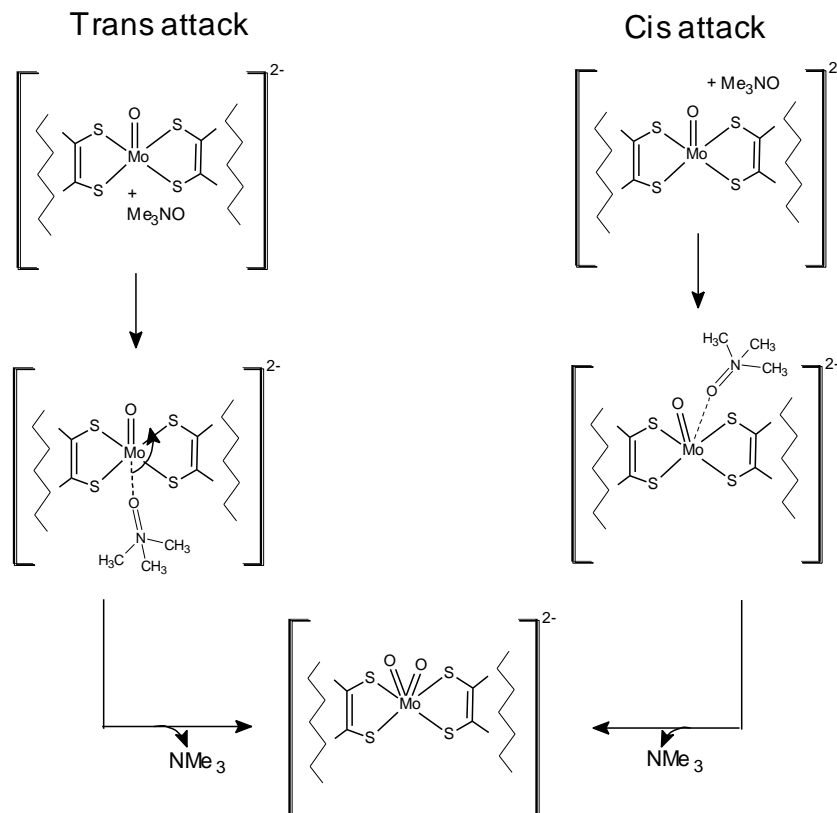
In 2006, Okamura's group¹⁷ investigated the role played by NH \cdots S hydrogen bond, introducing four intramolecular NH \cdots S hydrogen bonds into the bis-1,2-benzenedithiolato monooxomolybdenum(IV) complex, demonstrating that their presence accelerates the reduction process of Me₃NO to Me₃N. However the oxidized corresponding dioxomolybdenum(VI) complex proved to be unstable to be isolated¹⁷.

More recently Okamura et al¹⁸, have synthesized new series of monooxomolybdenum(IV) complexes containing only two intramolecular NH \cdots S hydrogen bonds. In the first series a carbamoyl group (tBuNHCO) was used (see **Scheme 1c**) to introduce the formation of a flexible six-membered NH \cdots S hydrogen bond¹⁸. In the next series, instead, new ligands with acylamino groups (tBuCONH), as shown in **Scheme 1d**, were designed and synthesized¹⁹. In this last case the formed five-membered NH \cdots S hydrogen bond, is more reminiscent of the intraligand interaction present in the natural molybdopterin cofactor (see **Scheme 1a**), allowing a better investigation of the relationship between the strength of the hydrogen bond and the reactivity of the molybdoenzyme models.

3.2.2 The proposed reaction mechanisms: Cis and Trans attacks

For the trimethylamine-N-oxide reduction process, catalysed by the previous described monooxomolybdenum(IV) complexes, two possible reaction mechanisms were proposed.^{17,18}

In the first proposed mechanism¹⁷, the Me₃NO attacks the molybdenum centre in trans position respect to the oxo ligand sited on the initial complex, leading to the formation of an adduct as intermediate. The formed adduct undergoes a trans-cis rearrangement, where the trimethylamine-N-oxide moves from the trans position to the cis one respect to the oxo ligand. Simultaneously, the dissociation of the N-O bond leads to the formation of the dioxomolybdenum(VI) complex. This mechanism is known as trans attack (see left side of **Scheme 2**). In the second proposed reaction mechanism¹⁸, the Me₃NO directly attacks the molybdenum centre in cis position to the oxo ligand. After that, the N-O bond dissociation occurs generating the dioxomolybdenum(VI) complex. This second proposed mechanism is known as cis attack. (see right side of **Scheme 2**).



Scheme 2. The two alternative proposed reaction mechanisms

3.2.3 Our results on the mechanistic aspects of the investigated molybdoenzyme models (Paper III)

In our study, we performed a detailed theoretical DFT investigation of the mechanistic aspects of the reduction process of Me₃NO using the bis-(1,2-benzenedithiolate)monooxomolybdenum(IV) complex, and its derivatives [Mo(IV)O-(1,2-S₂-3-tBuNHCOC₆H₃)₂]²⁻ and [Mo(IV)O-(1,2-S₂-3-tBuCONHC₆H₃)₂]²⁻, in both cis and trans arrangements. Both the possible cis and trans attacks were explored together with the structural properties of formed dioxo-molybdenum products to verify the assumption, formulated on the basis of ¹H-NMR analysis, that independently from the starting isomer, the only formed dioxo isomer has both oxo ligands in trans to each of two hydrogen-bonded thiolate ligands.

DFT studies of the reaction pathways revealed that the two possible reaction mechanism are both viable for the monooxomolybdenum(IV) complexes with the carbamoyl and the acylamino substituents, whereas for the unsubstituted bis-(bdt)monooxomolybdenum(IV) complex only the cis-attack occurs.

The reaction pathway for the cis-attack evolves by the approach of the substrate to the molybdenum centre in cis to the oxo ligand sited on the initial complex, causing a distortion of the initial square-pyramidal geometry of the complex. As a consequence, an energy barrier corresponding to the movement of one of the sulphur atoms from its position to allow the entrance of Me₃NO substrate in the metal coordination sphere, has to be overcome. This is the step that is calculated to be the rate-determining one for all the investigated compounds, involved in the cis attack. The following step is the definitive breaking of the N-O bond and the formation of a new Mo-O bond, leading to the exothermic formation of an adduct between the dioxomolybdenum(VI) complex and trimethylamine.

Our computational investigation about the trans attack revealed that the initial charge distribution of the complexes does not allow a direct attack to the molybdenum centre in trans to the oxo ligand sited on the initial complex and, consequently, minima and transition states relative to such trans attack do not correspond to those previously hypothesized¹⁷. Indeed the oxygen atom is transferred before to a sulphur atom and in the next step to the metal centre with a concomitant reorganization in the coordination sphere of the ligands. This result confirmed that, according to the molybdenum chemistry, formation of a linear dioxo species is not allowed and the assistance of a sulphur atom is required.

The cis-attack is the preferred mechanism for all the investigated substituted molybdenum compounds, whereas the attack at the trans position is energetically unfavourable.

The investigation of the influence of the presence of substituents on the benzene rings able to form intramolecular NH···S hydrogen bond confirmed, according to experimental findings, that such interactions contribute to the reactivity tuning of the molybdoenzyme models and cause an acceleration of Me₃NO reduction process.

Moreover, our computations revealed that, independently from the nature of substituents on benzene rings, the cis isomer leads to the formation of a dioxo product with one of the hydrogen-bonded thiolato ligand in trans to the Mo=O bonds and one in cis, whereas starting from the trans isomer the formed dioxo product has both hydrogen-bonded thiolato ligands in trans to the Mo=O bonds. In **Figure1** their M06L optimized structures are reported.

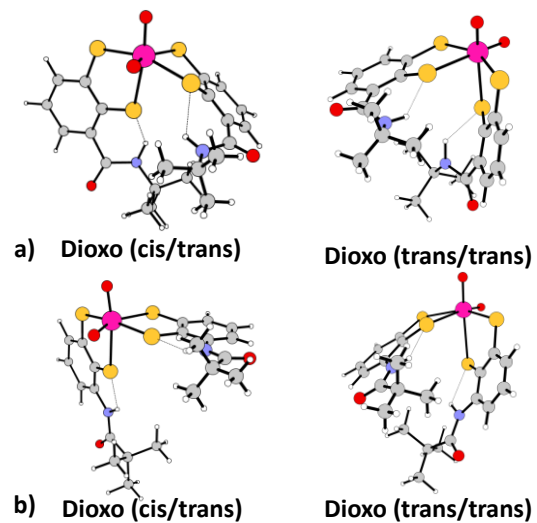


Figure 1. a) cis/trans and trans/trans $[\text{Mo(VI)}\text{O}_2\text{-(1,2-S}_2\text{-3-tBuNHCOC}_6\text{H}_3)]^{2-}$;
b) cis/trans and trans/trans $[\text{Mo(VI)}\text{O}_2\text{-(1,2-S}_2\text{-3-tBuCONHC}_6\text{H}_3)_2]^{2-}$

Bibliography

1. Hille, R. *Chem. Rev.*, **1996**, *96*, 2757.
2. Hille, R. *Met. Ions. Biol. Syst.*, **2002**, *39*, 187.
3. Zhang, Y.; Gladyshev, V. N. *J. Mol. Biol.*, **2008**, *379*, 881.
4. Hille, R. *Trend Biochem. Sci.*, **2002**, *27*, 360.
5. Kim, J.; Rees, D. C. *Science*, **1992**, *257*, 1677.
6. Lancaster, K. M.; Roemelt, M.; Ettenhuber, P.; Hu, Y.; Ribbe, M. W.; Neese, F.; Bergmann, U.; DeBeer, S. *Science*, **2011**, *334*, 974.
7. Spatzal, T.; Aksoyoglu, M.; Zhang, L.; Andrade, S. L. A.; Schleicher, E.; Weber, S.; Rees, D. C.; Einsle, O. *Science*, **2011**, *334*, 940.
8. Holm, R. H. *Chem. Rev.*, **1987**, *87*, 1401.
9. Cerqueira, N. M. F. S. A.; Pakhira, B.; Sarkar, S. *J. Biol. Inorg. Chem.*, **2015**, *20*, 323.
10. Boyde, S.; Ellis, S. R.; Garner, C. D.; Clegg, W. *J. Chem. Soc. Chem. Commun.*, **1986**, 1541.
11. a) Adman, E. T. *Adv. Protein. Chem.*, **1991**, *42*, 145; b) Adman, E.; Watenpaugh, K.; Jensen, L. H. *Proc. Natl. Acad. Sci. USA*, **1975**, *72*, 4954; c) Tsukihara, T.; Fukuyama, K.; Nakamura, M.; Katsume, Y.; Kanaka, N.; Kakudo, M.; Hase, T.; Wada, K.; Matsubara, H. *J. Biochem. (Tokyo)*, **1979**, *90*, 1763; d) Watenpaugh, K. D.; Sieker, L. C.; Jensen, L. H. *J. mol. Biol.*, **1979**, *131*, 509.
12. a) Nakamura, A.; Ueyama, N. *Adv. Inorg. Chem.*, **1989**, *33*, 39; b) Ueyama, N.; Terakawa, T.; Nakata, M.; Nakamura, A. *J. Am. Chem. Soc.*, **1983**, *105*, 7098; c) Ohno, R.; Ueyama, N.; Nakamura, A. *Inorg. Chem.*, **1991**, *30*, 4887; d) Sun, W. Y. Ueyama, N.; Nakamura, A. *Inorg. Chem.*, **1993**, *32*, 1095 e) Sun, W. Y. Ueyama, N.; Nakamura, A. *Inorg. Chem.*, **1991**, *30*, 4026 f) Sun, W. Y. Ueyama, N.; Nakamura, A. *Inorg. Chem.*, **1992**, *31*, 4053.
13. Ueyama, N.; Okamura, T.; Nakamura, A. *J. Am. Chem. Soc.*, **1992**, *114*, 8129.
14. Oku, H.; Ueyama, N.; Nakamura, A. *Inorg. Chem.*, **1997**, *36*, 1504.
15. Oku, H.; Ueyama, N.; Nakamura, A. *Inorg. Chem.*, **1995**, *34*, 3667.

16. Oku, H.; Ueyama, N.; Kondo, M.; Nakamura, A. *Inorg. Chem.*, **1994**, *33*, 209.
17. Baba, K.; Okamura, T.; Suzuki, C.; Yamamoto, H.; Yamamoto, T.; Ohama, M.; Ueyama, N. *Inorg. Chem.*, **2006**, *45*, 894.
18. Okamura, T.; Tatsumi, M.; Omi, Y.; Yamamoto, H.; Onitsuka, K. *Inorg. Chem.*, **2012**, *51*, 11688.
19. Okamura, T.; Ushijima, Y.; Omi, Y.; Onitsuka, K. *Inorg. Chem.*, **2013**, *52*, 381.

4 | Silver ion-mediated mismatched DNA base pairs

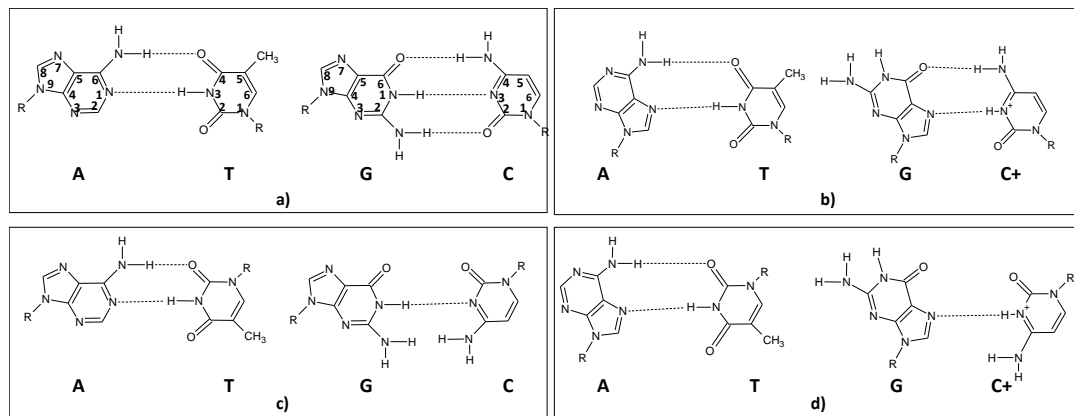
4.1 DNA base pairs and mispairs

Four nucleobases adenine (A), thymine (T) guanine (G) and cytosine (C) are used by nature for storing information of life. Of the all possible pairing schemes, involving two or three hydrogen bonds, nature uses relatively few only¹.

In double-stranded DNA, pairing occurs between the complementary nucleobases, G and C as well as A and T, mostly according to the Watson-Crick (W-C) fashion (see **Scheme 1a**). This pairing scheme allows an antiparallel strand orientation (aps-DNA).

Disorder of the regular duplex structure may led to a switch from Watson-Crick (W-C) to Hoogsten (H) pattern (see **Scheme 1b**), with the principal features of complementary and aps-orientation maintained.

In 1986², the possibility that DNA may adopt a structure with two strands running parallel was proposed and was later confirmed by de Sande et al³. The parallel strand orientation of DNA (ps-DNA) in Watson-Crick and Hoogsten models, has been called respectively reverse Watson-Crick (rW-C) and reverse Hoogsten (rH)⁴(see **Scheme 1c** and **1d**).



Scheme 1. Base pairing schemes: a) Watson-Crick; b) Hoogsten; c) reverse Watson-Crick; d) reverse Hoogsten.

The properties of nucleic acid base pairs can be influenced by a variety of contributions, including interaction with metal ions.

Metal ions have two favoured sites of interaction: the backbone phosphate of the sugar moieties and the electron-donor groups on the nucleobases. At very low concentration of cationic metal species, independently from the attack site of the metal, a thermal stabilization of duplex DNA structures is observed. However at higher level of metallation, depending on the type of metal (main group or transition metal, d-electron configuration, hardness and softness) its binding preference can change, leading to thermal stabilization or destabilization⁵.

Moreover, the interaction of DNA base pairs with metal ions can lead to the formation of non-complementary pairing schemes (base mispairing or

mismatching), which are the major source of errors affecting DNA replication⁶.

Several cases of mispairing have been experimentally observed using X-ray crystallography and ¹H-NMR spectroscopy⁷.

Lippert highlighted, through some crystal structure investigations, that such interactions can, in certain cases, increase the stability of mismatches and thereby sustain the formation, by altering the acid-base and hydrogen bonding properties^{7,8,9}

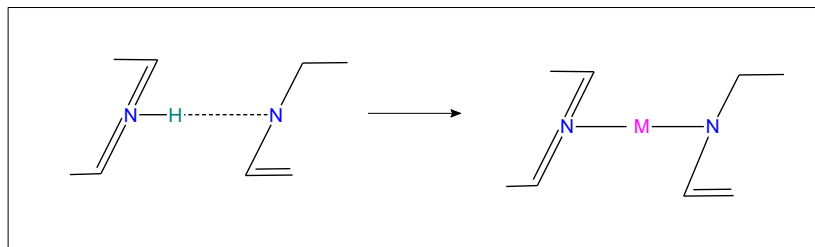
4.2 Metal-modified DNA base pairs: some features and their applications

In the last three decades, using new synthetic methodology, the chemically modified nucleic acids were used to experimentally address questions relative to their function and structure. Consequently, sugar-, phosphate- and base-modified nucleic acid analogues have recently been studied and used in therapeutic applications, in biotechnology and, due to the predictable molecular recognition properties of DNA, also in nanotechnology and in the material sciences¹⁰.

Several groups have reported artificial base pairs formed by non-Watson-Crick hydrogen bonding, hydrophobic interaction based on shape complementarity and modified base pairs using metal ions¹¹⁻¹³.

The metal-modified base pairs have attracted more interest in the last decade, in particular for the developing of nanodevices¹⁴.

The basic idea is to replace the hydrogen atoms, responsible for the hydrogen bond in natural DNA duplex, with a metal entities able to retain the natural duplex structure (see **Scheme 2**) and obtain a major stability, as expected considering that energies of metal coordination bonds are generally twice or three times larger than those of hydrogen bonds¹⁵.



Scheme 2. Schematization of metal mediated base pairs.

This analogy relates both to W-C, rW-C, H and rH pairs of complementary bases as well as nucleobase mismatches.

The incorporation of more than one type of metal-mediated base pairs into the DNA duplex backbones allows to obtain a completely synthetic information storage system.

4.2.1 Ag(I)-mediated mismatched base pairs

Complexes of Ag(I) ion with cytosine and guanine have been observed by X-ray diffraction, since 1979. In contrast to most divalent cations (such as Mg(II), Mn(II) and Co(II)) which interact preferably with the backbone phosphates or the sugar moieties¹⁶, it is well-accepted that Ag(I) has a propensity for binding to endocyclic ring nitrogen atoms of the DNA bases¹⁷. Very recently, Ono et al¹⁰ have found that thymine-thymine (T-T) and cytosine-cytosine (C-C) mispairs, selectively capture Hg(II) and Ag(I) ions, respectively, and the metal-mediated base pairs T-Hg(II)-T and C-Ag(I)-C are formed in DNA duplexes.

Starting from this experimental evidence, novel DNA structure-based sensors capable of selectively detecting Hg(II) and Ag(I) ions in aqueous solutions have been developed¹⁸.

Due to the high toxicity of mercury, interactions of Hg(II) ion with the nucleic acids and their structural features have been widely investigated, whereas a survey of the recent literature has revealed that the

characterization of the binding scheme and structural properties of **C-Ag(I)-C** system are limited¹⁰.

In addition, in 2012, Ono's group¹⁴ for the first time investigated the possibility that DNA polymerase may recognize Ag(I)-mediated base pairs into a primer strand to synthesize a full-length product. They showed that the Klenow Fragment (KF) of DNA polymerase incorporates adenine into the opposite site of a cytosine residue in the template strand in presence of Ag(I) ions, probably through the formation of a **C-Ag(I)-A** base pair.

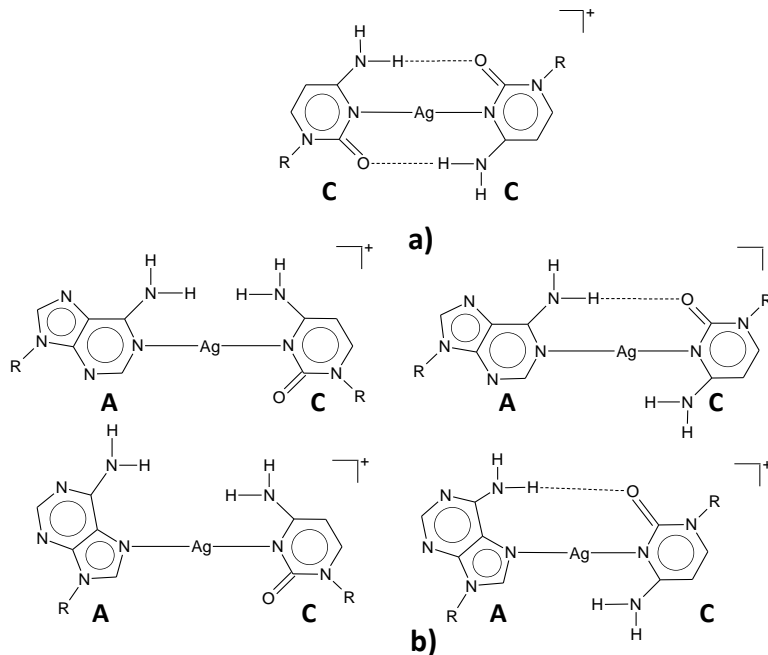
Our research interest is focused on the elucidation of some structural and energetic aspects of these Ag(I)-mediated base pairs.

4.3 A brief overview on our investigation (Paper II).

A DFT investigation was performed on the above mentioned silver ion-mediated base pairs, in order to get more information about their structural features and electronic properties, that could be useful to progress the potential applications of metal-mediated base pairs in nanotechnology.

For the considered non-complementary base pair, all possible orientation and pairing scheme was probed (W-C, rW-C, H and rH), and the sugar moiety was substituted by a methyl group.

Their thermodynamic stability was evaluated considering relative Gibbs free energy, whereas the binding energy was calculated as the difference between the electronic energy of the complex and the respective monomers.



Scheme 3. Ag(I)-mediated base pairs: a) C-Ag-C in rW-C arrangement; b) C-Ag-A in W-C, rW-C, H and rH arrangements.

For the C-Ag-C system, only the W-C pairing scheme, both in parallel and antiparallel orientation, appears to be possible. Indeed, Hoogsten base pair scheme applies the N7 position of the purine base as a hydrogen bond acceptor (see **Scheme 1**) and, consequently, in the metal-modified base pair model, the N7 position should be the atom coordinating the metal centre. In the C-Ag-C system the absence of a purine base implies the impossibility of a Hoogsten pairing mood.

In addition, our calculations showed that the parallel orientation collapses during the geometry optimization into the antiparallel one, in which the Ag(I) ion is coordinated by the N3 atoms and two hydrogen bonds are maintained (see **Scheme 3a**).

For the C-Ag-A model, the W-C and Hoogsten pairing schemes, in both the parallel and antiparallel orientation, are possible (see **Scheme 3b**).

Their relative energies showed that these four isomers are very close in energy. The reverse-Hoogsten arrangement, in which the silver ion is coordinated by the N3 and N7 positions of cytosine and adenine respectively, with a parallel orientation showed a major stability.

The geometrical and energetic investigation of their behaviour was extended to the duplex form $(dC\text{-Ag}\text{-}dC)_2$ and $(dC\text{-Ag}\text{-}dA)_2$, in which also the phosphate and sugar moieties were considered.

Moreover, for all the considered systems the nature of the metal-ligand interactions was investigated and the natural bond analysis revealed that this interaction is an electrostatic-type one. The BEs of the $(dC\text{-Ag}\text{-}dC)_2$ and $(dC\text{-Ag}\text{-}dA)_2$ systems are about two times of the corresponding C-Ag-C and C-ag-A monomers, showing the additivity of the BE.

Bibliography

1. Saenger, W. *Principles of Nucleic Acid Structures*, 1984, Springer, New York.
2. Pattabiraman, N. *Biopolymers*, 1986, 25, 1603.
3. Van de Sande, J. H.; Ramsing, N. B.; German, N. W.; Elhorst, W.; Kalisch, B. W.; Kitzing, V. E.; T. Pon, R.; Clegg, C.; Jovin, T. M.; *Science*, 1988, 241, 551.
4. Liu, K.; Miles, T.; Frazier, J.; Sasisekharan, V.; *Biochemistry*, 1993, 32, 11, 802.
5. Lippert, B.; *J. Chem. Soc., Dalton Trans.*, 1997, 3971.
6. Sirover, M.; Loeb, L. *Science*, 1976, 194, 1434.
7. a) Kennard, O.; Hunter, W. *Angew. Chem. Int. Ed.*, 1991, 30, 1254; b) Echols, H.; Goodman, M. *Annu. Rev. Biochem.*, 1991, 60, 477.
8. Sponer, J.; Gorb, L.; Leszczynski, J.; Lippert, B. *J. Phys. Chem. A*, 1999, 103, 11406.
9. Lippert, B. *Prog. Inorg. Chem.*, 2005, 54, 385.
10. Wojciechowski, F.; Leumann, C. *J. Chem. Soc. Rev.* 2011, 40, 5855.
11. Wojciechowski, F.; Leumann, C. *J. Chem. Soc. Rev.* 2011, 40, 5669.
12. Voegel, J. J.; Benner, S. A.; *J. Am. Chem. Soc.*, 1994, 116, 6929.
13. Schweitzer, B. A., Kool, E. T. *J. Am. Chem. Soc.*, 1995, 117, 1863.
14. Funai, T.; Miyazaki, Y.; Aotani, M.; Yamaguchi, E.; Nakagawa, O.; Wada, S.; Torigoe, H.; Ono, A.; Urata, H. *Angew. Chem. Int. Ed.*, 2012, 51, 6464.
15. Takezawa, Y.; Shionoya, M. *Acc. Chem. Res.*, 2012, 45, 2066.
16. Sigel, H. *Chem. Soc.*, 1993, 22, 255.
17. Sponer, J.; Sabat, M.; Burda, J.; Leszczynski, J.; Hobza, P.; Lippert, B. *J. Biol. Inorg. Chem.*, 1999, 4, 537.
18. a) Ono, A.; Togashi, H. *Angew. Chem. Int. Ed.*, 2004, 43, 4300; b) Miyaka, Y.; Ono, A.; *TetrahedronLett.*, 2005, 46, 2441; c) Ono, A.; Cao, S.; Togashi, M.; Tashiro, M.; Fujimoto, T.; Machinami, T.; Oda, s.; Miyake, Y.; Okamoto, I.; Tanaka, Y. *Chem. Commun.*, 2008, 4825; Torigoe, H.; Kawahashi, K.; Takamori, A.; Ono, A. *Nucleosides, NucleotidesNucleicAcids*, 2005, 24(5-7),

915; d) Torigoe, H.; Ono, A; Kozasa, T. *TransitionMet. Chem.*, 2011, **36**(2), 131; e) Ma, D.-L.; Chan, S.-H.; Man, Y.-W.; Leung, C.-H. *Chem. Asian. J.*, **2011**, **6**, 986.

Density Functional Theory

Mechanism of Thyroxine Deiodination by Naphthyl-Based Iodothyronine Deiodinase Mimics and the Halogen Bonding Role: A DFT Investigation

Mariagrazia Fortino,^[a] Tiziana Marino,^[a] Nino Russo,^[a, b] and Emilia Sicilia^{*[a]}

Abstract: This paper deals with a systematic density functional theory (DFT) study aiming to unravel the mechanism of the thyroxine (T4) conversion into 3,3',5-triiodothyronine (rT3) by using different bio-inspired naphthyl-based models, which are able to reproduce the catalytic functions of the type-3 deiodinase ID-3. Such naphthalenes, having two selenols, two thiols, and a selenol-thiol pair in *peri* positions, which were previously synthesized and tested in their deiodinase activity, are able to remove iodine selectively from the inner ring of T4 to produce rT3. Calculations were performed including also an imidazole ring that, mimicking the role of the His residue, plays an essential role deprotonating the selenol/thiol moiety. For all the used complexes, the cal-

culated potential energy surfaces show that the reaction proceeds via an intermediate, characterized by the presence of a X–I–C (X = Se, S) halogen bond, whose transformation into a subsequent intermediate in which the C–I bond is definitively cleaved and the incipient X–I bond is formed represents the rate-determining step of the whole process. The calculated trend in the barrier heights of the corresponding transition states allows us to rationalize the experimentally observed superior deiodinase activity of the naphthyl-based compound with two selenol groups. The role of the *peri* interactions between chalcogen atoms appears to be less prominent in determining the deiodination activity.

Introduction

The human thyroid prohormone 3,5,3',5'-tetraiodothyronine (thyroxine, T4) and its corresponding biologically active hormone 3,5,3'-triiodothyronine (T3) represent the main substrates of the type-3 iodothyronine deiodinase (ID-3) enzyme. ID-3 is a member of the iodothyronine deiodinase family, which includes three mammalian selenium-containing enzymes, type-1, -2, and -3, which are isozymes involved in the activation and inactivation of thyroid hormones.^[1] In particular, ID-3 catalyzes the conversion of T4 to 3,3',5'-triiodothyronine (rT3) by a selective inner-ring (5') deiodination.^[2,3] Furthermore, ID-3 is implicated in the maintenance of serum T3 concentration by the conversion of T3 into 3,3'-T2, an essential step for the protection of tissues from an excess of thyroid hormone, and also in preventing accumulation of T4 in cells and tissues.^[2–4] It was reported that the selenocysteine (Sec) residue in the active site of ID-3 is essential for efficient inner-ring deiodination as it is

confirmed by a reduction of the catalytic efficiency due to the substitution of Sec by a cysteine (Cys).^[5] Although the deiodinases are involved in basic functions of thyroid hormones,^[1] information about their structures and working mechanism is still incomplete. This lack of information can delay the development of more selective and suitable drugs with reduced side effects useful in contrasting the hyper- or hypo-activity of the thyroid gland. For such reasons, in the last decade, several selenium-containing compounds able to mimic the catalytic functions of ID-3^[6–9] were extensively investigated to shed light on the chemical mechanism of the type-3 iodothyronine deiodinase, the role played by the selenocysteine (Sec) residue in the catalytic site of the enzyme, and the effects of the substitution of Sec with Cys. In particular, in 2010, Manna and Mugesh^[8] proposed a series of *peri*-substituted naphthalenes containing thiol and selenol groups (Scheme 1) as model sys-

[a] M. Fortino, Prof. Dr. T. Marino, Prof. N. Russo, Prof. Dr. E. Sicilia

Department of Chemistry, Università della Calabria

87036, Arcavacata di Rende

Fax: (+39) 0964-492044

E-mail: emilia.sicilia@unical.it

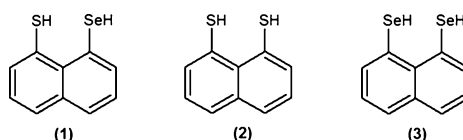
[b] Prof. N. Russo

División de Ciencias Básicas e Ingeniería

Departamento de Química, Universidad Autónoma Metropolitana-Iztapalapa

Av. San Rafael Atlixco No. 186, Col. Vicentina, CP 09340 (Mexico)

Supporting information for this article is available on the WWW under
<http://dx.doi.org/10.1002/chem.201406466>.



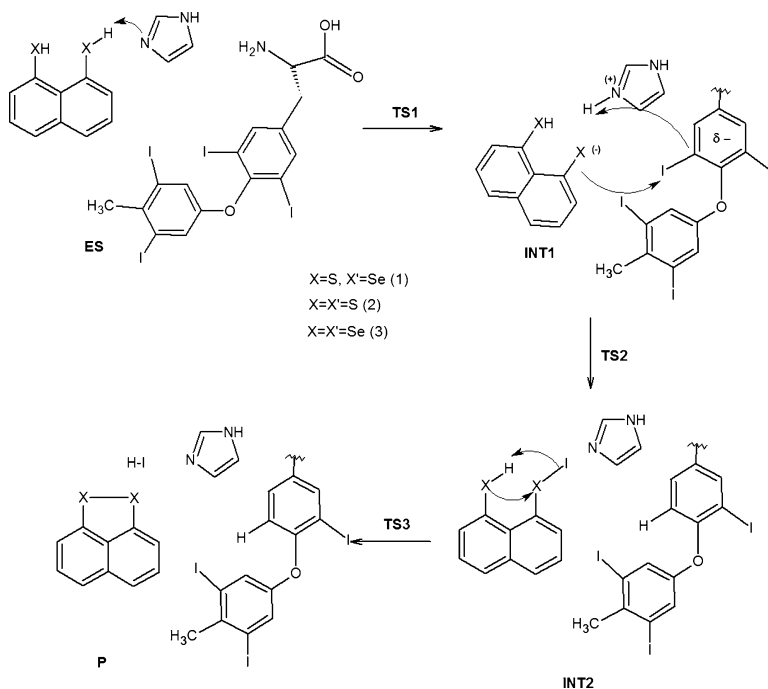
Scheme 1.

tems able to catalyze the selective inner-ring deiodination of T4 and T3 by ID-3 under physiological conditions. As no deiodination was observed when pure rT3 was used instead of T4, the high selectivity of these compounds was demonstrated.

Compound **1** has triggered an extensive research effort through the synthesis of a long series of substituted naphthalene derivatives aimed to satisfy the chemical and geometrical requirements that explain its special selectivity.^[9–11] Indeed, the reduced activity in the inner-ring deiodination of the synthesized compound **2**, bearing two thiol moieties on the naphthalene ring, with respect to compound **1** was proved.^[8] A further replacement of the –SH group in compound **1** with a selenol, compound **3** in Scheme 1, causes a remarkable increase in the deiodinase activity.^[9–11] Moreover, a second substitution with a selenol group should highlight the role that the thiol/selenol co-factor could play, not only in the deiodination process but also in the release of iodide from the involved intermediates. From the studies of the deiodination mechanism of T4 carried out so far by employing these simple models, the formation of a halogen bond between the thiol/selenol group and an iodine atom emerges as a key structural motif, as well as the role played by halogen bonds in the molecular recognition of thyroid hormones.

A survey of the recent literature reveals that the theoretical studies dedicated to the characterization of the nature of the S–I and Se–I halogen bonds are limited to the investigation of small systems mimicking Sec in the active site of ID by simple CH₃SeH or CH₃SH models interacting with a truncated model for thyroxine.^[12] More recently, a more extended model has been used in which the tyrosine substrate is modeled by a simple iodobenzene group.^[10] Detailed theoretical investigations of the whole deiodination process by ID-3 on T4 (and T3), as well as crystallographic data for these enzymes, are still lacking in the literature.

In this paper we present a systematic density functional theory (DFT) study of the mechanistic aspect of the deiodination process. The study was performed considering the entire T4 structure and by using different naphthyl-based models for ID-3, having S–S, S–Se and Se–Se sites, which have been previously synthesized and tested in their deiodinase activity.^[9–11] Calculations were performed including also a histidine residue, simulated by an imidazole ring (Im), because its presence appears to be essential for the activation of the –SeH group toward the nucleophilic attack by forming a selenolate-imidazolium zwitterionic species (see Scheme 2). The influence of the two thiols in **2**, the selenol and thiol pair in **1**, and the two selenols in **3** on the catalyzed reaction was rationalized on the



Scheme 2.

basis of the geometrical, electronic, and energetic properties of all stationary points present on the potential energy surfaces (PESs). On the basis of the experimental evidence, a deiodination mechanism was proposed,^[10] which involves a direct interaction of one of the selenol (selenolate) moieties with an iodine atom leading to the formation of a halogen bond.^[13] Generation of a σ hole or partial positive charge on the selenium atom should facilitate the selenium–selenium interaction, which strengthens the halogen bond, leading to the heterolytic cleavage of the C–I bond. With respect to the proposed mechanism, the outcomes of our calculations, as shown in Scheme 2, support the hypothesis that the process occurs in more steps and underscore the role of proton shuttle of the imidazole ring. Proton transfer from the formed imidazolium ion to the carbon atom causes the heterolytic cleavage of the C–I bond. Formation of the chalcogen–chalcogen (Se–Se, Se–S and S–S) bond, instead, concludes the process with elimination of the iodide as HI. The role the imidazole moiety could play in assisting the proton transfer in the last part of the process leading to the formation of the chalcogen bond was also explored.

Results and Discussion

According to Scheme 2, the mechanism of enzymatic deiodination of thyroxine by iodothyronine deiodinase has been probed by using naphthyl-based models to mimic ID3. Comparison of the calculated energy profile for compound **3**, containing two selenol groups, with those for compounds **1** and

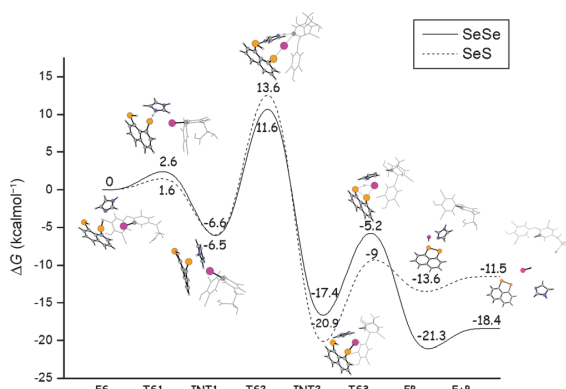


Figure 1. Calculated B3LYP-D3 free energy profile for inner ring 5 deiodination of thyroxine by naphthyl-based compound 3 (—) and 1 (----). Energies are in kcal mol^{-1} and relative to reactants asymptote.

2, having a selenol–thiol pair and two thiol groups, respectively, allows us to rationalize the observed activity trend.

The B3LYP-D3 free energy profile, calculated by including water-solvent effects, for the deiodination reaction of T4 by compound 3 in presence of an imidazole group (mimicking a histidine residue), is shown in Figure 1. Solvent effects have been accounted for implicitly by using the continuum approximation for the solvent.^[14]

Continuum salvation models represent a solvated molecule at an atomic level of detail inside a molecule-shaped electrostatic cavity surrounded by a solvent medium identified by its dielectric constant. The charge distribution of the solute induces polarization in the surrounding dielectric medium and the self-consistently determined interaction between the solute charge distribution and the electric polarization field of the solvent. Continuum models, based on the assumption that the electrostatic interactions of the solute and the surrounding solvent do not depend on the molecular structure of the solvent, reveal their inadequacy when strong, specific interactions between a solute and one or more first-shell solvent molecules are present. In the case under examination, however, the solvent does not play a key role; all the species directly involved in the deiodination process are included in the model system and the effects of the highly anisotropic electrostatic potential of ID-3 is properly considered. Relative free energies are calculated with respect to the first formed adduct (ES) and expressed in kcal mol^{-1} . Fully optimized geometrical structures of ES, INT1, and INT2 stationary points intercepted along the reaction pathway are schematically depicted in Figure 2, whereas complete geometries of all minima and transition states can be found in the Supporting Information. According to the hypothesized mechanism,^[9] many unsuccessful attempts to simulate the deiodination process in absence of the imidazole group were performed at the very beginning of the exploration of the deiodination reaction pathway. Indeed, the first step of the whole process is the proton abstraction by the imidazole moiety from one of the Se–H groups of compound 3 to form the selenolate anion. The proton transfer takes place

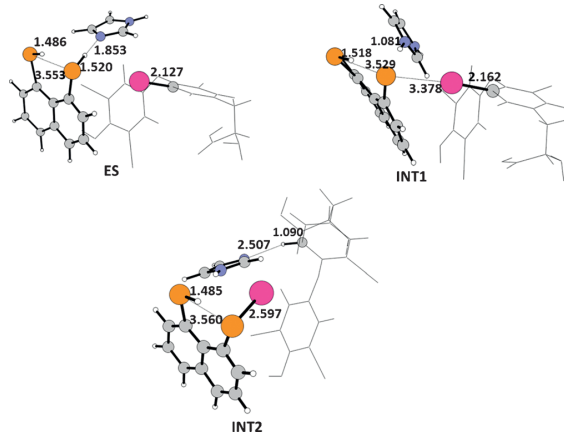


Figure 2. B3LYP-D3-optimized geometrical structure of stationary points intercepted along the pathway for T4 deiodination by compound 3. Selected bond lengths are in Å and angles in degrees.

by overcoming an energy barrier of only 2.6 kcal mol^{-1} for the TS1 transition state, and leads to the formation of a selenolate-imidazolium zwitterionic species. The key feature of such intermediate is that a halogen bond is formed between the selenolate group and the iodine atom, which is confirmed by structural and charge analysis of the INT1 intermediate. Even though it was proven that halogen bonds play a crucial role in thyroid hormone recognition,^[15] the importance they have in the mechanism of thyroid hormone deiodination was only recently highlighted.^[9,12] The increase of the C–I bond length (from 2.127 to 2.162 Å), the almost linear C–I–Se bond angle (173.5°), and the increase in electron density on the I atom (the NBO^[16] positive charge 0.227 becomes 0.189) are clear indications that a halogen bond is formed.^[13] The reaction is exothermic by 6.6 kcal mol^{-1} with respect to the reference energy of reactants. The proton transfer from the formed imidazolium ion to the carbon atom gives rise to the concerted heterolytic cleavage of the C–I bond and formation of the Se–I halogen bond. The barrier for the corresponding TS2 transition state is 18.2 kcal mol^{-1} , whereas the formed products lie 17.4 kcal mol^{-1} below the entrance channel energy. The chalcogen Se–Se interaction drives the proton transfer from the Se–H group to the I atom with consequent elimination of HI and formation of the Se–Se bond. The energetic cost for the formation of the TS3 transition state is 12.2 kcal mol^{-1} . The whole process is calculated to be exothermic by 21.3 kcal mol^{-1} , and even an additional 2.9 kcal mol^{-1} is required to release the deiodinated product.

As anticipated above, the possibility that imidazole can assist also the final step of the reaction by abstracting the proton from the Se–H group and transferring it to the iodine atom, either in a stepwise or concerted manner, was examined. Results of our computational exploration show that the process can occur in two steps, but it is not competitive with respect to the direct interaction between H and I atoms. Indeed, 11.0 and 9.1 kcal mol^{-1} are required for the proton shift to the

imidazole and the subsequent proton transfer from the imidazolium ion to I₁, respectively. Details are given in the Supporting Information (Figure S33). It is worth underlining that, additionally, in analogy with the model previously proposed,^[12] which involves two imidazole moieties acting as proton donor/acceptors, the influence of the contemporary presence of two Im molecules was examined. Nevertheless, any attempt to model the concerted protonation and deprotonation steps assisted by two Im molecules, one acting as proton acceptor and a second, protonated, to serve as the proton donor failed. The computational description of the deiodination process does not involve, as previously assumed, formation of an initial halogen-bonded adduct between T4 and the diselenol compound **3**. Instead, proton transfer occurs, thanks to the assistance of a basic imidazole group, and the rate-determining step of the whole process (requiring 18.2 kcal mol⁻¹ to occur) appears to be the concerted proton transfer from the formed imidazolium ion to the carbon atom, definitive C—I bond cleavage, and formation of the Se—I bond. To demonstrate that proton transfer and C—I bond cleavage occur simultaneously, Figure S34 in the Supporting Information shows intercepted structures along the reaction coordinate from the transition state to the products.

To check the influence that the polarity of the solvent might have on the described energy profile, additional calculations in a much less polar solvent (see the Supporting Information for more details, Figure S35) have been carried out. The calculated relative free energies along the reaction pathway show only small changes with respect to analogous values in water.

Deiodination of T4 was experimentally investigated by using compounds **1–3**, which are all able to mediate deiodination to form the corresponding chalcogenides.^[8–11] However, it has been shown that compound **3**, having two selenol moieties, is about 75-fold more active than compound **2**, whereas only a 13-fold enhancement in the activity was observed when only one of the thiols in compound **2** was replaced by a selenol (compound **1**).

To rationalize the observed behaviors, analogous calculations to generate the free energy profiles for **1** and **2** compounds were performed. The calculated B3LYP-D3 free energy profile for compound **2** is sketched in Figure 3 along with a schematic view of the structures of the intercepted stationary points. For compound **1**, instead, two alternatives pathways were explored. Indeed, initial proton transfer can occur from either the selenol SeH or thiol SH groups. The free energy profile calculated for the former and the latter are reported in Figures 1 and 3, respectively. Schematic views of all the intercepted stationary points are sketched in the same Figures, whereas the Supporting Information gives the geometries of all the optimized structures shown here. For the sake of clarity, from now on, compound **3** will be indicated as **SeSe**, compound **2** as **SS** and the two alternatives of compound **1** will be indicated as **SeS** and **SSe** when the first deprotonation occurs on Se and S, respectively.

Deiodination by compound **2** begins by surmounting an energy barrier of only 1.3 kcal mol⁻¹; the imidazole molecule abstracts the proton from one of the thiol groups and forms

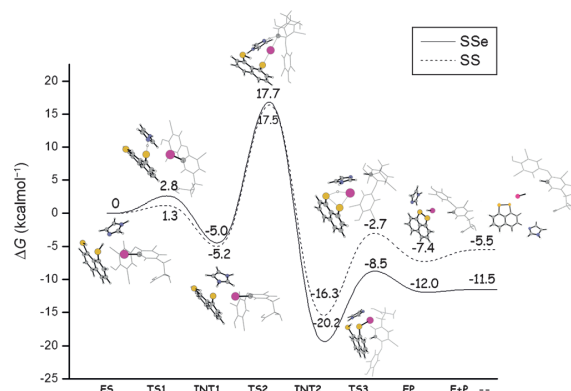


Figure 3. Calculated B3LYP-D3 free energy profile for inner ring 5 deiodination of thyroxine by naphthyl-based compounds **1** (—) and **2** (----). Energies are in kcal mol⁻¹ and relative to reactants asymptote.

the imidazolium thiolate complex, which is stabilized by 5.2 kcal mol⁻¹ with respect to the ES energy. Once again it is confirmed that a halogen-bonded adduct is formed. The TS2 transition state lies 22.7 kcal mol⁻¹ higher in energy than the minimum leading to it, whereas the next connected minimum is stabilized by 16.3 kcal mol⁻¹ with respect to the entrance channel energy. The last barrier relative to the TS3 transition state that allows for the elimination of a HI unit and formation of the S—S bond is 13.6 kcal mol⁻¹. The last step of the process is calculated to be exothermic by 7.4 kcal mol⁻¹, whereas the release of the deiodinated product costs 1.9 kcal mol⁻¹. The alternative stepwise proton transfer from the S atom to I assisted by the Im molecule entails two energy barriers of 13.2 and 12.1 kcal mol⁻¹, respectively, as reported in Figure S33 of the Supporting Information.

The deiodinase activity of compound **1** was explored by considering the possibility that both thiol and selenol groups can first act as proton donors to the Im group. As shown in Figure 1, when the SeH group transfers the proton to the imidazole, the corresponding transition state barrier is only 1.6 kcal mol⁻¹, whereas the formed product is stabilized by 6.5 kcal mol⁻¹ with respect to the reference energy. The height of the barrier that is necessary to overcome to simultaneously transfer the H atom from the imidazolium ion to the C atom and the I atom from C to Se is 20.1 kcal mol⁻¹. Once again, formation of the Se—I bond driven by the proton transfer to carbon atom results to be the rate-determining step of the whole process. Indeed, the subsequent intermediate INT2, in which the iodine is bonded to the Se atom, resides in a well 20.9 kcal mol⁻¹ deep and the transition state leading to the elimination of a HI molecule lies at 9.0 kcal mol⁻¹ below the energy of the entrance channel. Then, 11.9 kcal mol⁻¹ is the height of barrier for such TS, which leads to the formation of rT3, HI, the corresponding selenenyl sulfide, and the regenerated Im unit. The adduct formed by such species is stabilized by 13.6 kcal mol⁻¹, and 2.1 kcal mol⁻¹ is required to yield the separated products. Alternatively, to eliminate HI in the presence of an imidazole molecule, the heights of the barriers to overcome

are $14.4 \text{ kcal mol}^{-1}$ for the release of the H atom from the SH group and $11.7 \text{ kcal mol}^{-1}$ for the release of the I atom from Se. The free energy profile can be found in the Supporting Information, Figure S33.

The effect of the inversion of the role of the S and Se atoms in compound **1** is illustrated by the energy profile reported in Figure 3. To transfer the proton to the Im unit, a low barrier of $2.8 \text{ kcal mol}^{-1}$ has to be overcome to form the INT1 intermediate, which lies $5.0 \text{ kcal mol}^{-1}$ below the reference energy of the reactant. From this intermediate, following the C–I and N–H bond-breaking and Se–I and C–H bond-forming coordinate, the concerted transition state TS2 is intercepted, which lies $17.7 \text{ kcal mol}^{-1}$ above the reactant complex; that is, the corresponding activation energy barrier is $22.7 \text{ kcal mol}^{-1}$, and, in analogy with the energy profiles described above, represents the highest barrier along the deiodination pathway. Formation of the next intermediate INT2 is exothermic by $20.2 \text{ kcal mol}^{-1}$, whereas the elimination of a HI molecule from it and the concomitant formation of a new S–Se bond requires $11.7 \text{ kcal mol}^{-1}$ to occur. The final adduct formation and, therefore the whole process, is exothermic by $12.0 \text{ kcal mol}^{-1}$, although $0.5 \text{ kcal mol}^{-1}$ are needed to liberate the final deiodinated product. The calculated energy barriers along the alternative two-step pathway involving an imidazole molecule as acceptor–donor of an H atom are 14.0 and $11.6 \text{ kcal mol}^{-1}$, respectively (see Figure S33 of the Supporting Information). In analogy with **SeSe** compound, the influence of the polarity of the solvent on the energy profile has been checked also for **SS**. As the PES reported in the Supporting Information (Figure S35) clearly shows, the described behavior does not change appreciably when a much less polar solvent is considered.

In summary, the outcomes of the DFT computational analysis carried out in the present paper suggest that the inner-ring deiodination of thyroxine (T4) by ID-3 takes place in four steps. The importance of the presence of histidine residue, simulated by an imidazole ring, was demonstrated. The first step of the whole process is the proton abstraction by the imidazole moiety from one of the Se/S–H groups to form the corresponding selenolate/thiolate anion. The proton transfer from the formed imidazolium ion to the carbon atom gives rise to the consequent heterolytic cleavage of the C–I bond and formation of a Se/S–I bond. The chalcogen interaction forces the proton transfer from the remaining Se/S–H group to I with consequent elimination of HI and formation of a chalcogen–chalcogen bond. The role of proton acceptor/donor of the imidazole/imidazolium ion appears to be crucial for the process to occur. The rate-determining step of the entire process is calculated to be the simultaneous proton transfer from the imidazolium ion to the C atom of the ring, the heterolytic cleavage of the C–I bond, and the formation of a chalcogen–iodine bond. The described behaviors can be rationalized invoking several kinds of noncovalent interactions: Hydrogen, halogen, and chalcogen bonds. Common features of all these interactions are the directionality of the bond, bond lengths smaller than the corresponding sum of van der Waals radii, and anisotropy in electron density distribution, which causes the generation of an electropositive region of the electrostatic potential,

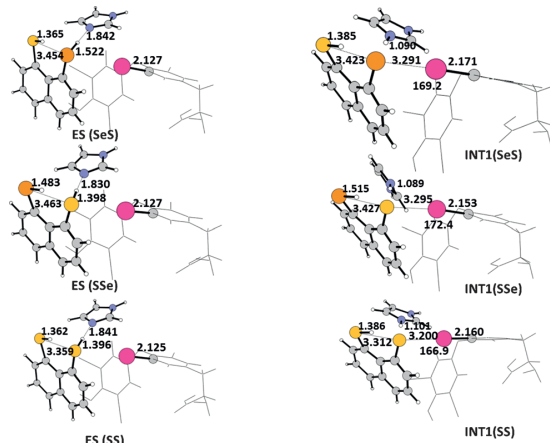


Figure 4. B3LYP-D3-optimized geometrical structure of stationary points intercepted along the pathway for T4 deiodination by both alternatives (**SeS** and **SSe**) of compounds **1** and **2**. Selected bond lengths are in Å and angles in degrees.

called σ -hole. The step that determines the rate of the whole process involves the transformation of the halogen-bonded adduct, INT1, into the corresponding intermediate, INT2, in which the C–I bond has been definitively broken and a new chalcogen–iodine bond has been formed.

In Figures 2 and 4 the most relevant geometrical parameters for the INT1 intermediates are reported, whereas Figure 5 shows the maps of the molecular electrostatic potential (MEP) for both ES and INT1 species formed by reaction of compounds **1**, **2**, and **3** with T4. The colors have been chosen such

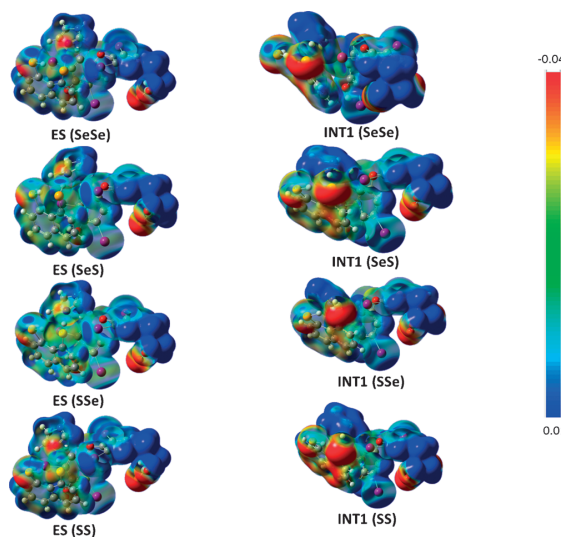


Figure 5. Maps of the molecular electrostatic potential (MEP) for both ES and INT1 species formed by reaction of compounds **1**, **2**, and **3** with T4. The electrostatic potential is represented with a color scale going from red (-0.04 au) to blue (0.01 au).

that regions of attractive potential appear in red and those of repulsive potential appear in blue. As anticipated above, the chalcogen–I–C bond angle in INT1 intermediates is almost linear (see Figures 2 and 4) indicating donation of the Se/S lone pair into the σ^* orbital of the C–I bond. For both INT1 intermediates, the C–I bond lengths are elongated by about 0.035 Å. The maps of the MEP clearly show a region of positive potential, that is, a σ -hole, located on the iodine atom in ES. A region of negative electrostatic potential, instead, corresponding to a dark-red area is located on the chalcogen atom in INT1, whereas the electrostatic potential becomes significantly less positive on I, which confirms the lone pair donation to the iodine σ hole and formation of a halogen bond. The strength of the halogen-bonding interaction was estimated by performing NBO second order energy analysis.^[16] The halogen bond energy, which is confirmed to be due to the donation of a S/Se lone pair into the σ^* C–I orbital, is calculated to be 13.5 kcal mol⁻¹ for **SeSe**, 11.1 kcal mol⁻¹ for **SeS**, 7.8 kcal mol⁻¹ for **SSe**, and 7.4 kcal mol⁻¹ for **SS**. The stronger Se–I interaction corresponds to a lower barrier (18.2 kcal mol⁻¹ for **SeSe** and 20.1 kcal mol⁻¹ for **SeS**), which is necessary to overcome for the definitive cleavage of the C–I bond and formation of a covalent Se–I bond with respect to the analogous barriers of 22.7 kcal mol⁻¹, for both **SSe** and **SS**, for the formation of a S–I bond. Contrary to the proposed mechanism,^[9] which assumes that the S/Se–I bond formation is facilitated by the interaction between the halogen-bonded S/Se atom with the adjacent thiol/selenol (thiolate/selenolate) moiety, elimination of a HI unit and formation of a chalcogen–chalcogen bond occurs in the next steps. As a consequence, *peri* interactions do not play the central role in the rate-determining step that was previously hypothesized, even if the proximity of a selenol or thiol in their protonated forms causes a weakening of the halogen bond, due to electron density donation to the selenium or sulfur atom of the SeH or SH groups. Electron density donation from lone pairs on S/Se atom to the antibonding σ S–H/Se–H orbital is confirmed by both the presence of a region of positive potential on the SH/SeH groups and NBO second order analysis.

Conclusion

A systematic DFT study of the mechanistic details of the inner-ring deiodination process of thyroxine T4 by ID-3 to 3,3',5'-triiodothyronine (rT3) was carried out by considering different *peri*-substituted naphthalenes mimicking the catalytic activity of type-3 deiodinase ID-3. The superior catalytic activity of the naphthalyl compound having two selenol groups in the *peri* positions with respect to the ones having two thiol groups or a thiol-selenol pair was investigated and rationalized. The importance of the presence of a histidine residue, simulated by an imidazole ring, was demonstrated. The computational analysis presented here reveals that the mechanism encompasses four steps. The first step is the proton abstraction by the imidazole moiety from one of the Se/S–H groups to form the corresponding selenolate/thiolate anion. The subsequent heterolytic cleavage of the C–I bond and formation of a Se/S–I bond

occur simultaneously to the proton transfer from the formed imidazolium ion to the carbon atom. The interaction between the two chalcogens forces the proton transfer from the remaining Se/S–H group to the iodine atom followed by the elimination of a HI unit and formation of a chalcogen–chalcogen bond. The rate-determining step of the whole process is the transformation of the intermediate characterized by the presence of a S/Se–I–C halogen bond into the intermediate in which the C–I bond is definitively broken and the chalcogen–I bond formed. The strongest Se–I interaction for the naphthalyl compound having two selenol groups corresponds to a barrier lower than those calculated for the other examined compounds and, as a consequence, deiodination is faster. The presence of an adjacent selenol or thiol group influences the strength of the chalcogen–iodine bond due to electron density donation from lone pairs on the S/Se atom to S–H/Se–H antibonding σ orbital.

Acknowledgements

This research was supported by Università della Calabria. M.F. gratefully acknowledges the Commissione Europea, Fondo Sociale Europeo, Regione Calabria for the financial support.

Keywords: amino acids • bioorganic chemistry • density functional calculations • enzyme models • iodine

- [1] a) G. W. Crabtree, M. S. Dresselhaus, M. V. Buchanan, *Phys. Today* **2004**, 57, 39; b) D. Behne, A. Kyriakopoulos, H. Meinhold, J. Köhrle, *Biochem. Biophys. Res. Commun.* **1990**, 173, 1143–1149; c) J. L. Leonard, T. J. Visser, *Biochemistry of Deiodination in Thyroid Hormone Metabolism* (Ed.: G. Hennemann), Marcel Dekker, New York, **1986**, p. 189; d) M. J. Berry, L. Banu, P. R. Larsen, *Nature* **1991**, 349, 438–440; e) P. R. Larsen, M. J. Berry, *Annu. Rev. Nutr.* **1995**, 15, 323; f) J. L. Leonard, J. Köhrle in *The Thyroid* (Eds.: L. E. Braverman, R. D. Utiger), Lippincott-Raven, Philadelphia, **1996**, p. 144; g) D. L. St. Germain, V. A. Galton, *Thyroid* **1997**, 7, 655–668.
- [2] a) A. C. Bianco, D. Salvatore, B. Gereben, M. J. Berry, P. R. Larsen, *Endocr. Rev.* **2002**, 23, 38–89; b) J. Köhrle, *Methods Enzymol.* **2002**, 347, 125–167; c) G. G. J. Kuiper, M. H. A. Kester, R. P. Peeters, T. J. Visser, *Thyroid* **2005**, 15, 787–798.
- [3] a) T. J. Visser, C. H. H. Schoenmakers, *Acta Med. Austriaca* **1992**, 19, 18–21; b) J. Köhrle, *Mol. Cell. Endocrinol.* **1999**, 151, 103–119; c) J. Köhrle, F. Jakob, B. Contempré, J. E. Dumont, *Endocr. Rev.* **2005**, 26, 944–984.
- [4] A. C. Bianco, B. W. J. Kim, *Clin. Invest.* **2006**, 116, 2571–2579.
- [5] G. G. J. M. Kuiper, W. Klootwijk, T. J. Visser, *Endocrinology* **2003**, 144, 2505–2513.
- [6] a) C. Beck, S. B. Jensen, J. Reglinski, *Bioorg. Med. Chem. Lett.* **1994**, 4, 1353–1356; b) A. A. Vasil'ev, L. J. Engman, *Org. Chem.* **1998**, 63, 3911–3917.
- [7] K. Goto, D. Sonoda, K. Shimada, S. Sase, T. Kawashima, *Angew. Chem. Int. Ed.* **2010**, 49, 545–547; *Angew. Chem.* **2010**, 122, 555–557.
- [8] D. Manna, G. Mugesh, *Angew. Chem. Int. Ed.* **2010**, 49, 9246–9249; *Angew. Chem.* **2010**, 122, 9432–9435.
- [9] D. Manna, G. Mugesh, *J. Am. Chem. Soc.* **2012**, 134, 4269–4279.
- [10] D. Manna, G. Mugesh, *J. Am. Chem. Soc.* **2011**, 133, 9980–9983.
- [11] D. Manna, G. Roy, G. Mugesh, *Acc. Chem. Res.* **2013**, 46, 2706–2715.
- [12] C. A. Bayse, E. R. Rafferty, *Inorg. Chem.* **2010**, 49, 5365–5367.
- [13] a) F. Guthrie, *J. Chem. Soc.* **1863**, 16, 239–244; b) B. Vonnegut, B. E. Warren, *J. Am. Chem. Soc.* **1936**, 58, 2459–2461; c) O. Hassel, *Science* **1970**, 170, 497–502; d) H. A. Bent, *Chem. Rev.* **1968**, 68, 587–648; e) P. Politzer, P. Lane, M. C. Concha, Y. Ma, J. S. Murray, *J. Mol. Model.* **2007**, 13, 305–311; f) P. Politzer, J. S. Murray, P. Lane, *Int. J. Quantum Chem.*

- 2007, 107, 3046–3052; g) F. F. Awwadi, R. D. Willett, K. A. Peterson, B. Twamley, *Chem. Eur. J.* **2006**, 12, 8952–8960; h) S. Tsuzuki, A. Wakisaka, T. Ono, T. Sonoda, *Chem. Eur. J.* **2012**, 18, 951–960.
- [14] The reaction mechanism was investigated employing the hybrid three-parameter gradient corrected (B3LYP) exchange-correlation functional including dispersion Grimme D3 corrections. The influence of solvent effects was estimated by using the COSMO (conductor-like screening model) approach. All the details can be found in the Supporting Information.
- [15] a) T. Eneqvist, E. Lundberg, A. Karlsson, S. Huang, C. R. A. Santos, D. M. Power, A. E. Sauer-Eriksson, *J. Biol. Chem.* **2004**, 279, 26411–26416; b) D. Lévesque, J. D. Beaudoin, S. Roy, J. P. Perreault, *Biochem. J.* **2007**, 403, 129–138; c) P. Metrangolo, F. Meyer, T. Pilati, G. Resnati, G. Terraneo, *Angew. Chem. Int. Ed.* **2008**, 47, 6114–6127; *Angew. Chem.* **2008**, 120, 6206–6220.
- [16] a) A. E. Reed, L. A. Curtiss, F. Weinhold, *Chem. Rev.* **1988**, 88, 899–926; b) E. D. Glendening, J. E. Reed, J. E. Carpenter, F. Weinhold, *NBO Program 3.1*, Madison, WI, 1988.

Received: December 12, 2014

Published online on April 23, 2015

CHEMISTRY

A European Journal

Supporting Information

Mechanism of Thyroxine Deiodination by Naphthyl-Based Iodothyronine Deiodinase Mimics and the Halogen Bonding Role: A DFT Investigation

Mariagrazia Fortino,^[a] Tiziana Marino,^[a] Nino Russo,^[a, b] and Emilia Sicilia*^[a]

chem_201406466_sm_miscellaneous_information.pdf

Supporting Information

Cartesian coordinates (Å) and absolute energies, (Hartrees) of optimized structures	S1-S32
Energy profiles for the alternative protonation/deprotonation two-steps pathways	S33
IRC path	S34
Energy profiles in a less polar solvent (diethylether)	S35
Computational Details	S36

S-1

Cartesian coordinates (Å) and absolute energies (Hartrees) of optimized structures

ES(SeSe): E(B3LYP/D3) = -7529.697402
Gas-phase zero-point energy = -7529.245832
Gas-phase free energy = -7529.335150

C	2.0225553	-2.0171256	3.3832453
C	3.1547756	-1.2166891	3.0659616
C	3.4402663	-0.8172180	1.6935273
C	2.4913131	-1.2809570	0.6976177
C	1.4129126	-2.0721174	1.0701093
C	1.1655482	-2.4468742	2.4056567
H	1.8402248	-2.2649764	4.4307168
H	0.7175277	-2.4102726	0.3022212
H	0.2892442	-3.0513763	2.6485774
C	3.9918460	-0.8231032	4.1460551
C	5.1199938	-0.0717812	3.9225695
C	5.4355468	0.3078836	2.6072761
C	4.6414163	-0.0271326	1.5134271
H	3.7235066	-1.1489803	5.1543992
H	5.7743199	0.2246822	4.7463718
H	6.3451995	0.8909727	2.4380621
Se	2.5228535	-1.0228758	-1.2473123
Se	5.3910486	0.7339233	-0.1012854
H	4.5571654	-0.0524844	-1.0474682
H	2.1804459	0.4584407	-1.2618242
C	-5.5774642	0.2848951	-0.6130398
C	-4.3795817	-0.3051665	-1.0431778
C	-3.1476889	0.2519313	-0.6955288
C	-3.0859506	1.4146365	0.0951942
C	-4.2899538	1.9984490	0.5250035
C	-5.5231112	1.4421720	0.1771038
C	-6.9079873	-0.3590510	-0.9289089
C	-7.3309213	-1.4084581	0.1383896
C	-6.3152406	-2.5714887	0.1632576
N	-7.5017345	-0.7799586	1.4304312
O	-1.8870829	1.9958722	0.3972489
O	-5.6052023	-2.8060938	1.1006610
O	-6.2248073	-3.3071929	-0.9714828
I	-1.3331281	-0.6553570	-1.3355077
H	-4.4081863	-1.2168471	-1.6436031
H	-6.4495946	1.8963338	0.5319820
H	-6.8655538	-0.8289713	-1.9254498
H	-7.7012331	0.4021724	-0.9639180
H	-8.3049902	-1.8226538	-0.1835664
H	-6.5788684	-0.5976337	1.8309809
H	-7.9406424	-1.4354882	2.0772861
H	-6.8872282	-3.0255519	-1.6189622
C	1.6990493	4.4250742	-0.7300273
C	2.4589272	3.2770511	-0.7577831
C	0.5514661	2.7564185	-1.6275597
N	0.4865076	4.0738834	-1.2927028
H	-0.3264577	4.6707706	-1.3916636
H	1.9046256	5.4291682	-0.3683774
H	3.4738510	3.1127229	-0.3992481
H	-0.2847987	2.2095887	-2.0575270
N	1.7294436	2.2548449	-1.3178998
I	-4.2274030	3.7548800	1.7236132
C	-1.1942170	1.5961039	1.5282124
C	-1.6603709	0.6129669	2.4014073

C	-0.8933783	0.2737931	3.5185382
C	0.3449352	0.8877314	3.7899260
C	0.7708837	1.8792429	2.8792640
C	0.0200068	2.2381043	1.7629831
O	1.0403006	0.5205925	4.8811793
I	-1.6281174	-1.2162516	4.8458606
I	2.6284610	2.8666530	3.2227505
H	-2.6085619	0.1092128	2.2146070
H	0.3605789	3.0127619	1.0808977
H	1.9342926	0.9017951	4.8456764

**TS1(SeSe): E(B3LYP/D3) = -7529.690311
 Gas-phase zero-point energy = -7529.240993
 Gas-phase free energy = -7529.332580**

C	3.6717836	-1.4204957	3.3836343
C	4.5699338	-0.7851205	2.4827779
C	4.3291495	-0.8161842	1.0487736
C	3.0587470	-1.3684724	0.6272765
C	2.2339592	-1.9998634	1.5500672
C	2.5452066	-2.0584581	2.9239973
H	3.9025713	-1.3897455	4.4519896
H	1.2886871	-2.4231771	1.2047785
H	1.8642181	-2.5648781	3.6130332
C	5.7095344	-0.1255640	3.0215094
C	6.6283673	0.4768712	2.1964432
C	6.4721690	0.3697214	0.8004166
C	5.3945077	-0.2915863	0.2212138
H	5.8342749	-0.1092853	4.1074860
H	7.4948576	1.0021280	2.6069962
H	7.2501054	0.7811306	0.1506664
Se	2.2453109	-1.1970673	-1.1374670
Se	5.6944302	-0.5840472	-1.6707300
H	4.3088438	-1.0630300	-1.9710302
H	2.3475909	0.4860808	-1.2085988
C	-5.5036112	-0.0754102	-0.7602050
C	-4.1798970	-0.5362982	-0.8013705
C	-3.1199339	0.2755003	-0.3869648
C	-3.3688462	1.5712411	0.0964291
C	-4.6958279	2.0380040	0.1210022
C	-5.7511948	1.2273399	-0.2993012
C	-6.6512236	-0.9613898	-1.1945689
C	-7.3778891	-1.6887486	-0.0259285
C	-6.4231783	-2.6719106	0.6844848
N	-7.9821737	-0.7383467	0.8848366
O	-2.3303438	2.3957389	0.4544914
O	-6.0608548	-2.5343803	1.8200894
O	-5.9762996	-3.7108455	-0.0594183
I	-1.1031214	-0.4445043	-0.5628843
H	-3.9679941	-1.5435136	-1.1675635
H	-6.7751640	1.6025229	-0.2706710
H	-6.2831403	-1.7015707	-1.9244579
H	-7.4143724	-0.3583623	-1.7091865
H	-8.1854588	-2.2884390	-0.4863855
H	-7.2674852	-0.4070027	1.5366984
H	-8.6710615	-1.2109585	1.4701782
H	-6.3817549	-3.7039282	-0.9385698
C	3.1376462	4.0059508	-1.4141391
C	3.4891946	2.6853915	-1.5475905
C	1.4026255	2.7152490	-0.9261642
N	1.8139401	4.0013527	-1.0213473
H	1.2455725	4.8179391	-0.8246591

H 3.6996037 4.9251682 -1.5564815
 H 4.4397698 2.2360562 -1.8324020
 H 0.3975750 2.4098545 -0.6361918
 N 2.3984648 1.9065496 -1.2408103
 I -5.1197221 4.0268771 0.7501967
 C -1.9583139 2.5190722 1.7777312
 C -1.1617953 3.6243914 2.0927159
 C -0.7040054 3.8048083 3.3946590
 C -1.0337076 2.9017683 4.4272640
 C -1.8472158 1.8083997 4.0706958
 C -2.3091270 1.6010722 2.7685547
 O -0.5708254 3.1256573 5.6680058
 I 0.5088408 5.4904538 3.8413058
 I -2.3809500 0.4090999 5.5929383
 H -0.9234778 4.3429892 1.3087072
 H -2.9276515 0.7357998 2.5314279
 H -0.8737296 2.4168334 6.2610300

INT1(SeSe): E(B3LYP/D3) =-7529.709217
 Gas-phase zero-point energy =-7529.254226
 Gas-phase free energy =-7529.339941

C 1.6623909 -1.0307765 3.0223924
 C 2.7666430 -0.3794262 2.4099554
 C 3.1567411 -0.7126384 1.0509242
 C 2.2459785 -1.5540593 0.2960729
 C 1.2178203 -2.2080204 0.9729363
 C 0.9360336 -1.9738209 2.3325242
 H 1.4067725 -0.7623852 4.0492247
 H 0.5597813 -2.8683511 0.4048420
 H 0.0998721 -2.4913062 2.8088743
 C 3.4718538 0.6124382 3.1505578
 C 4.5778585 1.2312454 2.6167299
 C 5.0551344 0.8281760 1.3514259
 C 4.4059628 -0.1406612 0.5917692
 H 3.1056777 0.8754390 4.1460827
 H 5.1100235 2.0044998 3.1776210
 H 5.9810274 1.2669024 0.9693023
 Se 2.1145566 -1.6640757 -1.6402287
 Se 5.4410359 -0.7242593 -0.9296942
 H 4.2444603 -1.3433553 -1.6298523
 H 2.3371969 0.4791769 -1.6864143
 C -5.3260446 0.2601450 -0.8133547
 C -4.0516783 -0.2135223 -1.1535598
 C -2.9042274 0.5300547 -0.8670814
 C -3.0263357 1.7680011 -0.2177413
 C -4.3061169 2.2727204 0.0674872
 C -5.4500875 1.5315617 -0.2325272
 C -6.5272259 -0.6487764 -0.9163074
 C -6.8104555 -1.3662589 0.4402904
 C -5.5479614 -2.1433513 0.8744092
 N -7.2536097 -0.4197429 1.4434157
 O -1.9096086 2.4768010 0.1582837
 O -4.8504704 -1.8031136 1.7914764
 O -5.2182577 -3.2149604 0.1200479
 I -0.9619452 -0.3067372 -1.3166097
 H -3.9459211 -1.2032853 -1.6037866
 H -6.4383708 1.9128590 0.0282766
 H -6.3664290 -1.3957132 -1.7111265
 H -7.4357327 -0.0834986 -1.1721286
 H -7.6235148 -2.0940292 0.2617150
 H -6.4364188 0.0746247 1.8079897

H -7.6348965 -0.9217491 2.2454736
 H -5.8875929 -3.3757980 -0.5608414
 C 3.6646418 3.2729365 -0.7106749
 C 3.5686392 2.3083714 -1.6772110
 C 2.0259080 1.8834761 -0.1583826
 N 2.6826794 2.9857119 0.2209119
 H 2.5400904 3.4602319 1.1141941
 H 4.3406708 4.1153326 -0.6009236
 H 4.1695709 2.1262903 -2.5625044
 H 1.2303132 1.3900062 0.3917792
 N 2.5339638 1.4753510 -1.3163492
 I -4.5076729 4.1630077 1.0306473
 C -1.3782455 2.2311915 1.3998258
 C -0.3699583 3.1015004 1.8244735
 C 0.2551004 2.8863157 3.0522055
 C -0.1139740 1.8259744 3.9030558
 C -1.1676698 1.0016151 3.4577422
 C -1.7927307 1.1798268 2.2233542
 O 0.5398052 1.6565338 5.0681787
 I 1.8038898 4.2182869 3.6633135
 I -1.8456610 -0.5722477 4.7278441
 H -0.1006312 3.9373864 1.1784911
 H -2.5897147 0.5055293 1.9090651
 H 0.1475794 0.9121027 5.5562711

TS2(SeSe): E(B3LYP/D3) =-7529.678509
 Gas-phase zero-point energy =-7529.226216
 Gas-phase free energy =-7529.315229

C -4.0496271 2.0076651 -2.0135073
 C -4.2100955 1.2208243 -0.8390951
 C -3.4733556 -0.0240895 -0.6572521
 C -2.5907474 -0.3992240 -1.7490161
 C -2.4867636 0.4126530 -2.8743298
 C -3.2060683 1.6140224 -3.0202370
 H -4.6079904 2.9434454 -2.0927661
 H -1.7972827 0.1171503 -3.6672848
 H -3.0578764 2.2258798 -3.9110246
 C -5.1128776 1.7039756 0.1488111
 C -5.3253209 1.0002516 1.3130921
 C -4.6232686 -0.2025856 1.5213638
 C -3.7151214 -0.7187113 0.5944813
 H -5.6443173 2.6392224 -0.0446492
 H -6.0339288 1.3541334 2.0665981
 H -4.7989352 -0.7563550 2.4480684
 Se -1.4074770 -1.9440626 -1.8923950
 Se -2.8931327 -2.3284656 1.2765942
 H -2.1262949 -2.6065292 0.0090610
 H 0.9649345 1.2802481 1.4093927
 C 4.7283364 0.0976735 1.2404374
 C 3.3385235 -0.1018148 1.2888227
 C 2.4191120 0.8193758 0.7632288
 C 2.9447108 1.9834810 0.1765462
 C 4.3262891 2.2058153 0.1094136
 C 5.2184206 1.2640735 0.6332831
 C 5.6842411 -0.9584102 1.7478442
 C 6.0688598 -1.9968971 0.6577395
 C 4.8222325 -2.7665997 0.1665945
 N 6.7934663 -1.3576098 -0.4208031
 O 2.0868964 3.0003714 -0.2326922
 O 4.4375368 -2.7425812 -0.9690099
 O 4.1578121 -3.4848935 1.1046437

I 0.6209841 -0.7315295 -0.5658557
 H 2.9629735 -1.0297724 1.7347080
 H 6.2952933 1.4281617 0.5631815
 H 5.2375499 -1.4714903 2.6168617
 H 6.6215330 -0.4993775 2.0959789
 H 6.7371470 -2.7391346 1.1359219
 H 6.1386635 -0.7853378 -0.9587456
 H 7.1136203 -2.0672940 -1.0803823
 H 4.5956948 -3.4105868 1.9645771
 C -1.6095586 3.3028664 1.8605765
 C -0.2554649 3.1257337 1.7441722
 C -1.1723483 1.1280294 1.8370822
 N -2.1570786 2.0358465 1.9221257
 H -3.1509841 1.8000801 1.9281374
 H -2.2191167 4.2014205 1.8885709
 H 0.5522975 3.8423845 1.6321801
 H -1.3163459 0.0480296 1.8234938
 N -0.0126021 1.7701244 1.7372027
 I 5.0948508 3.9875216 -0.7945795
 C 1.4229093 2.9354471 -1.4272161
 C 0.3895187 3.8591568 -1.6183703
 C -0.3542305 3.8389020 -2.7962813
 C -0.1060009 2.8941727 -3.8121505
 C 0.9524528 1.9915464 -3.5872735
 C 1.7285684 2.0121281 -2.4283160
 O -0.8811724 2.8897463 -4.9179913
 I -1.9030410 5.2774286 -3.0537452
 I 1.3295501 0.4767144 -5.0453179
 H 0.1806454 4.5881027 -0.8368106
 H 2.5343768 1.2952152 -2.2821597
 H -0.5615216 2.2079635 -5.5333436

INT2(SeSe): E(B3LYP/D3) =-7529.726487
 Gas-phase zero-point energy =-7529.271388
 Gas-phase free energy =-7529.366932

C 4.8498343 -1.5769520 2.6552394
 C 4.7900299 -0.5358134 1.6855478
 C 4.2801050 -0.7842254 0.3433297
 C 3.8047099 -2.1356599 0.1040194
 C 3.8761806 -3.1072405 1.0975370
 C 4.4149611 -2.8461249 2.3725324
 H 5.2459818 -1.3338617 3.6446794
 H 3.4864680 -4.1043933 0.8847027
 H 4.4578895 -3.6405681 3.1208744
 C 5.2306216 0.7529440 2.0869963
 C 5.2036564 1.8078360 1.2074840
 C 4.7615541 1.5861796 -0.1067996
 C 4.3176558 0.3452854 -0.5584420
 H 5.5838206 0.8870863 3.1119693
 H 5.5308815 2.8048501 1.5110553
 H 4.7841600 2.4245515 -0.8090077
 Se 3.0412456 -2.8836887 -1.5164764
 Se 3.8551044 0.4569163 -2.4383140
 H 3.5778419 -0.9914787 -2.6146508
 H -3.0780798 2.9160367 1.2090281
 C -5.1027433 0.5425305 -0.1869341
 C -4.2296812 1.6355527 -0.0902891
 C -3.7914171 2.0937118 1.1506631
 C -4.1937667 1.4504224 2.3240386
 C -5.0819544 0.3640848 2.2389463
 C -5.5400860 -0.0782614 0.9947640

C -5.4918455 -0.0234706 -1.5333195
 C -4.5832745 -1.2095104 -1.9706208
 C -3.1146729 -0.7475987 -2.0357142
 N -4.7739862 -2.3534203 -1.1073299
 O -3.7452243 1.8979446 3.5419399
 O -2.2614016 -1.1836790 -1.3022180
 O -2.8070343 0.2031073 -2.9363811
 I 0.5959853 -2.0171436 -1.3871858
 H -3.8568741 2.1272020 -0.9926539
 H -6.2233128 -0.9277603 0.9352170
 H -5.4618589 0.7752461 -2.2944289
 H -6.5214520 -0.4105809 -1.5160560
 H -4.8825338 -1.4908461 -2.9982125
 H -4.3512638 -2.1606823 -0.1968233
 H -4.2611767 -3.1556783 -1.4733731
 H -3.5865383 0.4629956 -3.4493193
 C 1.3778706 2.9792868 -0.3713766
 C 0.3277240 3.5153911 0.3420456
 C -0.3985220 1.6746301 -0.5003733
 N 0.8941514 1.8061465 -0.9031391
 H 1.4269901 1.1493439 -1.4722117
 H 2.3987931 3.3104667 -0.5363730
 H 0.3093237 4.4397637 0.9183503
 H -1.0123031 0.8169101 -0.7721042
 N -0.7714177 2.6949192 0.2515021
 I -5.7201026 -0.6310563 4.0076494
 C -2.5556846 1.3980670 4.0409710
 C -2.4969599 1.1685920 5.4177840
 C -1.3183199 0.6906839 5.9884573
 C -0.1752900 0.4145069 5.2094050
 C -0.2777253 0.6665226 3.8252645
 C -1.4415898 1.1576312 3.2335177
 O 0.9337827 -0.0610129 5.8066353
 I -1.2542322 0.3401866 8.0873799
 I 1.4340572 0.2950121 2.5945969
 H -3.3844593 1.3605520 6.0201196
 H -1.4634023 1.3836054 2.1677147
 H 1.6201277 -0.2036489 5.1326237

TS3(SeSe): E(B3LYP/D3) =-7529.708922
 Gas-phase zero-point energy =-7529.251743
 Gas-phase free energy =-7529.347387

C 4.8507905 -1.5766882 2.6551911
 C 4.7909862 -0.5355501 1.6855000
 C 4.2810615 -0.7839620 0.3432827
 C 3.8056667 -2.1353958 0.1039726
 C 3.8771374 -3.1069758 1.0974896
 C 4.4159176 -2.8458604 2.3724842
 H 5.2469378 -1.3335980 3.6446306
 H 3.4874250 -4.1041280 0.8846554
 H 4.4588459 -3.6403031 3.1208258
 C 5.2315776 0.7532065 2.0869483
 C 5.2046124 1.8080979 1.2074366
 C 4.7625104 1.5864417 -0.1068464
 C 4.3186123 0.3455482 -0.5584885
 H 5.5847764 0.8873488 3.1119207
 H 5.5318373 2.8051115 1.5110077
 H 4.7851163 2.4248131 -0.8090541
 Se 3.1233368 -2.5503976 -1.6084208
 Se 3.7753798 0.1260106 -2.3469737
 H 2.0502322 -0.3470326 -2.2627554

H -3.0780780 2.9160351 1.2090275
 C -5.1027405 0.5425301 -0.1869339
 C -4.2296788 1.6355517 -0.0902891
 C -3.7914149 2.0937106 1.1506625
 C -4.1937643 1.4504216 2.3240372
 C -5.0819516 0.3640846 2.2389451
 C -5.5400828 -0.0782614 0.9947634
 C -5.4918425 -0.0234706 -1.5333187
 C -4.5832719 -1.2095098 -1.9706196
 C -3.1146711 -0.7475983 -2.0357130
 N -4.7739836 -2.3534189 -1.1073293
 O -3.7452221 1.8979436 3.5419379
 O -2.2614004 -1.1836784 -1.3022172
 O -2.8070327 0.2031071 -2.9363795
 I 0.6372242 -1.3651273 -1.7299898
 H -3.8568719 2.1272008 -0.9926533
 H -6.2233094 -0.9277597 0.9352164
 H -5.4618559 0.7752457 -2.2944277
 H -6.5214484 -0.4105807 -1.5160552
 H -4.8825310 -1.4908453 -2.9982109
 H -4.3512614 -2.1606811 -0.1968231
 H -4.2611743 -3.1556765 -1.4733723
 H -3.5865363 0.4629954 -3.4493173
 C -0.0167269 5.7422355 -1.6322675
 C -1.0984662 6.5564878 -1.8892078
 C -1.9034583 4.6083563 -1.4622765
 N -0.5507709 4.5029248 -1.3640926
 H -0.0191759 3.6704837 -1.1119068
 H 1.0528431 5.9280896 -1.6065085
 H -1.0971217 7.6174994 -2.1365568
 H -2.5712581 3.7674706 -1.2800624
 N -2.2654213 5.8379821 -1.7822123
 I -5.7200994 -0.6310559 4.0076472
 C -2.5556832 1.3980662 4.0409688
 C -2.4969585 1.1685914 5.4177810
 C -1.3183191 0.6906835 5.9884539
 C -0.1752900 0.4145067 5.2094020
 C -0.2777251 0.6665222 3.8252623
 C -1.4415890 1.1576306 3.2335159
 O 0.9337821 -0.0610129 5.8066321
 I -1.2542314 0.3401864 8.0873753
 I 1.4340564 0.2950119 2.5945955
 H -3.3844573 1.3605512 6.0201162
 H -1.4634015 1.3836046 2.1677135
 H 1.6201267 -0.2036487 5.1326209

EP(SeSe): E(B3LYP/D3) =-7529.723448
 Gas-phase zero-point energy =-7529.270310
 Gas-phase free energy =-7529.363727

C 2.2501567 0.2962914 2.9768016
 C 1.6767296 1.0116790 1.8883938
 C 1.0190106 0.2722780 0.8498849
 C 0.9541002 -1.1507359 0.9385574
 C 1.5240662 -1.8176823 2.0107319
 C 2.1736211 -1.0809629 3.0302509
 H 2.7515469 0.8559828 3.7708187
 H 1.4739658 -2.9073220 2.0813256
 H 2.6170114 -1.6206178 3.8715275
 C 1.7257901 2.4303464 1.7854946
 C 1.1539682 3.0809989 0.7109692
 C 0.5066401 2.3566093 -0.3193918

C	0.4431110	0.9755052	-0.2479842
H	2.2236115	2.9983014	2.5759552
H	1.1959097	4.1715731	0.6463815
H	0.0602337	2.8948671	-1.1596326
Se	0.0380835	-2.0931110	-0.4625623
Se	-0.4529249	-0.0653176	-1.6066837
H	-2.3033877	0.1040101	-0.3598414
I	-3.5540337	0.1949760	0.7737741
H	-8.0675391	-6.3038409	-3.6323672
C	-6.4928641	-9.3350501	-3.8662621
C	-6.9102131	-8.0386388	-4.2019447
C	-7.7418461	-7.3077599	-3.3552806
C	-8.1726129	-7.8564250	-2.1388537
C	-7.7582610	-9.1548583	-1.7920840
C	-6.9300844	-9.8824060	-2.6497664
C	-5.5346815	-10.1007291	-4.7492866
C	-4.0433398	-9.8216124	-4.4042441
C	-3.7226957	-8.3326628	-4.6451266
N	-3.7418728	-10.2565541	-3.0588646
O	-9.0121842	-7.1974268	-1.2873163
O	-3.4390498	-7.5693196	-3.7601677
O	-3.8155631	-7.8938690	-5.9194343
H	-6.5774736	-7.5874337	-5.1406880
H	-6.6018838	-10.8833981	-2.3634742
H	-5.7283437	-9.8557810	-5.8073232
H	-5.6892082	-11.1838708	-4.6366403
H	-3.4273968	-10.4099994	-5.1108755
H	-4.1818083	-9.6146894	-2.3962165
H	-2.7404738	-10.1746357	-2.8828928
H	-4.0199602	-8.6235348	-6.5226989
C	-2.7232418	-4.3453848	-3.4103899
C	-1.6207085	-3.5233195	-3.4991513
C	-3.1295547	-2.3756736	-2.4814376
N	-3.6753116	-3.5905672	-2.7587563
H	-4.6101820	-3.8836420	-2.4967681
H	-2.9097336	-5.3716066	-3.7208421
H	-0.6509126	-3.7457315	-3.9423188
H	-3.6707356	-1.5939792	-1.9504733
N	-1.8876478	-2.3038641	-2.9177830
I	-8.3886986	-10.0118189	0.0481473
C	-9.1158002	-5.8248957	-1.3445169
C	-8.0348495	-5.0151900	-0.9804419
C	-8.1731332	-3.6288921	-0.9995253
C	-9.3932920	-3.0157001	-1.3681811
C	-10.4605893	-3.8689954	-1.7198479
C	-10.3335837	-5.2600839	-1.7166690
O	-9.4702237	-1.6762442	-1.3616104
I	-6.5236750	-2.4045745	-0.4406796
I	-12.3311223	-2.9998941	-2.2831536
H	-7.0955927	-5.4825604	-0.6808258
H	-11.1618824	-5.9132795	-1.9916489
H	-10.3608848	-1.3912663	-1.6259299

**ES(SeS): E(B3LYP/D3) =-5526.428192
 Gas-phase zero-point energy =-5525.974988
 Gas-phase free energy =-5526.063697**

C	2.0711826	-2.0258960	3.3579216
C	3.1880580	-1.2047462	3.0384333
C	3.4494703	-0.7881633	1.6681492
C	2.5056840	-1.2637420	0.6745725
C	1.4409758	-2.0718621	1.0483512

C	1.2102556	-2.4575891	2.3840964
H	1.9034932	-2.2891409	4.4040539
H	0.7479870	-2.4188300	0.2821261
H	0.3452150	-3.0767636	2.6303316
C	4.0335725	-0.8075941	4.1107896
C	5.1472457	-0.0367266	3.8774263
C	5.4369933	0.3662744	2.5637568
C	4.6297310	0.0329653	1.4773632
H	3.7855612	-1.1472411	5.1198037
H	5.8092742	0.2598069	4.6950724
H	6.3295554	0.9702547	2.3798513
Se	2.5532024	-1.0112424	-1.2712764
H	4.5072123	0.0334254	-0.9124490
H	2.1646435	0.4605285	-1.2902065
C	-5.5724534	0.2709839	-0.6247607
C	-4.3772521	-0.3282124	-1.0491587
C	-3.1429307	0.2274421	-0.7071819
C	-3.0766611	1.3944437	0.0766504
C	-4.2783343	1.9893025	0.4977019
C	-5.5136754	1.4373291	0.1518675
C	-6.9053511	-0.3729120	-0.9294813
C	-7.3458656	-1.3783777	0.1732729
C	-6.3333321	-2.5413735	0.2522411
N	-7.5269318	-0.7004293	1.4388726
O	-1.8759052	1.9696487	0.3813857
O	-5.6176124	-2.7285560	1.1961283
O	-6.2498700	-3.3326437	-0.8445956
I	-1.3322376	-0.6850660	-1.3494797
H	-4.4096368	-1.2459586	-1.6401367
H	-6.4385339	1.8995121	0.5002635
H	-6.8578804	-0.8807816	-1.9068847
H	-7.6923296	0.3924047	-0.9992908
H	-8.3186407	-1.7995524	-0.1431402
H	-6.6077619	-0.5213586	1.8493562
H	-7.9910506	-1.3229713	2.1005012
H	-6.9158068	-3.0825374	-1.5012995
C	1.6882910	4.4059408	-0.7035381
C	2.4398472	3.2529315	-0.7449400
C	0.5286953	2.7570467	-1.6224007
N	0.4734385	4.0706828	-1.2713700
H	-0.3352844	4.6745179	-1.3628456
H	1.9007904	5.4035698	-0.3281746
H	3.4522335	3.0744781	-0.3859087
H	-0.3109872	2.2211790	-2.0593755
N	1.7028916	2.2435976	-1.3186133
I	-4.2071885	3.7566455	1.6796380
C	-1.1889666	1.5669351	1.5152066
C	-1.6511482	0.5703083	2.3752046
C	-0.8878002	0.2274311	3.4937893
C	0.3425675	0.8508002	3.7796027
C	0.7627002	1.8580426	2.8837188
C	0.0158361	2.2201830	1.7659821
O	1.0359629	0.4778251	4.8700379
I	-1.6157635	-1.2836576	4.8008039
I	2.6027643	2.8681883	3.2538555
H	-2.5925814	0.0581856	2.1769433
H	0.3526088	3.0060603	1.0950654
H	1.9285177	0.8630006	4.8404766
S	5.2349122	0.7776443	-0.0297502

TS1(SeS): E(B3LYP/D3) = -5526.430574
 Gas-phase zero-point energy = -5525.973364

Gas-phase free energy =-5526.062018

C	1.8784190	-0.6738304	3.0810304
C	2.9467626	-0.0100187	2.4181386
C	3.3274687	-0.4001691	1.0742149
C	2.4342130	-1.3091918	0.3904793
C	1.4278568	-1.9539251	1.0982056
C	1.1684818	-1.6706915	2.4550660
H	1.6320325	-0.3647195	4.0985944
H	0.7676038	-2.6439534	0.5689634
H	0.3569874	-2.1877760	2.9723594
C	3.6254560	1.0429602	3.0936661
C	4.6964640	1.6723733	2.5028906
C	5.1693492	1.2186541	1.2553767
C	4.5510450	0.1815898	0.5616560
H	3.2660289	1.3464912	4.0795526
H	5.2063598	2.4968927	3.0080920
H	6.0706740	1.6672212	0.8295950
Se	2.3143716	-1.5241902	-1.5445741
H	4.5442499	-1.1591146	-1.4181026
H	2.4065839	0.1297943	-1.7558618
C	-5.3830830	0.0799635	-0.6739546
C	-4.0973198	-0.3706272	-1.0033128
C	-2.9697670	0.4036590	-0.7190670
C	-3.1160494	1.6496714	-0.0867131
C	-4.4070859	2.1077865	0.2278812
C	-5.5324393	1.3352225	-0.0656017
C	-6.5809839	-0.8199243	-0.8681637
C	-6.8991725	-1.6531987	0.4088372
C	-5.6777953	-2.5275441	0.7684133
N	-7.3099085	-0.7895654	1.4960471
O	-2.0195917	2.4213162	0.2013423
O	-4.9971059	-2.3387601	1.7389991
O	-5.3659545	-3.5068871	-0.1120617
I	-1.0237769	-0.3476446	-1.1915828
H	-3.9697423	-1.3534227	-1.4622056
H	-6.5288628	1.6893658	0.2025524
H	-6.4065655	-1.4923608	-1.7243031
H	-7.4801134	-0.2282545	-1.0952676
H	-7.7404186	-2.3257702	0.1576400
H	-6.4777719	-0.3512672	1.8966030
H	-7.6996160	-1.3509831	2.2534910
H	-6.0219679	-3.5532178	-0.8226656
C	3.6721286	3.4147271	-1.0616922
C	3.5619471	2.3797374	-1.9579664
C	2.0324724	2.0628721	-0.4468134
N	2.6881436	3.1964540	-0.1177577
H	2.5442246	3.7279017	0.7386664
H	4.3497806	4.2623206	-1.0094366
H	4.1664721	2.1627468	-2.8349831
H	1.2316691	1.6270509	0.1449325
N	2.5317712	1.5565168	-1.5632989
I	-4.6521434	3.9914354	1.1888231
C	-1.4023179	2.2797139	1.4196849
C	-0.3998820	3.2086924	1.7148707
C	0.2932119	3.1153960	2.9202271
C	0.0070425	2.1127612	3.8692596
C	-1.0312162	1.2168037	3.5447048
C	-1.7303735	1.2799379	2.3379590
O	0.7244516	2.0615884	5.0090371
I	1.8034475	4.5538204	3.3531688
I	-1.5693175	-0.2885597	4.9598816

H	-0.1888419	3.9933866	0.9885464
H	-2.5166784	0.5591890	2.1147885
H	0.3801476	1.3551630	5.5814897
S	5.5146882	-0.4011900	-0.8209435

INT1(SeS): E(B3LYP/D3) = -5526.431728
 Gas-phase zero-point energy = -5525.975642
 Gas-phase free energy = -5526.062235

C	2.1642208	-0.6759919	3.2896059
C	3.2405537	-0.1553519	2.5202130
C	3.4562667	-0.6012554	1.1539068
C	2.4377161	-1.4577914	0.5753146
C	1.4464337	-1.9823651	1.4004500
C	1.3139770	-1.6141392	2.7531799
H	2.0307399	-0.3150876	4.3126378
H	0.7075867	-2.6577908	0.9649678
H	0.5028993	-2.0398902	3.3485673
C	4.1031810	0.8012751	3.1240180
C	5.1876477	1.2995438	2.4417058
C	5.4774699	0.8101391	1.1535464
C	4.6773180	-0.1406042	0.5239763
H	3.8812670	1.1297415	4.1418058
H	5.8446913	2.0437720	2.8999326
H	6.3818790	1.1538765	0.6432675
Se	2.1619830	-1.7776930	-1.3235268
H	4.2817357	-1.3999632	-1.4697136
H	2.2581959	0.3503711	-1.4287087
C	-5.2674942	0.3307763	-0.8710904
C	-4.0407426	-0.2887756	-1.1487467
C	-2.8324314	0.3054238	-0.7785001
C	-2.8443940	1.5395219	-0.1108749
C	-4.0677730	2.1902443	0.1162141
C	-5.2725443	1.5956710	-0.2629128
C	-6.5632887	-0.4148638	-1.0835516
C	-7.0203357	-1.1435134	0.2177088
C	-5.9050616	-2.1092053	0.6767242
N	-7.3868068	-0.1876403	1.2428036
O	-1.6676825	2.1034811	0.3408526
O	-5.2327083	-1.9182309	1.6534833
O	-5.6711397	-3.1740833	-0.1229804
I	-0.9436754	-0.7053447	-1.1309629
H	-4.0271679	-1.2748916	-1.6190506
H	-6.2222781	2.0879293	-0.0487997
H	-6.4461240	-1.1435078	-1.9028523
H	-7.3752487	0.2715160	-1.3655635
H	-7.9139678	-1.7421723	-0.0395318
H	-6.5322932	0.1665837	1.6784375
H	-7.8853891	-0.6634325	1.9949561
H	-6.3079379	-3.2043069	-0.8516805
C	3.1985859	3.4585145	-1.1465123
C	3.4933386	2.1633025	-1.4758484
C	1.3668883	2.2220042	-0.8748180
N	1.8644211	3.4658554	-0.7757703
H	1.3316426	4.2736766	-0.4703718
H	3.8134423	4.3534898	-1.1295746
H	4.4199924	1.6800582	-1.7809635
H	0.3448732	1.9232766	-0.6462489
N	2.3416757	1.4293239	-1.3023457
I	-4.1002363	4.0835920	1.0967390
C	-1.2836685	1.8282808	1.6423919
C	-0.3063844	2.6602786	2.1895064

C	0.1684635	2.4238794	3.4774379
C	-0.3276173	1.3620020	4.2606584
C	-1.3351724	0.5644711	3.6816337
C	-1.8126898	0.7735905	2.3873012
O	0.1777817	1.1637283	5.4916151
I	1.6551890	3.7139775	4.2752036
I	-2.1529131	-1.0454700	4.8210434
H	0.0625710	3.5026526	1.6060529
H	-2.5817818	0.1241368	1.9698656
H	-0.2633121	0.4028630	5.9064977
S	5.4161580	-0.7737632	-0.9785851

**TS2(SeS): E(B3LYP/D3) = -5526.409075
 Gas-phase zero-point energy = -5525.954945
 Gas-phase free energy = -5526.040548**

C	-4.0895500	2.0103968	-1.9800862
C	-4.2296762	1.2071510	-0.8140338
C	-3.4664826	-0.0227107	-0.6543072
C	-2.5892908	-0.3743423	-1.7561602
C	-2.5018184	0.4536990	-2.8705086
C	-3.2418058	1.6451389	-2.9947798
H	-4.6670702	2.9356495	-2.0463973
H	-1.8140210	0.1782943	-3.6719929
H	-3.1082377	2.2709128	-3.8782026
C	-5.1338771	1.6578976	0.1885007
C	-5.3196312	0.9334605	1.3452913
C	-4.5881955	-0.2542301	1.5352619
C	-3.6731220	-0.7355931	0.5949668
H	-5.6875177	2.5836741	0.0129371
H	-6.0300072	1.2613865	2.1088494
H	-4.7350915	-0.8271650	2.4549869
Se	-1.4125960	-1.9214209	-1.9182558
H	-2.1569452	-2.4804363	0.0197538
H	0.9643585	1.2938782	1.3788657
C	4.7240513	0.0948939	1.2493721
C	3.3328940	-0.0993090	1.2752105
C	2.4250719	0.8265896	0.7383107
C	2.9636373	1.9911058	0.1636895
C	4.3470690	2.2081155	0.1193767
C	5.2276149	1.2614855	0.6541282
C	5.6668637	-0.9679413	1.7669042
C	6.0567531	-2.0077880	0.6799809
C	4.8104288	-2.7678880	0.1732270
N	6.7982632	-1.3720228	-0.3890599
O	2.1182958	3.0142762	-0.2555892
O	4.4386099	-2.7387157	-0.9664891
O	4.1309067	-3.4841388	1.1020606
I	0.6266409	-0.7165608	-0.5945868
H	2.9470004	-1.0272007	1.7123504
H	6.3059774	1.4220401	0.6014718
H	5.2063263	-1.4790363	2.6298659
H	6.6031236	-0.5158094	2.1265666
H	6.7141047	-2.7554575	1.1647953
H	6.1546152	-0.7906000	-0.9307025
H	7.1169431	-2.0824927	-1.0485384
H	4.5597290	-3.4152099	1.9669548
C	-1.6139499	3.3086876	1.8250811
C	-0.2597216	3.1361274	1.7033703
C	-1.1686974	1.1352369	1.8137541
N	-2.1563787	2.0400621	1.8973636
H	-3.1494692	1.8011805	1.9107446

H -2.2269573 4.2050306 1.8495867
 H 0.5454005 3.8544987 1.5838092
 H -1.3082056 0.0546470 1.8042619
 N -0.0120397 1.7814703 1.7042782
 I 5.1364971 3.9896959 -0.7667956
 C 1.4483125 2.9422352 -1.4465269
 C 0.4144241 3.8650625 -1.6389320
 C -0.3390870 3.8336245 -2.8104570
 C -0.1009473 2.8773714 -3.8179704
 C 0.9633211 1.9807526 -3.5557914
 C 1.7493771 2.0131760 -2.4437295
 O -0.8901362 2.8569593 -4.9135767
 I -1.8851227 5.2746979 -3.0709552
 I 1.3326248 0.4555435 -5.0445729
 H 0.2123663 4.6024698 -0.8636459
 H 2.5583745 1.2995850 -2.2985732
 H -0.5739471 2.1708994 -5.5259564
 S -2.8303355 -2.1893736 1.1894353

INT2(SeS): E(B3LYP/D3) =-5526.477072
 Gas-phase zero-point energy =-5526.019244
 Gas-phase free energy =-5526.105636

C 2.6004054 -1.6918100 3.3369655
 C 2.4962812 -0.6155358 2.4112214
 C 2.6308880 -0.8486208 0.9855133
 C 2.7241745 -2.2336014 0.5773949
 C 2.8106756 -3.2481791 1.5243699
 C 2.7877288 -2.9836052 2.9089912
 H 2.5202778 -1.4644692 4.4022388
 H 2.8611807 -4.2842908 1.1830048
 H 2.8708683 -3.8062520 3.6230371
 C 2.2492856 0.6866215 2.9238056
 C 2.1200857 1.7601342 2.0755720
 C 2.3318735 1.5747714 0.6961022
 C 2.6414222 0.3318260 0.1497445
 H 2.1405777 0.8100238 4.0017275
 H 1.8812302 2.7529769 2.4636267
 H 2.2932425 2.4443361 0.0351929
 Se 2.5963574 -2.9316166 -1.2313162
 H 2.9906920 -0.8355725 -1.9240244
 H -0.1020152 -0.3747694 1.3962058
 C -3.1504776 0.5365796 0.1222088
 C -1.7673983 0.3012654 0.1823639
 C -1.1738329 -0.1797706 1.3463515
 C -1.9537195 -0.4275509 2.4796724
 C -3.3342620 -0.1848410 2.4386543
 C -3.9281998 0.2859979 1.2633431
 C -3.8042336 0.9805861 -1.1654804
 C -4.2648148 -0.2135697 -2.0477561
 C -3.0461773 -1.0608138 -2.4676327
 N -5.2849535 -0.9849575 -1.3639644
 O -1.3606492 -0.9362047 3.6126756
 O -2.8580707 -2.1695812 -2.0040230
 O -2.2006331 -0.5444092 -3.3432401
 I 0.0444791 -2.6288763 -1.6733856
 H -1.1467875 0.4795059 -0.6969627
 H -5.0063688 0.4496031 1.2224523
 H -3.1099617 1.6138656 -1.7359431
 H -4.7037591 1.5769087 -0.9507571
 H -4.6970542 0.2145132 -2.9692552
 H -4.8340286 -1.5472848 -0.6385757

H -5.6849608 -1.6682724 -2.0077271
 H -2.1878435 0.4572162 -3.4429159
 C 0.1596408 3.6274774 -3.0724811
 C -1.1262516 3.2528626 -3.3961993
 C -0.0346002 1.4283447 -3.0159884
 N 0.8338617 2.4498431 -2.8358695
 H 1.8035545 2.3093913 -2.5554461
 H 0.6360943 4.6012632 -2.9942770
 H -1.9717245 3.8899859 -3.6508014
 H 0.2366809 0.3816328 -2.8813310
 N -1.2310110 1.8818427 -3.3568214
 I -4.5200586 -0.5235555 4.1716037
 C -0.7214289 -0.0866740 4.4725185
 C 0.0289356 -0.6826992 5.4916705
 C 0.7367915 0.1125345 6.3890074
 C 0.7130897 1.5239260 6.3147964
 C -0.0635691 2.0817821 5.2802410
 C -0.7800814 1.3044387 4.3675108
 O 1.4235919 2.2392183 7.2058276
 I 1.9339032 -0.8294475 7.8715830
 I -0.1041225 4.2099822 5.0605124
 H 0.0576194 -1.7707109 5.5475360
 H -1.3593839 1.7704903 3.5719726
 H 1.3032518 3.1883141 7.0379543
 S 3.2550299 0.4498163 -1.5285547

TS3(SeS): E(B3LYP/D3) =-5526.445634
 Gas-phase zero-point energy =-5525.991206
 Gas-phase free energy =-5526.084598

C 4.7862421 -1.6282322 2.6564499
 C 4.7264377 -0.5870939 1.6867586
 C 4.2165129 -0.8355058 0.3445409
 C 3.7411179 -2.1869400 0.1052306
 C 3.8125886 -3.1585203 1.0987479
 C 4.3513690 -2.8974048 2.3737430
 H 5.1823894 -1.3851420 3.6458896
 H 3.4228761 -4.1556728 0.8859137
 H 4.3942974 -3.6918477 3.1220848
 C 5.1670292 0.7016631 2.0882070
 C 5.1400641 1.7565548 1.2086949
 C 4.6979619 1.5348985 -0.1055883
 C 4.2540637 0.2940046 -0.5572306
 H 5.5202281 0.8358054 3.1131797
 H 5.4672891 2.7535687 1.5122661
 H 4.7205678 2.3732702 -0.8077962
 Se 3.0702990 -2.5565322 -1.6180020
 H 2.0466620 -0.3556791 -2.2562811
 H -3.0780789 2.9160359 1.2090278
 C -5.1027419 0.5425303 -0.1869340
 C -4.2296800 1.6355522 -0.0902891
 C -3.7914160 2.0937112 1.1506628
 C -4.1937655 1.4504220 2.3240379
 C -5.0819530 0.3640847 2.2389457
 C -5.5400844 -0.0782614 0.9947637
 C -5.4918440 -0.0234706 -1.5333191
 C -4.5832732 -1.2095101 -1.9706202
 C -3.1146720 -0.7475985 -2.0357136
 N -4.7739849 -2.3534196 -1.1073296
 O -3.7452232 1.8979441 3.5419389
 O -2.2614010 -1.1836787 -1.3022176
 O -2.8070335 0.2031072 -2.9363803

I	0.6044800	-1.3348248	-1.7365272
H	-3.8568730	2.1272014	-0.9926536
H	-6.2233111	-0.9277600	0.9352167
H	-5.4618574	0.7752459	-2.2944283
H	-6.5214502	-0.4105808	-1.5160556
H	-4.8825324	-1.4908457	-2.9982117
H	-4.3512626	-2.1606817	-0.1968232
H	-4.2611755	-3.1556774	-1.4733727
H	-3.5865373	0.4629955	-3.4493183
C	1.1549285	6.0435676	1.0720493
C	0.3921482	6.9816406	1.7333897
C	-0.9113683	6.0564743	0.2944967
N	0.3060512	5.4653887	0.1565553
H	0.5506153	4.7119042	-0.4850048
H	2.1915346	5.7362322	1.1729396
H	0.6965676	7.6476455	2.5400471
H	-1.7735865	5.7686290	-0.3054806
N	-0.8902024	6.9806175	1.2383548
I	-5.7201010	-0.6310561	4.0076483
C	-2.5556839	1.3980666	4.0409699
C	-2.4969592	1.1685917	5.4177825
C	-1.3183195	0.6906837	5.9884556
C	-0.1752900	0.4145068	5.2094035
C	-0.2777252	0.6665224	3.8252634
C	-1.4415894	1.1576309	3.2335168
O	0.9337824	-0.0610129	5.8066337
I	-1.2542318	0.3401865	8.0873776
I	1.4340568	0.2950120	2.5945962
H	-3.3844583	1.3605516	6.0201179
H	-1.4634019	1.3836050	2.1677141
H	1.6201272	-0.2036488	5.1326223
S	3.7283000	0.0391846	-2.2375718

P(SeS): E(B3LYP/D3) =-5526.446548
 Gas-phase zero-point energy =-5525.992352
 Gas-phase free energy =-5526.086261

C	2.2501567	0.2962914	2.9768016
C	1.6767296	1.0116790	1.8883938
C	1.0190106	0.2722780	0.8498849
C	0.9541002	-1.1507359	0.9385574
C	1.5240662	-1.8176823	2.0107319
C	2.1736211	-1.0809629	3.0302509
H	2.7515469	0.8559828	3.7708187
H	1.4739658	-2.9073220	2.0813256
H	2.6170114	-1.6206178	3.8715275
C	1.7257901	2.4303464	1.7854946
C	1.1539682	3.0809989	0.7109692
C	0.5066401	2.3566093	-0.3193918
C	0.4431110	0.9755052	-0.2479842
H	2.2236115	2.9983014	2.5759552
H	1.1959097	4.1715731	0.6463815
H	0.0602337	2.8948671	-1.1596326
Se	0.0380835	-2.0931110	-0.4625623
Se	-0.4529249	-0.0653176	-1.6066837
H	-2.3033877	0.1040101	-0.3598414
I	-3.5540337	0.1949760	0.7737741
H	-8.0675391	-6.3038409	-3.6323672
C	-6.4928641	-9.3350501	-3.8662621
C	-6.9102131	-8.0386388	-4.2019447
C	-7.7418461	-7.3077599	-3.3552806
C	-8.1726129	-7.8564250	-2.1388537

C -7.7582610 -9.1548583 -1.7920840
 C -6.9300844 -9.8824060 -2.6497664
 C -5.5346815 -10.1007291 -4.7492866
 C -4.0433398 -9.8216124 -4.4042441
 C -3.7226957 -8.3326628 -4.6451266
 N -3.7418728 -10.2565541 -3.0588646
 O -9.0121842 -7.1974268 -1.2873163
 O -3.4390498 -7.5693196 -3.7601677
 O -3.8155631 -7.8938690 -5.9194343
 H -6.5774736 -7.5874337 -5.1406880
 H -6.6018838 -10.8833981 -2.3634742
 H -5.7283437 -9.8557810 -5.8073232
 H -5.6892082 -11.1838708 -4.6366403
 H -3.4273968 -10.4099994 -5.1108755
 H -4.1818083 -9.6146894 -2.3962165
 H -2.7404738 -10.1746357 -2.8828928
 H -4.0199602 -8.6235348 -6.5226989
 C -2.7232418 -4.3453848 -3.4103899
 C -1.6207085 -3.5233195 -3.4991513
 C -3.1295547 -2.3756736 -2.4814376
 N -3.6753116 -3.5905672 -2.7587563
 H -4.6101820 -3.8836420 -2.4967681
 H -2.9097336 -5.3716066 -3.7208421
 H -0.6509126 -3.7457315 -3.9423188
 H -3.6707356 -1.5939792 -1.9504733
 N -1.8876478 -2.3038641 -2.9177830
 I -8.3886986 -10.0118189 0.0481473
 C -9.1158002 -5.8248957 -1.3445169
 C -8.0348495 -5.0151900 -0.9804419
 C -8.1731332 -3.6288921 -0.9995253
 C -9.3932920 -3.0157001 -1.3681811
 C -10.4605893 -3.8689954 -1.7198479
 C -10.3335837 -5.2600839 -1.7166690
 O -9.4702237 -1.6762442 -1.3616104
 I -6.5236750 -2.4045745 -0.4406796
 I -12.3311223 -2.9998941 -2.2831536
 H -7.0955927 -5.4825604 -0.6808258
 H -11.1618824 -5.9132795 -1.9916489
 H -10.3608848 -1.3912663 -1.6259299

ES(SSe): E(B3LYP/D3) =-5526.427391
 Gas-phase zero-point energy =-5525.974227
 Gas-phase free energy =-5526.062701

C 1.9095072 -2.0973068 3.1910557
 C 2.9759976 -1.2133104 2.8719539
 C 3.2797202 -0.8729198 1.4906550
 C 2.3724487 -1.4080375 0.4951617
 C 1.3702378 -2.2958047 0.8647873
 C 1.1389513 -2.6598065 2.2052710
 H 1.7060878 -2.3062014 4.2432572
 H 0.7099666 -2.6898603 0.0909520
 H 0.3200211 -3.3390197 2.4513423
 C 3.7380356 -0.6803927 3.9480406
 C 4.7940086 0.1650488 3.7077930
 C 5.1486766 0.4606516 2.3791644
 C 4.4585563 -0.0574580 1.2871553
 H 3.4651946 -0.9668220 4.9667419
 H 5.3755340 0.5886174 4.5306672
 H 6.0257535 1.0899682 2.2012678
 H 4.4350851 -0.3431056 -1.2564123
 H 2.1639402 0.3727504 -1.1472039

C	-5.5209966	0.2915330	-0.6631256
C	-4.3021372	-0.2649828	-1.0772133
C	-3.0900464	0.3253050	-0.7157337
C	-3.0717373	1.4856232	0.0800250
C	-4.2965650	2.0453221	0.4817284
C	-5.5098777	1.4591988	0.1138120
C	-6.8235830	-0.4131006	-0.9634343
C	-7.2241840	-1.4109806	0.1623490
C	-6.1349297	-2.4964552	0.3024127
N	-7.4795514	-0.7069346	1.4009597
O	-1.8914295	2.0815823	0.4288759
O	-5.4198573	-2.5909911	1.2606287
O	-5.9804896	-3.3252657	-0.7580370
I	-1.2422443	-0.5413574	-1.3133402
H	-4.2975668	-1.1833736	-1.6678721
H	-6.4534561	1.8911457	0.4509414
H	-6.7468062	-0.9422162	-1.9276777
H	-7.6443479	0.3134567	-1.0547269
H	-8.1588976	-1.9067810	-0.1603481
H	-6.5841017	-0.4538936	1.8250743
H	-7.9171261	-1.3380367	2.0724849
H	-6.6508990	-3.1482490	-1.4336980
C	2.0366295	4.3358107	-0.4277461
C	2.6650575	3.1112273	-0.4164847
C	0.7540168	2.7962571	-1.3730391
N	0.8194629	4.1157287	-1.0452277
H	0.0889867	4.8013044	-1.1984832
H	2.3361375	5.3141020	-0.0612229
H	3.6443693	2.8437742	-0.0238032
H	-0.1166128	2.3406104	-1.8396181
N	1.8537991	2.1709726	-1.0064219
I	-4.2964825	3.8014593	1.6825949
C	-1.2307120	1.6615299	1.5713437
C	-1.6648269	0.5913957	2.3546665
C	-0.9281712	0.2290180	3.4841571
C	0.2502135	0.9048974	3.8566082
C	0.6383625	1.9912450	3.0431078
C	-0.0819292	2.3721347	1.9138617
O	0.9226931	0.5055995	4.9516602
I	-1.6305631	-1.3812797	4.6815426
I	2.3659529	3.1246970	3.5788869
H	-2.5645459	0.0368167	2.0887996
H	0.2291394	3.2158533	1.3022652
H	1.7684476	0.9811477	5.0065435
S	2.3418927	-1.0083542	-1.2665851
Se	5.4034163	0.3320924	-0.3587715

TS1(SSe): E(B3LYP/D3) =-5526.414872
 Gas-phase zero-point energy =-5525.964832
 Gas-phase free energy =-5526.055999

C	3.6371311	-2.0167538	2.9886352
C	4.5844027	-1.3838384	2.1373526
C	4.2294101	-1.0057880	0.7783269
C	2.8399833	-1.1939261	0.4010079
C	1.9672372	-1.8408676	1.2710857
C	2.3588150	-2.2719032	2.5534439
H	3.9519546	-2.2977313	3.9973062
H	0.9314022	-1.9827580	0.9571605
H	1.6334971	-2.7712075	3.2013908
C	5.8876820	-1.1368191	2.6514523
C	6.8517291	-0.5467478	1.8700683

C	6.5573841	-0.2412429	0.5275707
C	5.3105007	-0.4908565	-0.0369376
H	6.1047257	-1.4287139	3.6825043
H	7.8505810	-0.3441965	2.2655703
H	7.3531693	0.1649135	-0.1039345
H	3.8935661	-0.4990642	-2.1462392
H	2.4159648	0.9875140	-0.8125209
C	-5.5692661	-0.3389889	-0.6511567
C	-4.1919581	-0.5981081	-0.6994941
C	-3.2590410	0.4142277	-0.4529453
C	-3.7010177	1.7090971	-0.1367390
C	-5.0817303	1.9621869	-0.0604036
C	-6.0093099	0.9525513	-0.3222310
C	-6.5753267	-1.4390973	-0.9068682
C	-7.1000538	-2.1105098	0.3935684
C	-5.9271115	-2.7691718	1.1499144
N	-7.8323045	-1.1612051	1.2063268
O	-2.8021667	2.7324842	0.0347499
O	-5.5323414	-2.3835744	2.2153969
O	-5.3170251	-3.8004265	0.5204137
I	-1.1538185	-0.0102360	-0.5972024
H	-3.8399021	-1.6050709	-0.9349947
H	-7.0794896	1.1573827	-0.2636958
H	-6.1276930	-2.1991423	-1.5684070
H	-7.4537078	-1.0338700	-1.4309649
H	-7.7948891	-2.9132277	0.0828349
H	-7.1618751	-0.5726721	1.7060667
H	-8.3402618	-1.6566447	1.9393042
H	-5.7667400	-4.0127363	-0.3102873
C	3.6218723	4.1905024	0.0478217
C	3.8181546	2.9919473	-0.5953442
C	1.7891918	2.9590711	0.2132629
N	2.3357636	4.1468146	0.5485980
H	1.8745592	4.8709781	1.0990837
H	4.2717093	5.0493873	0.1924992
H	4.6878162	2.5977141	-1.1183002
H	0.7816009	2.6412974	0.4795795
N	2.6655624	2.2525764	-0.4821158
I	-5.7727987	3.9106661	0.4510862
C	-2.3030558	3.0088667	1.2798633
C	-1.5291906	4.1688940	1.3901134
C	-0.9845730	4.5160254	2.6246073
C	-1.1888743	3.7369788	3.7825216
C	-1.9747702	2.5765742	3.6242135
C	-2.5301623	2.2042738	2.3985026
O	-0.6417882	4.1328171	4.9450084
I	0.1717009	6.3022127	2.7781134
I	-2.3273954	1.3410920	5.3308130
H	-1.3851042	4.7868675	0.5034847
H	-3.1315913	1.2994290	2.3127217
H	-0.8757224	3.5047464	5.6493050
S	2.0687193	-0.5665224	-1.0953359
Se	5.3570360	-0.2481308	-1.9605299

INT1 (SeS): E(B3LYP/D3) = -5526.432669
 Gas-phase zero-point energy = -5525.977074
 Gas-phase free energy = -5526.065484

C	3.6371311	-2.0167538	2.9886352
C	4.5844027	-1.3838384	2.1373526
C	4.2294101	-1.0057880	0.7783269
C	2.8399833	-1.1939261	0.4010079

C	1.9672372	-1.8408676	1.2710857
C	2.3588150	-2.2719032	2.5534439
H	3.9519546	-2.2977313	3.9973062
H	0.9314022	-1.9827580	0.9571605
H	1.6334971	-2.7712075	3.2013908
C	5.8876820	-1.1368191	2.6514523
C	6.8517291	-0.5467478	1.8700683
C	6.5573841	-0.2412429	0.5275707
C	5.3105007	-0.4908565	-0.0369376
H	6.1047257	-1.4287139	3.6825043
H	7.8505810	-0.3441965	2.2655703
H	7.3531693	0.1649135	-0.1039345
H	3.8935661	-0.4990642	-2.1462392
H	2.4159648	0.9875140	-0.8125209
C	-5.5692661	-0.3389889	-0.6511567
C	-4.1919581	-0.5981081	-0.6994941
C	-3.2590410	0.4142277	-0.4529453
C	-3.7010177	1.7090971	-0.1367390
C	-5.0817303	1.9621869	-0.0604036
C	-6.0093099	0.9525513	-0.3222310
C	-6.5753267	-1.4390973	-0.9068682
C	-7.1000538	-2.1105098	0.3935684
C	-5.9271115	-2.7691718	1.1499144
N	-7.8323045	-1.1612051	1.2063268
O	-2.8021667	2.7324842	0.0347499
O	-5.5323414	-2.3835744	2.2153969
O	-5.3170251	-3.8004265	0.5204137
I	-1.1538185	-0.0102360	-0.5972024
H	-3.8399021	-1.6050709	-0.9349947
H	-7.0794896	1.1573827	-0.2636958
H	-6.1276930	-2.1991423	-1.5684070
H	-7.4537078	-1.0338700	-1.4309649
H	-7.7948891	-2.9132277	0.0828349
H	-7.1618751	-0.5726721	1.7060667
H	-8.3402618	-1.6566447	1.9393042
H	-5.7667400	-4.0127363	-0.3102873
C	3.6218723	4.1905024	0.0478217
C	3.8181546	2.9919473	-0.5953442
C	1.7891918	2.9590711	0.2132629
N	2.3357636	4.1468146	0.5485980
H	1.8745592	4.8709781	1.0990837
H	4.2717093	5.0493873	0.1924992
H	4.6878162	2.5977141	-1.1183002
H	0.7816009	2.6412974	0.4795795
N	2.6655624	2.2525764	-0.4821158
I	-5.7727987	3.9106661	0.4510862
C	-2.3030558	3.0088667	1.2798633
C	-1.5291906	4.1688940	1.3901134
C	-0.9845730	4.5160254	2.6246073
C	-1.1888743	3.7369788	3.7825216
C	-1.9747702	2.5765742	3.6242135
C	-2.5301623	2.2042738	2.3985026
O	-0.6417882	4.1328171	4.9450084
I	0.1717009	6.3022127	2.7781134
I	-2.3273954	1.3410920	5.3308130
H	-1.3851042	4.7868675	0.5034847
H	-3.1315913	1.2994290	2.3127217
H	-0.8757224	3.5047464	5.6493050
S	2.0687193	-0.5665224	-1.0953359
Se	5.3570360	-0.2481308	-1.9605299

TS2(SSe): E(B3LYP/D3) = -5526.398134

Gas-phase zero-point energy =-5525.945793

Gas-phase free energy =-5526.033562

C -4.0006530 1.9682050 -2.0607498
C -4.1563714 1.2110607 -0.8663634
C -3.4151196 -0.0247031 -0.6556085
C -2.5178796 -0.4177278 -1.7316825
C -2.4248965 0.3639715 -2.8809682
C -3.1571628 1.5515806 -3.0596484
H -4.5621658 2.8997046 -2.1634009
H -1.7261133 0.0482156 -3.6579093
H -3.0161765 2.1419307 -3.9661640
C -5.0610406 1.7108520 0.1115289
C -5.2722616 1.0289678 1.2891941
C -4.5722493 -0.1714423 1.5198320
C -3.6652157 -0.7037209 0.6012750
H -5.5958730 2.6401426 -0.1005402
H -5.9824981 1.3962864 2.0348896
H -4.7533938 -0.7122798 2.4532156
H -2.0897915 -2.5751555 0.0148212
H 0.9984683 1.2860186 1.4515744
C 4.6945789 0.0909479 1.2291554
C 3.3039454 -0.0872911 1.3147189
C 2.3861929 0.8401453 0.7952098
C 2.9142308 1.9870650 0.1752582
C 4.2966868 2.1873329 0.0720586
C 5.1861476 1.2399064 0.5906550
C 5.6487595 -0.9689708 1.7313627
C 6.0040467 -2.0224900 0.6453821
C 4.7391446 -2.7820866 0.1867777
N 6.7138505 -1.4015811 -0.4537043
O 2.0572947 3.0029528 -0.2306437
O 4.3253439 -2.7539755 -0.9383944
O 4.0904416 -3.4903577 1.1431020
I 0.5804514 -0.6768702 -0.5249518
H 2.9243973 -1.0011699 1.7853703
H 6.2633893 1.3857563 0.4920716
H 5.2124368 -1.4684574 2.6132304
H 6.5963124 -0.5149971 2.0576897
H 6.6744504 -2.7654110 1.1191099
H 6.0498226 -0.8452152 -0.9969972
H 7.0328615 -2.1225489 -1.1014723
H 4.5538470 -3.4244561 1.9902516
C -1.5884649 3.3325352 1.9054309
C -0.2341759 3.1471049 1.8006608
C -1.1577052 1.1571903 1.9129603
N -2.1414740 2.0688102 1.9794870
H -3.1357411 1.8351879 1.9750784
H -2.1945665 4.2338427 1.9184645
H 0.5747618 3.8618743 1.6843217
H -1.3084912 0.0783219 1.9106770
N 0.0064895 1.7908157 1.8128648
I 5.0687574 3.9409625 -0.8788712
C 1.3993830 2.9435455 -1.4299021
C 0.3562027 3.8565541 -1.6160067
C -0.3763062 3.8442284 -2.8010920
C -0.1064396 2.9182395 -3.8286961
C 0.9576547 2.0218860 -3.6050864
C 1.7222347 2.0345569 -2.4384759
O -0.8676709 2.9249314 -4.9438069
I -1.9431601 5.2635129 -3.0522532
I 1.3652859 0.5317575 -5.0803288

H 0.1295817 4.5687772 -0.8240258
H 2.5323355 1.3221251 -2.2934928
H -0.5373171 2.2534025 -5.5646713
S -1.4028407 -1.8259516 -1.7777328
Se -2.8741373 -2.3325763 1.2731653

INT2(SSe): E(B3LYP/D3) =-5526.465277
Gas-phase zero-point energy =-5526.008154
Gas-phase free energy =-5526.104019

C 2.4224324 -1.7804914 3.4928959
C 2.3959143 -0.7194139 2.5442738
C 2.5524451 -0.9883566 1.1280886
C 2.5705096 -2.3846222 0.7447528
C 2.5852828 -3.3824791 1.7151591
C 2.5514957 -3.0893402 3.0928076
H 2.3299535 -1.5286487 4.5518961
H 2.5831814 -4.4237660 1.3864478
H 2.5761405 -3.9001772 3.8245669
C 2.2021630 0.6056015 3.0218345
C 2.1476587 1.6647130 2.1477341
C 2.3927318 1.4377024 0.7783239
C 2.6537116 0.1687686 0.2711293
H 2.0717018 0.7590285 4.0938726
H 1.9468973 2.6765147 2.5078856
H 2.4213930 2.2966286 0.1024477
H 3.0539008 -1.1423096 -1.8887915
H -0.1396344 -0.2860778 1.4611779
C -3.1169379 0.6215245 0.0283046
C -1.7395877 0.3841820 0.1608323
C -1.2062751 -0.0847790 1.3584674
C -2.0423227 -0.3148980 2.4552105
C -3.4179559 -0.0666845 2.3424887
C -3.9512661 0.3894256 1.1329337
C -3.7049041 1.0436008 -1.2977793
C -4.1354319 -0.1664513 -2.1743824
C -2.9033345 -1.0299231 -2.5101367
N -5.1951451 -0.9133704 -1.5249285
O -1.5148956 -0.8198892 3.6214152
O -2.7377527 -2.1198033 -1.9919372
O -2.0199168 -0.5511570 -3.3658946
I 0.0488906 -2.6433128 -1.5058001
H -1.0754902 0.5479835 -0.6892634
H -5.0256269 0.5550134 1.0356983
H -2.9780439 1.6569320 -1.8493188
H -4.6075512 1.6525977 -1.1393911
H -4.5174079 0.2431720 -3.1257029
H -4.7873697 -1.4634448 -0.7653964
H -5.5728720 -1.6057188 -2.1724306
H -1.9939718 0.4481614 -3.4998263
C 0.3592424 3.6092146 -3.2372533
C -0.9238312 3.2254795 -3.5601607
C 0.1405088 1.4202118 -3.0324263
N 1.0155314 2.4442196 -2.9050703
H 1.9815518 2.3169532 -2.6094113
H 0.8449234 4.5814266 -3.2184991
H -1.7572110 3.8511210 -3.8754919
H 0.3996062 0.3822963 -2.8247022
N -1.0435849 1.8614029 -3.4283192
I -4.6886077 -0.3797433 4.0191509
C -0.8561297 0.0134108 4.4820100
C -0.1654523 -0.5997700 5.5330048

C 0.5575183 0.1757653 6.4354379
 C 0.6086131 1.5846499 6.3346519
 C -0.1106739 2.1608782 5.2689727
 C -0.8411323 1.4034580 4.3504347
 O 1.3319047 2.2802556 7.2309179
 I 1.6663777 -0.7971177 7.9657869
 I -0.0348852 4.2835429 5.0087699
 H -0.1937436 -1.6866256 5.6096721
 H -1.3734336 1.8828808 3.5303383
 H 1.2677853 3.2305630 7.0405544
 S 2.4590602 -3.0303607 -0.9228323
 Se 3.4345929 0.2417829 -1.5007997

TS3(SSe): E(B3LYP/D3) =-5526.450913
 Gas-phase zero-point energy =-5525.989513
 Gas-phase free energy =-5526.085378

C 4.8232174 -1.6836239 2.6806767
 C 4.7634132 -0.6424858 1.7109855
 C 4.2534885 -0.8908977 0.3687682
 C 3.7780936 -2.2423315 0.1294581
 C 3.8495643 -3.2139115 1.1229751
 C 4.3883446 -2.9527961 2.3979698
 H 5.2193647 -1.4405337 3.6701161
 H 3.4598519 -4.2110637 0.9101410
 H 4.4312728 -3.7472388 3.1463113
 C 5.2040045 0.6462708 2.1124338
 C 5.1770393 1.7011622 1.2329221
 C 4.7349374 1.4795060 -0.0813608
 C 4.2910393 0.2386125 -0.5330029
 H 5.5572033 0.7804131 3.1374062
 H 5.5042642 2.6981758 1.5364932
 H 4.7575433 2.3178774 -0.7835685
 S 3.1133795 -2.5463090 -1.6088323
 H 2.1175008 -0.3257272 -2.2627165
 H -3.0780780 2.9160351 1.2090275
 C -5.1027405 0.5425301 -0.1869339
 C -4.2296788 1.6355517 -0.0902891
 C -3.7914149 2.0937106 1.1506625
 C -4.1937643 1.4504216 2.3240372
 C -5.0819516 0.3640846 2.2389451
 C -5.5400828 -0.0782614 0.9947634
 C -5.4918425 -0.0234706 -1.5333187
 C -4.5832719 -1.2095098 -1.9706196
 C -3.1146711 -0.7475983 -2.0357130
 N -4.7739836 -2.3534189 -1.1073293
 O -3.7452221 1.8979436 3.5419379
 O -2.2614004 -1.1836784 -1.3022172
 O -2.8070327 0.2031071 -2.9363795
 I 0.6885330 -1.3305459 -1.7473239
 H -3.8568719 2.1272008 -0.9926533
 H -6.2233094 -0.9277597 0.9352164
 H -5.4618559 0.7752457 -2.2944277
 H -6.5214484 -0.4105807 -1.5160552
 H -4.8825310 -1.4908453 -2.9982109
 H -4.3512614 -2.1606811 -0.1968231
 H -4.2611743 -3.1556765 -1.4733723
 H -3.5865363 0.4629954 -3.4493173
 C 0.6176852 4.0936263 -1.3250111
 C -0.0251641 5.0964997 -0.6320647
 C -1.4909238 3.5556297 -0.9526374
 N -0.3346589 3.1203464 -1.5219343

H -0.1813428 2.2268883 -1.9881703
 H 1.6388424 3.9821148 -1.6771309
 H 0.3881903 6.0403620 -0.2782410
 H -2.4038548 2.9616566 -0.9531038
 N -1.3364890 4.7498099 -0.4090942
 I -5.7200994 -0.6310559 4.0076472
 C -2.5556832 1.3980662 4.0409688
 C -2.4969585 1.1685914 5.4177810
 C -1.3183191 0.6906835 5.9884539
 C -0.1752900 0.4145067 5.2094020
 C -0.2777251 0.6665222 3.8252623
 C -1.4415890 1.1576306 3.2335159
 O 0.9337821 -0.0610129 5.8066321
 I -1.2542314 0.3401864 8.0873753
 I 1.4340564 0.2950119 2.5945955
 H -3.3844573 1.3605512 6.0201162
 H -1.4634015 1.3836046 2.1677135
 H 1.6201267 -0.2036487 5.1326209
 S 3.7767868 0.0292021 -2.2241824

EP(SSe): E(B3LYP/D3) = -5526.475309
 Gas-phase zero-point energy = -5526.019913
 Gas-phase free energy = -5526.110840

C 2.0348774 1.1284133 3.1913685
 C 1.7295089 1.4433017 1.8378458
 C 1.1127926 0.4367944 1.0284156
 C 0.8192203 -0.8447337 1.5818079
 C 1.1291843 -1.1199273 2.9059619
 C 1.7389871 -0.1208377 3.7020989
 H 2.5057944 1.8888886 3.8196769
 H 0.9056652 -2.0988943 3.3369677
 H 1.9770974 -0.3530123 4.7438176
 C 2.0040469 2.7066570 1.2419150
 C 1.6832856 2.9493720 -0.0793045
 C 1.0740495 1.9535540 -0.8830241
 C 0.7959906 0.7161217 -0.3292783
 H 2.4738899 3.4843538 1.8497619
 H 1.9006513 3.9252288 -0.5217993
 H 0.8305802 2.1724900 -1.9257214
 H -2.0642461 -0.0223502 -0.5839489
 I -3.4906875 0.4699007 0.1807573
 H -8.1930355 -6.2553593 -3.5876953
 C -6.7066616 -9.2929178 -4.1169547
 C -7.1465042 -7.9827590 -4.3544173
 C -7.8520343 -7.2718264 -3.3848418
 C -8.1305959 -7.8558859 -2.1409652
 C -7.6961508 -9.1706260 -1.8935487
 C -6.9937641 -9.8763483 -2.8726973
 C -5.8763138 -10.0353519 -5.1384732
 C -4.3510649 -9.7749450 -4.9779151
 C -4.0496425 -8.2795616 -5.2060488
 N -3.8836802 -10.2574264 -3.6976910
 O -8.8336698 -7.2153805 -1.1610742
 O -3.6430293 -7.5517689 -4.3403813
 O -4.3033423 -7.7951228 -6.4417501
 H -6.9301165 -7.5021492 -5.3125568
 H -6.6470446 -10.8902916 -2.6633054
 H -6.2003338 -9.7549397 -6.1549740
 H -6.0258377 -11.1207474 -5.0413438
 H -3.8348792 -10.3394958 -5.7777099
 H -4.2262738 -9.6346590 -2.9630660

H -2.8670054 -10.1892127 -3.6497363
 H -4.5969433 -8.5016160 -7.0358396
 C -2.5471374 -4.7328027 -3.0707281
 C -1.3512492 -4.0761782 -2.8761919
 C -2.7373713 -3.2036298 -1.4786313
 N -3.4168777 -4.1595500 -2.1675956
 H -4.4007284 -4.3744806 -2.0525095
 H -2.8494830 -5.5444348 -3.7284191
 H -0.4051568 -4.2340640 -3.3922382
 H -3.1935408 -2.5951032 -0.6993756
 N -1.4858836 -3.1308855 -1.8856572
 I -8.1059601 -10.0879121 -0.0203454
 C -9.0111659 -5.8500695 -1.2217347
 C -7.9354961 -4.9859503 -0.9938925
 C -8.1354927 -3.6076657 -1.0319239
 C -9.4154465 -3.0581546 -1.2773793
 C -10.4765058 -3.9644457 -1.4875956
 C -10.2869766 -5.3481862 -1.4682618
 O -9.5508167 -1.7235639 -1.2974102
 I -6.4906412 -2.2942235 -0.7186361
 I -12.4350770 -3.1903865 -1.8571370
 H -6.9508180 -5.4086229 -0.7898408
 H -11.1097231 -6.0430790 -1.6376207
 H -10.4770357 -1.4844291 -1.4693918
 Se -0.0585291 -0.7182427 -1.2961275
 S 0.0609877 -2.0547053 0.5245296

ES(SS): E(B3LYP/D3) =-3523.158022
 Gas-phase zero-point energy =-3522.703147
 Gas-phase free energy =-3522.790597

C 1.9676324 -2.0761510 3.2516063
 C 3.0599675 -1.2176460 2.9473381
 C 3.3404058 -0.8175048 1.5774408
 C 2.4135697 -1.3050708 0.5733430
 C 1.3807422 -2.1613890 0.9306309
 C 1.1512433 -2.5593808 2.2622092
 H 1.7831738 -2.3293397 4.2973872
 H 0.7074632 -2.5193608 0.1513653
 H 0.3104755 -3.2151662 2.4974513
 C 3.8673747 -0.7716138 4.0295389
 C 4.9574186 0.0348909 3.8041111
 C 5.2789982 0.4026307 2.4872967
 C 4.5236208 -0.0015307 1.3880257
 H 3.6082127 -1.0992561 5.0395104
 H 5.5833261 0.3796755 4.6312280
 H 6.1664316 1.0166873 2.3108172
 H 4.4218928 -0.1118194 -0.9933162
 H 2.1554601 0.4169519 -1.1522229
 C -5.5458429 0.3047379 -0.6384600
 C -4.3465559 -0.2639951 -1.0917346
 C -3.1171325 0.2986771 -0.7440477
 C -3.0606525 1.4446146 0.0707016
 C -4.2665513 2.0138597 0.5143317
 C -5.4968416 1.4528484 0.1654331
 C -6.8700491 -0.3620987 -0.9301783
 C -7.2628607 -1.3945853 0.1668791
 C -6.2106171 -2.5235169 0.2092334
 N -7.4393342 -0.7391090 1.4450140
 O -1.8629958 2.0172141 0.3941499
 O -5.4519711 -2.6821362 1.1244978
 O -6.1386450 -3.3109584 -0.8909875

I -1.2992746 -0.5876136 -1.3975389
 H -4.3709240 -1.1680283 -1.7037198
 H -6.4249208 1.8907045 0.5358722
 H -6.8305630 -0.8547226 -1.9156065
 H -7.6756899 0.3857300 -0.9712306
 H -8.2286869 -1.8398010 -0.1374260
 H -6.5179847 -0.5467655 1.8445120
 H -7.8813604 -1.3800209 2.1041380
 H -6.8392951 -3.0874979 -1.5206836
 C 1.8780384 4.3894893 -0.5561158
 C 2.5597122 3.1934712 -0.5594542
 C 0.6463244 2.7966735 -1.4801980
 N 0.6603485 4.1172257 -1.1510003
 H -0.1046131 4.7686897 -1.2829087
 H 2.1413551 5.3793894 -0.1928484
 H 3.5550681 2.9648012 -0.1823158
 H -0.2121979 2.3045508 -1.9316560
 N 1.7787063 2.2190060 -1.1354516
 I -4.2114350 3.7480960 1.7450235
 C -1.1950368 1.5989852 1.5336309
 C -1.6456555 0.5551417 2.3422491
 C -0.9044324 0.1977293 3.4704740
 C 0.2963239 0.8490080 3.8136973
 C 0.7044227 1.9051431 2.9702795
 C -0.0230215 2.2848638 1.8453795
 O 0.9717973 0.4562940 4.9086749
 I -1.6299196 -1.3706361 4.7092207
 I 2.4855691 2.9792762 3.4415300
 H -2.5621457 0.0185457 2.0978507
 H 0.3018426 3.1093871 1.2154268
 H 1.8458179 0.8817428 4.9252703
 S 5.2384139 0.5750303 -0.1460347
 S 2.4376687 -0.9494625 -1.2032456

TS1(SS): E(B3LYP/D3) =-3523.159457
 Gas-phase zero-point energy =-3522.702353
 Gas-phase free energy =-3522.789687

C 0.9890555 -1.7794222 2.2200559
 C 2.2309034 -1.1084524 2.0483248
 C 2.7408179 -0.8449076 0.7173361
 C 1.8464754 -1.1147597 -0.3900457
 C 0.6715291 -1.8249746 -0.1616683
 C 0.2430620 -2.1775333 1.1342092
 H 0.6344545 -1.9686092 3.2364343
 H 0.0230829 -2.0441174 -1.0115448
 H -0.7164361 -2.6826876 1.2699006
 C 2.9590875 -0.6894181 3.1979381
 C 4.1738768 -0.0570685 3.0678429
 C 4.7446013 0.0985927 1.7878364
 C 4.0927711 -0.3302358 0.6351676
 H 2.5310254 -0.8821646 4.1851423
 H 4.7245905 0.2837072 3.9491607
 H 5.7495790 0.5196901 1.6972969
 H 4.1574811 -0.5455003 -1.7332900
 H 2.3554098 1.0499306 -1.4496047
 C -5.2007142 -0.3496665 -0.2981222
 C -3.9406889 -0.2834664 -0.9081181
 C -3.1835984 0.8901092 -0.8732058
 C -3.6869253 2.0283299 -0.2214054
 C -4.9601267 1.9688328 0.3701793
 C -5.7133040 0.7925054 0.3342669

C -5.9355909 -1.6678618 -0.2196454
 C -5.5221518 -2.4924624 1.0347901
 C -4.0123559 -2.8173206 0.9805735
 N -5.9066735 -1.8021150 2.2466029
 O -2.9558561 3.1867854 -0.1674202
 O -3.2149672 -2.3769473 1.7642380
 O -3.6031584 -3.6068052 -0.0378714
 I -1.2155805 0.8474987 -1.6948503
 H -3.5248041 -1.1719651 -1.3877880
 H -6.6878358 0.7500215 0.8229340
 H -5.7500395 -2.2534125 -1.1354504
 H -7.0209645 -1.5049862 -0.1518839
 H -6.0702445 -3.4522315 0.9886672
 H -5.2700618 -1.0165325 2.3958789
 H -5.7644979 -2.4118513 3.0519813
 H -4.3543573 -3.9084086 -0.5692934
 C 3.8461704 3.5690118 0.4959689
 C 3.7815314 2.8907499 -0.6956440
 C 2.0018838 2.3492593 0.4386068
 N 2.7126262 3.2097516 1.1961351
 H 2.4401387 3.5409810 2.1216869
 H 4.5804345 4.2606370 0.8989847
 H 4.4933308 2.8596456 -1.5159651
 H 1.0672512 1.8827763 0.7423990
 N 2.6237928 2.1482801 -0.7131822
 I -5.7305135 3.6792476 1.3746773
 C -2.0166940 3.3368966 0.8190895
 C -1.2617708 4.5135777 0.7788082
 C -0.2705986 4.7295157 1.7329197
 C -0.0023239 3.7807146 2.7401101
 C -0.7997444 2.6229462 2.7676808
 C -1.8004045 2.3877521 1.8217359
 O 1.0495023 3.9893671 3.5779635
 I 0.8783721 6.5168128 1.6440994
 I -0.4539224 1.1729605 4.2933702
 H -1.4619907 5.2369568 -0.0113563
 H -2.3861379 1.4698269 1.8534997
 H 1.0445011 3.3129334 4.2791448
 S 5.1475122 -0.3509121 -0.8050416
 S 2.0270017 -0.4079495 -2.0341698

INT1(SS): E(B3LYP/D3) =-3523.156290
 Gas-phase zero-point energy =-3522.699199
 Gas-phase free energy =-3522.787639

C 2.3343827 -0.5623761 3.3764353
 C 3.3894006 -0.0919865 2.5480396
 C 3.5058634 -0.5442200 1.1734596
 C 2.4167496 -1.3514955 0.6478840
 C 1.4541868 -1.8374613 1.5321668
 C 1.4156616 -1.4626392 2.8880672
 H 2.2677120 -0.1943053 4.4030600
 H 0.6679608 -2.4833648 1.1373863
 H 0.6212985 -1.8528616 3.5290510
 C 4.3312081 0.8224538 3.0973152
 C 5.3961814 1.2686042 2.3509105
 C 5.5876569 0.7675060 1.0485533
 C 4.7071981 -0.1437774 0.4707839
 H 4.1865612 1.1601173 4.1261291
 H 6.1146334 1.9792998 2.7687128
 H 6.4765066 1.0677936 0.4857681
 H 4.1205765 -1.4210049 -1.4444611

H	2.2092699	0.3295724	-1.3153502
C	-5.2816459	0.3368537	-0.8876032
C	-4.0513559	-0.2898575	-1.1321142
C	-2.8504834	0.2954009	-0.7245837
C	-2.8735838	1.5288604	-0.0535749
C	-4.1001219	2.1811640	0.1495138
C	-5.2971484	1.5946451	-0.2653462
C	-6.5762995	-0.3921174	-1.1585906
C	-7.0773869	-1.1562908	0.1047109
C	-5.9932939	-2.1607605	0.5543360
N	-7.4489921	-0.2288422	1.1534241
O	-1.7058944	2.0951329	0.4149512
O	-5.3422842	-2.0207315	1.5535650
O	-5.7604022	-3.1994006	-0.2802385
I	-0.9630533	-0.7124671	-1.0206889
H	-4.0308878	-1.2725048	-1.6090185
H	-6.2499166	2.0892167	-0.0710312
H	-6.4421616	-1.0955930	-1.9970447
H	-7.3733419	0.3106723	-1.4424070
H	-7.9763645	-1.7272182	-0.1939673
H	-6.5975062	0.1003735	1.6139548
H	-7.9658123	-0.7217436	1.8818787
H	-6.3815047	-3.1903487	-1.0229443
C	3.1444974	3.4636073	-1.2043006
C	3.4362192	2.1551716	-1.4806728
C	1.3235133	2.2352885	-0.8436387
N	1.8175361	3.4847262	-0.8088989
H	1.2871512	4.3039496	-0.5311599
H	3.7572039	4.3594902	-1.2405889
H	4.3567046	1.6615971	-1.7876420
H	0.3067496	1.9461565	-0.5829499
N	2.2914001	1.4254102	-1.2529911
I	-4.1469425	4.0666756	1.1422944
C	-1.3161989	1.8002011	1.7108134
C	-0.3079665	2.5996287	2.2511970
C	0.1764483	2.3386418	3.5305256
C	-0.3358304	1.2815825	4.3103479
C	-1.3729501	0.5181411	3.7384570
C	-1.8644393	0.7546194	2.4536561
O	0.1845420	1.0562509	5.5300266
I	1.7138627	3.5740139	4.3170099
I	-2.2077551	-1.0921893	4.8652641
H	0.0835723	3.4314907	1.6671714
H	-2.6550773	0.1290934	2.0400765
H	-0.2584598	0.2934505	5.9387814
S	5.3112915	-0.8162457	-1.0749065
S	2.1011623	-1.6314505	-1.0928162

**TS2(SS): E(B3LYP/D3) = -3523.128901
 Gas-phase zero-point energy = -3522.674813
 Gas-phase free energy = -3522.761549**

C	-4.0256892	1.9690568	-2.0423863
C	-4.1719656	1.2022531	-0.8528936
C	-3.4119738	-0.0218961	-0.6538083
C	-2.5163195	-0.4018311	-1.7338135
C	-2.4297914	0.3893134	-2.8765177
C	-3.1750640	1.5708616	-3.0434789
H	-4.6001456	2.8932714	-2.1396312
H	-1.7303321	0.0850178	-3.6573358
H	-3.0410371	2.1700073	-3.9452162
C	-5.0816965	1.6795214	0.1320211

C -5.2777218 0.9830534 1.3043641
 C -4.5556947 -0.2051056 1.5269328
 C -3.6380051 -0.7122793 0.6029451
 H -5.6325034 2.6016091 -0.0699726
 H -5.9927520 1.3318513 2.0543394
 H -4.7170918 -0.7598443 2.4554406
 H -2.1326720 -2.4500837 0.0462150
 H 0.9995506 1.2879778 1.4336568
 C 4.6943124 0.0877637 1.2330798
 C 3.3027425 -0.0882195 1.3074735
 C 2.3903846 0.8413513 0.7824456
 C 2.9250573 1.9882137 0.1677539
 C 4.3087001 2.1857233 0.0748370
 C 5.1926785 1.2363572 0.5993827
 C 5.6424115 -0.9741804 1.7423933
 C 6.0039681 -2.0283164 0.6591347
 C 4.7408995 -2.7843701 0.1899153
 N 6.7244500 -1.4088562 -0.4337973
 O 2.0743950 3.0076761 -0.2422927
 O 4.3357245 -2.7539956 -0.9383392
 O 4.0829720 -3.4919508 1.1404982
 I 0.5847177 -0.6759281 -0.5412833
 H 2.9181904 -1.0019117 1.7743645
 H 6.2708549 1.3806255 0.5092559
 H 5.1981643 -1.4729186 2.6207411
 H 6.5883676 -0.5222819 2.0761540
 H 6.6684639 -2.7731149 1.1381583
 H 6.0666766 -0.8494920 -0.9816033
 H 7.0458915 -2.1303092 -1.0798004
 H 4.5402148 -3.4284556 1.9911893
 C -1.5902892 3.3312243 1.8828290
 C -0.2357712 3.1474924 1.7778548
 C -1.1565951 1.1565204 1.8954353
 N -2.1415094 2.0670681 1.9602188
 H -3.1355066 1.8323623 1.9582221
 H -2.1976673 4.2316787 1.8937321
 H 0.5724291 3.8628994 1.6597468
 H -1.3059799 0.0775273 1.8936037
 N 0.0067543 1.7915564 1.7931996
 I 5.0909248 3.9387808 -0.8689008
 C 1.4121646 2.9451333 -1.4390444
 C 0.3697921 3.8592367 -1.6247946
 C -0.3685937 3.8423343 -2.8060902
 C -0.1057400 2.9103355 -3.8301064
 C 0.9598489 2.0153473 -3.6086125
 C 1.7303865 2.0326572 -2.4458748
 O -0.8746710 2.9104289 -4.9399071
 I -1.9333206 5.2642042 -3.0564098
 I 1.3601996 0.5193654 -5.0797960
 H 0.1483956 4.5761538 -0.8355648
 H 2.5410744 1.3206246 -2.3020541
 H -0.5481299 2.2358572 -5.5594758
 S -2.8330838 -2.1851059 1.2027535
 S -1.4120005 -1.8180620 -1.7842872

INT2(SS): E(B3LYP/D3) =-3523.195788
 Gas-phase zero-point energy =-3522.736797
 Gas-phase free energy =-3522.825484

C 2.4230464 -1.7825499 3.4830530
 C 2.4039353 -0.7133098 2.5428578
 C 2.5291963 -0.9754295 1.1222759

C	2.5281522	-2.3698246	0.7303651
C	2.5318022	-3.3749221	1.6927657
C	2.5156631	-3.0909990	3.0727589
H	2.3551236	-1.5362382	4.5451885
H	2.5141762	-4.4135316	1.3563978
H	2.5328654	-3.9074301	3.7984303
C	2.2482514	0.6106028	3.0349407
C	2.2023859	1.6777124	2.1691060
C	2.4050062	1.4567662	0.7938182
C	2.6247658	0.1859918	0.2675058
H	2.1407066	0.7582251	4.1104757
H	2.0337298	2.6911559	2.5407800
H	2.4310777	2.3167399	0.1193006
H	2.9540108	-1.0773930	-1.7368234
H	-0.1164094	-0.2668635	1.4389871
C	-3.1039424	0.6315425	0.0219150
C	-1.7250263	0.4004621	0.1476948
C	-1.1842963	-0.0707143	1.3411210
C	-2.0141421	-0.3105453	2.4401369
C	-3.3913254	-0.0673874	2.3349187
C	-3.9319317	0.3922561	1.1299757
C	-3.7001079	1.0565513	-1.2997612
C	-4.1493194	-0.1497309	-2.1726910
C	-2.9292018	-1.0245245	-2.5226235
N	-5.2091296	-0.8881885	-1.5135378
O	-1.4785709	-0.8205455	3.6001290
O	-2.7677864	-2.1154707	-2.0042282
O	-2.0527005	-0.5571841	-3.3910597
I	0.0084163	-2.6504958	-1.5271611
H	-1.0650407	0.5717438	-0.7038807
H	-5.0072102	0.5548540	1.0385953
H	-2.9734362	1.6636111	-1.8584645
H	-4.5965944	1.6728838	-1.1341523
H	-4.5371677	0.2642607	-3.1196760
H	-4.7986078	-1.4433181	-0.7591580
H	-5.6001364	-1.5758819	-2.1581815
H	-2.0140428	0.4416594	-3.5254846
C	0.3841845	3.5672404	-3.2278112
C	-0.8986448	3.2039557	-3.5746377
C	0.1300310	1.3811489	-3.0376863
N	1.0175405	2.3913300	-2.8905153
H	1.9732671	2.2490049	-2.5712940
H	0.8836370	4.5319837	-3.1947556
H	-1.7169503	3.8434470	-3.9012871
H	0.3704352	0.3394559	-2.8279435
N	-1.0406325	1.8410929	-3.4514933
I	-4.6532734	-0.3945892	4.0153232
C	-0.8266172	0.0110431	4.4676881
C	-0.1395582	-0.6056791	5.5188495
C	0.5749346	0.1671866	6.4299718
C	0.6208305	1.5767695	6.3381279
C	-0.0928354	2.1564001	5.2706304
C	-0.8150659	1.4017409	4.3432399
O	1.3335368	2.2697823	7.2449582
I	1.6765840	-0.8108746	7.9621070
I	-0.0230566	4.2811164	5.0244989
H	-0.1647813	-1.6930331	5.5893604
H	-1.3451296	1.8840958	3.5234167
H	1.2671336	3.2209962	7.0599539
S	3.2221524	0.2259494	-1.4189343
S	2.4274268	-3.0017690	-0.9439591

TS3(SS): E(B3LYP/D3) =-3523.165681
 Gas-phase zero-point energy =-3522.698244
 Gas-phase free energy =-3522.803833

C	4.8232174	-1.6836239	2.6806767
C	4.7634132	-0.6424858	1.7109855
C	4.2534885	-0.8908977	0.3687682
C	3.7780936	-2.2423315	0.1294581
C	3.8495643	-3.2139115	1.1229751
C	4.3883446	-2.9527961	2.3979698
H	5.2193647	-1.4405337	3.6701161
H	3.4598519	-4.2110637	0.9101410
H	4.4312728	-3.7472388	3.1463113
C	5.2040045	0.6462708	2.1124338
C	5.1770393	1.7011622	1.2329221
C	4.7349374	1.4795060	-0.0813608
C	4.2910393	0.2386125	-0.5330029
H	5.5572033	0.7804131	3.1374062
H	5.5042642	2.6981758	1.5364932
H	4.7575433	2.3178774	-0.7835685
S	3.1133795	-2.5463090	-1.6088323
H	2.1175008	-0.3257272	-2.2627165
H	-3.0780780	2.9160351	1.2090275
C	-5.1027405	0.5425301	-0.1869339
C	-4.2296788	1.6355517	-0.0902891
C	-3.7914149	2.0937106	1.1506625
C	-4.1937643	1.4504216	2.3240372
C	-5.0819516	0.3640846	2.2389451
C	-5.5400828	-0.0782614	0.9947634
C	-5.4918425	-0.0234706	-1.5333187
C	-4.5832719	-1.2095098	-1.9706196
C	-3.1146711	-0.7475983	-2.0357130
N	-4.7739836	-2.3534189	-1.1073293
O	-3.7452221	1.8979436	3.5419379
O	-2.2614004	-1.1836784	-1.3022172
O	-2.8070327	0.2031071	-2.9363795
I	0.6885330	-1.3305459	-1.7473239
H	-3.8568719	2.1272008	-0.9926533
H	-6.2233094	-0.9277597	0.9352164
H	-5.4618559	0.7752457	-2.2944277
H	-6.5214484	-0.4105807	-1.5160552
H	-4.8825310	-1.4908453	-2.9982109
H	-4.3512614	-2.1606811	-0.1968231
H	-4.2611743	-3.1556765	-1.4733723
H	-3.5865363	0.4629954	-3.4493173
C	0.6176852	4.0936263	-1.3250111
C	-0.0251641	5.0964997	-0.6320647
C	-1.4909238	3.5556297	-0.9526374
N	-0.3346589	3.1203464	-1.5219343
H	-0.1813428	2.2268883	-1.9881703
H	1.6388424	3.9821148	-1.6771309
H	0.3881903	6.0403620	-0.2782410
H	-2.4038548	2.9616566	-0.9531038
N	-1.3364890	4.7498099	-0.4090942
I	-5.7200994	-0.6310559	4.0076472
C	-2.5556832	1.3980662	4.0409688
C	-2.4969585	1.1685914	5.4177810
C	-1.3183191	0.6906835	5.9884539
C	-0.1752900	0.4145067	5.2094020
C	-0.2777251	0.6665222	3.8252623
C	-1.4415890	1.1576306	3.2335159
O	0.9337821	-0.0610129	5.8066321

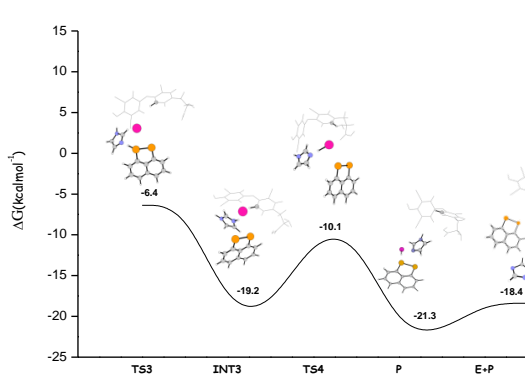
I	-1.2542314	0.3401864	8.0873753
I	1.4340564	0.2950119	2.5945955
H	-3.3844573	1.3605512	6.0201162
H	-1.4634015	1.3836046	2.1677135
H	1.6201267	-0.2036487	5.1326209
S	3.7767868	0.0292021	-2.2241824

EP(SS): E(B3LYP/D3) = -3523.170250
 Gas-phase zero-point energy = -3522.715085
 Gas-phase free energy = -3522.804034

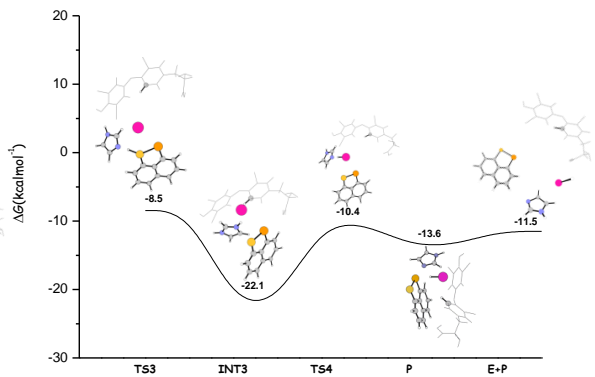
C	3.8917327	-2.5930899	1.7747039
C	3.5315117	-1.3688668	1.1430695
C	3.1069199	-1.4190596	-0.2196144
C	3.0662079	-2.6593826	-0.9132164
C	3.4195241	-3.8370184	-0.2756336
C	3.8317786	-3.7858218	1.0797953
H	4.2138524	-2.5754294	2.8188562
H	3.3839703	-4.7932618	-0.8021064
H	4.1062342	-4.7189633	1.5789481
C	3.5667334	-0.0971587	1.7804891
C	3.2013824	1.0449150	1.0928443
C	2.7727892	1.0007425	-0.2577477
C	2.7248533	-0.2281742	-0.8929318
H	3.8894712	-0.0377186	2.8231351
H	3.2388663	2.0150630	1.5957854
H	2.4712482	1.9012064	-0.7950775
H	0.1555871	-0.9184382	-1.7431836
I	-1.2049998	-1.3673494	-0.8823478
H	-2.8458202	-4.0163902	-0.7603693
C	-3.9526880	-7.2260305	-1.2058633
C	-3.0650564	-6.1474861	-1.0554891
C	-3.5400051	-4.8507639	-0.8777524
C	-4.9184177	-4.6009181	-0.8502212
C	-5.8142404	-5.6701692	-0.9989925
C	-5.3316500	-6.9725304	-1.1662056
C	-3.4430871	-8.6428001	-1.3437432
C	-3.2259425	-9.3476691	0.0237638
C	-2.1316263	-8.6270551	0.8413857
N	-4.4784681	-9.4657402	0.7384292
O	-5.4070351	-3.3401659	-0.6218563
O	-2.3299089	-8.1219300	1.9102721
O	-0.9019627	-8.5701209	0.2707018
H	-1.9862622	-6.3235871	-1.0612255
H	-6.0332544	-7.8028639	-1.2653946
H	-2.5037180	-8.6418988	-1.9218765
H	-4.1634085	-9.2540382	-1.9071631
H	-2.8490110	-10.3658948	-0.1925986
H	-4.7498516	-8.5419150	1.0821226
H	-4.3416243	-10.0254684	1.5804678
H	-0.8931587	-9.0467951	-0.5716673
C	-0.7140627	2.5783762	-4.0714323
C	0.6468324	2.5458649	-3.8571916
C	-0.2716181	2.1560112	-1.9521502
N	-1.2831459	2.3330097	-2.8416827
H	-2.2788333	2.2150217	-2.6651403
H	-1.3108870	2.7608650	-4.9618407
H	1.4469079	2.6938223	-4.5815618
H	-0.4479388	1.9172193	-0.9038443
N	0.9073471	2.2801226	-2.5336913
I	-7.9091470	-5.3080025	-0.9791163
C	-4.9976035	-2.2802799	-1.3869221

C	-5.0327396	-1.0175981	-0.7863632
C	-4.6718387	0.1071883	-1.5250877
C	-4.2617173	0.0078881	-2.8681945
C	-4.2336314	-1.2795913	-3.4353635
C	-4.6034632	-2.4180992	-2.7208146
O	-3.9019378	1.1302182	-3.5348694
I	-4.6565364	2.0102735	-0.5768983
I	-3.5549933	-1.4956435	-5.4504501
H	-5.3371786	-0.9416160	0.2575911
H	-4.5746532	-3.4035428	-3.1850256
H	-3.6467527	0.8968014	-4.4446422
S	2.1262441	-0.4568263	-2.5624994
S	2.5806994	-2.5613527	-2.6178474

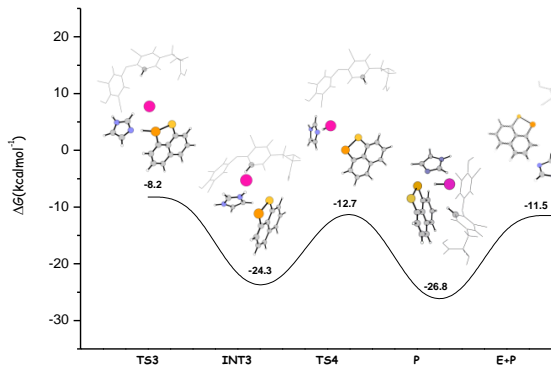
a)



b)



c)



d)

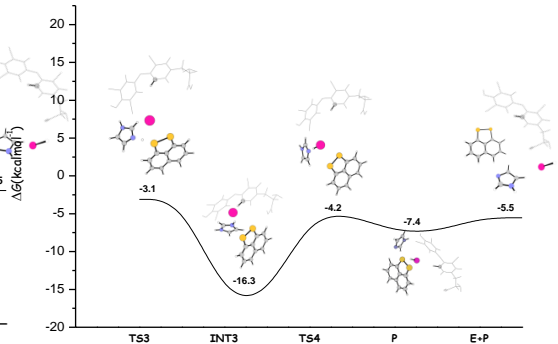


Figure S33. Calculated B3LYP-D3 free energy alternative two-steps deprotonation/protonation profile for naphthyl-based compounds **a) SeSe**, **b) SeS**, **c) SSe** and **d) SS**. Energies are in kcal mol⁻¹ and relative to reactants asymptote.

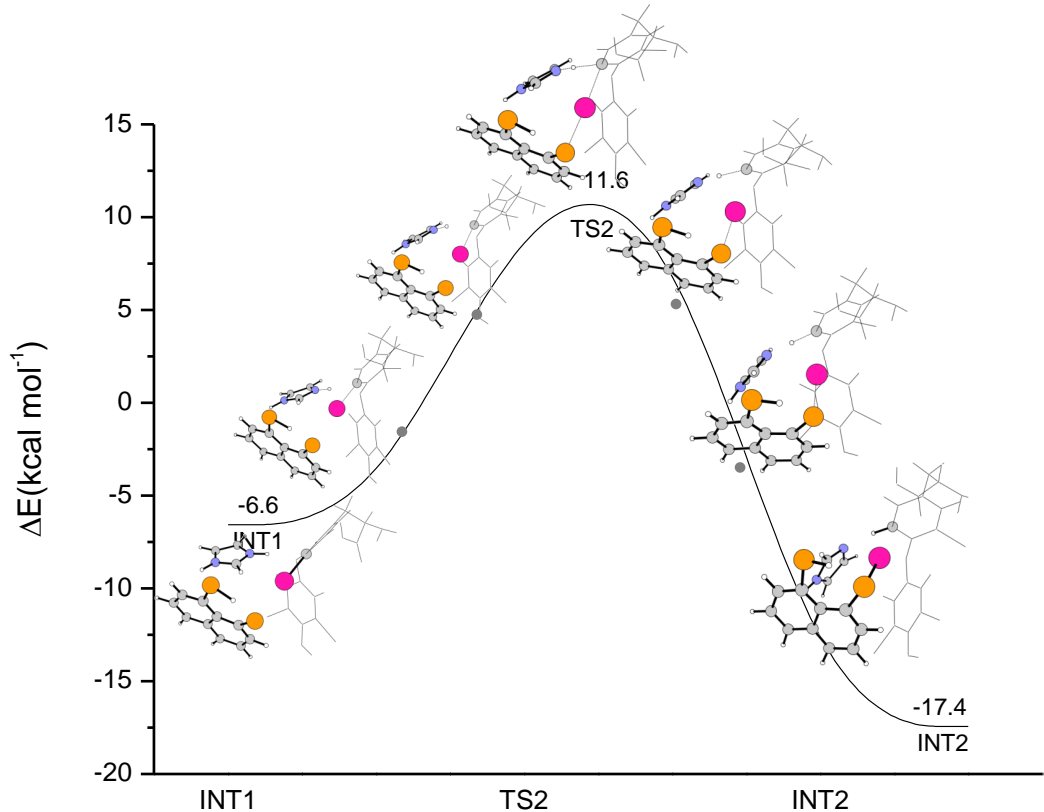


Figure S34. IRC path of TS2 for SeSe naphthyl-based compound. Energies are in kcal mol^{-1} and relative to reactants' asymptote.

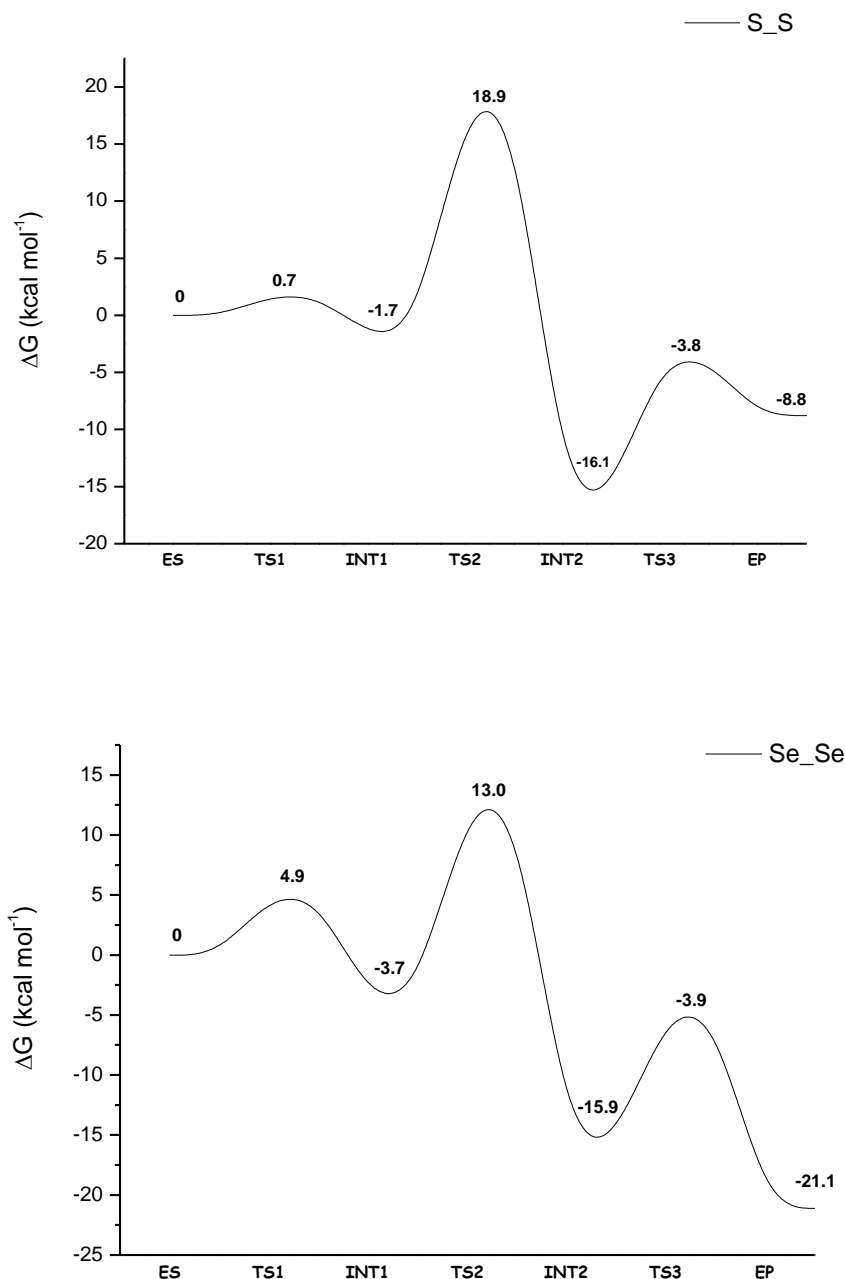


Figure S34. Calculated B3LYP-D3 free energy profile for inner ring deiodination of thyroxine by naphthyl-based compound (**2**) and (**3**) in diethylether as a less polar solvent. Energies are in kcal mol⁻¹ and relative to reactants asymptote.

Computational Details

Molecular geometry optimizations were carried out without symmetry constraints at the density functional level of theory, by using TURBOMOLE code^[1,2]. For this purpose, the exchange correlation functional, belonging to the pure hybrid Becke semiempirical three-parameter gradient corrected (B3LYP)^[3-5] was employed. The dispersion corrections were taken into account using the corresponding Grimme D3-parametrized XC functional^[6,7] denoted here by a “·D3” suffix. The SVP split-valence basis set of Ahlrichs et al.,^[1,2] which includes polarization functions, was used on C, N, O, H, S, Se. For iodine, a scalar relativistic effective core potential (ECP) was used for the description of the 46 innermost electrons with the def2-SV(P) associated basis set.^[1,2] Final energies were evaluated by performing single-point calculations on the optimized geometries employing the same B3LYP-D3 functional together the SVP split-valence basis set on C, N, O and H and more extended Dunning double-zeta basis sets aug-cc-pVQZ,^[1,2] including diffuse functions, on Se, S and I. All of the reported structures represent genuine minima or transition states on the respective potential energy surfaces, as confirmed by analysis of the corresponding Hessian matrices. The influence of solvent effects on the energetics of the process was estimated using the COSMO (conductor-like screening model) approach,^[8] where the solute molecule is embedded within a dielectric of permittivity ϵ , that represents the solvent, that is water in the present case. Single-point calculations on all stationary points structures obtained from vacuum calculations by using the same B3LYP-D3 computational approach were performed. Reaction Gibbs free energies in solution, ΔG_{sol} , were calculated for each process as the sum of two contributions: a gas-phase reaction free energy, ΔG_{gas} , and a solvation reaction free energy term calculated with the conductor-like approach, ΔG_{solv} . NBO and electrostatic potential calculations were performed for some key species using the Gaussian 09 suite of quantum chemical programs^[9], whereas the electrostatic potential maps were visualized with the GaussView 5.0

- [1] R. Ahlrichs, *TURBOMOLE* (v.5.6), Universitat Karlsruhe, **2003**.
- [2] R. Ahlrichs, M. Bar, M. Haser, H. Horn, C. Kolmel, *Chem. Phys. Lett.* **989**, 162, 165-169.
- [3] A. D. Becke, *J. Chem. Phys.* **1993**, 98, 5648-5652.
- [4] R. G. Parr, W. Yang, *Density Functional Theory of Atoms and Molecules*; Oxford University Press: Oxford, U.K., **1989**.
- [5] C. T. Lee, W. Yang, R. G. Parr, *Phys. Rev. B: Condens. Matter* **1988**, 37, 785-789.
- [6] S. Grimme, *J. Comput. Chem.*, **2004**, 25, 1463-1473.
- [7] S. Grimme, J. Antony, S. Ehrlich, H. Krieg, *J. Chem. Phys.*, **2010**, 132, 154104.
- [8] A. Klamt, G. Schüürmann, *J. Chem. Soc. Perkin Trans. 2*, **1993**, 5, 799-805.
- [9] Gaussian 09, Revision D.01, M. J. Frisch, G. W. Trucks, H. B. Schlegel, G. E. Scuseria, M. A. Robb, J. R. Cheeseman, G. Scalmani, V. Barone, B. Mennucci, G. A. Petersson, H. Nakatsuji, M. Caricato, X. Li, H. P. Hratchian, A. F. Izmaylov, J. Bloino, G. Zheng, J. L. Sonnenberg, M. Hada, M. Ehara, K. Toyota, R. Fukuda, J. Hasegawa, M. Ishida, T. Nakajima, Y. Honda, O. Kitao, H. Nakai, T. Vreven, J. A. Montgomery, Jr., J. E. Peralta, F. Ogliaro, M. Bearpark, J. J. Heyd, E. Brothers, K. N. Kudin, V. N. Staroverov, R. Kobayashi, J. Normand, K. Ragahavachari, A. Rendell, J. C. Burant, S. S. Iyengar, J. Tomasi, M. Cossi, N. Rega, J. M. Millam, M. Klene, J. E. Knox, J. B. Cross, V. Bakken, C. Adamo, J. Jaramillo, R. Gomperts, R. E. Stratmann, O. Yazyev, A. J. Austin, R. Cammi, C. Pomelli, J. W. Ochterski, R. L. Martin, K. Morokuma, V. G. Zakrzewski, G. A. Voth, P. Salvador, J. J. Dannenberg, S. Dapprich, A. D. Daniels, Ö. Farkas, J. B. Foresman, J. V. Ortiz, J. Cioslowski, and D. J. Fox, Gaussian, Inc., Wallingford CT, **2009**.

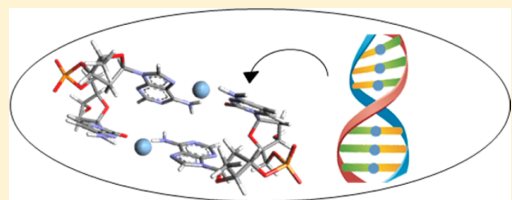
Theoretical Study of Silver-Ion-Mediated Base Pairs: The Case of C–Ag–C and C–Ag–A Systems

Mariagrazia Fortino, Tiziana Marino,* and Nino Russo*

Dipartimento di Chimica e Tecnologie Chimiche, Università della Calabria, 87036 Rende, Italy

Supporting Information

ABSTRACT: Silver-mediated base pairs applied to DNA represent a new biomacromolecular nanomaterial useful for generating nanodevices as ion sensors. Reported herein is a full quantum chemical study devoted to give further knowledge on the electronic and energetic properties of C–Ag–C and mixed C–Ag–A mismatched base pairs. The B3LYP functional in conjunction with the dispersion effects (D3) has been applied. Single-point calculations have been also performed by using the M06-L functional. The investigation of their behavior has been extended to the duplex DNA modeled by the (dC–Ag–dC)₂ and (dC–Ag–dA)₂ more complex systems. The solvent effect has been taken into account by the conductor-like screening model, COSMO. In the case of mixed C–Ag–A and (dC–Ag–dA)₂ systems, both the Watson–Crick and Hoogsteen arrangements have been taken into account. Results show that for (dC–Ag–dA)₂ systems, the binding energies are almost double that of the corresponding values of C–Ag–A ones.



INTRODUCTION

In the past decade, interest in DNA duplexes containing metal-mediated natural mismatch base pairs has considerably grown due to their potential use in the development of new materials, (e.g., DNAzymes, logic gates, metal DNA wires, sensors able to detect different metal ions in aqueous environment, nanomaterials containing metals).^{1–6} The basic idea into building up this kind of system is to replace the hydrogen atoms responsible for the H-bond in natural DNA with a metal ion having, possibly, coordination properties such to retain the DNA duplex structure. The presence of the metal ion often does not allow the formation of interbase hydrogen bonds (H-bonds) essentially due to noncomplementarity,⁵ while in the Hoogsteen arrangement, the involvement of H-bonds has been observed.⁵ Starting from the pioneering work of Tanaka and Shionoya in 1999,⁷ numerous metal-mediated base pairs containing different metal ions, natural and artificial bases, and organic ligands have been synthesized and characterized.^{4,5,8–21} Very recently, the Ono and Urata groups in a series of articles have reported that silver and mercury ions specifically stabilize the thymine-thymine (T-T) and cytosine-cytosine (C-C) mismatches in oligodeoxynucleotide (ODN) duplexes through the formation of the T-Hg-T, C-Ag-C, and C-Ag-A base pairs.^{3,4,6,7,22,23}

Here, we report a theoretical analysis on the C–Ag–C and C–Ag–A systems for which a series of experimental data are available.^{4,8–10} Hoogsteen (H) geometries and energies compared to that corresponding Watson–Crick (WC) have been studied. In addition, we have considered the relative duplex forms (dC–Ag–dC)₂ and (dC–Ag–dA)₂.

COMPUTATIONAL METHOD

All the computations have been performed at the density functional theory level by using the long-range corrected hybrid B3LYP-D3 exchange–correlation potential^{24,25} as implemented in TURBOMOLE code.^{26,27} The choice to use dispersion-corrected density functional theory represents an accurate method to overcome the London dispersion problem of DFT that in these molecular systems plays a crucial role.^{24,25} Aug-cc-pVDZ orbital basis sets have been employed for all atoms excepts for Ag, for which the Stuttgart pseudopotential (SDD) (including 28 core electrons) with the optimized valence basis set has been considered.²⁸ Full structure optimizations have been performed without geometrical constraints. The vibrational analysis has been carried out at the same level of theory in order to verify the minimum nature of the optimized structures as well as to compute the zero-point energy corrections.

The solvent effects have been considered by using the conductor-like screening model (COSMO)²⁹ as a continuum solvation model, on every examined system.

The Gibbs free energy has been obtained fixing the temperature at 298 K. The binding energies (BEs) have been computed following the equation $BE = G_{\text{complex}} - \sum G_{\text{monomer}}$.

NBO analysis³⁰ as implemented in the Gaussian03 code³¹ has been performed by using the same basis set.

Special Issue: Jacopo Tomasi Festschrift

Received: September 24, 2014

Revised: November 19, 2014

Published: November 20, 2014



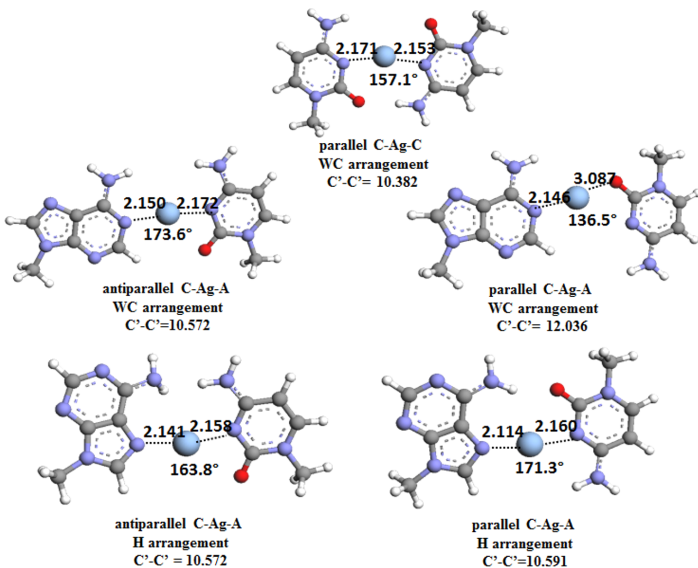


Figure 1. Optimized geometries of C–Ag–C and C–Ag–A monomers; distances are in Å, and angles are in degrees.

Because the calculation of BEs is subject to basis set superposition error (BSSE) when a finite basis set is used,³² the counterpoise (CP) approach as implemented in the Gaussian03 code has been applied for calculating the BSSE by performing all of the calculations using the mixed basis sets, through introducing “ghost” atoms.

As carried out on similar systems,³³ the influence of another functional, M06-L,³⁴ on the energetic values has been taken into account by means of single-point energy calculations performed on the previously optimized geometries.

The Cartesian coordinates of all of the optimized species are given in the Supporting Information.

RESULTS AND DISCUSSION

In the first part of the work, we have considered the silver cation interacting with two naturally occurring cytosine and adenine nucleobases, generating mismatched base pairs (C–Ag–C, C–Ag–A) in the WC and Hoogsteen-like (H) arrangements and considering both the cis (antiparallel) and trans (parallel) conformations. The optimized structures are shown in Figure 1 along with the main geometrical parameters. Relative energy values and BEs, obtained in aqueous solution, for the investigated C–Ag–C and C–Ag–A systems are collected in Table 1. The C–Ag–C mismatched pair has been recently studied experimentally⁴ owing to the fact that the C base selectively captures the Ag(I) ion in aqueous solution for generating the C–Ag–C base pair in the DNA duplex. In this system, only the WC coupling in both the trans and cis geometries is possible. Our computations show that the cis form collapses during the geometry optimization procedure into the trans one. In this last conformation, the vibrational analysis confirms the minimum nature of the obtained structure characterized by the Ag(I) linked to the N3 nitrogens of the bases by almost linear coordination geometries, as can be evinced by the valence angle value (157.1°). The two Ag(I)–N3' distances have about the same value (2.153 versus 2.171 Å), and the presence of a H-bond of 2.125 Å between N–H

Table 1. Relative Energy Values ($\Delta\Delta G$) and BEs in Water for the Investigated Base Pair Complexes

	H_2O phase				
	$\Delta\Delta G$	BE _{B3LYP-D3}	BE _{M06L}	BE _{B3LYP-D3/BSSE}	BE _{M06L/BSSE}
C–Ag–C					
trans		35.1	32.6	34.0	31.5
C–Ag–A					
WC					
cis	2.9	35.1	34.8	34.1	33.8
trans	6.0	30.7	30.2	29.8	29.3
Hoogsteen					
cis	23.0	38.0	36.5	36.8	35.2
trans	0.0	41.3	39.4	40.0	38.1

and C–O groups of the two bases contributes to stabilize the system for which the computed BE is 34.0 and 31.5 kcal/mol at B3LYP-D3 and M06L, respectively (Table 1). This value is lower than the BE previously found (42.9 kcal/mol), at almost the same level of theory (B3LYP-D3) but in a gas-phase environment, for the GC naturally occurring nucleobases that incorporate the silver ion.³⁵ The formation of this kind of WC structure has been observed experimentally also in the case of a silver ion interacting with artificial pyridine and imidazole.^{36–38}

As far as the (dC–Ag–dC)₂ complex is concerned, the optimized structure depicted in Figure 2 shows a planar geometry on the upper base pair fragment, characterized by Ag–N distances of 2.169 and 2.147 Å with two H-bonds involving the C=O and H₂N groups equal to 3.062 and 3.497 Å. In the lower base pair, the distances between the silver ion and the cytosine nitrogens are slightly larger than the corresponding values in the upper base pair (2.204 and 2.194 Å). This layer shows a significant deviation from the planarity, as evidenced by the value of the propeller twist angle of 78.3° and by the loss of one H-bond (4.619 Å). The Ag–Ag interlayer length is 3.921 Å and falls in the range of values proposed experimentally on similar systems (~4 Å).³⁹ The

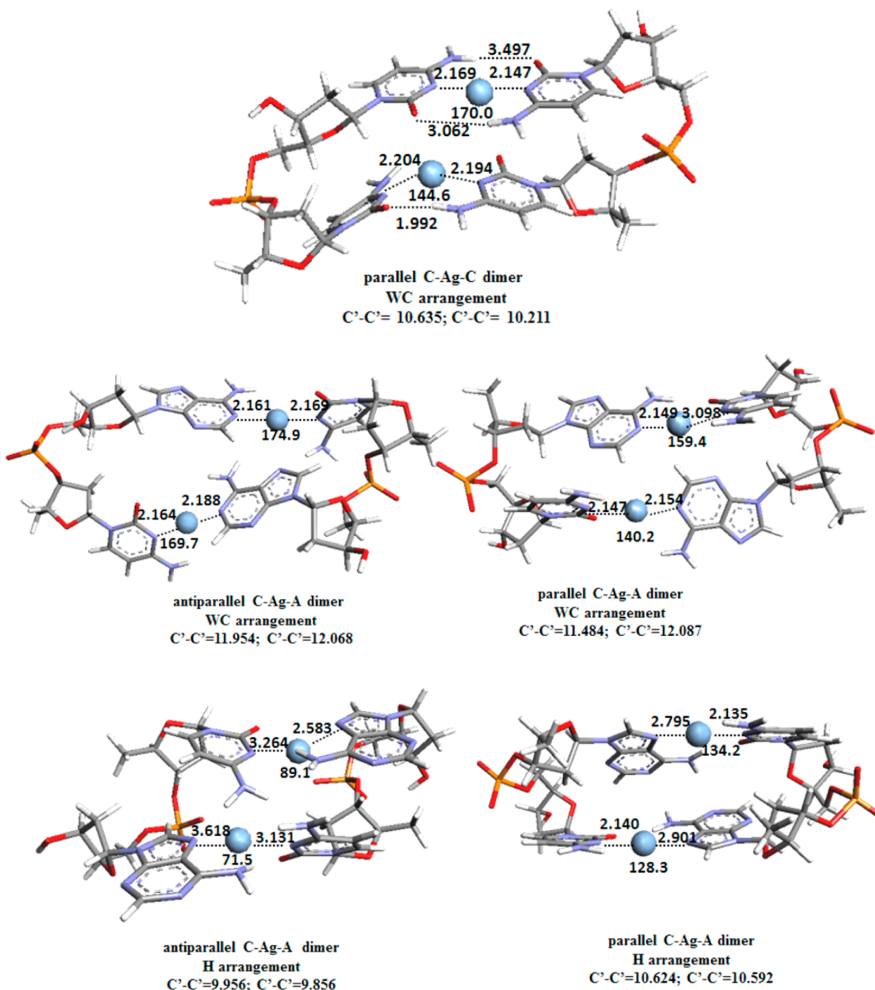


Figure 2. Optimized geometries of $(dC\text{--Ag--}dC)_2$ and $(dC\text{--Ag--}dA)_2$. Distances are in Å, and angles are in degrees.

computed BE (BE = 73.0 and 66.3 kcal/mol at B3LYP-D3 and M06L, respectively) is slightly higher than that obtained by addition of the BE found for the C–Ag–C species at both the B3LYP-D3 (68.0 kcal/mol) and M06L (63.0 kcal/mol) levels of theory and accounts for different factors, including the constraints of the phosphate and the sugar ring linkages and the $\text{Ag}^+–\text{Ag}^+$ and cytosine ring $\pi–\pi$ interactions other than the electrophilicity of the metal center.

Natural bond order (NBO) analysis shows that the positive charge is located on the silver cation with a value of about 0.71 lel for the C–Ag–C system and 0.76 and 0.72 lel for the two Ag^+ ions in the $(dC\text{--Ag--}dC)_2$ complex. The negative charge assumes almost the same value as the positive ones and is concentrated on the N3 nitrogen atoms. In the C–Ag–C system, the nitrogen reaches a net charge of –0.73 lel, while that involved in the two interactions present in the $(dC\text{--Ag--}dC)_2$ have net charges of –0.74 and –0.75 lel, respectively. Second-order perturbation analysis always indicates that the bond is electrostatic in nature.

In the C–Ag–A model system, the WC and Hoogsteen couplings in both the parallel (trans) and antiparallel (cis) arrangements are possible. Relative energies reported in Table 1 show that these four isomers are very close in energy, with the trans-Hoogsteen and the cis-Hoogsteen species being the absolute minimum and the low-lying one, respectively. In the most stable isomer, the BEs are 40.0 (B3LYP-D3) and 38.1 kcal/mol (M06L), and the Ag–N distances are 2.160 and 2.114 Å for cytosine and adenine, respectively. Only one H-bond between the cytosine C=O group and the adenine NH₂ one (2.033 Å) contributes to stabilize this structure. The two WC arrangements are less stable in energy also because of the lack of any kind of H-bonds (see Figure 1). The obtained value in the antiparallel arrangement in the WC base pair (34.1 kcal/mol at B3LYP-D3 level) is slightly higher than the BE previously calculated (42.9 kcal/mol), at almost the same level of theory, for the naturally occurring G–Ag–C system.³⁵ Also in this case, the previous computed value does not take into account the solvent effect. If we compare the present gas-phase

value of 42.4 kcal/mol (B3LYP-D3) with the value reported in ref 35, we note that the substitution of G with an adenine does not affect significantly the BE value. M06-L values propose a stability trend similar to that obtained at B3LYP-D3.

The corresponding $(dC-Ag-dA)_2$ system also prefers the Hoogsteen-type coupling over the WC one, with the trans isomer more stable than the cis one by only 1.2 kcal/mol. The WC base pair structures appear very different from the corresponding Hoogsteen ones. In fact, in the former, the two base pairs interacting with the Ag ion lie in two perpendicular planes, and the Ag–Ag distances are 5.040 and 7.180 Å for the trans and cis positions, respectively. In the Hoogsteen arrangement, the Ag ion lies at the center of a planar layer, and the distances between the metal ions are 5.180 (cis form) and 3.911 Å (trans form). In the cis conformer, the structure presents an interaction between the silver cation and the oxygen atom of the phosphate moiety (2.108 Å) that is absent in the trans arrangement, making the trans arrangement a structure more similar to that of regular DNA. The presence of the sugar and phosphate moieties imposes a constraint such that the driving force during the optimization procedure is represented by the metal–base pair attractions and by the ion–ion distance that minimizes the effect of the plane's distortion.

From the examination of the BEs (Table 2) emerges that B3LYP-D3 proposes the $(dC-Ag-dA)_2$ Hoogsteen pair in the

been studied by means of density functional theory, including the long-range interactions. Results show that in the mixed C–Ag–A and $(dC-Ag-dA)_2$ systems, the Hoogsteen arrangement is preferred over the WC ones at the B3LYP-D3 level of theory; the BE of the $(dC-Ag-dC)_2$ and $(dC-Ag-dA)_2$ is about two times that of the corresponding C–Ag–C and C–Ag–A monomers, showing the additivity of the BE; and natural bond analysis indicates that in all cases the nature of the metal–ligand interactions are prevalently electrostatic in nature.

■ ASSOCIATED CONTENT

S Supporting Information

The Cartesian coordinates of all of the optimized geometries of the investigated species are given. This material is available free of charge via the Internet at <http://pubs.acs.org>.

■ AUTHOR INFORMATION

Corresponding Authors

*E-mail: nrusso@unical.it (N.R.).

*E-mail: tmarino@unical.it (T.M.).

Author Contributions

The manuscript was written through contributions of all authors. All authors have given approval to the final version of the manuscript.

Notes

The authors declare no competing financial interest.

■ ACKNOWLEDGMENTS

This work was supported by Dipartimento di Chimica e Tecnologie Chimiche, Università della Calabria.

■ ABBREVIATIONS

BE, binding energy; COSMO, conductor-like screening model; BSSE, basis set superposition error

■ REFERENCES

- Torigoe, H.; Ono, A.; Kozasa, T. Hg^{II} Ion Specifically Binds with T:T Mismatched Base Pair in Duplex DNA. *Chem.—Eur. J.* **2010**, *16*, 13218–13225.
- Ono, A.; Togashi, H. Highly Selective Oligonucleotide-Based Sensor for Mercury(II) in Aqueous Solutions. *Chem. Int. Ed.* **2004**, *43*, 4300–4302.
- Ono, A.; Torigoe, H.; Tanaka, Y.; Okamoto, I. Binding of Metal Ions by Pyrimidine Base Pairs in DNA Duplexes. *Chem. Soc. Rev.* **2011**, *40*, 5855–5866.
- Ono, A.; Cao, S.; Togashi, H.; Tashiro, M.; Fujimoto, T.; Machinami, T.; Oda, S.; Miyake, Y.; Okamoto, I.; Tanaka, Y. Specific Interactions between Silver (I) Ions and Cytosine-Cytosine Pairs in DNA Duplexes. *Chem. Commun.* **2008**, 4825–4827.
- Takezawa, Y.; Shionoya, M. Metal-Mediated DNA Base Pairing: Alternatives to Hydrogen-Bonded Watson–Crick Base Pairs. *Chem. Res.* **2012**, *45*, 2066–2076.
- Krishnan, Y.; Simmel, F. C. Nucleic Acid Based Molecular Devices. *Chem. Int. Ed.* **2011**, *50*, 3124–3156.
- Kanaka, K.; Shionoya, M. Efficient Incorporation of a Copper Hydroxypyridone Base Pair in DNA. *J. Org. Chem.* **1999**, *64*, 5002–5003.
- Torigoe, H.; Okamoto, I.; Dairaku, T.; Tanaka, Y.; Ono, A.; Kozasa, T. Thermodynamic and Structural Properties of the Specific Binding between Ag^+ Ion and C:C Mismatched Base Pair in Duplex DNA to form C–Ag–C Metal-Mediated Base Pair. *Biochimie* **2012**, *94*, 2431–2440.
- Funai, T.; Miyazaki, Y.; Aotoni, M.; Yamaguchi, E.; Nakagawa, O.; Wada, S.; Torigoe, H.; Ono, A.; Urata, H. AgI Ion Mediated

Table 2. Relative Energy Values ($\Delta\Delta G$) and BEs in Water for the $(dC-Ag-dC)_2$ and $(dC-Ag-dA)_2$ Complexes

H_2O phase					
$\Delta\Delta G$	BE _{B3LYP-D3}	BE _{M06L}	BE _{B3LYP-D3/BSSE}	BE _{M06L/BSSE}	
$(dC-Ag-dC)_2$					
trans	75.6	68.9	73.0	66.3	
$(dC-Ag-dA)_2$					
WC					
cis	11.2	65.8	60.2	63.5	57.8
trans	10.7	75.0	70.6	72.6	68.2
Hoogsteen					
cis	1.2	80.2	67.1	74.9	61.8
trans	0.0	78.0	58.3	72.6	53.0

antiparallel arrangement as the system having the highest BE, while M06-L suggests the $(dC-Ag-dA)_2$ WC pair in the parallel conformation. Although this result is different, both functionals provide, as favored, the molecular system having similar geometry as far as the Ag^+-Ag^+ distance is concerned (about 5 Å), which represents a “measure” of the metallophilic attraction typically found in the nucleic acids complexed with metal ions.^{2,33}

For both Hoogsteen and WC arrangements, NBO analysis indicates that the concentration of the net positive charge is on the silver cation (about 0.7 lel) and that the negative one is on the nitrogen atoms (about -0.7 lel). The charge on the two silver cations in $(dC-Ag-dA)_2$ has almost the same values (0.85 versus 0.86 lel in the most stable Hoogsteen trans isomer). As observed in the previously examined cases, from the NBO analysis also in these systems, no evidence for the presence of a covalent bond between the metal ions and the nitrogen atoms occurs.

■ CONCLUSIONS

The structures of silver-mediated natural mismatch base pairs C–Ag–C, C–Ag–A, $(dC-Ag-dC)_2$, and $(dC-Ag-dA)_2$ have

- Formation of C–A Mispair by DNA Polymerases. *Ang. Chem., Int. Ed.* **2012**, *51*, 6464–6466.
- (10) Urata, H.; Yamaguchi, E.; Nakamura, Y.; Wada, S. I. Pyrimidine–Pyrimidine Base Pairs Stabilized by Silver (I) Ions. *Chem. Commun.* **2011**, *47*, 941–943.
 - (11) Clever, G. H.; Kaul, C.; Carell, T. DNA–Metal Base Pairs. *Angew. Chem.* **2007**, *119*, 6340–6350; *Angew. Chem., Int. Ed.* **2007**, *46*, 6226–6236.
 - (12) Tanaka, K.; Tengeiji, A.; Kato, T.; Toyama, N.; Sionoya, M. A Discrete Self-Assembled Metal Array Inartificial DNA. *Science* **2003**, *299*, 1212–1213.
 - (13) Clever, G. H.; Carell, T. Controlled Stacking of 10 Transition-Metal Ions Inside a DNA Duplex. *Angew. Chem., Int. Ed.* **2007**, *119*, 254; *Angew. Chem., Int. Ed.* **2007**, *46*, 250–253.
 - (14) Switzer, C.; Sinha, S.; Kim, P. H.; Heuberger, B. D. A Purine-Like Nickel (II) Base Pair for DNA. *Angew. Chem.* **2005**, *117*, 1553; *Angew. Chem., Int. Ed.* **2005**, *44*, 1529–1532.
 - (15) Meggers, E.; Holland, P. L.; Tolman, W. B.; Romesberg, F. E.; Schultz, P. G. A Novel Copper-Mediated DNA Base Pair. *J. Am. Chem. Soc.* **2000**, *122*, 10714–10715.
 - (16) Johansen, S.; Megger, N.; Böhme, D.; Sigel, R. K. O.; Müller, J. Solution Structure of a DNA Double Helix with Consecutive Metal-Mediated Base Pairs. *Nat. Chem.* **2010**, *2*, 229–234.
 - (17) Megger, D. A.; Megger, N.; Müller, J. Metal-Mediated Base Pairs in Nucleic Acids with Purine- and Pyrimidine-Derived Nucleosides. *Metal Ions Life Sci.* **2012**, *10*, 295–317.
 - (18) Petrovec, K.; Ravoo, B. J.; Müller, J. Cooperative Formation of Silver (I)-Mediated Base Pairs. *Chem. Commun.* **2012**, *48*, 11844–11846.
 - (19) Šponer, J.; Šponer, J. E.; Gorb, L.; Leszczynski, J.; Lippert, B. Metal-Stabilized Rare Tautomers and Mispairs of DNA Bases: N6-Metalated Adenine and N4-Metalated Cytosine, Theoretical and Experimental Views. *J. Phys. Chem. A* **1999**, *103*, 11406–11413.
 - (20) Hobza, P.; Šponer, J. Structure, Energetics, and Dynamics of the Nucleic Acid Base Pairs: Nonempirical Ab Initio Calculations. *Chem. Rev.* **1999**, *99*, 3247–3276.
 - (21) Benda, L.; Straka, M.; Sychrovský, V.; Bour, P.; Tanaka, Y. Detection of Mercury–TpT Dinucleotide Binding by Raman Spectra: A Computational Study. *J. Phys. Chem. A* **2012**, *116*, 8313–8320.
 - (22) Miyake, Y.; Togashi, H.; Tashiro, M.; Yamaguchi, H.; Oda, S.; Kudo, M.; Tanaka, Y.; Kondo, Y.; Sawa, R.; Fujimoto, T.; et al. Mercury^{II}-Mediated Formation of Thymine–Hg^{II}–Thymine Base Pairs in DNA Duplexes. *J. Am. Chem. Soc.* **2006**, *128*, 2172–2173.
 - (23) Tanaka, Y.; Oda, S.; Yamaguchi, H.; Kondo, Y.; Kojima, C.; Ono, A. ¹⁵N–¹⁵N J-Coupling across Hg^{II}. Direct Observation of Hg^{II}-Mediated T-T Base Pairs in a DNA Duplex. *J. Am. Chem. Soc.* **2007**, *129*, 244–245.
 - (24) Grimme, S. Accurate Description of a Van Der Waals Complexes by Density Functional Theory including Empirical Corrections. *J. Comput. Chem.* **2004**, *25*, 1463–1473.
 - (25) Grimme, S.; Antony, J.; Ehrlich, S.; Krieg, H. A Consistent and Accurate Ab Initio Parametrization of Density Functional Dispersion Correction (DFT-D) for the 94 Elements H–Pu. *J. Chem. Phys.* **2010**, *132*, 154104.
 - (26) Ahlrichs, R. *TURBOMOLE*, v. 5.6; Universitat Karlsruhe: Karlsruhe, Germany, 2003.
 - (27) Ahlrichs, R.; Bar, M.; Haser, M.; Horn, H.; Kolmel, C. Electronic Structure Calculations on Workstation Computers: The Program System Turbomole. *Chem. Phys. Lett.* **1989**, *162*, 165–169.
 - (28) Figgen, D.; Rauhut, G.; Dolg, M.; Stoll, H. Energy-Consistent Pseudopotentials for Group 11 and 12 Atoms Adjustment to Multi-Configuration Dirac–Hartree–Fock Data. *Chem. Phys.* **2005**, *311*, 227–244.
 - (29) Klamt, A.; Schüürmann, G. COSMO: A New Approach to Dielectric Screening Solvents with Explicit Expressions for the Screening Energy and Its Gradient. *J. Chem. Soc., Perkin Trans. 2* **1993**, *S*, 799–805.
 - (30) Glendening E. D.; Reed, A. E.; Carpenter Weinhold, J. E. F. NBO, version 3.1; University of Wisconsin, Madison, WI, 1988.
 - (31) Frisch, M. J.; Trucks, G. W.; Schlegel, H. B.; Scuseria, G. E.; Robb, M. A.; Cheeseman, J. R.; Montgomery, J. A., Jr.; Vreven, T.; Kudin, K. N.; Burant, J. C.; et al. *Gaussian 03*; Gaussian, Inc.: Pittsburgh, PA, 2003.
 - (32) Boys, S.; Bernardi, F. The Calculation of Small Molecular Interactions by the Differences of Separate Total Energies. Some Procedures with Reduced Errors. *Mol. Phys.* **1970**, *19*, 553–566; *Mol. Phys.* **2002**, *100*, 65–73.
 - (33) Marino, T. DFT Investigation of the Mismatched Base pairs (T–Hg–T)₃, (U–Hg–U)₃, d(T–Hg–T)₂ and d(U–Hg–U)₂. *J. Mol. Model.* **2014**, *20*, 2303–2308.
 - (34) Zhao, Y.; Truhlar, D. G. A New Local Density Functional for Main-Group Thermochemistry Transition Metal Bonding, Thermochemical Kinetics, and Noncovalents Interactions. *J. Chem. Phys.* **2006**, *125*, 194101–194118.
 - (35) Marino, T.; Russo, N.; Toscano, M.; Pavelka, M. Theoretical Investigation on DNA/RNA Base Pairs Mediated by Copper, Silver and Gold Cations. *Dalton Trans.* **2012**, *41*, 1816–1823.
 - (36) Johansen, S.; Megger, N.; Böhme, D.; Sigel, R. K. O.; Müller, J. Solution Structure of a DNA Double Helix with Consecutive Metal-Mediated Base Pairs. *Nat. Chem.* **2010**, *2*, 229–234.
 - (37) Ono, T.; Saotome, Y.; Sakabe, R.; Okamoto, I.; Ono, A. Synthesis of Covalently Linked Parallel and Antiparallel DNA Duplexes, Containing the Metal-Mediated Base Pairs T–Hg(II)–T and C–Ag(I)–C. *Chem. Commun.* **2009**, *47*, 1542–1544.
 - (38) Takezawa, Y.; Tanaka, K.; Yori, M.; Tashiro, S.; Shiro, M.; Shionoya, M. Soft Metal-Mediated Base Pairing with Novel Synthetic Nucleosides Possessing an O,S-Donor Ligand. *J. Org. Chem.* **2008**, *73*, 6092–6098.
 - (39) Pyykkö, P.; Straka, M. Ab Initio Studies of the Dimers(HgH₂)₂ and (HgMe₂)₂ Metallophilic Attraction and the Van Der Waals Radii of Mercury. *Phys. Chem. Chem. Phys.* **2000**, *2*, 2489–2493.

Supporting Information

Theoretical study of silver ion-mediated base pairs: the case of C-Ag-C and C-Ag-A systems

Mariagrazia Fortino, Tiziana Marino*, Nino Russo*

Dipartimento di Chimica e Tecnologie Chimiche, Università della Calabria, 87036 Rende, Italy

Cartesian coordinates

Base pair			
C-Ag-C			
33			
C	-0.6271533	5.0561032	0.5559548
H	-0.4233654	6.1305797	0.6428618
N	-1.4688732	4.8055192	-0.6197826
C	-2.6881193	4.2137215	-0.5281351
H	-3.0126857	3.9321532	0.4738765
C	-3.4608386	3.9841877	-1.6241605
H	-4.4345116	3.5087353	-1.5335893
C	-2.9402220	4.3894832	-2.8915487
N	-3.6446684	4.1939634	-4.0132430
H	-3.2779680	4.4798386	-4.9140158
H	-4.5591457	3.7624747	-3.9876581
N	-1.7350441	4.9716530	-2.9812849
C	-0.9544359	5.2037200	-1.8643119
O	0.1497449	5.7335961	-1.9241312
H	-1.1508955	4.6992486	1.4490767
H	0.3292703	4.5302190	0.4452416
C	1.6439175	7.0883445	-9.3686672
H	1.4453823	6.0699334	-9.7256111
N	1.8816932	7.0674642	-7.9224101
C	3.0312651	7.5243977	-7.3624307
H	3.7810236	7.9102347	-8.0537893
C	3.2419024	7.5039696	-6.0173588
H	4.1713433	7.8748176	-5.5919957
C	2.1975525	6.9761167	-5.1939309
N	2.3249668	6.9195788	-3.8625674
H	1.5895867	6.5374487	-3.2645319
H	3.1713286	7.2503681	-3.4188989
N	1.0649309	6.5266094	-5.7559687
C	0.8484011	6.5462004	-7.1185849
O	-0.1843139	6.1342576	-7.6197033
H	2.5282081	7.4978958	-9.8690363

H	0.7649126	7.7065356	-9.5914025
Ag	-0.6060021	5.6792689	-4.6948820
C-Ag-A cis (WC)			
35			
C	-6.6518419	-2.5113012	-19.3230576
H	-6.4494087	-3.5433099	-19.0105940
N	-5.4354064	-1.9197466	-19.8915432
C	-5.3762878	-1.4451640	-21.1614828
H	-6.2922979	-1.5243328	-21.7476961
C	-4.2402885	-0.9001559	-21.6785265
H	-4.2151128	-0.5249874	-22.6987454
C	-3.0912637	-0.8379957	-20.8299634
N	-1.9402723	-0.3118916	-21.2720468
H	-1.1127436	-0.2416450	-20.6796011
H	-1.8700180	0.0293584	-22.2217245
N	-3.1546310	-1.3059206	-19.5746600
C	-4.3075557	-1.8653986	-19.0518329
O	-4.3545898	-2.2975103	-17.9125037
H	-7.4427207	-2.4950785	-20.0807840
H	-6.9628805	-1.9396343	-18.4396625
C	2.9511068	-2.4839020	-14.9018321
H	3.4406489	-1.7123463	-14.2939314
N	2.0808431	-1.8517629	-15.8883715
C	0.7346198	-1.9725041	-16.0143226
H	0.1425315	-2.6059730	-15.3586016
N	0.2445670	-1.2513106	-17.0146435
C	1.3422686	-0.6152313	-17.5784402
C	1.5267198	0.2944920	-18.6382036
N	0.4759633	0.8158004	-19.3830790
H	0.8058728	1.5660984	-19.9916953
H	-0.3110183	1.1299186	-18.8162018
N	2.7689327	0.6548800	-18.9555135
C	3.8008041	0.1782699	-18.2346861
H	4.7932098	0.5074263	-18.5500288
N	3.7469546	-0.6297129	-17.1740813
C	2.5012417	-0.9984351	-16.8923778
H	2.3488308	-3.1368717	-14.2607882
H	3.7209961	-3.0712286	-15.4175119
Ag	-1.6158522	-1.3947069	-18.0645364
C-Ag-A trans (WC)			
35			
C	-6.6695241	-2.7089640	-2.6050854
H	-5.9972675	-2.9374722	-3.4398730
N	-6.0580599	-1.6484016	-1.8149888
C	-6.5781588	-1.0177698	-0.6998020
H	-7.5579233	-1.2873243	-0.3102675
N	-5.7886604	-0.0997307	-0.1927264
C	-4.6897853	-0.1253367	-1.0154332
C	-3.4961826	0.6239594	-0.9960858
N	-3.2748496	1.5585885	-0.0617423
H	-2.4135365	2.0879152	-0.0244041
H	-3.9834740	1.7130628	0.6459360
N	-2.5813908	0.3576716	-1.9681705
C	-2.8565932	-0.6076832	-2.9014539
H	-2.0761978	-0.7656570	-3.6481351
N	-3.9363914	-1.3492203	-2.9925902
C	-4.8326676	-1.0775045	-2.0286471

C	3.3110138	3.9945746	-2.0318786
H	2.5011049	4.7343600	-2.0124394
N	3.0900438	3.0452352	-3.1289047
C	3.9941745	2.8751145	-4.1349159
H	4.8947724	3.4866315	-4.0809397
C	3.7748535	1.9903846	-5.1433611
H	4.5016216	1.8613102	-5.9424538
C	2.5505428	1.2470708	-5.0974619
N	2.2555247	0.3532133	-6.0519978
H	1.3846619	-0.1608764	-5.9989066
H	2.8804411	0.1763079	-6.8265767
N	1.6654270	1.4156124	-4.1105182
C	1.9124029	2.2971481	-3.1300696
O	1.1161901	2.4984785	-2.1742985
H	-7.6399469	-2.3782744	-2.9981165
H	-6.8080809	-3.6104800	-1.9931475
H	4.2725351	4.4957923	-2.1868818
H	3.3160914	3.4602364	-1.0738215
Ag	-0.7073578	1.3901153	-2.1364725
C-Ag-A cis (H)			
35			
C	-6.6518419	-2.5113012	-19.3230576
H	-6.4494087	-3.5433099	-19.0105940
N	-5.4354064	-1.9197466	-19.8915432
C	-5.3762878	-1.4451640	-21.1614828
H	-6.2922979	-1.5243328	-21.7476961
C	-4.2402885	-0.9001559	-21.6785265
H	-4.2151128	-0.5249874	-22.6987454
C	-3.0912637	-0.8379957	-20.8299634
N	-1.9402723	-0.3118916	-21.2720468
H	-1.1127436	-0.2416450	-20.6796011
H	-1.8700180	0.0293584	-22.2217245
N	-3.1546310	-1.3059206	-19.5746600
C	-4.3075557	-1.8653986	-19.0518329
O	-4.3545898	-2.2975103	-17.9125037
H	-7.4427207	-2.4950785	-20.0807840
H	-6.9628805	-1.9396343	-18.4396625
C	2.9511068	-2.4839020	-14.9018321
H	3.4406489	-1.7123463	-14.2939314
N	2.0808431	-1.8517629	-15.8883715
C	0.7346198	-1.9725041	-16.0143226
H	0.1425315	-2.6059730	-15.3586016
N	0.2445670	-1.2513106	-17.0146435
C	1.3422686	-0.6152313	-17.5784402
C	1.5267198	0.2944920	-18.6382036
N	0.4759633	0.8158004	-19.3830790
H	0.8058728	1.5660984	-19.9916953
H	-0.3110183	1.1299186	-18.8162018
N	2.7689327	0.6548800	-18.9555135
C	3.8008041	0.1782699	-18.2346861
H	4.7932098	0.5074263	-18.5500288
N	3.7469546	-0.6297129	-17.1740813
C	2.5012417	-0.9984351	-16.8923778
H	2.3488308	-3.1368717	-14.2607882
H	3.7209961	-3.0712286	-15.4175119
Ag	-1.6158522	-1.3947069	-18.0645364
C-Ag-A trans (H)			

35

C	-3.3891844	2.2014461	-2.5911165
H	-3.7584393	1.2230887	-2.9214853
N	-2.3546296	2.6564349	-3.5116791
C	-1.1188742	3.1226640	-3.2138897
H	-0.7533992	3.1942296	-2.1934131
N	-0.4322585	3.4689019	-4.2963088
C	-1.2751726	3.2120634	-5.3757032
C	-1.1802904	3.3494122	-6.7881492
N	-0.1102221	3.8187885	-7.4540026
H	-0.1795931	3.8215959	-8.4656308
H	0.8063348	3.9856156	-7.0501854
N	-2.2578792	2.9959531	-7.5132801
C	-3.3524870	2.5293596	-6.9042369
H	-4.1827355	2.2623788	-7.5628262
N	-3.5535738	2.3467983	-5.5944967
C	-2.4854638	2.7065278	-4.8891553
H	-2.9645205	2.1207837	-1.5841540
H	-4.2265711	2.9116419	-2.5889372
C	4.9894285	5.3470758	-8.2540006
H	4.2201803	5.9445860	-8.7592439
N	4.8331655	5.4655093	-6.7985744
C	5.7965091	5.9952945	-6.0022302
H	6.7055420	6.3303544	-6.5022911
C	5.6374525	6.1023709	-4.6546849
H	6.4189705	6.5298523	-4.0312442
C	4.4111867	5.6302805	-4.0963738
N	4.1906820	5.7000848	-2.7774545
H	3.3198116	5.3700822	-2.3794000
H	4.8839082	6.0886755	-2.1515509
N	3.4591968	5.1062437	-4.8842931
C	3.6248916	5.0084758	-6.2534587
O	2.7607346	4.5397165	-6.9837767
H	4.8650274	4.2988700	-8.5516853
H	5.9867252	5.7032232	-8.5326774
Ag	1.5098606	4.2943484	-4.4275555

Dimers			
C-Ag-C			
118			
P	13.0050951	7.8011363	-1.1227664
O	12.0603467	7.9355969	0.0684496
O	13.8615266	9.2190431	-1.3063107
C	13.5197861	10.4078928	-0.6488113
H	14.4526317	10.9897682	-0.5494423
H	13.1350775	10.2116140	0.3686426
C	12.5229331	11.2723885	-1.4198631
H	12.8498254	11.3550920	-2.4655755
O	11.1973910	10.6936388	-1.4244829
C	10.3061923	11.4873983	-0.6795046
H	9.6256376	12.0419967	-1.3362367
N	9.4406686	10.5932666	0.1197726
C	10.0061871	9.5867394	0.8381159
H	11.0877852	9.4316109	0.7492030
C	9.2430514	8.6687174	1.4958020
H	9.7247226	7.8437176	2.0153237
C	7.8394307	8.7391964	1.3195850
N	7.0170711	7.8202923	1.8670610
H	6.0412510	7.7868856	1.5921349
H	7.4076722	6.9901884	2.2917182
N	7.2904260	9.7160907	0.5844066
C	8.0476393	10.6979290	-0.0218981
O	7.5264747	11.6023967	-0.6681604
C	12.3418510	12.6672664	-0.8040779
H	13.2537998	13.0064975	-0.2804636
C	11.1702998	12.4347135	0.1542104
H	11.5165888	11.9350513	1.0715431
H	10.6422009	13.3564805	0.4363714
O	11.9842659	13.5504888	-1.8565554
H	11.8222017	14.4256169	-1.4737871
C	11.4022341	5.0553832	-2.0162358
H	11.0853497	4.0099573	-2.1494599
H	12.4927504	5.1363202	-2.1169495
C	10.7050624	5.9280508	-3.0419607
H	11.0162557	5.6288201	-4.0530738
O	9.2592310	5.7282909	-3.0001104
C	8.6155824	6.8258963	-2.3988826
H	7.9359100	7.3176626	-3.1077380
N	7.6979967	6.2903087	-1.3352112
C	8.1120857	5.2664016	-0.5514033
H	9.1500684	4.9682264	-0.6848455
C	7.2749980	4.6379855	0.3229588
H	7.6252927	3.8046816	0.9285599
C	5.9024070	5.0340095	0.3132342
N	4.9830015	4.3939879	1.0530303
H	3.9762490	4.5624765	0.9317424
H	5.2476759	3.5484464	1.5412107
N	5.5118078	6.0768359	-0.4365307
C	6.3831068	6.7700661	-1.2497171
O	6.0186759	7.7600140	-1.8811642
C	10.8481214	7.4641452	-2.8562178
C	9.6972500	7.7573289	-1.8771936
H	10.0148597	7.4900642	-0.8634566
H	9.3999179	8.8102556	-1.8880188

O	12.1106428	7.9617315	-2.5518513
O	13.9624635	6.6657939	-1.2789466
H	10.5848935	7.9205519	-3.8273608
P	-4.0980038	5.0975697	-0.1854337
O	-3.8177814	4.7853301	-1.6359532
O	-4.0592291	6.7770025	-0.0115737
C	-3.1631248	7.5287167	-0.8194208
H	-3.5472562	8.5575391	-0.8788624
H	-3.0887533	7.0976608	-1.8286390
C	-1.8147890	7.5363700	-0.1250976
H	-1.3840056	6.5280448	-0.1446699
O	-0.8912293	8.4260886	-0.7964650
C	0.0946868	8.6444927	0.1825161
H	0.7236421	7.7518240	0.3109542
N	1.0004267	9.6941807	-0.3050456
C	0.5339739	10.7460413	-1.0294005
H	-0.5439760	10.7543275	-1.1880729
C	1.37777620	11.6897525	-1.5318112
H	0.9988252	12.5288728	-2.1107864
C	2.7783798	11.5169196	-1.2912257
N	3.6848685	12.3764703	-1.7733417
H	4.6759517	12.2392038	-1.5876330
H	3.4051152	13.1774511	-2.3226883
N	3.2196491	10.4719809	-0.5772510
C	2.3647361	9.5531349	-0.0287703
O	2.7750286	8.6180949	0.6610109
C	-1.8785924	8.0085695	1.3605081
C	-0.6711848	8.9568757	1.4659589
H	-1.0508191	9.9886756	1.4328005
H	-0.0587086	8.8207432	2.3655037
C	-3.6263042	1.8960999	0.1308761
H	-3.5128725	0.8324212	-0.1230584
H	-4.5972559	2.0654183	0.6135200
C	-2.5181841	2.3124759	1.0691633
H	-2.5326199	1.6594211	1.9620020
O	-1.2251324	2.1032645	0.4107778
C	-0.3047682	3.0525651	0.8354218
H	0.6496972	2.5893192	1.1113835
N	0.0311844	3.9744788	-0.3187414
C	-0.8381607	4.1448713	-1.3452064
H	-1.7255885	3.5236847	-1.3509762
C	-0.6228182	5.0852954	-2.3092123
H	-1.3689956	5.2351320	-3.0848756
C	0.5293368	5.8955267	-2.1822703
N	0.8009123	6.8727747	-3.0752411
H	1.5030225	7.5609334	-2.8307867
H	0.0495941	7.1951686	-3.6716046
N	1.4051431	5.7028263	-1.1799756
C	1.1956778	4.7315956	-0.2245808
O	1.9974421	4.5426455	0.6998678
C	-2.4504587	3.7627001	1.5896654
C	-0.9703470	3.8226625	1.9893123
H	-0.5921322	4.8452327	2.1019023
H	-0.7927790	3.2739275	2.9258893
O	-2.6125952	4.7599528	0.6030778
O	-5.1982758	4.5812441	0.6810665
H	-3.1565300	3.9067757	2.4230297

Ag	3.4044002	6.5553371	-0.8165449
Ag	5.2625631	9.9307614	-0.0888224
H	-1.7510792	7.1215822	2.0053833
H	11.1788922	5.3758872	-0.9865743
H	-3.6232856	2.4892493	-0.7929196
O	-3.0489832	8.7129363	1.6955165
H	-3.7868268	8.0963600	1.5178728
C-Ag-A cis (WC)			
122			
C	2.3119400	0.4022417	35.0849010
H	1.1222152	-1.6975852	33.1311412
C	3.3479517	0.1009814	34.0094024
H	3.4204326	-0.9782481	33.8325463
O	2.8625143	0.7213928	32.7919367
C	3.9948439	1.1098908	32.0566897
H	4.4228142	0.2768809	31.4727176
N	3.5392201	2.1017890	31.0851753
C	2.7205069	3.1814879	31.3540935
H	2.3573698	3.3578850	32.3625657
N	2.4316569	3.9036520	30.2954716
C	3.0902676	3.2606725	29.2741271
C	3.1788029	3.5464376	27.8996306
N	2.5428753	4.5968325	27.3476243
H	2.7814144	4.88959470	26.4081802
H	2.1071113	5.2642206	27.9738480
N	3.9124166	2.6993169	27.1307983
C	4.5377713	1.6376825	27.7198638
H	5.1163291	1.0094460	27.0399017
N	4.5130406	1.2904532	28.9892458
C	3.7788674	2.1314027	29.7400400
C	4.7904210	0.6318028	34.2547566
H	4.8377894	1.1455251	35.2339653
C	4.9873283	1.6260856	33.1002332
H	4.6975517	2.6452714	33.3961429
H	6.0271635	1.6276549	32.7518923
O	5.7390581	-0.3889938	34.1519328
H	5.4832261	-1.0289107	34.8748134
C	-0.7240971	-4.3158836	36.0291217
H	-0.9889396	-5.3818504	36.0862860
H	-0.7158419	-3.9045620	37.0486540
C	0.6452490	-4.1384082	35.4094910
H	1.4267712	-4.5774393	36.0429848
O	0.6803669	-4.8187510	34.1067652
C	1.0979463	-3.8966531	33.1383240
H	2.1895204	-3.8983010	33.0029164
N	0.5226251	-4.2935006	31.8265808
C	-0.4910693	-5.1778896	31.7178874
H	-0.8443544	-5.5835845	32.6652210
C	-1.0027000	-5.5293106	30.4998865
H	-1.8178605	-6.2444107	30.4190905
C	-0.4077548	-4.9489709	29.3436746
N	-0.8389313	-5.2664849	28.1093131
H	-0.4261517	-4.8314884	27.2941072
H	-1.6071061	-5.9089593	27.9761776
N	0.6046780	-4.0780543	29.4589746
C	1.0948699	-3.6940823	30.6972549

O	1.9935432	-2.8721879	30.7955503
C	1.0340378	-2.6793185	35.0971697
H	0.5369091	-1.9720571	35.7785540
C	0.6239516	-2.5347631	33.6307671
H	1.3166149	0.1748742	34.6558901
O	2.4353120	-2.5343757	35.1141893
H	-0.4685376	-2.4594334	33.5108956
C	4.6974215	-1.5095166	20.4082296
H	4.3736710	-1.8822572	19.4220410
C	6.2269455	-1.6421425	20.4606917
H	6.6637470	-1.2644323	19.5311162
O	6.8136706	-0.8637738	21.5319099
C	6.7214916	-1.5878431	22.7136928
H	7.6150307	-1.3860941	23.3200595
N	5.5553934	-1.0598926	23.4902734
C	5.0200823	0.1998671	23.3303376
H	5.3611884	0.8627546	22.5401279
N	4.0550444	0.4619543	24.1933960
C	3.9501916	-0.6821059	24.9548310
C	3.1110149	-1.0234457	26.0297865
N	2.1684789	-0.1814449	26.5105842
H	1.8399795	-0.3145181	27.4618677
H	2.2153472	0.7821711	26.1954712
N	3.2576689	-2.2657623	26.5627200
C	4.2264618	-3.0946329	26.0743934
H	4.3067046	-4.0641496	26.5703556
N	5.0623342	-2.8522891	25.0872641
C	4.8847630	-1.6403024	24.5372773
C	6.6646196	-3.0643775	20.7901721
H	5.9822295	-3.8078165	20.3367390
C	6.5602426	-3.0785503	22.3329362
H	5.6005329	-3.4804174	22.6752400
H	7.3522779	-3.6903350	22.7831721
O	7.9926435	-3.2207521	20.3334945
H	8.2746016	-4.1286603	20.5180824
C	6.4681098	3.1573536	17.7914022
H	6.8327134	3.9593568	17.1336160
H	6.3827027	2.2171776	17.2315780
C	7.4230999	2.9669298	18.9473509
H	8.4139348	2.6713964	18.5602765
O	7.6356373	4.2423272	19.6515814
C	7.5473710	4.0579717	21.0296330
H	8.2660164	4.7024113	21.5489588
N	6.1550031	4.4489809	21.4884480
C	5.2067213	4.7493033	20.5552021
H	5.5886055	5.1587856	19.6248512
C	3.9012622	4.4448352	20.7461423
H	3.1688635	4.5717143	19.9554949
C	3.6055689	3.6694091	21.9060076
N	2.4959659	2.9037644	21.9413732
H	2.5214395	2.1860550	22.6646784
H	2.3296732	2.4968859	21.0011615
N	4.4574860	3.6755125	22.9429823
C	5.7726840	4.0620601	22.7749506
O	6.5928145	3.9816187	23.6861316
C	7.0432216	1.9495999	20.0451196
H	7.4106451	0.9497351	19.7830100

C	7.7712343	2.5528473	21.2473854
H	8.8518257	2.3598266	21.1710165
O	5.6544551	1.9144327	20.3659067
H	7.4196325	2.1752569	22.2102115
Ag	1.9123934	-3.0832819	28.0424798
Ag	4.1823320	3.0010585	24.9806342
H	4.2289471	-2.1382818	21.1835736
O	4.2299037	-0.2019811	20.6496688
P	4.5173168	1.0031167	19.5053080
O	3.2661553	1.8446890	19.4905182
O	5.1965284	0.3671384	18.3246747
H	2.3268292	1.4863108	35.2935064
O	2.4850632	-0.2665419	36.3131697
P	3.1488724	-1.8068892	36.4741244
O	4.6142990	-1.7525063	36.1151611
O	2.5492817	-2.4086322	37.7018896
H	5.4590662	3.4088348	18.1414937
H	-1.5000732	-3.7955196	35.4452292
C-Ag-A trans (WC)			
122			
Ag	-1.0321445	-1.2283668	-2.9528097
Ag	0.5505867	-2.3119312	1.7079171
C	7.6202354	0.8016513	2.8642897
H	7.0555561	1.4295109	2.1520723
H	8.0105759	1.4684764	3.6511842
C	6.6138806	-0.1304349	3.5253804
H	6.0203621	0.4749866	4.2390001
O	5.7317131	-0.6582774	2.5310775
C	5.1684470	-1.8484770	3.0228530
H	4.2309998	-1.6480409	3.5576666
N	4.7848216	-2.6457009	1.8384870
C	5.7641961	-3.0645165	0.9814469
C	5.4288158	-3.7302585	-0.1602736
H	6.2051250	-4.0591275	-0.8485684
C	4.0491903	-3.9667928	-0.4006894
N	3.6366630	-4.6392948	-1.5014239
H	2.6719235	-4.9435277	-1.5372363
H	4.3089632	-5.1319288	-2.0734715
N	3.0970529	-3.5255089	0.4264925
C	3.4451054	-2.8226364	1.5149018
O	2.5748219	-2.3142016	2.2843384
C	7.1603995	-1.3380392	4.3275905
H	8.1772938	-1.5754388	3.9911134
C	6.2190005	-2.4926831	3.9449413
H	6.7851297	-3.2710399	3.4240044
H	5.7536871	-2.9130076	4.8456244
O	7.1020617	-1.1027838	5.7293178
H	7.9110042	-0.6329429	5.9773844
P	8.8386594	-1.0090699	1.1318149
O	8.4422285	-2.3003802	1.8276617
O	8.7621194	0.2377613	2.2533016
C	8.0683994	2.5581964	-1.6773297
H	7.9646333	3.6073958	-1.3660441
H	9.1275841	2.3678190	-1.9049887
C	7.6094644	1.6360464	-0.5636135

H	8.2525993	1.7568115	0.3167624
O	6.2435893	1.9772573	-0.1642407
C	5.3948427	0.8876950	-0.4485914
N	4.0992496	1.4099005	-0.8962065
C	3.7215825	2.7108436	-1.1491933
H	4.4253928	3.5226912	-0.9956055
N	2.4748274	2.8234319	-1.5624830
C	2.0194635	1.5278815	-1.5883802
C	0.7800701	0.9779345	-1.9812492
N	-0.2371837	1.7434321	-2.3895474
H	-1.1699691	1.3809385	-2.6101346
H	-0.0903029	2.7460754	-2.3864303
N	0.6739642	-0.3876534	-1.9417142
C	1.7195767	-1.1359549	-1.4739341
H	1.5486325	-2.2135553	-1.4287941
N	2.8927153	-0.7043865	-1.0707617
C	3.0107482	0.6345374	-1.1688920
C	7.5286398	0.1483534	-0.9533755
H	8.3388730	-0.1398025	-1.6404863
C	6.1127228	0.0584814	-1.5149138
H	6.0183456	0.5420401	-2.4983501
H	5.7451370	-0.9722872	-1.5644536
O	7.4866847	-0.6885074	0.1828814
O	10.0722826	-0.7825095	0.3224382
H	7.4795074	2.4152501	-2.5965290
C	-8.8547962	0.5568831	-1.7652924
H	-8.4401367	-0.0385543	-0.9330710
H	-9.5884943	1.2582319	-1.3348888
C	-7.7170778	1.3937631	-2.3382696
H	-7.5184027	2.2169576	-1.6238815
O	-6.5402509	0.5866050	-2.4463412
C	-5.6930251	1.1353854	-3.4270708
H	-4.9447892	1.8008145	-2.9767818
N	-4.9168744	-0.0043700	-3.9688684
C	-5.5786875	-1.0003546	-4.6190866
C	-4.9385671	-2.1554999	-4.9652288
H	-5.4805233	-2.9435853	-5.4836383
C	-3.5909146	-2.3123307	-4.5697838
N	-2.9169259	-3.4560798	-4.8121122
H	-1.9180136	-3.4963657	-4.6542157
H	-3.3318536	-4.1711283	-5.3940696
N	-2.9508851	-1.3320926	-3.9115655
C	-3.5748520	-0.1357229	-3.6070977
O	-2.9644871	0.7721311	-3.0387545
C	-7.9376793	2.0543598	-3.7209670
H	-8.7113178	1.5055678	-4.2716822
C	-6.5865335	1.8782530	-4.4367444
H	-6.7206806	1.3031571	-5.3591605
H	-6.1674324	2.8622827	-4.6823212
O	-8.2506368	3.4352839	-3.5959431
H	-9.2121847	3.5094535	-3.5181300
P	-9.0345214	-1.3922111	-3.7454940
O	-8.3880689	-0.6506926	-4.9034128
O	-9.5988806	-0.2612853	-2.6488669
C	-9.2050368	-4.1082137	-0.1449931
H	-9.6457178	-3.8333415	0.8239242
H	-9.9929862	-4.5548593	-0.7687756

C	-8.6481910	-2.8752553	-0.8329475
H	-9.4582416	-2.1711251	-1.0565966
O	-7.7049786	-2.1856254	0.0423980
C	-6.3954149	-2.3004338	-0.4655706
N	-5.5097178	-2.6307688	0.6617432
C	-5.8626548	-3.3082635	1.8116779
H	-6.8984296	-3.5801873	1.9886767
N	-4.8514552	-3.5378983	2.6207614
C	-3.7797538	-2.9843441	1.9656780
C	-2.4173851	-2.9228040	2.3126753
N	-1.9561420	-3.4806772	3.4437909
H	-1.0046206	-3.3310047	3.7556454
H	-2.6304514	-3.8762486	4.0882358
N	-1.5821759	-2.2932699	1.4434656
C	-2.0980100	-1.7448071	0.3025607
H	-1.3709797	-1.2206386	-0.3202188
N	-3.3448235	-1.7767182	-0.1170964
C	-4.1637863	-2.4087197	0.7466226
C	-7.8353097	-3.1672864	-2.1046130
H	-8.2568434	-4.0150383	-2.6669459
C	-6.4395330	-3.4012664	-1.5324132
H	-6.3522064	-4.3899032	-1.0587540
H	-5.6584790	-3.2842168	-2.2929879
O	-7.7033145	-2.0219629	-2.9171508
O	-10.0766746	-2.4559959	-3.8579537
H	-8.4272106	-4.8674070	0.0329571
H	5.2100372	0.2887002	0.4557781
H	-6.0470800	-1.3439237	-0.8846566
H	6.8101281	-2.8258476	1.2649174
H	-6.6588328	-0.8380699	-4.8280845

C-Ag-A cis (H)

122			
P	-1.5694893	3.3693385	5.3196157
O	-1.3710482	4.4078389	6.3890005
O	-2.8164787	2.4957134	5.1578564
O	-0.2874545	2.3334235	5.2500753
C	0.8666078	2.5055904	6.0772684
H	1.2219570	1.4969656	6.3308094
H	0.5941480	3.0332678	7.0046812
C	1.9675084	3.2877842	5.3882328
H	2.7753872	3.4647890	6.1203505
O	2.5221827	2.5493211	4.2685469
C	2.5369014	3.3753172	3.1296249
H	3.4161636	3.1265878	2.5208984
N	1.3153334	3.0632882	2.3244553
C	0.5054315	1.9711067	2.5269592
H	0.7605630	1.2207288	3.2632377
N	-0.5882607	1.9765031	1.7927443
C	-0.4910239	3.1374468	1.0447324
C	-1.3284880	3.7352924	0.0800144
N	-2.5447505	3.2374576	-0.2547453
H	-2.9399715	3.5595505	-1.1312561
H	-2.8491679	2.3240118	0.0890458
N	-0.9187085	4.8786983	-0.5073520
C	0.2434899	5.4213868	-0.1146377

H	0.5242055	6.3509135	-0.6191124
N	1.0964357	4.9808627	0.8111761
C	0.6897744	3.8288794	1.3593036
C	1.5218128	4.6333094	4.7966417
H	0.5472830	4.4968498	4.3218646
C	2.5162888	4.8131723	3.6566358
H	2.2139379	5.5440561	2.8991914
H	3.5189103	5.0659852	4.0347248
O	1.4586309	5.6763756	5.7376473
H	0.6013228	5.5564213	6.1925343
C	-0.8577467	7.2665937	3.6089743
H	-0.9940883	8.3195441	3.8933150
H	0.0035889	6.8771608	4.1683963
C	-2.0949597	6.4741126	3.9581604
H	-2.1925608	6.3763427	5.0514439
O	-3.2815761	7.1600166	3.4476110
C	-4.2512950	6.2332035	3.0506780
H	-5.2302633	6.4811787	3.4753893
N	-4.4193238	6.3065320	1.5481596
C	-3.4950521	6.9072515	0.7592372
H	-2.7442548	7.4900592	1.2878036
C	-3.5155484	6.7487896	-0.5921082
H	-2.7372439	7.1766956	-1.2168602
C	-4.5234401	5.8941355	-1.1201887
N	-4.5271315	5.5488404	-2.4238095
H	-5.3341653	5.0567812	-2.8043064
H	-3.8651621	5.9672521	-3.0631793
N	-5.4857304	5.3669795	-0.3489272
C	-5.4518334	5.5553749	0.9854800
O	-6.2905005	5.0668835	1.7784129
C	-2.2220415	5.0850791	3.3183911
H	-1.9490968	5.1760753	2.2552673
C	-3.7312093	4.8444073	3.4256259
H	-4.1012956	4.0461499	2.7728507
H	-4.0178399	4.5951730	4.4550139
O	-1.3590306	4.0906284	3.8125173
P	-9.1653010	0.5486741	3.0461453
O	-9.8307907	1.1906744	4.2070466
O	-8.0510262	1.2259488	2.2058466
O	-10.2651176	0.0975234	1.8718237
C	-11.6578613	0.2043433	2.1598916
H	-11.8622874	1.1424618	2.6956880
H	-11.9851941	-0.6292437	2.8079015
C	-12.4559121	0.1664058	0.8671177
H	-13.5235646	0.2328659	1.1435517
O	-12.1436115	1.2918842	0.0381206
C	-11.5098962	0.8777912	-1.1616361
H	-12.1836759	1.0358835	-2.0159535
N	-10.3562995	1.7310196	-1.4101444
C	-9.2221986	1.8011206	-0.6375875
N	-8.4054413	2.7680563	-1.0027328
C	-9.0443465	3.3858879	-2.0620707
C	-8.7294144	4.5131513	-2.8385941
N	-7.5873383	5.2457014	-2.6229145
H	-7.6243086	6.1756427	-3.0327766
H	-7.2066746	5.2188953	-1.6714554
N	-9.5706187	4.8728929	-3.8171254

C	-10.6909764	4.1513010	-3.9980130
H	-11.3371899	4.4847271	-4.8143083
N	-11.1205756	3.0948800	-3.3021945
C	-10.2641222	2.7555418	-2.3382859
C	-12.2294221	-1.0779572	-0.0174476
H	-11.9086242	-1.9477814	0.5841832
C	-11.1461971	-0.6010171	-0.9723258
H	-10.1683836	-0.6959287	-0.4886160
H	-11.1588980	-1.1628928	-1.9140277
O	-13.3651267	-1.3772734	-0.8134459
H	-14.1158524	-1.5558598	-0.2279544
C	-8.8423701	-3.1587345	1.1473524
H	-8.8549975	-4.2103595	0.8296775
H	-9.8031383	-2.9160608	1.6233959
C	-7.7346605	-2.8960910	2.1404557
H	-7.8641798	-3.5391631	3.0291760
O	-6.4289272	-3.1910935	1.5497105
C	-5.4731008	-2.2518942	1.9868259
H	-4.5330225	-2.7507805	2.2403407
N	-5.1719205	-1.2699875	0.8698478
C	-6.0022753	-1.1568181	-0.2019200
H	-6.6074351	-2.0359552	-0.4121161
C	-6.0835529	0.0000430	-0.9108838
H	-6.7621121	0.1065066	-1.7532499
C	-5.3079999	1.1034954	-0.4284623
N	-5.5129618	2.3408138	-0.9286663
H	-5.0952095	3.1087714	-0.4091461
H	-6.4829118	2.5498695	-1.2023332
N	-4.3761856	0.9428031	0.5140950
C	-4.2761810	-0.2330366	1.1754713
O	-3.4728189	-0.4273478	2.1081730
C	-7.5612794	-1.4438809	2.5697170
H	-7.5584661	-0.8390012	1.6548780
C	-6.1406785	-1.4677274	3.1190934
H	-5.7136843	-0.4755785	3.2928723
H	-6.0990236	-2.0388513	4.0584377
O	-8.5419927	-0.9380854	3.4469638
Ag	-7.2777459	3.1614509	1.8909948
Ag	-2.6259691	1.3310740	3.2426903
H	-9.0583718	1.1484516	0.2139200
H	-8.7414019	-2.5209234	0.2569048
H	-0.6304759	7.2145820	2.5324955
C-Ag-A trans (H)			
122			
P	-2.3481331	-2.1769407	-5.9569215
O	-3.0601302	-1.0470276	-6.6653035
O	-3.6146784	-2.9010505	-5.0825393
C	-3.4051335	-4.0790093	-4.3314559
H	-2.9378895	-3.8469941	-3.3590896
H	-2.7523420	-4.7803959	-4.8787991
C	-4.7589828	-4.7102677	-4.0621234
H	-4.6352405	-5.5840105	-3.4063268
O	-5.6336513	-3.7907930	-3.3738619
C	-6.5246526	-3.1768008	-4.2644980
H	-7.5356770	-3.2860260	-3.8556709

N	-6.2981504	-1.6881184	-4.2682367
C	-5.5971808	-1.0308416	-5.2270676
H	-5.2143195	-1.5859034	-6.0746627
C	-5.3036850	0.2971224	-5.1360702
H	-4.6744277	0.7400023	-5.9039521
C	-5.7208555	0.9804068	-3.9761801
N	-5.4005077	2.2761997	-3.7790659
H	-5.7866747	2.7861981	-2.9946406
H	-4.9692122	2.8046778	-4.5253709
N	-6.4109486	0.3396218	-3.0163016
C	-6.7129195	-1.0094418	-3.1116655
O	-7.3256423	-1.5825785	-2.2142647
C	-5.5519337	-5.1227234	-5.3060719
H	-4.8790052	-5.3954590	-6.1373990
C	-6.3641017	-3.8596786	-5.6339467
H	-5.8030389	-3.2563994	-6.3508452
H	-7.3411007	-4.1068581	-6.0711339
O	-6.3823011	-6.2069673	-4.9180212
H	-6.8790348	-6.4989233	-5.6962795
C	-0.8891158	1.7981572	-3.1191687
H	-0.1565490	2.1742908	-2.3907575
H	-0.6721508	2.2549932	-4.0961660
C	-0.8119657	0.2859451	-3.2175476
H	0.1504928	-0.0400380	-3.6366610
O	-0.9243018	-0.2730683	-1.8730892
C	-1.9882230	-1.1896994	-1.8621610
H	-1.6479252	-2.2188062	-2.0608769
N	-2.5886529	-1.1885624	-0.5261507
C	-2.4176648	-0.2979902	0.4767063
H	-1.6803222	0.4944231	0.4164938
N	-3.2413835	-0.5327823	1.4955514
C	-4.0008387	-1.6421795	1.1250540
C	-5.0727785	-2.3755871	1.7059471
N	-5.5625645	-2.1813093	2.9386204
H	-6.4514639	-2.6212933	3.1636425
H	-5.2460560	-1.4648087	3.5885967
N	-5.6421607	-3.3356030	0.9411103
C	-5.1606233	-3.5970875	-0.2809177
H	-5.6917238	-4.3538339	-0.8609397
N	-4.1226174	-3.0219611	-0.8916993
C	-3.6002425	-2.0497265	-0.1493434
C	-1.9551835	-0.3490264	-4.0363784
H	-2.3714895	0.3505361	-4.7774824
C	-2.9556725	-0.7172490	-2.9364215
H	-3.4884114	0.1714805	-2.5650068
H	-3.6703729	-1.4834327	-3.2427747
O	-1.4689742	-1.5125628	-4.6693628
O	-1.4977972	-3.2510018	-6.5423011
H	-1.8933418	2.1199959	-2.7988659
P	-8.0069863	4.6227539	7.8103492
O	-6.5613420	4.9640853	8.0903499
O	-7.9525667	2.9288704	7.6669771
C	-9.1306712	2.1783232	7.4592839
H	-9.4752638	2.2652042	6.4144678
H	-9.9401379	2.5262291	8.1237966
C	-8.8077310	0.7190193	7.7272267
H	-9.6792336	0.0961136	7.4790060

O	-7.7178200	0.2696856	6.8941202
C	-6.5094809	0.2570112	7.6060514
H	-6.0570766	-0.7335115	7.4843120
N	-5.5261212	1.1854102	6.9474986
C	-5.2737337	2.4493856	7.3751683
H	-5.7527618	2.8044310	8.2793049
C	-4.4837716	3.3121409	6.6756193
H	-4.3889410	4.3327135	7.0380353
C	-3.9550467	2.8653592	5.4476016
N	-3.2283560	3.6867578	4.6632137
H	-2.7807889	3.3359339	3.8261276
H	-2.9591651	4.5995966	5.0042396
N	-4.2024217	1.6177478	5.0103541
C	-5.0043269	0.7419154	5.7229958
O	-5.2445766	-0.3838656	5.2926349
C	-8.3492807	0.3982534	9.1532552
H	-8.8019192	1.0901335	9.8844678
C	-6.8255800	0.5823384	9.0752834
H	-6.5817247	1.6116304	9.3466703
H	-6.2960636	-0.0971746	9.7569888
O	-8.7132916	-0.9508959	9.4047609
H	-8.4516200	-1.1690300	10.3112148
C	-6.4912864	6.3526321	3.2715098
H	-6.8056308	6.7776314	2.3074799
H	-6.0398432	7.1558107	3.8728344
C	-7.6801491	5.7544064	4.0016194
H	-8.4010102	6.5297397	4.2967924
O	-8.3639602	4.8316622	3.1001965
C	-8.4281855	3.5715343	3.7174654
H	-9.3742345	3.4278882	4.2635427
N	-8.3751293	2.5439881	2.6749021
C	-8.0147338	2.6795998	1.3783926
H	-7.8324676	3.6524995	0.9361903
N	-7.9285480	1.5039990	0.7603835
C	-8.2450670	0.5446375	1.7207470
C	-8.2831426	-0.8761879	1.7528023
N	-8.1187228	-1.6769738	0.6889659
H	-7.9137763	-2.6556581	0.8754609
H	-7.8713481	-1.3541532	-0.2440015
N	-8.4941214	-1.4554243	2.9569953
C	-8.7220293	-0.6964744	4.0367492
H	-8.8506473	-1.2271240	4.9822455
N	-8.7834633	0.6350201	4.1051591
C	-8.5163870	1.1935943	2.9275876
C	-7.2973494	4.9244433	5.2437556
H	-6.3406082	5.2520016	5.6777498
C	-7.2360798	3.5089598	4.6609398
H	-6.3232065	3.3594199	4.0641264
H	-7.3202231	2.7241664	5.4167591
O	-8.3341126	5.0199544	6.1951100
O	-9.2176178	4.9973856	8.5926975
H	-5.7224908	5.5867193	3.0800885
Ag	-3.6163676	0.6357551	3.2093266
Ag	-7.1551539	1.0512414	-1.1484401



Mechanistic investigation of the trimethylamine-N-oxide reduction catalysed by biomimetic molybdenum enzyme models

Received 00th January 20xx,
Accepted 00th January 20xx

DOI: 10.1039/x0xx00000x

www.rsc.org/

M. Fortino,^a T. Marino,*^a N. Russo,^a E. Sicilia*^a

In this paper, we report a theoretical investigation of the reduction reaction mechanism of Me_3NO by molybdenum containing systems that are functional and structural analogues of trimethylamine N-oxide reductase mononuclear molybdenum enzyme. The reactivity of monooxomolybdenum(IV) benzenedithiolato complex and its derivatives with carbamoyl (*t*-BuNHCO) and acylamino (*t*-BuCONH) substituents on the benzene rings in both *cis* and *trans* arrangements was explored. Calculated energy profiles describing the steps of two mechanisms of attack considered viable (named *cis*- and *trans*-attack) by the Me_3NO substrate at *cis* and *trans* positions with respect to the oxo ligand show that the attack in *cis* is energetically more favourable than the attack in *trans*. Along the pathway for the *cis*-attack the first step of the reaction, that is rate-determining for all the studied compounds, is the approach of the substrate to the Mo centre in *cis* to the oxo ligand that causes a distortion of the initial square-pyramidal geometry of the complex. The reaction steps involved in the *trans* position attack were also explored. Calculations confirm that, as previously suggested, the introduction of ligands able to form intramolecular $\text{NH}\cdots\text{S}$ hydrogen bonds accelerates the reduction of the Me_3NO substrate and contributes to the tuning of the reactivity of molybdoenzyme models.

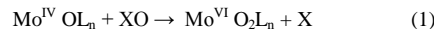
1. Introduction

Enzymes are essential for the life since they possess phenomenal capability to catalyse efficiently a huge number of reactions with high specificity and are able to work under mild and physiological conditions. Understanding how enzymes achieve these remarkable results is a fundamental problem in biochemistry. In fact, it can also contribute to develop more efficient inhibitors, to predict the drugs metabolism and to design new catalysts for specific reactions.¹⁻⁴

The highly efficiency of natural enzymes inspired the development of so called biomimetic catalysts that mimic the active sites of natural enzymes in order to promote catalysis in homogeneous phase.⁵ Furthermore, discovering how the natural enzymes work allows to design artificial enzymes with superior catalytic power.⁵⁻⁹

In metal-containing enzymes the active site is characterized by the presence of a metal cation coordinated to specific amino acid residues and represents the core of the catalytic event.¹⁰ This “catalytic core” is the reference for designing new biomimetic organometallic complexes with high catalytic efficiency. Nakamura and co-workers¹¹ and Okamura et al.¹²⁻¹⁴ showed as a series of bio-

inspired monooxomolybdenum(IV) complexes are able to catalyse the reduction of trimethylamine-N-oxide (Me_3NO) to trimethylamine (Me_3N) mimicking the activity of the trimethylamine-N-oxide reductase (TMAOR) enzyme. This enzyme belongs to the molybdenum containing family whose catalytic centre contains one or two pyranopterin dithiolene ligands, called molybdopterin cofactors, coordinated by the dithiolene sulphur atoms to the metal ion (Scheme 1). TMAOR is implicated in the catalysis of oxygen atom transfer reactions according to the following equation:¹⁵⁻¹⁷



The originally synthesized biomimetic TMAOR enzymes were characterized by the presence of the 1,2-benzenedithiolato (bdt) ligands in state of the natural pyranopterin dithiolene moieties (see Scheme 1a).¹²

Successively, Okamura’s group investigated the role played by $\text{NH}\cdots\text{S}$ hydrogen bonds for sulphur atoms bonded to the molybdenum¹² and demonstrated that the introduction of four intramolecular $\text{NH}\cdots\text{S}$ hydrogen bonds into a monooxomolybdenum(IV) complex $(\text{NEt}_4)_2[\text{Mo}(\text{IV})\text{O}(\text{bdt})_2]$ accelerates the reduction of Me_3NO to Me_3N along with the production of the corresponding dioxomolybdenum(VI) complex. More recently, in Okamura’s laboratory^{13,14} new series of monooxomolybdenum(IV) complexes containing only two $\text{NH}\cdots\text{S}$ hydrogen bonds were synthesized. In the first series, a carbamoyl group (RNHCO) was used (Scheme 1b) to introduce an amide

^a Department of Chemistry and Chemical Technologies, Università della Calabria, 87036, Arcavacata di Rende, Italy.

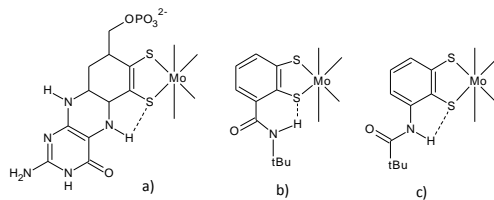
† M. Fortino, Prof. Dr. T. Marino, Prof. N. Russo, Prof. Dr. E. Sicilia

*tmarino@unical.it; siciliae@unical.it.

Electronic Supplementary Information (ESI) available: [details of any supplementary information available should be included here]. See DOI: 10.1039/x0xx00000x

moiety that led to the formation of a flexible NH···S hydrogen bond and resulted in a small contribution to the reduction of Me₃NO in polar solvent.¹³

For the next series, instead, new ligands with acylamino groups (RCONH), as shown in Scheme 1c, were designed and synthesized.¹⁴ In this case, the formed five-membered hydrogen bond, reminiscent of the intraligand interaction in the molybdopterin cofactor, allowed a better investigation of the relationship between the strength of the hydrogen bond and the reactivity of the molybdoenzyme models.



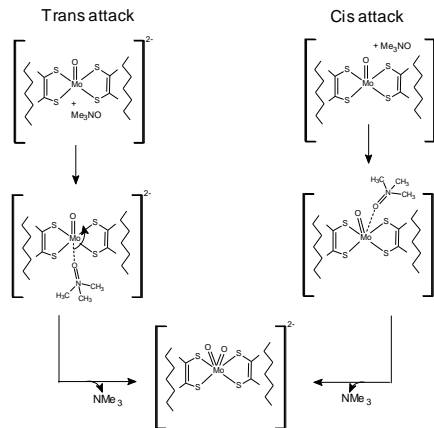
Scheme 1. Molybdopterin ligand a) present in the natural enzyme, compared with carbamoyl b) and acylamino c) groups containing model ligands.

For the Me₃NO reduction by such monooxomolybdenum(IV) complexes two reaction mechanisms are viable.^{12,13} In the traditional mechanism,¹² the attack by Me₃NO to Mo takes place at the position *trans* to the oxo ligand to yields an intermediate Me₃NO adduct. After that, the trimethylamine N-oxide ligand moves to the *cis* position through a *trans-cis* rearrangement and by the N-O bond dissociation a *cis*-dioxomolybdenum(VI) complex is formed. The *trans-cis* rearrangement becomes the rate-determining step at high Me₃NO concentrations when the substituent is bulky or the intermediate is stabilized. The alternative mechanism¹³ involves direct Me₃NO *cis* attack to Mo when very bulky groups hamper the *trans-cis* rearrangement. For the sake of clarity, from now on, the former mechanism will be indicated as *trans*-attack and the latter as *cis*-attack.

We present here the outcomes of a detailed theoretical Density functional investigation of the proposed reaction mechanisms for the oxo transfer from Me₃NO to the monooxomolybdenum(IV) benzenedithiolato complex, [Mo(IV)O-(bdt)₂]²⁻ labelled E, and its [Mo(IV)O-(1,2-S₂-3-t-BuNHCO₆H₃)₂]²⁻, E_(CONH) and [Mo(IV)O-(1,2-S₂-3-t-BuCONHC₆H₃)₂]²⁻, E_(NHCO), derivatives. A comparative analysis was performed with the aim to elucidate the influence on the course of the reaction of both the presence of substituents on the benzene ring and formation of NH···S hydrogen bonds.

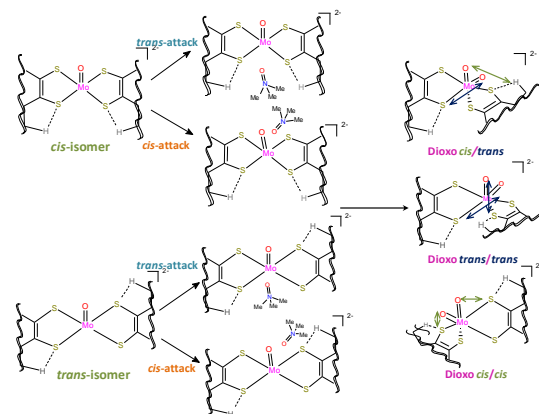
Trans- and *cis*-mechanisms were explored for all the complexes, whereas for E_(CONH) and E_(NHCO) monooxomolybdenum(IV) complexes the reactivity of both *cis* and *trans* isomers was examined.

Moreover, the structure and stability of the formed dioxomolybdenum(VI) complexes were carefully checked for confirming whether products exist as a single isomer where both oxo ligands are *trans* to each of the two hydrogen-bonded thiolate ligands.



Scheme 2. Schematic representation of the reaction steps for the *trans*- and *cis*-attack mechanisms.

All calculations were carried out with the support of the information coming from experiments and previous theoretical investigations of the reactivity of molybdenum enzymes.¹⁸⁻²² A summary of all the alternatives examined here is shown in Scheme 3.



Scheme 3. Schematic representation of the mechanistic alternatives for the Me₃NO attack to *cis* and *trans* isomers of monooxomolybdenum(IV) complexes.

2. Computational methods

Molecular geometry optimizations were carried out without symmetry constraints at the density functional level of theory, by using the Gaussian 09 code²³ employing the M06-L²⁴ functional, that is recommended for the calculation of transition metal containing systems thermochemistry.²⁵ Additional B3LYP^{26,27} and OPBE²⁸ preliminary calculations were performed to check the singlet ground state multiplicity of the examined complexes. The standard 6-31+G(d,p) basis set was used for the C, N, O, S, and H atoms, whereas the SDD pseudo-potential in connection with the relative orbital basis set²⁹ was employed for the molybdenum atom. All of the reported structures represent genuine minima or transition states

on the respective potential energy surfaces, as confirmed by analysis of the corresponding Hessian matrices. For transition states, the vibrational mode associated with the imaginary frequency was verified to be related to the correct movement of involved atoms. Furthermore, the IRC^{30,31} method was used to assess that the localized TSs correctly connect to the corresponding minima along the imaginary mode of vibration. The influence of dimethylformamide (DMF) solvent effects on the energetics of the process was estimated in the framework of the SMD³² model. Single-point calculations on all stationary points structures obtained from gas-phase calculations by using the same M06-L and basis sets computational approach were performed. Calculated reaction Gibbs free energies in solution, ΔG_{sol} , for each process were obtained as the sum of two contributions: a gas-phase reaction free energy, ΔG_{gas} , and a solvation reaction free energy term calculated with the SMD approach, ΔG_{solv} . NBO^{33,34} analysis of the charge density was performed for some key species intercepted along the reaction paths.

3. Results

3.1. Me₃NO reduction by the [Mo(IV)O(bdt)₂]²⁻ complex

The potential energy surface (PES) calculated to describe the oxo transfer from the Me₃NO substrate to the Mo(IV) bis-dithiolene [Mo(IV)O(bdt)₂]²⁻ complex is depicted in Figure 1 together with the stationary points optimized structures. The values of the most relevant geometrical parameters of minima and transition states can be found in Figure S1 of the Supporting Information (SI) together with atomic Cartesian coordinates (Table S1). Preliminary computations were performed considering different spin multiplicities for the reaction of Me₃NO with the monooxomolybdenum(IV) benzenedithiolato-Mo complex. Results show that the singlet is the ground state and the triplet the first excited state along the entire PES and no crossing between the two electronic spin states occurs (see Figure S2, in the SI). In particular, the calculated energy difference between the ground singlet and the excited triplet states is 15.2 kcal mol⁻¹ for the ES complex. Moreover, all the attempts to locate the stationary points along a pathway describing a *trans*-attack failed. As a consequence, only the PES for the singlet ground state describing the *cis*-attack is reported. To this proposal, it is worth noting that several investigations reported examples of *cis*-attack^[18,20-22] and that a second order kinetics is followed.^[35]

Me₃NO approaches the E complex causing a distortion of the initial square pyramidal geometry of the complex. A transition state lying 18.1 kcal mol⁻¹ in DMF solvent above the reference energy of separated reactants (E+S) was intercepted corresponding to the movement of one of the sulfur atoms from its position to allow the oxygen atom of Me₃NO to enter the coordination sphere of the Mo(IV) centre. The distance between the substrate oxygen and the Mo(IV) centre is 2.345 Å. The ES first adduct, stabilized by only 1.8 kcal mol⁻¹ with respect to the transition state leading to it, is formed.

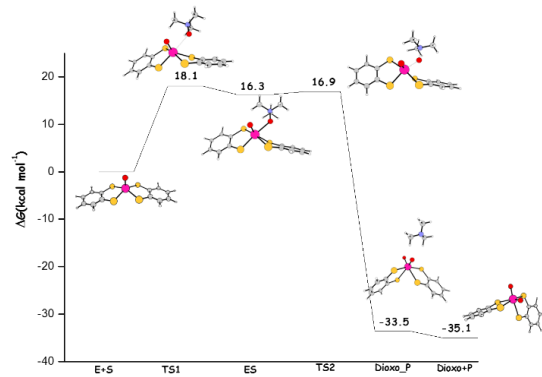


Figure 1. Calculated M06-L *cis*-attack free energy profile for the monooxomolybdenum(IV) benzenedithiolato complex (E). Energies are in kcal mol⁻¹ and relative to reactants' asymptote.

As a consequence of the distortion of the initial geometry, the bond distance between Mo and the S atom in *trans* position with respect to the M=O bond increases from 2.440 Å to 2.740 Å (Figure S1) and the O-Mo-S valence angle changes from 108.3° to 156.0°. The reaction proceeds toward the product formation by overcoming a very low energy barrier, only 0.6 kcal mol⁻¹ for a transition state that corresponds to the formation of a new Mo-O (2.058 Å) bond and the definitive cleavage of the N-O (1.547 Å) substrate bond. The vibrational N-O stretching mode associated to the imaginary frequency (570*i* cm⁻¹) well accounts for this event. From the computed PES it is clear that the most energy demanding step is the formation of the ES complex, whereas once the ES adduct is formed the reduction of Me₃NO and the oxidation of Mo easily occurs.

Me₃NO reduction by the [Mo(IV)O-(1,2-S₂-t-BuNHCO₆H₃)₂]²⁻, E_(CONH), complex

In their detailed experimental investigations Okamura and collaborators demonstrated as the introduction of intramolecular NH···S hydrogen bonds^[13] can stabilize the intermediate in the reduction path of Me₃NO resulting in more favourable reaction kinetics. In this section is examined what is the effect of the unsymmetrical introduction of t-BuNHCO groups on both benzene rings of 1,2-benzenedithiolato ligands and the reactivity of both *cis* and *trans* isomers is investigated. M06-L fully optimized structure of the *trans*-E_(CONH) complex is shown in Figure 2, where the experimental and theoretical values of the most significant geometrical parameters are compared. Calculated geometrical parameters agree with those extracted from the crystallographic characterization^[13] of the complex indicating a good modeling of the investigated systems. The main deviation concerns, as expected, the NH···S hydrogen bond distances that seem to be underestimated at theoretical level. This apparent discrepancy can be explained considering that calculations allow a more secure location of the hydrogen atoms involved in the NH···S hydrogen bonding interaction with respect to the values extracted from the crystallographic characterization of the complex where a fixed N-H

distance of 0.881 Å is assumed. In fact, if we compare the N···S distances, the agreement between theory and experiment (see Figure 2) becomes quite good. Supporting Information gives atomic coordinates for the complex (Table S2). More detailed geometrical information for all the intercepted stationary points are reported in Figure S3 of the SI.

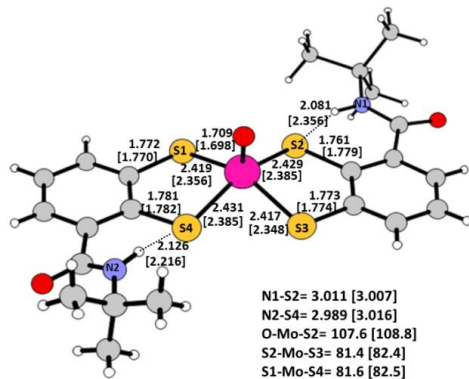


Figure 2. M06-L optimized structure of $\mathbf{E}_{(\text{CONH})}$ in its *trans* arrangement. Selected bond lengths (in Å) and angles (degrees) are compared with available experimental values in square brackets.

In contrast to what occurred in the unsubstituted \mathbf{E} complex, intramolecular NH···S hydrogen bond formation makes the Mo-S bonds distinguishable as (see Figure 2) the Mo-S bond with S2 and S4 sulphur atoms involved in the hydrogen bonds are longer than the Mo-S bond distances with S1 and S3 atoms. Reaction pathways for both *cis*, *cis*- $\mathbf{E}_{(\text{CONH})}$ and *trans*, *trans*- $\mathbf{E}_{(\text{CONH})}$ isomers were investigated together with the identity of the products, according to ^1H NMR analysis and DFT calculations,^[13] that proposed a single isomer to be formed in which both oxo ligands are *trans* to each of the two hydrogen-bonded thiolate ligands. Moreover, for each isomer both *cis*- and *trans*-attack mechanisms were explored. The calculated *cis*-attack free energy profiles for the Me_3NO reduction assisted by *cis*- $\mathbf{E}_{(\text{CONH})}$, and *trans*- $\mathbf{E}_{(\text{CONH})}$ isomers are depicted in **Path a** and **Path b**, respectively of Figure 3.

The PESs describing the *trans*-attack reaction steps for the same complexes can be found in the SI (Figure S4) together with detailed geometrical information (Table S3 and Figure S5). The two *cis* and *trans* isomers result to be isoenergetic in agreement with a previous gas-phase theoretical investigation on these two conformers employing the B3LYP exchange-correlation functional.^[13] The reaction evolves following the same steps described for the \mathbf{E} unsubstituted Mo(IV) complex for both *cis* and *trans* isomers. It is worth underlining that for the *cis*- $\mathbf{E}_{(\text{CONH})}$ complex the attack takes place from the unhindered side of the complex with sulphur atoms not involved in hydrogen bonds. Due to the symmetric disposition of the t-BuNHCO groups with respect to the Mo centre in the *trans*- $\mathbf{E}_{(\text{CONH})}$ complex, instead, for the coordination of the substrate the side of attack is unimportant, whereas different results are obtained whether the hydrogen-bonded sulphur is involved (i.e. S2 or S4 in Figure 2) or not (i.e. S1 or S3 in Figure 2).

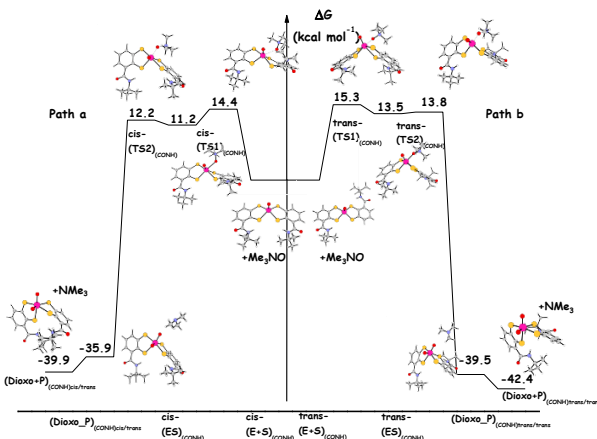


Figure 3. Calculated M06-L free energy profiles for the Me_3NO *cis*-attack to the monooxomolybdenum(IV) $\mathbf{E}_{(\text{CONH})}$ complex in its *cis* (**Path a**) and *trans* (**Path b**) arrangements. Energies are in kcal mol⁻¹ and relative to reactants' asymptote.

From the exploration of both possibilities resulted that the attack from the side of the hydrogen-bonded sulphur is the preferred one and, hence, in the next paragraphs the corresponding lowest energy pathway will be described. The *cis*-attack of the Me_3NO substrate to the metallic centre causes a distortion of the initial square pyramidal geometry and, as a consequence, to form the first weakly bound adducts between the *cis*- $\mathbf{E}_{(\text{CONH})}$ and *trans*- $\mathbf{E}_{(\text{CONH})}$ complexes and Me_3NO the overcoming of a transition state barrier is required. The height of the barrier is 14.4 kcal mol⁻¹ along the **Path a** for the *cis* isomer and 15.3 kcal mol⁻¹ along the **Path b** for the *trans* isomer. The formed intermediates are more stable by only a few kcal mol⁻¹ than the preceding transition states and even smaller is the difference in energy with respect to the next transition states. By surmounting the second transition state barrier the N-O bond is definitively broken and a new Mo-O bond is formed. The analysis of the imaginary frequencies in the *cis* (501*i* cm⁻¹) and *trans* (456*i* cm⁻¹) species shows that the main vector lies along the N-O bond. The whole reaction leading to the formation of the final weakly bound adducts between dioxomolybdenum complexes and trimethylamine is exothermic by 35.9 and 39.5 kcal mol⁻¹ for the *cis* and *trans* isomers, respectively. Release of trimethylamine is accompanied by an energy gain of 3.1 kcal mol⁻¹ along **Path a** and 2.9 kcal mol⁻¹ along **Path b**.

The proposed mechanism^[12] for the *trans*-attack involves that Me_3NO first approaches the Mo centre at the position *trans* to the oxo ligand to give an intermediate adduct. Then, the ligand moves to the *cis* position through a *trans*-*cis* rearrangement and the O-N bond is broken to afford a dioxomolybdenum(VI) complex. In spite of such indications, the effect of the *trans* attack explored in the present investigation does not reproduce (see Figure S4 of SI) what previously hypothesized.^[12] Our calculations lead to a completely different description of the reaction steps. That is, formation of a first adduct as a consequence of the *trans* to Mo=O approach of the substrate to the metal centre. The reaction proceeds by the transfer of the oxygen atom from the Me_3NO substrate to one sulphur atom and not, as suggested, to the Mo centre. The elongation of the S-O bond

together with the shortening of the Mo-O bond and a reorganization of the ligands leads to the formation of the final dioxo products. The outcomes of our calculations confirm that, in accordance with molybdenum chemistry^[36,37] the *trans* attack cannot allow the formation, albeit transient, of a linear dioxo species. A final product where the dioxo moiety adopts a bent geometry around the metal centre is formed as the result of a series of steps that bypass the direct transfer of the oxygen atom to the Mo centre.

Concerning the identity of the dioxomolybdenum complex products formed along the examined pathways for both *cis*- and *trans*-attacks on *cis* and *trans* Mo(IV) complexes, the structures are reported in Figure 4.

The *cis*-E_(CONH) isomer leads to the formation of a complex, labelled Dioxo_{(CONH)cis/trans}, in which one of the hydrogen-bonded thiolato ligand is *trans* to one of the Mo=O bonds and one is *cis* to the other oxo ligand. In the dioxo complex, indicated as Dioxo_{(CONH)trans/trans}, formed along the calculated pathways describing the reactions of the *trans*-E_(CONH) isomer, instead, both hydrogen-bonded thiolato ligands are *trans* to each of the oxo ligands. It is important to underline, for the sake of completeness, that when the attack to the *trans* isomer and consequent geometrical distortion occur from the side of the sulphur atom non involved in the hydrogen bond with the NH unit the Dioxo_{(CONH)cis/cis} species is formed, that is less stable by about 4 kcal mol⁻¹ than the most stable Dioxo_{(CONH)trans/trans} one.

Okamura and co-workers^[13], on the basis of the results ¹H NMR, and Raman analysis and DFT calculations concluded that the most stable dioxo isomer, in which both Mo=O bonds are *trans* to the

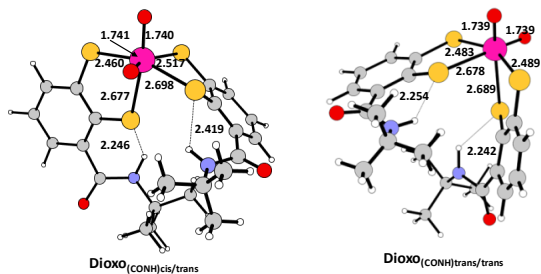


Figure 4. M06-L optimized structure of dioxomolybdenum(VI) complexes labelled as Dioxo_{(CONH)cis/trans} and Dioxo_{(CONH)trans/trans}. Most relevant geometrical parameters are reported. Bond lenghts are in Å and angles in degrees.

hydrogen-bonded thiolato ligands, is the sole product. Furthermore, the strong donation of the oxo ligand at the *trans* position via *trans* influence should cause the elongation of the Mo-S bond and, conversely, the NH···S hydrogen bond should stabilize the longer Mo-S bond and strengthen the Mo=O bond at *trans* position. Such conclusions are only partially supported by the outcomes of our computational analysis. Indeed, the Dioxo_{(CONH)trans/trans} isomer is calculated to be more stable than the Dioxo_{(CONH)cis/trans} one by 2.5 kcal mol⁻¹. The Mo-S bond in *trans* to the M=O bond is elongated

and, concurrently, the NH···S hydrogen bond is calculated to be stronger and shorter. However, in comparison with the structure of the dioxo product of the unsubstituted complex E the length of the Mo-O bond is not significantly influenced by the nature of the ligand in *trans*. Moreover, the Dioxo_{(CONH)trans/trans} complex is not the sole product. All the efforts, carried out in order to rationalize the experimental evidence, to intercept a low energy transition state for the interconversion of the Dioxo_{(CONH)cis/trans} isomer into the Dioxo_{(CONH)trans/trans} one were unsuccessful. We were able to locate a transition state, whose structure is shown in Figure S6 of SI for the interconversion between the two *cis* and *trans* isomers of the initial monooxo E_(CONH) complex. The height of the calculated energy barrier for such rearrangement is 27.4 kcal mol⁻¹ in condensed phase. As a consequence, even if a rearrangement able to cause the transformation of the Dioxo_{(CONH)cis/trans} into the Dioxo_{(CONH)trans/trans} exists it should be very high energy demanding and should require the heating of the solution. As consequence, for both *cis* and *trans* monooxomolybdenum(IV) complexes, the Me₃NO attack to Mo at the position *cis* to the oxo ligand is more favorable than the attack at the *trans* one. The slowest step of this process is, such as for the unsubstituted complex, the formation of the first adduct. However, a comparison of the barrier calculated for the E complex (18.1 kcal mol⁻¹) and those for the *cis*-E_(CONH) and *trans*-E_(CONH) isomers calculated to be 14.4 and 15.3 kcal mol⁻¹, respectively confirms that the introduction of benzene substituents able to form intramolecular NH···S hydrogen bonds accelerates the Me₃NO reduction process.

3.2. Me₃NO reduction by the [Mo(IV)O-(1,2-S₂-3-t-BuCONHC₆H₃)₂]²⁻, E_(NHCO), complex

More recently, Okamura and co-workers^[14] introduced at the 3-position of the 1,2-benzenedithiolato ligands a new series of acylamino groups (RCONH) designed and synthesized with the aim to provide a rigid and stable intraligand NH···S hydrogen bond and form a five-membered hydrogen bond that better reproduces the intraligand interaction in the natural enzyme molybdopterin cofactor (see Scheme 1). Also in this case the reaction pathways for both *cis* and *trans* isomers, indicated as *cis*-E_(NHCO), and *trans*-E_(NHCO), respectively were explored and for each isomer both *cis*- and *trans*-attack mechanisms were examined. M06-L free energy profiles illustrating the *cis*-attack leading to Me₃NO reduction by *cis*-E_(NHCO) (**Path A**) and *trans*-E_(NHCO) (**Path B**) complexes are depicted in Figure 5. Cartesian coordinates and the most relevant geometrical parameters of stationary points can be found in Table S4 and Figure S7, respectively of SI. Also for *cis*-E_(NHCO), and *trans*-E_(NHCO) species, *trans*-attack reaction steps are reported in the SI (Figure S8), where more detailed geometrical information and atomic Cartesian coordinates can be found (Figure S9 and Table S5, respectively).

At a first glance it clearly appears that the mechanistic steps for the Me₃NO *cis*-attack to both *cis*-E_(NHCO) and *trans*-E_(NHCO) complexes are very similar to those for the corresponding *cis* and

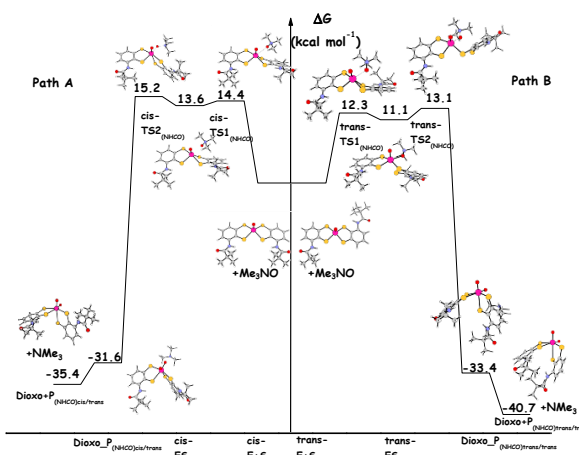


Figure 5. Calculated M06-L free energy profiles for the Me_3NO *cis*-attack to the monooxomolybdenum(IV) $\mathbf{E}_{(\text{NHCO})}$ complex in its *cis* (**Path A**) and *trans* (**Path B**) arrangements. Energies are in kcal mol^{-1} and relative to reactants' asymptote.

trans carbamoyl complexes and also the energetics do not differ significantly. In analogy with the results reported above, the attack to the *cis* isomer takes place from the less hindered side and, preferably, from the side of the hydrogen-bonded sulphur in the case of the *trans* isomer. The fully optimized structures of the two *cis*- $\mathbf{E}_{(\text{NHCO})}$ and *trans*- $\mathbf{E}_{(\text{NHCO})}$ minima are calculated to be isoenergetic. The substrate enters the Mo coordination sphere overcoming an energy barrier of 14.4 and 12.3 kcal mol^{-1} along the **Path A** for the *cis* isomer and **Path B** for the *trans* one, respectively. The formed adducts are slightly more stable, by 1.2 and 0.8 kcal mol^{-1} along **Path A** and **Path B**, respectively than the previous transition states. The formed adducts lead to the formation of the corresponding dioxomolybdenum(VI) products by the definitive oxygen atom transfer through two transition states with energy barriers of 1.6 kcal mol^{-1} along **Path A** and 2.0 kcal mol^{-1} along **Path B**. Dioxomolybdenum(VI) complexes formation is exothermic by 31.6 kcal mol^{-1} for the *cis* isomer and 33.4 kcal mol^{-1} for the *trans* one. Finally, the two dioxo complexes release the trimethylammonium product with an energy gain of about 3.8 kcal mol^{-1} in the former case and 7.3 kcal mol^{-1} in the latter.

The examination of the mechanism of the Me_3NO attack to Mo at the position *trans* to the oxo ligand, gives results superimposable to those previously described for the *cis*- $\mathbf{E}_{(\text{CONH})}$ and *trans*- $\mathbf{E}_{(\text{CONH})}$ carbamoyl complexes. An initial oxygen atom transfer to a sulphur atom is involved that avoids the direct transfer to the Mo centre.

In analogy to what happens in the case of complexes with carbamoyl substituents, along both *cis*- and *trans*-attack pathways two dioxo isomers are obtained. The difference in energy between them is 5.3 kcal mol^{-1} and is due to the different disposition of the t-BuCONH groups on thiolato ligands. Indeed, the complex formed along the pathways for the Me_3NO attack to the *cis*- $\mathbf{E}_{(\text{NHCO})}$ complex is the isomer in which one of the hydrogen-bonded thiolato ligand is *trans* to one of the Mo=O bonds and one is *cis* to the other oxo

ligand. In analogy with the labeling adopted in the previous section, such isomer will be indicated as $\mathbf{Dioxo}_{(\text{NHCO})\text{cis/trans}}$. Both Mo=O bonds are *trans* to the hydrogen-bonded thiolato ligands, instead, in the complex, labeled $\mathbf{Dioxo}_{(\text{NHCO})\text{trans/trans}}$, formed by oxidation of the *trans*- $\mathbf{E}_{(\text{NHCO})}$ complex. Fully optimized structures and most relevant geometrical parameters for these two complexes are shown in Figure 6.

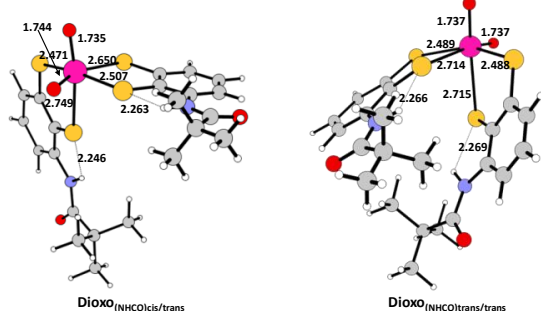


Figure 6. M06-L optimized structure of dioxomolybdenum(VI) complexes labelled as $\mathbf{Dioxo}_{(\text{NHCO})\text{cis/trans}}$ and $\mathbf{Dioxo}_{(\text{NHCO})\text{trans/trans}}$. Most relevant geometrical parameters are reported. Bond lengths are in Å and angles in degrees.

Results confirm that, in comparison with the Mo-O and Mo-S bond lengths calculated for the unsubstituted \mathbf{E} and carbamoyl $\mathbf{E}_{(\text{CONH})}$ complexes, NH···S hydrogen bonds in *trans* position strengthen the Mo-O and weaken the S-O bonds. The *cis*-attack is more favorable than the *trans* one. The introduction of benzene substituents able to form intramolecular NH···S hydrogen bonds influences the course of the reaction as it appears from the calculated values of the energy barriers for the rate determining step, 14.4 and 12.3 kcal mol^{-1} for the *cis* and *trans* isomers, respectively with respect to 18.1 kcal mol^{-1} for the \mathbf{E} complex.

Once again, we underscore that when the attack to the *trans* isomer from the side of the sulphur atom non involved in the hydrogen bond with the NH unit is explored, the dioxo product $\mathbf{Dioxo}_{(\text{NHCO})\text{cis/cis}}$ is formed that is less stable by about 4 kcal mol^{-1} than the most stable $\mathbf{Dioxo}_{(\text{NHCO})\text{trans/trans}}$ one.

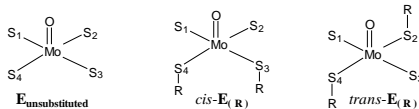
4. Discussion

The results of our computational analysis illustrated in the previous section show that for all the examined monooxomolybdenum(IV) benzenedithiolato complexes the oxo transfer reaction from Me_3NO to form the corresponding dioxomolybdenum(VI) products occurs by the attack to the Mo centre at the position *cis* to the oxo ligand. However, relevant differences in behaviour exist due to the introduction of benzene substituents able to form NH···S hydrogen bonds. NBO charge analysis^[33,34] Table 1, is helpful in rationalizing this behavior.

The oxygen atom of Me_3NO substrate carries a negative charge (-0.727), as well as negative is the charge on the Mo centre. When Me_3NO approaches the complex in *cis* position to the oxo ligand is the *trans* sulphur atom that allows to delocalize the negative charge.

In addition, the weakening and elongation of the bond between the Mo centre and the next hydrogen bonded S atom facilitates the distortion of the ligand.

Table 1. NBO analysis of charge density distribution for the investigated complexes.



	E_{unsubstituted}	cis-E_(CONH)	trans-E_(CONH)	cis-E_(NHCO)	trans-E_(NHCO)
Mo	-0.145	-0.149	-0.146	-0.172	-0.171
S ₁	-0.016	0.015	0.004	-0.031	-0.037
S ₂	-0.016	0.014	-0.007	-0.031	-0.061
S ₃	-0.016	-0.016	0.004	-0.067	-0.037
S ₄	-0.016	-0.020	-0.014	-0.067	-0.061

This is the reason why the barrier of the rate-determining step of the *cis*-attack mechanism lowers in going from **E** ($\Delta E^\# = 18.1 \text{ kcal mol}^{-1}$) to *trans*-**E_(CONH) ($\Delta E^\# = 15.3 \text{ kcal mol}^{-1}$) and *trans*-**E_(NHCO) ($\Delta E^\# = 12.3 \text{ kcal mol}^{-1}$). The rate-determining step barrier of the *cis*-attack mechanism, instead, becomes $14.4 \text{ kcal mol}^{-1}$ for both *cis*-**E_(CONH) and *cis*-**E_(NHCO) as the attack occurs from the side of the sulphur atoms non involved in the hydrogen bond due to the steric hindrance of the benzene substituents in conjunction with the positive charge on such sulphur atoms. It is noteworthy that such results confirm the experimental suggestion that t-BuCONH acylamino groups are more effective in enhancing the reactivity owing to the greater rigidity and stability of the formed intraligand NH···S hydrogen bonds. A further support to this assumption comes from the calculated energy differences in exothermicity, reported above, of the formation of dioxo products in their *cis/trans* and *trans/trans* arrangements for the two complexes **Dioxo_(CONH)** and **Dioxo_(NHCO)**. Indeed, the **Dioxo_{(CONH)trans/trans}** isomer is calculated to be more stable than the **Dioxo_{(CONH)cis/trans}** by $2.5 \text{ kcal mol}^{-1}$, whereas the **Dioxo_{(NHCO)trans/trans}** isomer is stabilized by $5.3 \text{ kcal mol}^{-1}$ with respect the **Dioxo_{(NHCO)cis/trans}**.********

Another important difference is that for both substituted **E_(CONH)** and **E_(NHCO)** complexes the *trans*-attack, even if less viable with respect to the *cis*-attack, can occur whereas for the **E** complex such attack is precluded. As already underlined above, the *trans*-attack cannot lead to the formation of a linear O-Mo-O arrangement. Therefore, the attack for both substituted **E_(CONH)** and **E_(NHCO)** complexes is redirected towards the sulphur atoms. The explanation of this difference in behaviour can be ascribed to the ability of sulphur atoms in substituted thiolates to delocalize the excess of negative charge.

5. Conclusions

In this paper, we performed a theoretical comparative analysis of the mechanistic aspects of the reduction reaction of trimethylamine N-oxide by bioinspired catalysts namely monooxomolybdenum(IV) benzenedithiolato complex and its derivatives carrying on benzene rings carbamoyl (t-BuNHCO) and acylamino (t-BuCONH) substituents in both *cis* and *trans* arrangements. The two most accredited mechanisms of attack

were explored, that is *cis*- and *trans*-attack of the Me₃NO substrate at *cis* and *trans* positions, respectively with respect the oxo ligand.

The theoretical exploration of the reaction pathways revealed that the *cis*-attack is the preferred mechanism for all the compounds under investigation, whereas the way of attack at the *trans* position is energetically unfavourable and in the case of unsubstituted monooxomolybdoenzyme cannot take place. The reaction along the pathway for the *cis*-attack evolves by the approach of the substrate to the Mo centre in *cis* to the oxo ligand. Therefore, a distortion of the initial square-pyramidal geometry of the complex is observed. As a consequence, an energy barrier has to be overcome corresponding to the movement of one of the sulphur atoms from its position to allow the oxygen atom of Me₃NO to enter the coordination sphere of the Mo centre. This step represents the rate-determining step for all the investigated compounds. The reaction proceeds by definitive breaking of the N-O bond and formation of a new Mo-O bond in the formed adduct. Very low barriers are required for this step leading to the exothermic formation of an adduct between the dioxo(VI) complex and trimethylamine. Final release of trimethylamine and formation of separated products causes further stabilization. Concerning the details of the *trans*-attack, from our calculations emerges that the oxygen atom is transferred before to a sulphur atom and in the next step to the metal centre with a concomitant reorganization in the coordination sphere of the ligands. This result confirms that, according to the molybdenum chemistry, formation of a linear dioxo species is not allowed and the assistance of a sulphur atom is required. The investigation of the influence on the course of the reaction of the presence of substituents on the benzene ring able to form intramolecular NH···S hydrogen bonds confirms, according to experimental findings, that such interactions contribute to the reactivity tuning of the molybdoenzyme models and cause an acceleration of the substrate reduction.

Acknowledgements

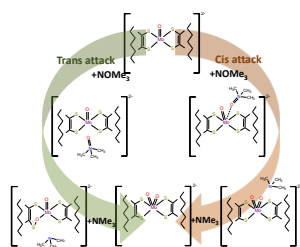
This research was supported by Università della Calabria and FP7- PEOPLE-2011-IRSES, Project no. 295172. Mariagrazia Fortino gratefully acknowledges Commissione Europea, Fondo Sociale Europeo, Regione Calabria for the financial support.

Notes and references

- V. L. Schramm *Chem. Rev.* 2006, **106**, 3029-3030.
- R. Wolfenden and M. J. Snider, *Acc. Chem. Res.* 2001, **34**, 938–945
- M. R. A. Blomberg, T. Borowski, F. Himo, R.-Z. Liao and P. E. M. Siegbahn, *Chem. Rev.* 2014, **114**, 3601–3658.
- S. F. Sousa, P. A. Fernandes and M. J. Ramos, *Phys. Chem. Chem. Phys.* 2012, **14**, 12431-12441.
- F. Yu, V. M. Cangelosi, M. L. Zastrow, M. Tegoni, J. S. Plegaria, A. G. Tebo, C. S. Mocny, L. Ruckthong, H.

- Qayyum and V. L. Pecoraro, *Chem. Rev.* 2014, **114**, 3495–3578.
- 6 V. M. Robles, E. Ortega-Carrasco, L. Alonso-Cotchico, J. Rodriguez-Guerra, A. Lledós and J.-D. Maréchal, *ACS Catal.* 2015, **5**, 2469–2480.
- 7 D. N. Bolon and S. L. Mayo, *Proc. Natl. Acad. Sci. U.S.A.* 2001, **98**, 14274–14279.
- 8 C. M. Thomas and T. R. Ward, *Chem. Soc. Rev.* 2005, **34**, 337–346
- 9 S. Chakraborty, P. Hosseinzadeh, Y. Lu, Encyclopedia of Inorganic and Bioinorganic Chemistry (Ed.: R.A. Scott) John Wiley and Sons, Ltd., Chichester, 2014, pp. 1–51.
- 10 S. W. Ragsdale *Chem. Rev.* 2006, **106**, 3317–3337
- 11 H. Oku, N. Ueyama, M. Kondo and A. Nakamura, *Inorg. Chem.* 1994, **33**, 209–216.
- 12 K. Baba, T. Okamura, C. Suzuki, H. Yamamoto, T. Yamamoto, M. Ohama and N. Ueyama, *Inorg. Chem.* 2006, **45**, 894–901.
- 13 T. Okamura, M. Tatsumi, Y. Omi, H. Yamamoto and K. Onitsuka, *Inorg. Chem.* 2012, **51**, 11688–11697.
- 14 T. Okamura, Y. Ushijima, Y. Omi and K. Onitsuka, *Inorg. Chem.* 2013, **52**, 381–394.
- 15 M Czjzek, Jean-Philippe Dos Santos, J. Pommier, G. Giordano, V. Méjean and R. Haser, *J. Mol. Biol.* 1998, **284**, 435–447.
- 16 R. Hille, J. Hall and P. Basu *Chem. Rev.* 2014, **114**, 3963–4038.
- 17 C. Lorber, M. R. Plutino, L. I. Elding and E. Nordlander, *J. Chem. Soc. Dalton Trans.*, 1997, 3997–4003.
- 18 N. M. F. S. A. Cerqueira, B. Pakhira and S. Sarkar, *J. Biol. Inorg. Chem.* 2015, **20**, 323–335.
- 19 A. L. Tenderholt, K. O. Hodgson, B. Hedman, R. H. Holm and E. I. Solomon *Inorg. Chem.* 2012, **51**, 3436–3442.
- 20 G. Moula, M. Bose and S. Sarkar *Inorg. Chem.* 2013, **52**, 5316–5327.
- 21 M. Leopoldini, N. Russo, M. Toscano, M. Dulak, T. A. Wesolowski, *Chem. Eur. J.* 2006, **12**, 2532–2541.
- 22 M. Leopoldini, S. G. Chiodo, M. Toscano and N. Russo, *Chem. Eur. J.* 2008, **14**, 8674–8681.
- 23 Gaussian 09, Revision D.01, M. J. Frisch, G. W. Trucks, H. B. Schlegel, G. E. Scuseria, M. A. Robb, J. R. Cheeseman, G. Scalmani, V. Barone, B. Mennucci, G. A. Petersson, H. Nakatsuji, M. Caricato, X. Li, H. P. Hratchian, A. F. Izmaylov, J. Bloino, G. Zheng, J. L. Sonnenberg, M. Hada, M. Ehara, K. Toyota, R. Fukuda, J. Hasegawa, M. Ishida, T. Nakajima, Y. Honda, O. Kitao, H. Nakai, T. Vreven, J. A. Montgomery, Jr., J. E. Peralta, F. Ogliaro, M. Bearpark, J. J. Heyd, E. Brothers, K. N. Kudin, V. N. Staroverov, R. Kobayashi, J. Normand, K. Raghavachari, A. Rendell, J. C. Burant, S. S. Iyengar, J. Tomasi, M. Cossi, N. Rega, J. M. Millam, M. Klene, J. E. Knox, J. B. Cross, V. Bakken, C. Adamo, J. Jaramillo, R. Gomperts, R. E. Stratmann, O. Yazyev, A. J. Austin, R. Cammi, C. Pomelli, J. W. Ochterski, R. L. Martin, K. Morokuma, V. G. Zakrzewski, G. A. Voth, P. Salvador, J. J. Dannenberg, S. Dapprich, A. D. Daniels, Ö. Farkas, J. B. Foresman, J. V. Ortiz, J. Cioslowski, and D. J. Fox, Gaussian, Inc., Wallingford CT, 2009.
- 24 Y. Zhao and D. G. Truhlar, *J. Chem. Phys.* 2006, **125**, 194101.
- 25 Y. Zhao and D. G. Truhlar, *Acc. Chem. Res.* 2008, **41**, 157–167.
- 26 A.D. Becke *Phys. Rev. B*, 1988, **38**, 3098.
- 27 C. Lee, W. Yang and R.G. Parr *Phys. Rev. B*, 1988, **37**, 785.
- 28 M. Swart, A.W. Ehlers and K. Lammertsma, *Molec. Phys.* 2004, **102**, 2467.
- 29 D. Andrae, U. Haussermann, M. Dolg, H. Stoll and H. Preuss, *Theor. Chim. Acta* 1990, **77**, 123–141.
- 30 K. Fukui, *J. Phys. Chem.* 1970, **74**, 4161–4163.
- 31 C. Gonzalez and H. B. Schlegel, *J. Chem. Phys.* 1989, **90**, 2154–2161.
- 32 A. V. Mareich, C. A. V. Marenich, C. J. Cramer and D. G. Truhlar, *J. Phys. Chem. B*, 2009, **113**, 6378–6396.
- 33 E. D. Glendening, J. E. Reed, J. E. Carpenter and F. Weinhold, NBO Program 3.1; Madison, WI, 1988.
- 34 A. E. Reed, L. A. Curtiss and F. Weinhold, *Chem. Rev.* 1988, **88**, 899–926.
- 35 H. Sugimoto, S. Tatemoto, K. Suyama, H. Miyake, S. Itoh, C. Dong, J. Yang and M. L. Kirk, *Inorg. Chem.* 2009, **48**, 10581–10590.
- 36 R. H. Holm *Chem. Rev.* 1987, **87**, 1401–1449.
- 37 K. Tatsumi, and R. Hoffmann *Inorg. Chem.*, **19**, 1980, 2656–2658.

Graphical Abstract



Supporting Information

Mechanistic investigation of the trimethylamine-N-oxide reduction catalysed by biomimetic molybdenum enzyme models

M. Fortino, T. Marino, N. Russo, E. Sicilia

Cartesian coordinates (Å) of all optimized structures

Tables S1-S5

The most relevant geometrical parameters of minima and transition states intercepted along the pathway for the Me_3NO reduction by the $[\text{Mo(IV)}\text{O}(\text{bdt})_2]^{2-}$ complex.

Figure S1

Me_3NO attack to the $[\text{Mo(IV)}\text{O}(\text{bdt})_2]^{2-}$ complex PESs for the examined singlet and the triplet electronic spin states.

Figure S2

M06-L optimized geometries for the Me_3NO cis-attack to the monooxomolybdenum(IV) $\text{E}_{(\text{CONH})}$ complex in its *cis* and *trans* arrangements.

Figure S3

M06-L free energy profiles for the Me_3NO trans-attack to the monooxomolybdenum(IV) $\text{E}_{(\text{CONH})}$ complex in its *cis* and *trans* arrangements. Energies are in kcal mol⁻¹ and relative to reactants' asymptote

Figure S4

M06-L optimized geometries for the Me_3NO *trans*-attack to the monooxomolybdenum(IV) $\text{E}_{(\text{CONH})}$ complex in its *cis* and *trans* arrangements.

Figure S5

M06-L optimized geometry of the transition state for the *cis* to *trans* interconversion of the initial monooxo(CONH) complex.

Figure S6

M06-L optimized geometries for the Me_3NO cis-attack to the monooxomolybdenum(IV) $\text{E}_{(\text{NHCO})}$ complex in its *cis* and *trans* arrangement

Figure S7

M06-L free energy profiles for the Me_3NO trans-attack to the monooxomolybdenum(IV) $\text{E}_{(\text{NHCO})}$ complex in its *cis* and *trans* arrangements. Energies are in kcal mol⁻¹ and relative to reactants' asymptote

Figure S8

M06-L optimized geometries for the Me_3NO *trans*-attack to the monooxomolybdenum(IV) $\text{E}_{(\text{NHCO})}$ complex in its *cis* and *trans* arrangement

Figure S9

Table S1**E**

Mo	0.00003500	-0.00000600	0.73683200
S	-1.66518800	-1.61056200	-0.03008700
S	1.66501600	1.61049700	-0.03073600
S	-1.66525900	1.61058800	-0.02989900
S	1.66509500	-1.61052600	-0.03057600
O	0.000039800	-0.00001700	2.44881700
C	-5.54517600	-0.69889800	-0.84242700
H	-6.46350400	-1.25293500	-1.03918300
C	-5.54521300	0.69884500	-0.84232700
H	-6.46357000	1.25286300	-1.03900400
C	-3.15648900	0.70808300	-0.32318000
C	3.15641400	0.70808300	-0.32343800
C	-4.35726100	-1.38441900	-0.58795800
C	4.35735000	-1.38438700	-0.58770300
H	4.34251700	-2.47463700	-0.59011800
C	-4.35733100	1.38439400	-0.58777900
C	-3.15645700	-0.70808000	-0.32326300
C	4.35726800	1.38443300	-0.58787700
C	5.54524300	0.69891600	-0.84208000
H	6.46360300	1.25295900	-1.03866500
C	5.54528200	-0.69883100	-0.84200000
H	6.46367400	-1.25284500	-1.03851700
C	3.15645700	-0.70807500	-0.32333500
H	-4.34237800	-2.47466800	-0.59046900
H	-4.34250500	2.47464400	-0.59014700
H	4.34237100	2.47468200	-0.59042100

TS1

Mo	0.25056600	-0.12233600	-0.64179600
S	-1.11098500	-0.34913800	1.57505900
S	2.03303400	-1.72022800	-0.81694400
S	-1.38150000	-1.88960300	-1.23757600
S	1.82175700	1.01615000	0.87168700
O	0.38364800	0.79374200	-2.08971800
C	-5.00948800	-1.48510600	1.53212300
H	-5.86629200	-1.39868200	2.20155200
C	-5.13030600	-2.13972200	0.30264400
H	-6.08512900	-2.56496800	-0.00881100
C	-2.77481300	-1.68176800	-0.18572500
C	3.46680100	-0.99711200	-0.06817900
C	-3.77957500	-0.93769400	1.89898500
C	4.54273800	0.72133200	1.26756600
H	4.45973800	1.64288700	1.84489800
C	-4.01757200	-2.23437600	-0.53377500
C	-2.64740600	-1.01815000	1.06919000
C	4.71518700	-1.62701300	-0.18828900
C	5.86490600	-1.09765700	0.39740400
H	6.82159300	-1.60760900	0.28024000
C	5.77857700	0.08779200	1.13256500
H	6.66634100	0.51769200	1.59760300
C	3.38150600	0.20458800	0.67459200
H	-3.67250900	-0.42984200	2.85812700
O	-1.85808600	1.70548000	-0.73231500
N	-1.55317500	2.96311900	-0.33321500
C	-2.70714700	3.84822600	-0.67655000
C	-0.32090900	3.47876700	-1.02484300
C	-1.32256900	3.01306900	1.14838500
Mo	0.26700900	0.03546200	-0.86165500
S	-0.82692500	-0.80450900	1.76042400
S	2.01048600	-1.70150400	-0.64522500
S	-1.40547600	-1.82924300	-1.27334600

H	-2.52705800	4.88520100	-0.36070000
H	-2.84050600	3.78430700	-1.75694700
H	-3.58097500	3.42816600	-0.17732500
H	-0.17421400	4.53877400	-0.77864200
H	0.52237900	2.86798700	-0.69288100
H	-0.46827700	3.31595900	-2.09192600
H	-1.11968700	4.04472100	1.46535300
H	-2.21304600	2.60045500	1.62400200
H	-0.48308200	2.34888200	1.36181900
H	-4.09946200	-2.74329300	-1.49416100
H	4.76769900	-2.55406600	-0.76016000

ES

Mo	0.26570300	-0.04139000	-0.73580700
S	-0.92849600	-0.57574600	1.67181400
S	2.04442100	-1.68372500	-0.76120700
S	-1.42699400	-1.80779000	-1.27794800
S	1.83775500	1.17982700	0.71693100
O	0.48862200	0.77689200	-2.23444400
C	-4.94166300	-1.21223000	1.60913600
H	-5.77286000	-1.07651100	2.30283900
C	-5.15806200	-1.73335400	0.33093600
H	-6.16214800	-2.00539300	0.00285200
C	-2.76466800	-1.53690100	-0.16785900
C	3.46529800	-0.93149400	-0.02496600
C	-3.64559500	-0.86622900	1.99762700
C	4.54096000	0.87455400	1.19577000
H	4.45886700	1.84205900	1.69252700
C	-4.07205400	-1.89183100	-0.53368600
C	-2.53480400	-1.01515900	1.14514200
C	4.70701600	-1.58709000	-0.05769900
C	5.85122300	-1.02951300	0.51223000
H	6.80072700	-1.56362800	0.46262100
C	5.76910000	0.21418400	1.14475600
H	6.65266700	0.66750000	1.59542400
C	3.38600300	0.32839200	0.61793300
H	-3.46591000	-0.46709100	2.99675600
O	-1.67407900	1.27585800	-0.69497400
N	-1.65510700	2.58114900	-0.26636600
C	-3.00080400	3.13153600	-0.58179100
C	-0.59702900	3.35826300	-0.98669600
C	-1.41817000	2.67065000	1.20999400
H	-3.08846500	4.17039400	-0.23916600
H	-3.13097900	3.05804600	-1.66167200
H	-3.72473100	2.48320800	-0.08551900
H	-0.66401200	4.41734700	-0.70773700
H	0.36747700	2.92417800	-0.70728000
H	-0.75510700	3.19895300	-2.05311200
H	-1.45102300	3.72366000	1.51768100
H	-2.18376300	2.06753300	1.69893000
H	-0.44734300	2.21515000	1.41493200
H	-4.22954500	-2.29176800	-1.53530100
H	4.75856800	-2.55903200	-0.54937800

TS2

S	1.85124300	1.33960700	0.50950400
O	0.59655400	0.67753100	-2.41947300
C	-4.88699500	-0.99966500	1.60058800
H	-5.71128600	-0.80538800	2.28923100

C -5.13617000 -1.42931800 0.29581600
 H -6.15673000 -1.57180100 -0.06174400
 C -2.72348300 -1.47983600 -0.15551300
 C 3.41952700 -0.90297900 0.04279800
 C -3.56837800 -0.81900500 2.02597800
 C 4.51964600 1.00166800 1.08748100
 H 4.45276500 2.02193500 1.46635300
 C -4.05274800 -1.66212800 -0.55919100
 C -2.45376900 -1.05209700 1.19057400
 C 4.64394500 -1.59007100 0.13100900
 C 5.78632400 -1.00371300 0.67295200
 H 6.71766900 -1.56898000 0.71778000
 C 5.72750100 0.30672100 1.15513800
 H 6.61049900 0.78373500 1.58109800
 C 3.36526800 0.42464000 0.54086200
 H -3.36819600 -0.49388000 3.04779900
 O -1.52613800 1.03327300 -0.70289700
 N -1.71966900 2.45381300 -0.12050300
 C -3.14262300 2.69833200 -0.375756300
 C -0.83004300 3.35410800 -0.86216500
 C -1.41922400 2.43611700 1.32012800
 H -3.44084000 3.68398500 0.00684900
 H -3.30492500 2.63247000 -1.45226800
 H -3.70165000 1.89956700 0.11643700
 H -0.90642900 4.37607700 -0.46770800
 H 0.18944600 2.96578800 -0.74933800
 H -1.10661700 3.31177700 -1.91654800
 H -1.54088500 3.44931300 1.72923100
 H -2.08682600 1.71649200 1.79728200
 H -0.39565200 2.07389000 1.45076100
 H -4.23246700 -1.98062500 -1.58597000
 H 4.68019000 -2.61312700 -0.24315600

Dioxo_P

Mo-0.31734300 -0.90196700 0.78554900
 S 1.34024500 0.64881300 1.79814300
 S -2.15608500 -1.69524400 -0.70088700
 S 0.17188600 0.79306800 -1.24259100
 S -2.31169000 0.81899200 1.36121200
 O -0.46730700 -1.48095500 2.42160100
 C 3.53030400 3.58678600 0.10691900
 H 4.34833300 4.23276300 0.42323000
 C 2.99347900 3.68869000 -1.17989400
 H 3.38696600 4.42057400 -1.88522300
 C 1.41618400 1.87257900 -0.69952500
 C -3.51783100 -0.58905900 -0.68048000
 C 3.000163700 2.64566400 0.98925700
 C -4.69315800 1.37298600 0.12426700
 H -4.72604500 2.23460200 0.78884800
 C 1.95389700 2.84843400 -1.56532600
 C 1.95236900 1.79211200 0.61637100
 C -4.58129800 -0.81569700 -1.56695000
 C -5.68945000 0.02908200 -1.61604500
 H -6.49707400 -0.16906300 -2.31986600
 C -5.73872500 1.13479500 -0.76178200
 H -6.59043900 1.81483400 -0.78846900
 C -3.56682000 0.52641200 0.20384100
 H 3.40529200 2.55470200 1.99692100
 O 0.58075000 -2.16918300 -0.01525200
 H 1.53775700 2.91956100 -2.56884000
 H -4.52102800 -1.67576000 -2.23265100
 N 4.30079700 -2.03012100 -1.24671300
 C 5.69620300 -1.96258600 -0.88923000
 H 6.20390500 -2.89781200 -1.16118800
 H 6.18211500 -1.13720800 -1.42291900
 H 5.85520200 -1.79639600 0.20031800
 C 3.65478600 -3.13179900 -0.55661600

H 2.58719500 -3.14410700 -0.78903500
 H 4.11419100 -4.08139300 -0.86210600
 H 3.73961600 -3.04416800 0.54655700
 C 3.62852400 -0.77584600 -0.92243300
 H 4.08153800 0.04838100 -1.48474200
 H 2.56658000 -0.83617100 -1.18143900
 H 3.69089600 -0.53412200 0.15547300

Dioxo

Mo 0.00004800 -1.38473600 -0.00004000
 S 2.13472700 -0.95157200 1.20912800
 S -2.13435700 -0.95109300 -1.20957600
 S 1.08653600 0.62264700 -1.45150800
 S -1.08673600 0.62239500 1.45175600
 O -0.28700200 -2.46536200 1.33596800
 C 5.16093800 1.59072800 0.38879600
 H 6.13654900 1.80813200 0.82215500
 C 4.70229200 2.28796000 -0.73287700
 H 5.31707700 3.06312600 -1.19130600
 C 2.61585100 0.99221000 -0.72667100
 C -3.08611000 0.29634500 -0.42375400
 C 4.34759000 0.60848800 0.95259000
 C -3.45334100 1.99172300 1.26921200
 H -3.09377800 2.53227400 2.14340600
 C 3.45306000 1.99216300 -1.26890200
 C 3.08624400 0.29618400 0.42355700
 C -4.34750500 0.60858400 -0.95274800
 C -5.16108800 1.59047400 -0.38867300
 H -6.13673800 1.80782600 -0.82200700
 C -4.70260600 2.28746100 0.73321300
 H -5.31755800 3.06237900 1.19183800
 C -2.61593400 0.99206100 0.72675200
 H 4.68588100 0.05783600 1.82950700
 O 0.28697800 -2.46564200 -1.33584000
 H 3.09335000 2.53292800 -2.14290900
 H -4.68566900 0.05811700 -1.82983000

Table S2**Cis-E_{CONH}**

Mo 0.01763500 -1.86266300 0.79488300
 S -1.63445000 -3.28460700 -0.24316600
 S 1.65696900 -0.14175100 0.29205500
 S -1.63469600 -0.16444400 0.26041000
 S 1.70096400 -3.26641300 -0.21807200
 O 5.80210200 1.75573400 -0.18414500
 O 0.00761500 -2.13861200 2.48152300
 O -5.82039700 1.68364800 -0.39288700
 N 3.56068500 2.09889000 -0.30152300
 H 2.65142000 1.63762600 -0.23352200
 N -3.59981200 2.05133500 -0.12097900
 H -2.68676400 1.60841900 0.00079700
 C -4.66470700 1.22786800 -0.30450200
 C -5.49141500 -2.35482800 -0.97973500
 H -6.38758100 -2.90352100 -1.26693000
 C -5.54074300 -0.98268800 -0.79369800
 H -6.46287000 -0.42480800 -0.92545800
 C -3.16418700 -0.93579200 -0.22221300
 C -2.24063300 3.97064200 0.30202100
 H -1.60462900 3.72376600 -0.55490000
 H -1.80438900 3.49118100 1.18504600
 H -2.21445700 5.05612900 0.44934300
 C 3.19551200 -0.89786300 -0.18626900
 C -4.28485800 -3.02630200 -0.79865900
 C 4.35628700 -2.97117400 -0.74128100
 H 4.30919800 -4.04935800 -0.88995100
 C -4.39780000 -0.24773400 -0.42818100
 C -3.12670100 -2.34261700 -0.41974100
 C 4.41997700 -0.19289100 -0.37932400
 C -3.67578100 3.49923200 0.07448700
 C 5.58149300 -0.90873700 -0.72114100
 H 6.49785800 -0.33758600 -0.83661000
 C -4.52980700 3.83740900 1.29984100
 H -4.55837600 4.92385900 1.45459400
 H -4.10741900 3.37272900 2.19694400
 H -5.54846000 3.46734500 1.16304200
 C -4.25137500 4.17980100 -1.17011900
 H -3.63505800 3.95411100 -2.04656700
 H -4.27010200 5.26884000 -1.03306700
 H -5.26702700 3.82532200 -1.35869800
 C 5.55540100 -2.28220300 -0.90568700
 H 6.46350500 -2.81800300 -1.17950000
 C 3.58283100 3.54503600 -0.07284000
 C 4.65183400 1.28749300 -0.26200500
 C 2.12663600 4.00353900 -0.12079500
 H 1.53008100 3.50401500 0.65025200
 H 1.67414400 3.77148900 -1.09092400
 H 2.06195700 5.08554300 0.04017000
 C 4.17834600 3.87024900 1.30031200
 H 5.21439400 3.52922200 1.35623900
 H 3.60477100 3.37368300 2.08966900
 H 4.14911300 4.95269300 1.48033500
 C 4.38327100 4.24636300 -1.17255100
 H 3.94520200 4.03714600 -2.15434700
 H 5.41682400 3.89249900 -1.17067700
 H 4.37185900 5.33274400 -1.01485500
 C 3.18206700 -2.30514800 -0.37891700
 H -4.21901800 -4.10346300 -0.94758300

S -2.15686200 0.15313400 0.11334500
 S 1.12799000 1.11306300 0.78655800
 S -1.24813700 -2.83600600 -0.33342300
 O -6.76445300 0.54234900 0.19524400
 O 0.22278000 -0.45960400 -2.03807500
 O 4.70053900 3.18429700 1.06288600
 N -4.76582500 1.60672700 0.11819200
 H -3.75149400 1.48525500 0.07298700
 N 3.93882400 1.73226700 -0.54709300
 H 3.40648200 0.86403200 -0.64697300
 C 4.14900300 2.12026800 0.74998600
 C 4.51060800 -0.54866800 3.37033300
 H 5.25688900 -0.89906500 4.08312900
 C 4.73180200 0.60905000 2.62907200
 H 5.66662300 1.16249000 2.70083700
 C 2.51596100 0.39035300 1.61411700
 C 3.22280400 1.84081600 -2.82761200
 H 2.28591100 1.34615700 -2.54140300
 H 3.93251600 1.06018700 -3.12870400
 H 3.03380700 2.48338000 -3.69553500
 C -3.41952300 -1.09191800 -0.11405300
 C 3.35308100 -1.29892200 3.14481200
 C -3.89723600 -3.46186800 -0.45558000
 H -3.51809800 -4.47452200 -0.59058400
 C 3.75738100 1.05578900 1.72457800
 C 2.36807300 -0.87803400 2.23989700
 C -4.82388600 -0.83919400 -0.08922200
 C 3.78668200 2.66569700 -1.67287400
 C -5.71832600 -1.91364600 -0.25105900
 H -6.77819900 -1.68061500 -0.22527900
 C 5.14622400 3.25560200 -2.05017500
 H 5.04497300 3.92896900 -2.91202100
 H 5.84978700 2.45774700 -2.31723500
 H 5.56213700 3.81401700 -1.20720200
 C 2.80230500 3.78304300 -1.31866200
 H 1.84234400 3.35076200 -1.01880100
 H 2.64732100 4.43806100 -2.18579500
 H 3.18328500 4.38223200 -0.48736800
 C -5.26672800 -3.21078700 -0.43315300
 H -5.97743700 -4.02726800 -0.55770200
 C -5.27662000 2.95991500 0.33957900
 C -5.52477200 0.48067900 0.09203400
 C -4.05957900 3.88221600 0.32214900
 H -3.53897300 3.82690600 -0.63965300
 H -3.34258100 3.60524800 1.10198500
 H -4.36843400 4.92017000 0.48914700
 C -6.24236900 3.36231100 -0.77844900
 H -7.10379500 2.69132600 -0.79555300
 H -5.74070600 3.31022200 -1.75056700
 H -6.59051800 4.39231600 -0.62530000
 C -5.97551600 3.05927600 1.69872900
 H -5.28175500 2.79048900 2.50192000
 H -6.83177100 2.38247600 1.73698900
 H -6.32256400 4.08622400 1.87252400
 C -2.97017800 -2.42661300 -0.30590000
 H 3.21016500 -2.25269000 3.65323200
 O 2.60822600 -1.00614900 -0.85707400
 N 3.19509900 -2.18619800 -1.21765300
 C 4.08837500 -2.64854400 -0.11041200
 C 3.98741000 -1.95234600 -2.45772000
 C 2.14726400 -3.22501100 -1.47753700
 H 4.60544600 -3.57414000 -0.39401800
 H 4.79469000 -1.84062000 0.08895400
 H 3.44403600 -2.79340100 0.75989700
 H 4.47966000 -2.87464700 -2.79167200
 H 3.28876200 -1.57960000 -3.20807800
 H 4.72241300 -1.17930000 -2.22561100
 H 2.62042800 -4.14860600 -1.83330800
 H 1.61801700 -3.37729000 -0.53301300
 H 1.45274000 -2.80573500 -2.20749100

Cis-TS1 CONH (Cis attack)

Mo -0.00296900 -0.74320400 -0.35621000
 S 1.04299200 -1.93207200 1.77994700

Cis-ES_{CONH} (Cis Attack)

Mo 0.10880500 -0.57344200 -0.40238800
S 0.67511800 -1.32984200 2.28463200
S-2.11571500 0.24790600 0.04807500
S 1.18488100 1.39615500 0.67980400
S-1.06048400 -2.70624400 -0.41515100
O-6.73498000 0.40405800 0.11647800
O 0.30805900 -0.25510300 -2.08367200
O 4.99104100 3.00968900 0.61908500
N-4.79113700 1.56941300 0.07827100
H-3.77100200 1.49582600 0.04623800
N 4.05121900 1.38835000 -0.71232000
H 3.35532800 0.64312400 -0.65444700
C 4.30458000 1.98702400 0.49725000
C 4.38087400 -0.22640700 3.52130200
H 5.09940300 -0.55772000 4.27165600
C 4.72950100 0.75807900 2.60184100
H 5.72910700 1.18854600 2.57484900
C 2.47340700 0.66879200 1.65268000
C 3.46705100 1.10689800 -3.01256200
H 2.46600100 0.77275500 -2.70759900
H 4.11154400 0.22146800 -3.10384400
H 3.39376600 1.57184100 -4.00269300
C-3.30753600 -1.05360700 -0.19859800
C 3.12475100 -0.83453500 3.44470800
C-3.67492600 -3.44040800 -0.58769500
H-3.24580900 -4.43043500 -0.73898500
C 3.79109200 1.17163100 1.64176900
C 2.15852700 -0.43946100 2.50148800
C-4.72489600 -0.87167100 -0.17736200
C 4.05165900 2.09225900 -2.00267200
C-5.56571100 -1.98472300 -0.36562600
H-6.63543900 -1.80158000 -0.34191300
C 5.48120900 2.46878500 -2.39156700
H 5.49212600 2.95374700 -3.37699600
H 6.11186800 1.57278800 -2.44163100
H 5.90914400 3.14920300 -1.65107800
C 3.16631800 3.33873200 -1.93570100
H 2.15277400 3.05697100 -1.63322900
H 3.12622400 3.83161900 -2.91596000
H 3.55866600 4.04698900 -1.20084400
C-5.05529600 -3.25589800 -0.57132700
H-5.72622800 -4.10182500 -0.71752800
C-5.36791300 2.89193600 0.31961800
C-5.49257000 0.40826400 0.02358500
C-4.19626900 3.87171300 0.32551600
H-3.66745600 3.85757100 -0.63338600
H-3.47150800 3.61672100 1.10560200
H-4.55582200 4.89083700 0.50675100
C-6.34494300 3.26754400 -0.79781800
H-7.17488900 2.55867500 -0.83141300
H-5.83589300 3.25383400 -1.76748200
H-6.74048200 4.27807700 -0.63086100
C-6.07804400 2.93493400 1.67569300
H-5.37696300 2.68516000 2.47855700
H-6.90127500 2.21768300 1.69684000
H-6.47445900 3.94115700 1.86429200
C-2.80246600 -2.36620000 -0.40759400
H 2.87273900 -1.65519200 4.11605900
O 2.29647400 -1.11707200 -0.44134200
N 2.77997800 -2.37480900 -0.78031000
C 4.26115800 -2.24612900 -0.78746600
C 2.26770500 -2.75812800 -2.12808800
C 2.37034900 -3.39130200 0.23629400
H 4.72372400 -3.20565200 -1.04289700
H 4.52058900 -1.47371300 -1.51349800
H 4.55565200 -1.91265400 0.20941900

H 2.67690700 -3.73342000 -2.41454600
H 1.17571700 -2.77838900 -2.06016200
H 2.56569900 -1.97150600 -2.82229200
H 2.79918100 -4.36094400 -0.04238700
H 2.72046200 -3.04364600 1.20910800
H 1.27917000 -3.42296800 0.25896900

Cis-TS2_{CONH} (Cis attack)

Mo-0.18735700 -1.71158900 -0.62180500
S 0.71077000 -1.87499200 1.95319000
S -1.72537600 0.03579500 0.11560000
S 1.73560500 0.10502800 -0.43413000
S -2.04807100 -3.14327800 -0.10376900
O -5.69373800 2.15993300 0.75039700
O -0.17307400 -1.42065900 -2.31930600
O 5.27149100 2.45499700 0.55699600
N -3.62288200 2.32103300 -0.17392500
H -2.76987900 1.78814300 -0.36234200
N 3.11900800 2.78938000 -0.13206700
H 2.24511500 2.26805800 -0.21126400
C 4.07768900 2.11651600 0.57446100
C 3.84003600 0.01798800 3.65176000
H 4.35079900 -0.03894400 4.61254400
C 4.24381800 0.93584800 2.69288500
H 5.07563900 1.61473900 2.86173800
C 2.50210700 0.13410700 1.15133000
C 2.04237800 4.01558000 -1.88242500
H 1.45292800 4.60180600 -1.16810100
H 1.46595800 3.11879900 -2.13710500
H 2.17318600 4.61062900 -2.79346200
C -3.35246700 -0.66390800 0.15267800
C 2.76074100 -0.81949400 3.38502300
C -4.71517900 -2.69008900 0.20248800
H -4.76242900 -3.77807500 0.16026900
C 3.57572900 1.02090200 1.46160900
C 2.06522700 -0.79189800 2.16181500
C -4.54815900 0.10411700 0.28970200
C 3.40097800 3.63894000 -1.29536400
C -5.78751000 -0.55219700 0.39697900
H -6.66989900 0.07096800 0.51173200
C 4.21660400 2.86872100 -2.33872300
H 4.42563400 3.50306300 -3.21035600
H 3.66335400 1.98446000 -2.67134900
H 5.16612500 2.54188100 -1.90623600
C 4.14791700 4.90185600 -0.86151500
H 3.60722500 5.40668700 -0.05832200
H 4.23079700 5.59586800 -1.71308900
H 5.14793400 4.65354900 -0.50432300
C -5.87784800 -1.93461100 0.35537000
H -6.84657900 -2.42704500 0.43593100
C -3.46278200 3.77121400 -0.04313800
C -4.66335700 1.60300600 0.32806900
C -2.08329400 4.10087300 -0.61260200
H -2.00009200 3.77936300 -1.65659500
H -1.29096000 3.59705100 -0.04833600
H -1.90128100 5.18080500 -0.56948400
C -4.54490900 4.49973100 -0.84267400
H -5.53469300 4.23187300 -0.46555500
H -4.48844700 4.22309000 -1.90099900
H -4.40945400 5.58642100 -0.76262100
C -3.52214000 4.19166100 1.42794300
H -2.74119400 3.67925600 1.99887600
H -4.49392300 3.93213800 1.85470500
H -3.36655200 5.27431300 1.52180500
C -3.46128200 -2.08289300 0.09768300
H 2.41824800 -1.52764800 4.13722400
O 0.84268700 -3.54513800 -0.82138000
N 2.32312200 -3.67829100 -1.10246500

C 3.12308200 -3.21005400 0.04823600
 C 2.62702200 -2.89324700 -2.31365400
 C 2.50810600 -5.11676000 -1.32667800
 H 4.18579900 -3.40386200 -0.15187700
 H 2.94162100 -2.14216000 0.16898500
 H 2.76987700 -3.72620800 0.94069700
 H 3.68214600 -3.02842400 -2.58466900
 H 1.95875300 -3.22915300 -3.10678900
 H 2.41499900 -1.84487800 -2.08559700
 H 3.55792900 -5.33706200 -1.56219600
 H 2.19943600 -5.63435700 -0.41821300
 H 1.85532900 -5.41265500 -2.14823500

Dioxo_P CONH (Cis/Trans) (Cis attack)

M o 1.48536800 -1.72622200 -0.59733900
 S 1.44448700 -1.24451400 2.06030800
 S -1.03697600 -0.85876100 -0.52528400
 S 1.78081000 0.76255000 -0.42533900
 S 0.21214900 -3.82115200 -0.43162600
 O -5.42117600 -0.72983800 -0.35524600
 O 1.69448800 -1.38731100 -2.29209900
 O 0.63115900 4.80089400 0.15901400
 N -3.63682300 0.08654000 0.81377900
 H -2.63811300 -0.06738100 0.93930600
 N -0.28658700 3.00651000 -0.92491800
 H -0.30341200 1.99168100 -0.89309800
 C 0.38378300 3.58862000 0.11328800
 C 0.35620100 2.31416600 3.62965800
 H 0.08490000 2.69394400 4.61405000
 C 0.33768200 3.15782900 2.52411800
 H 0.02669500 4.19702600 2.59958200
 C 1.09742800 1.32066800 1.10192600
 C -0.89691000 2.43606900 -3.16826700
 H -1.88046700 2.08372300 -2.83844700
 H -0.21373000 1.57903100 -3.14139900
 H -0.98495000 2.77907300 -4.20510200
 C -2.09104500 -2.23817600 -0.30891000
 C 0.67025500 0.96831000 3.46859300
 C -2.34713200 -4.67264700 -0.34198000
 H -1.87978000 -5.65382400 -0.40291400
 C 0.66104300 2.65981000 1.25581400
 C 1.04520500 0.43652700 2.22006600
 C -3.50108000 -2.13955200 -0.13458500
 C -0.38553200 3.56821400 -2.28115900
 C -4.29672600 -3.29205900 -0.13058900
 H -5.37106400 -3.15491700 -0.03809800
 C 0.98954200 4.02366300 -2.77708500
 H 0.91395100 4.38919400 -3.80896600
 H 1.69426300 3.18627900 -2.75453500
 H 1.38235100 4.82511300 -2.14669800
 C -1.36925600 4.73787200 -2.28090700
 H -2.35645300 4.40580600 -1.94146400
 H -1.47218700 5.15053400 -3.29289900
 H -1.01731400 5.52570800 -1.60977600
 C -3.73106300 -4.55552900 -0.23781500
 H -4.35673800 -5.44606100 -0.22632900
 C -4.03701500 1.50176100 0.86879800
 C -4.26108200 -0.86305000 0.06309900
 C -2.96050000 2.20596100 1.68635700
 H -1.96841400 2.04164100 1.25208800
 H -2.93369100 1.83629700 2.71721600
 H -3.13572300 3.28754100 1.70836500
 C -4.07736600 2.09256100 -0.54293100
 H -4.79715900 1.55457000 -1.16600200
 H -3.08607700 2.02308600 -1.00428600
 H -4.36175800 3.15167000 -0.50522700
 C -5.39793700 1.64674400 1.54852200
 H -5.37301600 1.20065900 2.54878000

H -6.17652400 1.14856900 0.96673600
 H -5.64854500 2.71022000 1.65272900
 C -1.52206400 -3.54234800 -0.37007800
 H 0.63990300 0.29130600 4.31997100
 O 2.88646800 -2.69253700 -0.20859200
 N 6.05218100 -0.45484500 0.28811500
 C 5.04777900 -0.62452900 1.33376900
 C 5.45581300 -0.68802900 -1.01985600
 C 6.60795800 0.87851300 0.34693900
 H 4.22562400 0.10966100 1.26045000
 H 4.59173000 -1.61516200 1.26123200
 H 5.52138500 -0.51773600 2.31721100
 H 4.67943100 0.05906100 -1.27158200
 H 6.23552200 -0.65027700 -1.79154300
 H 4.97373800 -1.66884000 -1.03803800
 H 5.84390100 1.67033800 0.19665400
 H 7.07589800 1.04727300 1.32466000
 H 7.37603900 1.00125900 -0.42749000

Dioxo CONH (Cis/Trans)

Mo-1.71708100 -2.20762700 -0.48215500
 S -1.29311200 -2.01213900 2.17520500
 S -0.88662800 0.33641100 -0.53014200
 S 0.77443300 -2.46786300 -0.23279700
 S -3.83030600 -0.95161700 -0.38909800
 O -0.88648000 4.78410100 -0.52823100
 O -1.34673100 -2.44975900 -2.16641300
 O 4.78773700 -1.12144100 0.39400700
 N 0.06774800 3.02132000 0.55630600
 H -0.02228000 2.01436200 0.68767800
 N 3.00614700 -0.42940500 -0.86093600
 H 1.99217200 -0.48691000 -0.89965000
 C 3.56649000 -0.95470500 0.26734500
 C 2.17782300 -0.64731000 3.72164400
 H 2.52066600 -0.27267100 4.68547500
 C 3.05166600 -0.70323500 2.64178100
 H 4.07810300 -0.35176900 2.71513300
 C 1.28125900 -1.65068500 1.24690800
 C 2.58627200 0.07999300 -3.15952100
 H 2.14991000 1.04739400 -2.88778100
 H 1.77213500 -0.65346800 -3.18333500
 H 3.00840800 0.16376100 -4.16714100
 C -2.27837600 1.38179700 -0.37687100
 C 0.84869700 -1.02435400 3.55643300
 C -4.71892000 1.59373100 -0.41815400
 H -5.69194400 1.10677800 -0.45262800
 C 2.60184700 -1.15982900 1.39545500
 C 0.36572200 -1.53017700 2.33505800
 C -2.20387800 2.80234400 -0.27894400
 C 3.66910100 -0.33539200 -2.16710100
 C -3.37316000 3.57452900 -0.30807600
 H -3.25485300 4.65400900 -0.26826000
 C 4.24856300 -1.69290500 -2.57492000
 H 4.70586300 -1.62493300 -3.57027200
 H 3.45566700 -2.44706600 -2.60572000
 H 5.00721000 -2.01562200 -1.85771300
 C 4.77183300 0.72234200 -2.11072800
 H 4.35506900 1.69153600 -1.81503100
 H 5.24268400 0.83418400 -3.09601400
 H 5.53355000 0.43668300 -1.38111500
 C -4.62615200 2.98283400 -0.38144100
 H -5.52742700 3.59311300 -0.39497600
 C 1.43698500 3.54665900 0.63356200
 C -0.94883400 3.61002100 -0.12748100
 C 2.25468800 2.48531000 1.36085900
 H 2.24754800 1.53995900 0.80832600

H	1.85396700	2.28374600	2.36034700
H	3.29861300	2.80422900	1.46248300
C	2.00327500	3.75811100	-0.77324400
H	1.40331900	4.48778700	-1.32307100
H	1.99585700	2.81046600	-1.32343900
H	3.03994400	4.11411400	-0.71805500
C	1.45416400	4.85913600	1.41840400
H	1.06065800	4.70134100	2.42839300
H	0.83966200	5.61226700	0.91912800
H	2.48356300	5.23023100	1.50481000
C	-3.57479400	0.78827100	-0.40854800
H	0.14652000	-0.94038600	4.38365100
O	-2.66581000	-3.60687600	-0.06855600

Trans-E CONH

Mo	-0.02129100	-0.02543200	0.81599700
S	-2.31277300	-0.25247300	0.03654900
S	2.29055100	0.23585300	0.11701700
S	-0.35429100	2.23878200	0.03223800
S	0.34216400	-2.24538600	-0.06748200
O	6.68875700	-0.98192800	-0.65996800
O	-0.04482300	-0.06447800	2.52451700
O	-6.59229800	0.89856800	-1.03368200
N	5.24433700	0.65687800	-0.06092500
H	4.26550500	0.89086300	0.11980300
N	-5.30749700	-0.54257300	0.16376400
H	-4.34307800	-0.73975800	0.43863800
C	-5.50418500	0.63371400	-0.49256700
C	-4.79783100	2.94155100	-0.75881500
H	-5.85484600	3.09276500	-0.95726200
C	-3.89880200	3.99616700	-0.77916100
H	-4.24197000	5.00851000	-0.98926300
C	-2.08946900	2.45894400	-0.25244400
C	-5.52525300	-2.82087800	0.86192000
H	-5.35535900	-2.53299100	1.90494400
H	-4.55319000	-3.06710100	0.42166500
H	-6.14813600	-3.72227000	0.84966100
C	2.99510400	-1.36067900	-0.23034900
C	-4.37872300	1.62825600	-0.48067800
C	2.55093100	-3.72732200	-0.63754300
H	1.82422200	-4.53592800	-0.70697600
C	-2.55138600	3.74963800	-0.52584400
H	-1.82590800	4.56226900	-0.53864700
C	-2.99994400	1.36903300	-0.22933800
C	4.38285300	-1.60922300	-0.45768300
C	-6.20907200	-1.69520000	0.08911900
C	4.80398000	-2.91600200	-0.76766700
H	5.86697900	-3.06404300	-0.93023600
C	-6.41769400	-2.12508800	-1.36613400
H	-7.06312400	-3.01164300	-1.41379500
H	-5.45643000	-2.37206800	-1.82868800
H	-6.88106400	-1.31680400	-1.93651600
C	-7.55402300	-1.36589900	0.74035300
H	-7.40772000	-1.06363100	1.78305100
H	-8.20652200	-2.24882800	0.72651400
H	-8.04418500	-0.54808900	0.20796500
C	3.90506700	-3.96559300	-0.86062700
H	4.25373900	-4.96863500	-1.10403900
C	6.22688400	1.73746900	0.01892900
C	5.52205300	-0.62758500	-0.40475500
C	5.44896800	2.99024500	0.41681100
H	4.95422200	2.85571400	1.38439500
H	4.67370400	3.22301400	-0.32064700
H	6.12547000	3.84899600	0.49134400
C	7.28474400	1.43147900	1.08302200
H	7.83426200	0.52421000	0.82355500
H	6.81052900	1.28480000	2.05900600

H	7.99114900	2.26793300	1.16537400
C	6.89833500	1.95980500	-1.33935400
H	6.14758700	2.20248700	-2.09855500
H	7.42979300	1.05798300	-1.65114000
H	7.60973300	2.79380000	-1.27876700
C	2.08537400	-2.44938200	-0.31939400

Trans-TS1 CONH (Cis Attack)

Mo	0.22372000	-0.23823500	1.28742500
S	-1.36198100	-0.04378800	-0.84837200
S	2.40636600	0.15486200	0.38030900
S	-0.15809100	2.26294400	1.00659200
S	0.57279400	-2.45608000	0.40609900
O	6.68202700	-0.68493100	-0.68136900
O	0.52023100	-0.37081400	2.97763700
O	-5.25661200	1.06221600	-2.78289400
N	4.97258600	0.76698300	-1.08154600
H	3.96955500	0.88208500	-0.93171600
N	-4.26879400	-0.51617000	-1.46051400
H	-3.36343700	-0.69879500	-1.00830600
C	-4.37646400	0.74792800	-1.96370000
C	-3.98433900	3.06797500	-1.34866200
H	-4.93110100	3.22384500	-1.85928600
C	-3.32950700	4.10101700	-0.69199600
H	-3.74812700	5.10698000	-0.68800800
C	-1.59024500	2.54536900	0.02615000
C	-4.37783000	-2.88656500	-1.23398800
H	-4.61852700	-2.77366000	-0.17057900
H	-3.28751800	-2.96019600	-1.31107600
H	-4.81843400	-3.82311700	-1.59475300
C	3.11014100	-1.40533700	-0.12201000
C	-3.45575400	1.76586700	-1.35718900
C	2.80595000	-3.80931000	-0.39321000
H	2.14346800	-4.67299500	-0.34252600
C	-2.15216500	3.82843000	0.00478500
C	-2.19684800	1.49359700	-0.73856600
C	4.45466300	-1.55893300	-0.563397700
C	-4.90999300	-1.70005200	-2.03605300
C	4.95031200	-2.83894200	-0.86511700
H	5.99191400	-2.91267200	-1.16585900
C	-4.53251300	-1.85688400	-3.51240400
H	-4.98152400	-2.76783400	-3.92947100
H	-3.44509500	-1.92654600	-3.61779500
H	-4.88310100	-0.99437900	-4.08545000
C	-6.42907900	-1.60742900	-1.88600000
H	-6.70044300	-1.49969300	-0.82943100
H	-6.90453000	-2.51923900	-2.27150500
H	-6.81177400	-0.74177500	-2.43162300
C	4.13504600	-3.95823700	-0.78505100
H	4.52681000	-4.94412900	-1.03381600
C	5.74952700	2.01033700	-1.01588000
C	5.46131200	-0.46349200	-0.75235100
C	4.75849600	3.14314000	-1.27502100
H	3.95556400	3.14504200	-0.52983700
H	4.29597000	3.03969300	-2.26227700
H	5.27065300	4.11119600	-1.23408000
C	6.37415600	2.18255800	0.37217300
H	7.06924000	1.36571400	0.58166300
H	5.59326200	2.18084200	1.13950200
H	6.91769500	3.13463000	0.43044100
C	6.83675600	2.01890200	-2.09131500
H	6.39070400	1.89670600	-3.08419700
H	7.54325900	1.20280000	-1.92667100
H	7.37808300	2.97419700	-2.07230800
C	2.28191500	-2.55785100	-0.05317100
O	-1.99898500	-0.95156700	2.04677500
N	-2.83683800	-0.21681700	2.85302800
C	-3.68521200	0.69588200	2.02597700

C	-2.07902200	0.60227900	3.85117500	H	5.16985500	-4.04177700	-1.27986700
C	-3.70509500	-1.19043000	3.56910300	H	6.60255000	-3.03393300	-0.98901400
H	-4.43952600	1.18533300	2.65344100	H	6.22917300	-3.60599400	-2.63870500
H	-3.02009700	1.43167100	1.57600500	C	2.27356700	0.80770700	2.40756500
H	-4.14400700	0.09379300	1.23890600	O	-1.68394400	2.90362500	0.71531800
H	-2.79138800	1.10470300	4.51687100	N	-2.68193100	3.42704200	-0.11567000
H	-1.40780700	-0.06939600	4.38403500	C	-3.50979100	2.33614400	-0.71224700
H	-1.47622800	1.32224100	3.29040400	C	-2.07553300	4.24994100	-1.20216900
H	-4.41665600	-0.67136600	4.22334100	C	-3.52436800	4.27616400	0.76057600
H	-4.22560600	-1.77219300	2.80803100	H	-4.36620900	2.77688900	-1.23668800
H	-3.04690800	-1.84439900	4.14079400	H	-2.87200200	1.78543400	-1.40363400
H	-1.65322900	4.61365400	0.57103400	H	-3.81741500	1.67643600	0.09955200

Trans-ES_{CONH} (Cis Attack)

Mo	0.19075200	1.88556300	-0.01115100
S	-1.50974900	-0.26917300	0.30873000
S	2.12221500	0.47489400	-0.31844900
S	-0.52324800	1.16043000	-2.40970900
S	0.67288400	1.57268300	2.31983200
O	6.23277400	-1.17121300	0.49083900
O	0.77939700	3.43859500	-0.45439600
O	-5.06368200	-3.02551200	-0.44153800
N	4.32968700	-1.53737100	-0.70362200
H	3.36498900	-1.21578500	-0.79938200
N	-3.30869000	-2.56768100	0.92971800
H	-2.50227900	-1.93991500	1.03404100
C	-3.96382600	-2.46765900	-0.25733400
C	-3.80082500	-2.00857300	-2.63143900
H	-4.59964900	-2.74263700	-2.67774100
C	-3.30690200	-1.40194800	-3.77523100
H	-3.70184600	-1.66502900	-4.75606600
C	-1.76927800	-0.08114700	-2.41342700
C	-2.84756100	-2.88096500	3.25514800
H	-2.58582600	-1.82253200	3.35944700
H	-1.92728600	-3.42496200	3.01849300
H	-3.22532100	-3.24257800	4.21849700
C	2.92260800	0.27515400	1.25981000
C	-3.28675500	-1.70093400	-1.35802400
C	2.88394300	0.71143700	3.66108300
H	2.35427400	1.12123900	4.52078900
C	-2.30357600	-0.44271700	-3.65794600
C	-2.23526800	-0.73498400	-1.21783100
C	4.18180400	-0.36884100	1.43340000
C	-3.89753700	-3.08613900	2.16452900
C	4.77311500	-0.41838300	2.70796500
H	5.74856000	-0.89067600	2.78596900
C	-4.21305900	-4.57716700	2.02815500
H	-4.60604200	-4.96840900	2.97610200
H	-3.30489200	-5.13502000	1.77617600
H	-4.94958900	-4.73905100	1.23826800
C	-5.16949300	-2.31033000	2.52328600
H	-4.93973300	-1.24584400	2.64249000
H	-5.59205600	-2.68099600	3.46647300
H	-5.91426300	-2.42130300	1.73120400
C	4.13270500	0.11222900	3.81711700
H	4.59670200	0.05501200	4.80165700
C	4.96381700	-1.98823300	-1.94688100
C	5.00369600	-1.03131000	0.36669600
C	3.82509000	-2.30707500	-2.91327700
H	3.20189600	-1.42516400	-3.09643500
H	3.17790200	-3.09295900	-2.50980900
H	4.22827400	-2.65086800	-3.87257000
C	5.84191500	-0.88021300	-2.53705000
H	6.65015200	-0.62593100	-1.84721800
H	5.24333200	0.01827500	-2.71902600
H	6.27818700	-1.20636400	-3.49015200
C	5.79723600	-3.24597900	-1.69565700

Trans-TS2_{CONH} (Cis Attack)

Mo	0.18404100	1.93449200	-0.13305900
S	-1.40776000	-0.32296400	0.28974300
S	2.10843800	0.44336700	-0.34957900
S	-0.55765300	1.08058600	-2.49307600
S	0.71577500	1.78829000	2.21043300
O	6.20603900	-1.18556100	0.54038300
O	0.82240200	3.40867900	-0.74187200
O	-5.03597600	-3.03896900	-0.28340200
N	4.28923100	-1.61516600	-0.60911500
H	3.32556500	-1.29480400	-0.71698300
N	-3.27859800	-2.51908800	1.06074000
H	-2.46286400	-1.89726900	1.12820100
C	-3.92939500	-2.48352400	-0.13287400
C	-3.79553100	-2.13546800	-2.52532200
H	-4.60048700	-2.86426400	-2.52548400
C	-3.33008200	-1.57128700	-3.70104000
H	-3.74740400	-1.86988000	-4.66224500
C	-1.76940500	-0.19314700	-2.42410800
C	-2.84085000	-2.69416400	3.40575300
H	-2.55234900	-1.63856000	3.44507000
H	-1.93410100	-3.27592600	3.21016600
H	-3.23354800	-2.98447700	4.38712200
C	2.92174800	0.36032100	1.22430100
C	-3.25245200	-1.78229700	-1.27556000
C	2.92074200	0.98637600	3.58534500
H	2.40976100	1.47554300	4.41399000
C	-2.33236200	-0.60050000	-3.64093700
C	-2.19183600	-0.81810200	-1.19479700
C	4.17372300	-0.28949000	1.43699000
C	-3.88929300	-2.94018700	2.32236800
C	4.77789500	-0.24918500	2.70526900
H	5.74705800	-0.72909600	2.80887700
C	-4.24699300	-4.42754200	2.28158600
H	-4.64945200	-4.74565600	3.25272000
H	-3.35516500	-5.02599000	2.06685600
H	-4.98829400	-4.61984900	1.50301500
C	-5.14059300	-2.10668300	2.61893100
H	-4.88033400	-1.04370400	2.66970100
H	-5.57976500	-2.40204100	3.58096000
H	-5.88249500	-2.24811400	1.82907100
C	4.16003200	0.37735100	3.77648700
H	4.63348900	0.38937500	4.75768200
C	4.90662800	-2.14834500	-1.82810000
C	4.97751500	-1.03999200	0.41616600
C	3.75412700	-2.51356900	-2.76126700
H	3.13605200	-1.63817200	-2.98810700

H	3.10486600	-3.26846500	-2.30536600	H	-0.11413000	0.13943600	5.48353900
H	4.14246200	-2.91644100	-3.70341400	C	-4.67021000	-0.79014000	0.19386800
C	5.78870400	-1.08690900	-2.49243300	C	-3.19855100	-0.84220400	2.22294700
H	6.60287300	-0.79651600	-1.82385300	C	-4.36491100	-0.57960700	-1.28709100
H	5.19526100	-0.19713200	-2.72651300	H	-3.62614000	-1.30617300	-1.64472900
H	6.21602900	-1.47580900	-3.42585900	H	-3.95781300	0.42024200	-1.46964800
C	5.72991000	-3.39746000	-1.50963300	H	-5.27713800	-0.69421000	-1.88339800
H	5.10134700	-4.15459400	-1.02854200	C	-5.19416400	-2.21241200	0.41889100
H	6.55301600	-3.15176900	-0.83515400	H	-5.39160600	-2.38398500	1.48042500
H	6.13745400	-3.82543500	-2.43508400	H	-4.45646900	-2.94636700	0.07870700
C	2.29780400	0.99485500	2.33480500	H	-6.12417800	-2.36756500	-0.14334200
O	-1.55660700	2.88241900	0.60512000	C	-5.70070200	0.23299100	0.67198800
N	-2.72210000	3.34625400	-0.22343800	H	-5.33322800	1.25102800	0.50640300
C	-3.51273400	2.19013800	-0.69778600	H	-5.89708600	0.10282100	1.73894200
C	-2.20254700	4.13729100	-1.35596700	H	-6.63896500	0.10949400	0.11554300
C	-3.500041600	4.17416600	0.70689500	C	0.64235300	-1.16970500	2.41762600
H	-4.44994700	2.55017400	-1.14296500	O	3.19308700	-1.74482600	-1.16032400
H	-2.91677000	1.65855000	-1.43969600	N	5.72275400	0.79665200	0.24100500
H	-3.69096000	1.53132500	0.15288100	C	6.42960600	1.73321700	1.07843200
H	-3.04232900	4.56978000	-1.91548000	C	5.66487400	-0.51184000	0.86857400
H	-1.54485600	4.90705100	-0.95175500	C	4.37622000	1.26924800	-0.04623500
H	-1.61916400	3.45920400	-1.98749500	H	5.94079100	1.88585300	2.06701900
H	-4.38499200	4.58771900	0.20453200	H	7.45183900	1.37888400	1.26416000
H	-3.79333000	3.54135400	1.54498000	H	6.48857200	2.71037000	0.58398700
H	-2.84947100	4.97043800	1.06838900	H	5.17350900	-0.48033800	1.86186200
H	-1.97030000	-0.12611500	-4.55168200	H	5.08337900	-1.19278300	0.24010400

Dioxo_P CONH(Trans/Trans) (Cis Attack)

Mo	1.50405500	-2.07679900	-0.86592700
S	0.96557200	0.53905700	-0.86478100
S	-0.85932000	-2.20779800	0.38604500
S	0.21765600	-1.77726200	-2.96045700
S	2.08762700	-1.59297200	1.50879900
O	-4.13331800	-0.94603000	3.03295100
O	1.33994100	-3.78028600	-1.16884000
O	-0.92919500	4.42694100	-1.71589000
N	-3.39746000	-0.59532700	0.89957300
H	-2.56721700	-0.72091700	0.32091900
N	-0.62321200	2.95383800	0.00253800
H	-0.35467200	1.98504900	0.17503900
C	-0.79611800	3.26084100	-1.31187000
C	-1.74431300	2.31504900	-3.35092300
H	-2.20581000	3.29546800	-3.43652200
C	-1.97058400	1.32023400	-4.29244800
H	-2.63201700	1.49794600	-5.13875100
C	-0.49150100	-0.17138500	-3.06133100
C	0.10188500	3.05703300	2.27718000
H	0.84266400	2.27047000	2.08751300
H	-0.81719900	2.56563200	2.61433400
H	0.47309700	3.68911100	3.09187400
C	-0.67108900	-1.34035400	1.88809500
C	-0.90781400	2.09423100	-2.24942800
C	0.81786900	-0.64165800	3.70194000
H	1.83246900	-0.53021400	4.08060800
C	-1.35195100	0.08124500	-4.13609700
C	-0.22822600	0.84882700	-2.10021800
C	-1.76681400	-0.87048300	2.66968500
C	-0.14407200	3.89472900	1.02469600
C	-1.55267600	-0.37058700	3.96050300
H	-2.42798700	-0.06539000	4.52822000
C	-1.20252100	4.96249700	1.29844200
H	-0.85776000	5.63950900	2.09091200
H	-2.13822200	4.49771900	1.62624300
H	-1.40046600	5.54165700	0.39343600
C	1.16528600	4.54900400	0.57241600
H	1.92309300	3.78364900	0.37542700
H	1.54449200	5.22016900	1.35378900
H	1.00875100	5.12720900	-0.34225700
C	-0.27149900	-0.26190700	4.48391000

H	-0.11413000	0.13943600	5.48353900
C	-4.67021000	-0.79014000	0.19386800
C	-3.19855100	-0.84220400	2.22294700
C	-4.36491100	-0.57960700	-1.28709100
H	-3.62614000	-1.30617300	-1.64472900
H	-3.95781300	0.42024200	-1.46964800
H	-5.27713800	-0.69421000	-1.88339800
C	-5.19416400	-2.21241200	0.41889100
H	-5.39160600	-2.38398500	1.48042500
H	-4.45646900	-2.94636700	0.07870700
H	-6.12417800	-2.36756500	-0.14334200
C	-5.70070200	0.23299100	0.67198800
H	-5.33322800	1.25102800	0.50640300
H	-5.89708600	0.10282100	1.73894200
H	-6.63896500	0.10949400	0.11554300
C	0.64235300	-1.16970500	2.41762600
O	3.19308700	-1.74482600	-1.16032400
N	5.72275400	0.79665200	0.24100500
C	6.42960600	1.73321700	1.07843200
C	5.66487400	-0.51184000	0.86857400
C	4.37622000	1.26924800	-0.04623500
H	5.94079100	1.88585300	2.06701900
H	7.45183900	1.37888400	1.26416000
H	6.48857200	2.71037000	0.58398700
H	5.17350900	-0.48033800	1.86186200
H	5.08337900	-1.19278300	0.24010400
H	6.68090200	-0.90717900	0.99684600
H	3.77266200	1.40994200	0.87319500
H	4.42122800	2.22606400	-0.57921700
H	3.85011000	0.54003900	-0.66752700
H	-1.52850100	-0.71719100	-4.85463900

Dioxo CONH (Trans/Trans)

Mo	3.05353100	0.01475800	-0.06562700
S	0.95372800	-1.08706100	-1.31043300
S	1.10353200	1.24032700	1.32231700
S	2.55154400	-1.97047500	1.33926100
S	2.47657800	1.96974800	-1.49309100
O	-2.82855200	3.13234200	1.98002700
O	4.14342500	0.46792400	1.21182800
O	-2.85958700	-3.19891200	-1.92495300
N	-1.87477000	1.05814800	1.92160400
H	-1.02214000	0.58937500	1.61467100
N	-2.05413200	-1.06749200	-1.76763800
H	-1.22934700	-0.55552600	-1.45413800
C	-2.04763100	-2.38978900	-1.44711900
C	-1.50073900	-3.84304600	0.43489400
H	-2.47557800	-4.27330300	0.21990900
C	-0.72326100	-4.29532800	1.49243900
H	-1.07985800	-5.09472200	2.13989500
C	0.99535700	-2.67091700	0.91312700
C	-2.27784600	0.96503600	-3.00554500
H	-1.18736200	1.06640700	-3.05721900
H	-2.61239000	1.49812800	-2.10915300
H	-2.71041200	1.46034900	-3.88252500
C	0.24529500	2.23979000	0.17820400
C	-1.06098500	-2.80331900	-0.39517200
C	0.33782100	3.57849800	-1.87071500
H	0.88099700	3.86298100	-2.77025800
C	0.51108200	-3.69572800	1.73391800
C	0.22906000	-2.22545600	-0.20421800
C	-1.06246600	2.76253800	0.40364000
C	-2.69440800	-0.50220600	-2.96331100
C	-1.59971000	3.72378500	-0.46334600
H	-2.58526000	4.11482700	-0.22293100
C	-4.21507900	-0.61465600	-2.85552100
H	-4.68792500	-0.15385600	-3.73280600
H	-4.57335900	-0.09597900	-1.96012600
H	-4.51588000	-1.66293600	-2.79557500
C	-2.19680400	-1.22341000	-4.22021800

H -1.10757900 -1.14277300 -4.29530100
H -2.64298800 -0.77557600 -5.11776300
H -2.46573700 -2.28256500 -4.18504400
C -0.90566600 4.14145800 -1.59075200
H -1.33834400 4.87701800 -2.26685900
C -2.45119900 0.51807700 3.15908700
C -1.97596100 2.35433200 1.52131600
C -1.91549300 -0.90630300 3.28244100
H -0.82025300 -0.91269900 3.33232900
H -2.20748300 -1.51632800 2.42066700
H -2.30347000 -1.38232800 4.19031200
C -2.00112200 1.35258400 4.36311700
H -2.35519800 2.38251800 4.26687700
H -0.90818100 1.36484800 4.42760800
H -2.40022600 0.92671100 5.29292200
C -3.97706400 0.50346500 3.06654600
H -4.30074800 -0.09758100 2.21038900
H -4.35903000 1.51993400 2.94289000
H -4.40445000 0.06525300 3.97794700
C 0.91861400 2.63429500 -1.01676100
O 4.09298500 -0.44932300 -1.38048200
H 1.12315900 -4.01566900 2.57535400

Table S3**Cis-ES_{CONH} (Trans Attack)**

Mo -0.59015600 -1.79852300 -1.45878700
 S 0.40300500 -3.34837500 0.11948300
 S -1.67205400 0.37956800 -1.60369700
 S 1.45146800 -0.55592900 -0.96646600
 S -2.81058100 -2.51453100 -0.71454000
 O -3.68941700 3.76482500 -0.48824900
 O -0.44057100 -2.41862800 -3.04153400
 O 5.69335900 0.39871000 0.56573900
 N -2.00319100 2.62234900 0.57532900
 H -1.66118500 1.66753600 0.74293400
 N 3.79060300 1.20376600 -0.36814400
 H 2.83970200 0.97005400 -0.66487000
 C 4.50448300 0.22090100 0.23837500
 C 4.08879500 -3.16272200 1.76822600
 H 4.69261400 -3.80241600 2.41068100
 C 4.56447800 -1.92684700 1.36275500
 H 5.54176900 -1.56746200 1.67032700
 C 2.51854200 -1.50526300 0.08400100
 C 3.19327300 3.22764800 -1.49429800
 H 2.35087700 3.38051900 -0.81210600
 H 2.82030000 2.65830900 -2.35264600
 H 3.53094700 4.20777100 -1.84926300
 C -3.20175400 0.23017700 -0.73399800
 C 2.82455700 -3.57607000 1.34973300
 C -5.06120700 -1.12702400 0.04311800
 H -5.49682700 -2.11536400 0.19163700
 C 3.80579800 -1.07825100 0.53544600
 C 2.03656400 -2.77151600 0.52375300
 C -3.86876500 1.37117800 -0.23136500
 C 4.33649200 2.49200300 -0.79997200
 C -5.15901000 1.26512200 0.30628100
 H -5.64958800 2.17088800 0.65904900
 C 5.49115300 2.28632500 -1.78512900
 H 5.87373500 3.25638600 -2.12807300
 H 5.14689500 1.72399400 -2.65938800
 H 6.30143000 1.72931400 -1.30938500
 C 4.81412200 3.30235700 0.40813300
 H 3.98768100 3.46303600 1.10880700
 H 5.18558900 4.28330200 0.08414700
 H 5.61352400 2.77003100 0.92841300
 C -5.76792000 0.01839200 0.41856300
 H -6.77041500 -0.07117400 0.83638200
 C -0.94913100 3.64535900 0.51186100
 C -3.18382200 2.69912600 -0.10757300
 C 0.28252100 3.04097800 1.18376700
 H 0.57740200 2.10056600 0.69921400
 H 0.08477100 2.81963100 2.24024900
 H 1.11986900 3.74829500 1.14032500
 C -0.61552200 3.97922700 -0.94468900
 H -1.49307000 4.38709700 -1.45369300
 H -0.30350000 3.07092700 -1.47135400
 H 0.19583100 4.71795400 -0.98956400
 C -1.39350500 4.90337500 1.25993600
 H -1.62540800 4.66388900 2.30484600
 H -2.28921600 5.32390300 0.79553700
 H -0.59391300 5.65603700 1.24857600
 C -3.77066700 -1.04615500 -0.49657800
 N -1.12514400 -0.54580900 2.56458600
 C 0.24784700 -0.88900500 3.05023100
 C -1.98202800 -1.77293900 2.58275900
 C -1.74416500 0.49141700 3.44219600
 H 0.21730800 -1.24933300 4.08612900
 H 0.63455600 -1.65528100 2.37509500
 H 0.85455400 0.01370100 2.95837800
 H -2.08098900 -2.14765200 3.60972200

H -2.94792900 -1.49114700 2.15857100
 H -1.50669200 -2.50457300 1.92551600
 H -1.11047000 1.37874900 3.39713000
 H -2.72099800 0.72493100 3.01401300
 H -1.83955600 0.12878400 4.47335500
 O -1.03400400 -0.06699200 1.29173400
 H 2.41995800 -4.53715400 1.66675400

Cis-TS1' CONH (Trans Attack)

Mo -0.43105300 -1.72952900 -1.17012200
 S 0.88817300 -3.32317800 0.10115800
 S -1.80507500 0.28299400 -1.38212100
 S 1.60718200 -0.35924800 -0.84957600
 S -2.62320700 -2.78991100 -0.64732700
 O -4.44266000 3.32916400 -0.34677900
 O -0.26882000 -2.21161200 -2.80127800
 O 5.72985100 0.92949900 0.71426000
 N -2.52350000 2.46924800 0.57586500
 H -2.00911400 1.58467900 0.63825400
 N 3.98062600 1.42782400 -0.64536800
 H 3.07902100 1.08275600 -0.98503900
 C 4.68524900 0.56845700 0.13996900
 C 4.76786300 -3.01893900 1.18680900
 H 5.50285300 -3.67956300 1.64488900
 C 5.09046200 -1.70395600 0.89449100
 H 6.06559800 -1.29215600 1.13738100
 C 2.86137200 -1.31789500 -0.05126100
 C 3.04938800 3.43756700 -1.54863900
 H 2.05801700 3.15416800 -1.17787400
 H 3.14373600 3.05227700 -2.56966300
 H 3.10195200 4.53163100 -1.58547300
 C -3.37022200 -0.09867100 -0.62070000
 C 3.48134100 -3.48013600 0.91059300
 C -5.04163100 -1.70770100 0.06307400
 H -5.34024200 -2.74740600 0.19499000
 C 4.16480200 -0.83390900 0.28880700
 C 2.52570100 -2.65417800 0.31699600
 C -4.21328200 0.93765800 -0.16583100
 C 4.15508900 2.88256800 -0.65161600
 C -5.49854100 0.64701800 0.31210400
 H -6.12990700 1.47159100 0.63609300
 C 5.52316100 3.26204400 -1.22106900
 H 5.62623400 4.35440700 -1.26223300
 H 5.63446200 2.86805100 -2.23710400
 H 6.31942800 2.84705200 -0.59944800
 C 3.99572800 3.44345300 0.76495400
 H 3.01694000 3.16577100 1.17130100
 H 4.06744900 4.53873000 0.75508400
 H 4.77118900 3.04168900 1.42154800
 C -5.91816900 -0.67684300 0.40138600
 H -6.91460700 -0.91286600 0.77435700
 C -1.64671200 3.64466100 0.42894900
 C -3.74452900 2.35600900 -0.03155000
 C -0.28207000 3.23104900 0.97761600
 H 0.07397200 2.31100200 0.49294700
 H -0.32845400 3.04659100 2.05807400
 H 0.45220100 4.02705700 0.80672100
 C -1.49766000 4.02518700 -1.04729700
 H -2.46702900 4.29529900 -1.47515900
 H -1.09412700 3.17864100 -1.61235100
 H -0.81467700 4.87844700 -1.15012600
 C -2.20780200 4.82061200 1.22745300
 H -2.30893900 4.55063200 2.28509400
 H -3.19301000 5.10165200 0.84654800
 H -1.53402300 5.68441500 1.15510900
 C -3.75027400 -1.45077700 -0.42586200
 N -0.82424900 -0.73995700 2.41775000
 C 0.60117800 -0.63465000 2.66860100

C -1.37645300 -2.06966200 2.61204600
 C -1.61531800 0.27632800 3.07793200
 H 0.82259100 -0.72286200 3.74783400
 H 1.11718800 -1.42791100 2.12391500
 H 0.95528300 0.32827200 2.28987000
 H -1.37706600 -2.33435400 3.68612000
 H -2.39611700 -2.08222900 2.21896100
 H -0.78003700 -2.78869400 2.04598300
 H -1.19298300 1.26087500 2.86612400
 H -2.63301900 0.24219200 2.67671000
 H -1.63837100 0.11458400 4.17093200
 O -1.10313500 -0.29291700 0.65274900
 H 3.19059600 -4.49932200 1.16352800

Cis-INT1_{CONH} (Trans Attack)

Mo-0.24889900 -1.84352400 -1.39865900
 S 0.63400200 -3.22681600 0.37759300
 S -2.76289200 0.20451500 -1.98676100
 S 1.62222200 -0.44104700 -0.75167800
 S -2.48268600 -2.83397500 -0.76185500
 O -4.62758400 3.08090600 0.15585700
 O 0.13344900 -2.52308500 -2.91458800
 O 5.64578300 0.80831600 1.07994000
 N -2.46639700 2.32264300 0.32459600
 H -1.90278400 1.47601100 0.31646000
 N 4.13349100 1.17548000 -0.57163500
 H 3.25120600 0.84773800 -0.96901300
 C 4.65376900 0.42394500 0.43523800
 C 4.32405100 -2.95709100 1.99744000
 H 4.94100400 -3.57654900 2.64681500
 C 4.77845300 -1.71843000 1.57373800
 H 5.74134500 -1.32969200 1.89098100
 C 2.73131500 -1.36397000 0.28591000
 C 3.56434800 3.03394800 -1.96478800
 H 2.50956700 2.93503800 -1.68661700
 H 3.72821100 2.43369100 -2.86627600
 H 3.75910100 4.08418900 -2.20854200
 C -3.56114700 -0.26512300 -0.51239600
 C 3.06378700 -3.39536100 1.59859100
 C -4.51976300 -2.00786800 0.86361300
 H -4.58845100 -3.06045300 1.13406900
 C 4.00634800 -0.90207700 0.72804000
 C 2.26028900 -2.61932900 0.75909800
 C -4.20766600 0.70372300 0.29413500
 C 4.47942300 2.57588900 -0.83074500
 C -5.12625400 0.30462300 1.26403800
 H -5.65151400 1.06278500 1.84140600
 C 5.94092400 2.69993800 -1.26576900
 H 6.17165200 3.74370800 -1.51548800
 H 6.12690200 2.08522700 -2.15305900
 H 6.60600000 2.36539600 -0.46693600
 C 4.22233100 3.42821900 0.41526700
 H 3.17140700 3.35399200 0.71484100
 H 4.44857800 4.48253100 0.21123500
 H 4.84614700 3.08453600 1.24383100
 C -5.30977400 -1.06205900 1.50990900
 H -6.02915100 -1.38694000 2.26097500
 C -1.73421700 3.54785600 -0.02183100
 C -3.81454600 2.14829200 0.21294000
 C -0.25193900 3.18554400 0.04154400
 H -0.02247600 2.35380200 -0.63592100
 H 0.03314000 2.86968400 1.05165300
 H 0.35969200 4.05182500 -0.23685100
 C -2.09708900 3.99264500 -1.44035900
 H -3.16236800 4.22975400 -1.50825100
 H -1.87744500 3.18884300 -2.14999100
 H -1.51708500 4.88208100 -1.71754100
 C -2.05649800 4.65312300 0.98474000

H -1.78508400 4.33789200 1.99876400
 H -3.12473100 4.88398600 0.96681500
 H -1.48912800 5.56137700 0.74397200
 C -3.59695200 -1.63870900 -0.13543500
 N -0.83272700 0.48181800 2.44065700
 C 0.55371000 0.14572700 2.69034500
 C -1.67237900 -0.69761300 2.53285800
 C -1.29184700 1.51208900 3.33960000
 H 0.72484100 -0.17105700 3.74239500
 H 0.85364000 -0.67263000 2.03203000
 H 1.20053200 1.00614900 2.47846400
 H -1.62847600 -1.16156900 3.54245000
 H -2.71311300 -0.43090200 2.32489200
 H -1.34856300 -1.44745500 1.80178300
 H -0.66382500 2.40658000 3.23856800
 H -2.32344300 1.79012600 3.09392100
 H -1.25704400 1.19463900 4.40703300
 O -1.10794600 -0.01161800 -1.60786700
 H 2.67291600 -4.35246200 1.94160600

Cis-TS2'_{CONH} (Trans Attack)

Mo-0.27763800 -1.79618700 -1.42267800
 S 0.57783200 -3.21243200 0.36401600
 S -2.83007600 0.24212400 -2.01250300
 S 1.59209900 -0.40766700 -0.70117300
 S -2.51069300 -2.80605200 -0.84741600
 O -4.59801700 3.09871100 0.24306700
 O 0.14843800 -2.45830000 -2.93554400
 O 5.61720200 0.77422600 1.12842600
 N -2.43776500 2.32087900 0.32979800
 H -1.88201100 1.46974100 0.29078600
 N 4.16843900 1.11433800 -0.58482300
 H 3.29342100 0.78814000 -0.99838200
 C 4.64213000 0.38567100 0.46110300
 C 4.25374200 -2.99148800 2.02090500
 H 4.85853400 -3.62282100 2.67002800
 C 4.72808700 -1.75761700 1.60398200
 H 5.69488800 -1.38444300 1.92718800
 C 2.68975000 -1.36705100 0.31137000
 C 3.66177000 2.94110400 -2.04147900
 H 2.59881500 2.85871500 -1.78967800
 H 3.84498200 2.31741400 -2.92322600
 H 3.87397000 3.98289900 -2.30594500
 C -3.57543100 -0.24145800 -0.53036600
 C 2.99079800 -3.41211800 1.61212400
 C -4.49599100 -2.00358800 0.85430300
 H -4.55734400 -3.06008600 1.11187500
 C 3.97101900 -0.92708000 0.75874100
 C 2.20132600 -2.62243800 0.77103000
 C -4.18871800 0.71694300 0.32223500
 C 4.53992000 2.50333300 -0.87114500
 C -5.08221700 0.30351900 1.30683600
 H -5.58621400 1.05380000 1.91310900
 C 6.01457800 2.59114600 -1.26789200
 H 6.27221700 3.62417400 -1.53461900
 H 6.21450800 1.95172900 -2.13436200
 H 6.64957200 2.26450500 -0.44132100
 C 4.26428800 3.39595200 0.34196400
 H 3.20345400 3.35520100 0.61013500
 H 4.52193600 4.43840200 0.11525300
 H 4.85429900 3.06287400 1.19877300
 C -5.26822900 -1.06723300 1.53552100
 H -5.96953700 -1.40145700 2.29931700
 C -1.70169200 3.54511400 -0.00821200
 C -3.78963200 2.15973900 0.25684200
 C -0.22236000 3.17299300 0.04241100
 H -0.00507200 2.33458900 -0.63176600
 H 0.07642100 2.86277100 1.05142000

H	0.39123800	4.03234700	-0.25203700	H	-7.22991300	-2.61854000	-0.23441800
C	-2.07162200	4.00255400	-1.42111200	C	-3.47799800	3.35014900	0.03922000
H	-3.13566500	4.24806800	-1.47919600	C	-4.88254400	1.32524800	-0.46235900
H	-1.86421700	3.20162700	-2.13787900	C	-2.27061000	3.53903000	0.95259600
H	-1.48738800	4.88969000	-1.69719800	H	-1.53565100	2.74644600	0.76912900
C	-2.00843900	4.64557800	1.00859000	H	-2.56342000	3.49708600	2.00718900
H	-1.73264900	4.32163000	2.01874100	H	-1.76497700	4.49384200	0.76399400
H	-3.07440900	4.88587300	0.99889000	C	-3.05877900	3.54500200	-1.42054100
H	-1.43396500	5.54995100	0.76968100	H	-3.90065100	3.34196400	-2.08825100
C	-3.60313900	-1.62033200	-0.16544600	H	-2.23503200	2.86660800	-1.66817000
N	-0.79077300	0.46908600	2.47626400	H	-2.72069000	4.57622400	-1.58596400
C	0.58774000	0.12850700	2.75617300	C	-4.59035000	4.32647800	0.41554400
C	-1.63942200	-0.70334700	2.56879300	H	-4.88758200	4.18449400	1.46051600
C	-1.25735800	1.51521800	3.35086400	H	-5.46653900	4.16778200	-0.21754600
H	0.73717600	-0.17650000	3.81557300	H	-4.23748200	5.35868400	0.29375800
H	0.89571900	-0.70056800	2.11513700	C	-3.81813400	-2.37547900	-0.16142900
H	1.24459500	0.98207900	2.54763000	N	0.72052500	3.21843900	-0.80781900
H	-1.60437500	-1.16290300	3.58090100	C	1.19350500	3.01933000	0.54842800
H	-2.67758200	-0.43203700	2.35518900	C	0.46017800	4.61045200	-1.07888100
H	-1.31662700	-1.45846400	1.84224000	C	1.64755400	2.63663200	-1.75458700
H	-0.61625200	2.40150800	3.25334600	H	2.20120400	3.45779900	0.71214800
H	-2.27982100	1.80254700	3.07929300	H	0.50391500	3.48129300	1.26205300
H	-1.24949600	1.21214900	4.42331800	H	1.24626000	1.94938300	0.76715500
O	-1.08892700	-0.01890500	-1.65108500	H	1.31810200	5.27669900	-0.83835400
H	2.58682700	-4.36656400	1.94709400	H	0.21413600	4.74429900	-2.13926900
				H	-0.41449700	4.92482000	-0.49639300
				H	1.76952000	1.56871400	-1.53691000
				H	1.25610200	2.74033300	-2.77304400
				H	2.65235100	3.11382500	-1.71557500
				O	0.09325400	-2.27671200	-1.80468400
				H	1.05048900	0.43799100	4.26689800

Dioxo_P CONH(Cis/Trans) (Trans Attack)

Mo	-0.25730500	-2.21442200	-0.10693100
S	-0.12335500	-0.82955700	2.07668000
S	-2.06702200	-0.32527200	-0.57789500
S	1.99088000	-0.96005100	-0.29670500
S	-2.43940300	-3.43191800	0.07726100
O	-5.78141800	1.93457200	-1.06166900
O	0.28989500	-3.71927000	0.55133900
O	5.84039900	1.24825800	0.72340300
N	-3.91912400	1.96351700	0.26339200
H	-3.16313600	1.34998800	0.55860500
N	4.93527400	-0.39100000	-0.55212900
H	4.10127100	-0.95790400	-0.71071200
C	4.91155900	0.44709400	0.51726500
C	3.05989900	0.99608000	3.71040600
H	3.27664500	1.48247500	4.66036400
C	4.01342700	0.96640200	2.70514700
H	4.98745900	1.42902000	2.83104100
C	2.48663500	-0.26908100	1.24098600
C	5.49980500	-1.39015500	-2.65048600
H	4.48817300	-1.20771000	-3.02862100
H	5.51024200	-2.38648300	-2.19565300
H	6.19065700	-1.39208200	-3.50093000
C	-3.66958000	-0.96945400	-0.35217800
C	1.81760900	0.40791000	3.49571100
C	-5.09927100	-2.93991300	-0.12021200
H	-5.18234900	-4.01688800	0.01270500
C	3.75516000	0.34379100	1.47307600
C	1.50750600	-0.22580000	2.28407400
C	-4.85103400	-0.17168900	-0.40230700
C	5.91053100	-0.32138200	-1.63962500
C	-6.11162900	-0.77923200	-0.38614400
H	-6.97885600	-0.12936300	-0.47185300
C	7.31849500	-0.61652900	-1.11728800
H	8.03743800	-0.61100800	-1.94680300
H	7.34961300	-1.60270900	-0.64175500
H	7.61421000	0.13378100	-0.37999300
C	5.87094800	1.05646000	-2.30704200
H	4.87025900	1.25629800	-2.70559100
H	6.58849200	1.09806200	-3.13661400
H	6.11796900	1.83601300	-1.58264900
C	-6.24425800	-2.15605100	-0.25271600

Dioxo CONH (Cis/Trans)

Mo	-1.71708100	-2.20762700	-0.48215500
S	-1.29311200	-2.01213900	2.17520500
S	-0.88662800	0.33641100	-0.53014200
S	0.77443300	-2.46786300	-0.23279700
S	-3.83030600	-0.95161700	-0.38909800
O	-0.88648000	4.78410100	-0.52823100
O	-1.34673100	-2.44975900	-2.16641300
O	4.78773700	-1.12144100	0.39400700
N	0.06774800	3.02132000	0.55630600
H	-0.02228000	2.01436200	0.68767800
N	3.00614700	-0.42940500	-0.86093600
H	1.99217200	-0.48691000	-0.89965000
C	3.56649000	-0.95470500	0.26734500
C	2.17782300	-0.64731000	3.72164400
H	2.52066600	-0.27267100	4.68547500
C	3.05166600	-0.70323500	2.64178100
H	4.07810300	-0.35176900	2.71513300
C	1.28125900	-1.65068500	1.24690800
C	2.58627200	0.07999300	-3.15952100
H	2.14991000	1.04739400	-2.88778100
H	1.77213500	-0.65346800	-3.18333500
H	3.00840800	0.16376100	-4.16714100
C	-2.27837600	1.38179700	-0.37687100
C	0.84869700	-1.02435400	3.55643300
C	-4.71892000	1.59373100	-0.41815400
H	-5.69194400	1.10677800	-0.45262800
C	2.60184700	-1.15982900	1.39545500
C	0.36572200	-1.53017700	2.33505800
C	-2.20387800	2.80234400	-0.27894400
C	3.66910100	-0.33539200	-2.16710100
C	-3.37316000	3.57452900	-0.30807600
H	-3.25485300	4.65400900	-0.26826000
C	4.24856300	-1.69290500	-2.57492000
H	4.70586300	-1.62493300	-3.57027200
H	3.45566700	-2.44706600	-2.60572000

H	5.00721000	-2.01562200	-1.85771300	H	3.97848400	5.08897800	0.22137100
C	4.77183300	0.72234200	-2.11072800	C	6.19483600	-1.62354000	0.52849100
H	4.35506900	1.69153600	-1.81503100	C	5.39390100	0.74456600	0.43369900
H	5.24268400	0.83418400	-3.09601400	C	5.53954000	-2.95277900	0.15920300
H	5.53355000	0.43668300	-1.38111500	H	5.27214400	-2.97761400	-0.90222600
C	-4.62615200	2.98283400	-0.38144100	H	4.62127900	-3.11378200	0.73374400
H	-5.52742700	3.59311300	-0.39497600	H	6.22535400	-3.78292200	0.36263100
C	1.43698500	3.54665900	0.63356200	C	7.46254300	-1.42492600	-0.30717800
C	-0.94883400	3.61002100	-0.12748100	H	7.92444000	-0.46363800	-0.07079300
C	2.25468800	2.48531000	1.36085900	H	7.21997100	-1.44219200	-1.37485200
H	2.24754800	1.53995900	0.80832600	H	8.18029200	-2.23037000	-0.10344100
H	1.85396700	2.28374600	2.36034700	C	6.54605700	-1.62042000	2.01929200
H	3.29861300	2.80422900	1.46248300	H	5.64803400	-1.79403500	2.62150400
C	2.00327500	3.75811100	-0.77324400	H	6.97628100	-0.65730400	2.30320700
H	1.40331900	4.48778700	-1.32307100	H	7.26833700	-2.41682300	2.24144200
H	1.99585700	2.81046600	-1.32343900	C	2.01003300	2.40105100	-0.54156900
H	3.03994400	4.11411400	-0.71805500	N	-0.59657200	0.30495800	2.19369900
C	1.45416400	4.85913600	1.41840400	C	0.65321200	1.07981900	2.47988100
H	1.06065800	4.70134100	2.42839300	C	-0.98351800	-0.49486100	3.39245400
H	0.83966200	5.61226700	0.91912800	C	-1.70937200	1.25436600	1.86455900
H	2.48356300	5.23023100	1.50481000	H	0.51960700	1.71861200	3.36200600
C	-3.57479400	0.78827100	-0.40854800	H	1.44904700	0.34858300	2.62518800
H	0.14652000	-0.94038600	4.38365100	H	0.87061000	1.67384300	1.59160600
O	-2.66581000	-3.60687600	-0.06855600	H	-1.20116600	0.15599600	4.24934300

Trans-ES_{CONH} (Trans Attack)

Mo	0.08085300	-0.27480500	-1.50142100
S	-2.35356800	-0.10039700	-1.28749900
S	2.35130500	-0.31872400	-0.57923600
S	-0.37486300	-2.60833600	-0.89633600
S	0.32491000	2.10807000	-1.02622600
O	6.47841800	1.17895300	0.86890000
O	0.30499400	-0.38310800	-3.18599600
O	-6.35296800	-0.77856400	0.88716300
N	5.20939700	-0.58490800	0.22823200
H	4.28564500	-0.88086500	-0.10081800
N	-4.88208700	0.71771800	0.02739000
H	-3.97143500	0.82638600	-0.43335500
C	-5.23901000	-0.54723000	0.37803800
C	-4.61918300	-2.86012200	0.77373800
H	-5.60109600	-2.89215200	1.23544400
C	-3.78485300	-3.96444700	0.76428600
H	-4.11014700	-4.90308400	1.21276200
C	-2.05562000	-2.66356300	-0.36036800
C	-4.87845800	3.07842900	-0.33140800
H	-4.63223200	2.93442600	-1.38877400
H	-3.93259800	3.17453900	0.21379000
H	-5.43339700	4.01787000	-0.22916900
C	2.93714700	1.33884200	-0.32605200
C	-4.22016600	-1.63797100	0.19265300
C	2.39900300	3.72710200	-0.33999500
H	1.66001800	4.50843000	-0.51499900
C	-2.51216100	-3.85905000	0.20511400
H	-1.82871800	-4.70736600	0.22166600
C	-2.93567800	-1.54106100	-0.42443900
C	4.25642300	1.67671100	0.11504200
C	-5.70668100	1.91062500	0.20231900
C	4.59972900	3.02966400	0.30020600
H	5.61250100	3.23680700	0.63184300
C	-6.01868800	2.13670400	1.68459900
H	-6.60801900	3.05387200	1.81508000
H	-5.08937100	2.24196200	2.25585600
H	-6.57976900	1.28936400	2.08530900
C	-7.00888400	1.79601200	-0.59536300
H	-6.79046200	1.65263300	-1.65881800
H	-7.60447000	2.71184400	-0.48546800
H	-7.59301600	0.94328300	-0.24291700
C	3.69014500	4.04873300	0.07406500

Trans-TS1'_{CONH} (Trans Attack)

Mo	0.07451300	0.07447700	-1.67448000
S	-2.19392800	0.26186400	-0.82435000
S	2.49121400	-0.10509800	-1.36201600
S	-0.33070700	-2.31905600	-1.20784100
S	0.50760100	2.48566900	-1.24080100
O	6.27236600	0.25778000	0.38438800
O	-0.06968500	0.11021700	-3.37503000
O	-6.38584800	-0.77352400	0.48061400
N	4.26826900	-0.66100800	1.02254300
H	3.25924300	-0.52886200	0.89395400
N	-4.66585100	0.67415400	0.84185000
H	-3.69515400	0.83898000	0.56820200
C	-5.16878200	-0.52909300	0.43967900
C	-4.64506300	-2.89072700	0.20437600
H	-5.66479900	-3.01215800	0.55853000
C	-3.82937600	-3.98088600	-0.06228600
H	-4.20245100	-4.99441500	0.08175800
C	-2.01666100	-2.48152200	-0.71045600
C	-4.46869400	3.01469000	1.28631000
H	-3.76797600	3.12961300	0.45157700
H	-3.88074700	2.80720700	2.18739100
H	-4.99376600	3.96580900	1.42869300
C	3.02222100	1.44129300	-0.64391700
C	-4.17248200	-1.57778200	0.03470900
C	2.69775600	3.80934700	-0.25712500
H	2.05982400	4.68941900	-0.33349900
C	-2.52486000	-3.77209300	-0.50087200
H	-1.86377700	-4.61603500	-0.69424400
C	-2.85689100	-1.35895700	-0.46283600
C	4.25601500	1.52624400	0.03718600
C	-5.46759400	1.89031400	1.01791500
C	4.74089600	2.76587100	0.47728600
H	5.70657900	2.79439000	0.97755800
C	-6.41053600	1.74124500	2.21210500
H	-6.97076100	2.67250100	2.36796700

H	-5.84088700	1.52651200	3.12272300	C	3.12208100	-1.41023300	-0.07544200
H	-7.11389200	0.92346900	2.04286400	C	-3.83475200	1.84402000	0.03235900
C	-6.26372000	2.20071000	-0.25299700	C	5.07366000	2.46990900	-0.71081000
H	-5.58529700	2.31482400	-1.10485900	C	-3.75573400	3.19104900	-0.33996200
H	-6.82972000	3.13331400	-0.13183700	H	-4.53243100	3.57036200	-0.99671900
H	-6.96151800	1.38856700	-0.47067400	C	6.02358500	2.79323800	-1.86399200
C	3.96985700	3.91062600	0.30542100	H	6.40664800	3.81677100	-1.76065600
H	4.33758900	4.87782800	0.64688100	H	5.49928900	2.71759400	-2.82274000
C	4.67949600	-2.07421000	1.08866900	H	6.86313600	2.09474400	-1.87303500
C	5.03678400	0.31777300	0.45444200	C	5.80525200	2.58223100	0.63003200
C	3.42246600	-2.87050700	1.43163800	H	5.12182100	2.35068400	1.45323200
H	2.61008900	-2.64871700	0.72771900	H	6.19114400	3.59992400	0.77183300
H	3.06897700	-2.63128800	2.44212700	H	6.64220300	1.87994400	0.66557100
H	3.63423900	-3.94510600	1.39786400	C	-2.70650600	4.00094800	0.08777000
C	5.21763500	-2.54127400	-0.26721900	H	-2.67329000	5.04985200	-0.20310400
H	6.11071800	-1.97403500	-0.54166900	C	-5.80338600	-1.17079400	-1.29068900
H	4.45835500	-2.39029700	-1.04101300	C	-4.94906300	1.10122800	-0.66201600
H	5.47409100	-3.60745800	-0.22451800	C	-5.39225800	-2.57129400	-0.84016900
C	5.74227900	-2.25787500	2.17191900	H	-5.59391800	-2.71583200	0.22700000
H	5.35976900	-1.92306300	3.14316500	H	-4.32009000	-2.73321300	-0.99913500
H	6.63238300	-1.67151200	1.92976800	H	-5.94565500	-3.33154000	-1.40225100
H	6.02161900	-3.31642600	2.25684700	C	-7.29306800	-0.94613100	-1.01909200
C	2.18660600	2.58414200	-0.71599400	H	-7.57744200	0.07018300	-1.30192800
N	0.39938100	0.09763700	2.09477700	H	-7.51263300	-1.08570300	0.04506000
C	1.51685500	0.09631900	3.01441600	H	-7.89753200	-1.66135000	-1.59219100
C	-0.49291800	-1.03644500	2.24590000	C	-5.50994100	-1.00684800	-2.78435700
C	-0.27120000	1.38588500	2.05806200	H	-4.44712100	-1.17638100	-2.98460400
H	1.18039200	0.27305500	4.05226800	H	-5.76766300	0.00135300	-3.11616300
H	2.03139900	-0.86511800	2.95683200	H	-6.09128500	-1.73359800	-3.36596200
H	2.21716700	0.88190100	2.71529700	C	-1.69831900	2.11098400	1.25037200
H	-0.96480300	-1.04250600	3.24532400	N	-0.34948900	0.14144100	-1.59598600
H	-1.26369400	-0.98090500	1.47530700	C	-0.58695800	1.53744000	-1.88838200
H	0.07586900	-1.95604400	2.08865100	C	-1.50989900	-0.67129700	-1.89151300
H	0.45417000	2.14929400	1.76565700	C	0.80396900	-0.33012700	-2.33050100
H	-1.05912200	1.35422700	1.30279400	H	-0.68718200	1.72304300	-2.98198100
H	-0.70137300	1.62756500	3.04825300	H	-1.50365800	1.87925600	-1.40166000
O	1.25037800	-0.11955600	0.48533600	H	0.24694100	2.14127100	-1.50923300

Trans-INT1_{CONH} (Trans Attack)

Mo	0.23704600	-0.89598800	1.73559100
S	2.36426100	-0.10113400	0.86175800
S	-2.99463200	-0.21215700	1.77621600
S	0.74225700	-2.81383400	0.32693400
S	-0.27683900	1.52496300	2.09194700
O	-5.75475700	1.69431600	-1.40124400
O	0.52525500	-1.46778600	3.31442400
O	6.45874900	-0.06171200	-0.84934000
N	-4.99179900	-0.24535000	-0.50138800
H	-4.32803700	-0.63506600	0.17486100
N	4.50941400	1.12546900	-0.87729500
H	3.53783700	1.04410500	-0.57764700
C	5.22083600	-0.03426600	-0.77027600
C	5.00157300	-2.40406800	-1.28805000
H	5.99929100	-2.27440900	-1.69921100
C	4.32738900	-3.61376000	-1.37487200
H	4.79311800	-4.47091700	-1.85930600
C	2.42115800	-2.63751400	-0.21266700
C	3.88260700	3.42602900	-0.73290800
H	3.17626500	3.19710600	0.07352500
H	3.34082600	3.34972400	-1.68250600
H	4.22191400	4.46081900	-0.61160600
C	-2.85165500	1.31700000	0.93760300
C	4.40622300	-1.29068900	-0.67513000
C	-1.67252100	3.45279000	0.83505000
H	-0.80420900	4.05044200	1.10774800
C	3.03737600	-3.71645400	-0.85742000
H	2.47767900	-4.64661200	-0.94797600

Trans-TS2'_{CONH} (Trans Attack)

Mo	0.14969000	-0.71089000	-1.87426500
S	-2.05051400	-0.13893500	-0.95278400
S	3.30502200	0.35511500	-1.93711000
S	-0.09788800	-2.58966500	-0.35657700
S	0.37138900	1.78143200	-2.04243400
O	5.75965600	1.21035100	1.34766700
O	-0.09055100	-1.29864100	-3.45798700
O	-6.17224800	-0.67524700	0.43094200
N	4.08551900	-0.31977300	0.99066400
H	3.23775900	-0.46141000	0.44382900
N	-4.43248000	0.77707000	0.71761700
H	-3.42588200	0.83065100	0.57706000
C	-4.95299800	-0.47077000	0.51769500
C	-4.40387300	-2.76261000	1.15681600
H	-5.42491700	-2.77818700	1.52957500
C	-3.55578900	-3.85123900	1.31302600
H	-3.90133600	-4.75040900	1.82110000
C	-1.78796000	-2.64145500	0.15618300
C	-4.12000900	3.14698000	0.55476000
H	-3.26037000	2.99671500	-0.10923900
H	-3.74816900	3.19148100	1.58429600

H	-4.57671500	4.11290800	0.31208700	H	-3.22823100	2.58415500	2.79291600
C	2.89123400	1.61346800	-0.82821300	C	-1.94848200	1.19055400	3.83432700
C	-3.96165700	-1.59396400	0.51980100	H	-1.87736300	1.78364900	4.74446800
C	1.51871100	3.54572300	-0.30256600	C	-1.34800800	-0.79857100	2.57197800
H	0.61505100	4.12944600	-0.47493500	C	-3.97947200	0.77081700	-3.08369800
C	-2.25138100	-3.77719300	0.83016500	H	-4.28581900	-0.26211800	-2.88625400
H	-1.56158600	-4.60843200	0.96954700	H	-2.90487300	0.76396300	-3.29704000
C	-2.65707300	-1.53639100	-0.03770300	H	-4.50574600	1.12489100	-3.97735900
C	3.71088000	1.92735500	0.29188800	C	2.26393400	-0.60447900	-1.06882600
C	-5.14178700	2.02446200	0.39273100	C	-2.77400800	0.91463700	1.55659300
C	3.53523200	3.13316000	0.96624600	C	2.56444800	-1.31881300	-3.39665100
H	4.20556000	3.37334700	1.78868800	H	2.30829600	-2.01338100	-4.19468900
C	-6.30694600	2.23498400	1.35936600	C	-1.28065100	-0.02798200	3.73551200
H	-6.80344700	3.19096800	1.14791400	H	-0.68449800	-0.40046900	4.56653400
H	-5.94610000	2.25676400	2.39351700	C	-2.08431800	-0.33542500	1.43312600
H	-7.03264400	1.42417900	1.26406600	C	3.16838100	0.47428200	-1.31999700
C	-5.64311100	1.99100600	-1.05360300	C	-4.29642500	1.67359800	-1.89315300
H	-4.80416200	1.83349700	-1.73898000	C	3.74836100	0.60449900	-2.59070300
H	-6.13171600	2.93987500	-1.30942300	H	4.43816800	1.43188200	-2.72985300
H	-6.36086400	1.17831400	-1.19047000	C	-3.84615500	3.10496700	-2.19631100
C	2.46210300	3.96676800	0.62969500	H	-4.39877900	3.50259600	-3.05773600
H	2.31978800	4.91137100	1.15326700	H	-2.77644100	3.12494200	-2.43395600
C	4.82467900	-1.55632300	1.27505300	H	-4.02145900	3.74795000	-1.33056600
C	4.64689000	0.92185700	0.88609900	C	-5.80256900	1.64210200	-1.61510400
C	3.82945300	-2.69402500	1.06293500	H	-6.13014800	0.61605800	-1.41583400
H	3.43319800	-2.68146900	0.04142700	H	-6.35513500	2.01712500	-2.48655800
H	2.97273700	-2.60282800	1.73946700	H	-6.04221100	2.25912900	-0.74648600
H	4.31304200	-3.66050600	1.24492900	C	3.45853600	-0.27582500	-3.62297000
C	5.99984700	-1.70501400	0.30460300	H	3.91936100	-0.15086900	-4.60137100
H	6.70794400	-0.88141600	0.43099000	C	3.26083100	2.58068000	1.90145500
H	5.63494600	-1.69156800	-0.72769400	C	3.60105000	1.55171100	-0.35997300
H	6.52264600	-2.65371500	0.48238000	C	2.24434700	2.30282100	3.00814200
C	5.32168700	-1.54471300	2.72042000	H	2.28103600	1.25503500	3.32658300
H	4.47831700	-1.43570900	3.41109200	H	1.22141700	2.50325600	2.66958700
H	6.01073500	-0.71166200	2.88076100	H	2.44714000	2.93760300	3.87802900
H	5.83693300	-2.48636700	2.95048600	C	4.67690500	2.29054700	2.40806600
C	1.68378000	2.35148000	-1.02601700	H	5.40234800	2.44061800	1.60444800
N	-0.14326100	0.94593300	2.83697800	H	4.74939500	1.25498900	2.75633700
C	-1.08780600	-0.15852100	2.89293500	H	4.92554400	2.95571200	3.24512200
C	1.07618700	0.52022200	2.16941200	C	3.15601500	4.04192500	1.45639800
C	-0.72507200	2.06468000	2.11338100	H	2.13599600	4.26802400	1.12564400
H	-1.35774200	-0.53804200	1.89300300	H	3.84230500	4.23576800	0.62842800
H	-0.65209600	-0.99164700	3.45657100	H	3.39903100	4.71062100	2.29247100
H	-2.00750500	0.16044000	3.39915500	C	1.96047000	-1.48664000	-2.14709200
H	0.89599600	0.17276200	1.12964800	N	0.58709400	2.18321100	-1.32171800
H	1.78973500	1.34999500	2.13053800	C	1.06484700	3.36076700	-1.99370000
H	1.53594700	-0.30986200	2.71828600	C	-0.22337300	2.48771500	-0.16711400
H	-1.65674400	2.37391400	2.60416300	C	-0.07509500	1.26886800	-2.22244400
H	-0.02692800	2.90930600	2.11789300	H	0.24737800	3.98226600	-2.42824000
H	-0.94937600	1.81938700	1.05532800	H	1.63112900	3.98710300	-1.29340600
O	2.05102600	-0.89946700	-1.41889700	H	1.74218000	3.07084300	-2.80630800

Dioxo_P CONH(Trans/Trans) (Trans Attack)

Mo	0.02387300	-3.11899400	0.30598900
S	-2.07851800	-1.35277900	0.01954400
S	1.48847700	-0.91716500	0.46399000
S	-0.50411800	-2.34580100	2.61105300
S	0.76125100	-2.77059100	-2.01627700
O	4.54718200	2.31256800	-0.64159700
O	-1.13843900	-4.22921000	-0.36415200
O	-4.27247400	2.62135500	0.79333200
N	2.92097300	1.67539300	0.80407600
H	2.15974400	0.10586600	0.96357200
N	-3.55095200	1.13015600	-0.75720600
H	-2.99808800	0.27974300	-0.90245900
C	-3.59672400	1.61389500	0.50897700
C	-2.69117700	1.64131700	2.75605700

Dioxo CONH (Trans/Trans)

Mo	3.05353100	0.01475800	-0.06562700
S	0.95372800	-1.08706100	-1.31043300
S	1.10353200	1.24032700	1.32231700
S	2.55154400	-1.970477500	1.33926100
S	2.47657800	1.96974800	-1.49309100
O	-2.82855200	3.13234200	1.98002700
O	4.14342500	0.46792400	1.21182800

O -2.85958700 -3.19891200 -1.92495300
 N -1.87477000 1.05814800 1.92160400
 H -1.02214000 0.58937500 1.61467100
 N -2.05413200 -1.06749200 -1.76763800
 H -1.22934700 -0.55552600 -1.45413800
 C -2.04763100 -2.38978900 -1.44711900
 C -1.50073900 -3.84304600 0.43489400
 H -2.47557800 -4.27330300 0.21990900
 C -0.72326100 -4.29532800 1.49243900
 H -1.07985800 -5.09472200 2.13989500
 C 0.99535700 -2.67091700 0.91312700
 C -2.27784600 0.96503600 -3.00554500
 H -1.18736200 1.06640700 -3.05721900
 H -2.61239000 1.49812800 -2.10915300
 H -2.71041200 1.46034900 -3.88252500
 C 0.24529500 2.23979000 0.17820400
 C -1.06098500 -2.80331900 -0.39517200
 C 0.33782100 3.57849800 -1.87071500
 H 0.88099700 3.86298100 -2.77025800
 C 0.51108200 -3.69572800 1.73391800
 C 0.22906000 -2.22545600 -0.20421800
 C -1.06246600 2.76253800 0.40364000
 C -2.69440800 -0.50220600 -2.96331100
 C -1.59971000 3.72378500 -0.46334600
 H -2.58526000 4.11482700 -0.22293100
 C -4.21507900 -0.61465600 -2.85552100
 H -4.68792500 -0.15385600 -3.73280600
 H -4.57335900 -0.09597900 -1.96012600
 H -4.51588000 -1.66293600 -2.79557500
 C -2.19680400 -1.22341000 -4.22021800
 H -1.10757900 -1.14277300 -4.29530100
 H -2.64298800 -0.77557600 -5.11776300
 H -2.46573700 -2.28256500 -4.18504400
 C -0.90566600 4.14145800 -1.59075200
 H -1.33834400 4.87701800 -2.26685900
 C -2.45119900 0.51807700 3.15908700
 C -1.97596100 2.35433200 1.52131600
 C -1.91549300 -0.90630300 3.28244100
 H -0.82025300 -0.91269900 3.33232900
 H -2.20748300 -1.51632800 2.42066700
 H -2.30347000 -1.38232800 4.19031200
 C -2.00112200 1.35258400 4.36311700
 H -2.35519800 2.38251800 4.26687700
 H -0.90818100 1.36484800 4.42760800
 H -2.40022600 0.92671100 5.29292200
 C -3.97706400 0.50346500 3.06654600
 H -4.30074800 -0.09758100 2.21038900
 H -4.35903000 1.51993400 2.94289000
 H -4.40445000 0.06525300 3.97794700
 C 0.91861400 2.63429500 -1.01676100
 O 4.09298500 -0.44932300 -1.38048200
 H 1.12315900 -4.01566900 2.57535400

Table S4**Cis-E NHCO**

Mo	-0.00001600	-1.77299400	0.75832000
S	-1.67729200	-0.09605900	0.17617000
S	1.67726200	-0.09607200	0.17614100
S	-1.65170000	-3.28616300	-0.18281400
S	1.65164600	-3.28617800	-0.18282700
O	-0.00000500	-1.96260900	2.45474900
C	-5.57976400	-0.95069400	-0.69618900
H	-6.49676800	-0.38621400	-0.81161700
C	-5.53807400	-2.33620000	-0.85747100
H	-6.45260500	-2.87208500	-1.10923600
C	-3.15556900	-2.37149500	-0.36543500
C	5.85187800	4.50300200	-0.03741800
H	6.34296200	4.48568100	-1.01452800
H	6.61692500	4.27302600	0.70982400
H	5.47167500	5.51515100	0.14885700
C	3.17425300	-0.97404100	-0.20483500
C	-4.39546800	-0.27973200	-0.37525900
C	4.34622300	-3.03654900	-0.69788500
C	-4.34628600	-3.03651500	-0.69781900
C	-3.17429400	-0.97401900	-0.20478000
C	4.39542700	-0.27976200	-0.37535400
C	4.70526300	3.49984900	0.02027600
C	5.57971000	-0.95073400	-0.69630900
H	6.49671400	-0.38625900	-0.81176700
C	4.05667200	3.54694900	1.40934400
H	3.71322200	4.56595700	1.62962300
H	4.77048400	3.25640100	2.18805800
H	3.18910900	2.88392000	1.49138000
C	3.65941100	3.85847500	-1.04247800
H	4.08705700	3.80371200	-2.04967300
H	3.29596600	4.88209300	-0.88457200
H	2.79174800	3.19145700	-1.01265000
C	5.53801100	-2.33624100	-0.85757000
H	6.45253300	-2.87213400	-1.10935100
C	-4.70516800	3.49990500	0.02018800
C	-5.85180600	4.50305500	-0.03708000
H	-6.61658800	4.27306300	0.71042900
H	-6.34323500	4.48575100	-1.01401600
H	-5.47154100	5.51520100	0.14908300
C	-4.05610300	3.54695700	1.40902900
H	-3.18853100	2.88389800	1.49073900
H	-4.76965100	3.25640400	2.18798400
H	-3.71255100	4.56595000	1.62921100
C	-3.65967400	3.85857000	-1.04291400
H	-4.08765900	3.80381800	-2.04996500
H	-2.79198700	3.19157100	-1.01339200
H	-3.29619300	4.88219200	-0.88511500
C	3.15551600	-2.37151900	-0.36548200
C	-5.27080500	2.08428000	-0.25887000
O	-6.46588300	1.90416800	-0.51324200
N	-4.32570200	1.11696400	-0.19718700
H	-3.37426600	1.40264000	0.02973500
N	4.32567700	1.11693900	-0.19732500
C	5.27081700	2.08422400	-0.25895000
O	6.46591300	1.90405800	-0.51319800
H	3.37424900	1.40263300	0.02960200
H	-4.31714000	-4.11766800	-0.82502900
H	4.31706900	-4.11770200	-0.82508200

Cis-TS1 NHCO (Cis Attack)

Mo	0.18659700	-1.23190200	0.28367100
S	-1.25809600	0.64521800	-0.46734700
S	2.11556400	0.12056200	-0.12612900

S	-0.90409700	-2.22414300	-1.84475300
S	1.74323900	-3.06325300	-0.10962300
O	0.00001900	-1.18593800	2.00495200
C	-4.96989900	-0.08398200	-2.01883500
H	-5.93307400	0.41247100	-2.01309400
C	-4.75764800	-1.29198800	-2.68566300
H	-5.58132300	-1.75076600	-3.23252500
C	-2.43259300	-1.37638100	-1.93987500
C	6.80621600	4.19044800	-0.09102000
H	7.39375400	3.99229200	-0.99205400
H	7.45359700	3.98295600	0.76559500
H	6.53079900	5.25229400	-0.07696700
C	3.53388900	-0.95616300	-0.09189500
C	-3.89106400	0.48821100	-1.33292600
C	4.50286500	-3.17397400	-0.08812000
C	-3.51830800	-1.92572700	-2.64536400
C	-2.61972700	-0.12971800	-1.29169300
C	4.84193900	-0.41906000	-0.08199900
C	5.54976800	3.32787700	-0.05221300
C	5.97120100	-1.24386100	-0.07014700
H	6.95800400	-0.79684900	-0.05809200
C	4.76482600	3.62681700	1.23132600
H	4.51272200	4.69400100	1.27949900
H	5.35491800	3.37844800	2.12046400
H	3.82809500	3.06285400	1.28520400
C	4.67375500	3.64543600	-1.27046700
H	5.19341900	3.40220900	-2.20377800
H	4.42789400	4.71488600	-1.28934200
H	3.72919400	3.09156600	-1.26439800
C	5.78278300	-2.62668500	-0.07624700
H	6.65243800	-3.28306700	-0.07051700
C	-4.65504600	3.65873900	0.63907400
C	-5.87626500	4.54781300	0.84369800
H	-6.71417700	3.97961600	1.25733000
H	-6.21669600	4.97416600	-0.10452400
H	-5.63222800	5.36821300	1.53038800
C	-4.21990800	3.06590200	1.98604000
H	-3.31085100	2.46092900	1.89465800
H	-5.00486600	2.42692700	2.40743000
H	-4.01408600	3.86834200	2.70630600
C	-3.50669300	4.49381800	0.05998800
H	-3.77219400	4.90372400	-0.92082700
H	-2.58659300	3.91239800	-0.06078100
H	-3.27924300	5.33522800	0.72730900
C	3.36353000	-2.35257400	-0.08692200
C	-5.03346000	2.50818000	-0.32913700
O	-6.18309900	2.37991400	-0.76399800
N	-3.98974700	1.69418300	-0.60455400
H	-3.09267800	1.91015100	-0.16666100
N	4.91073500	0.98907700	-0.07893400
C	5.97187600	1.83691100	-0.07198600
O	7.16075100	1.50179800	-0.07569500
H	3.98418500	1.39899000	-0.07292300
H	-3.37255800	-2.88141900	-3.14583000
H	4.36276500	-4.25427300	-0.09578200
N	-2.86958900	-2.35708800	1.86461700
C	-2.21495600	-2.97354200	3.06233700
H	-2.10295400	-4.03592400	2.84187700
H	-1.23314000	-2.50169100	3.13986300
H	-2.82502600	-2.81714100	3.96220500
C	-3.06380900	-0.88800000	2.10422200
H	-2.07271600	-0.45494700	2.24264200
H	-3.52112200	-0.47966400	1.20089300
H	-3.70869900	-0.73727400	2.97930900
C	-4.20469800	-2.97854200	1.63063100
H	-4.61626800	-2.50897400	0.73562400
H	-4.03284100	-4.03776500	1.43733200
H	-4.86484500	-2.83332800	2.49627600
O	-2.11160600	-2.59162100	0.75281300

Cis-ES NHCO (Cis Attack)

Mo 0.16853700 -1.16006700 0.30985200
S -1.29806900 0.70986400 -0.47644000
S 2.11221100 0.15910600 -0.16696900
S -0.83108900 -2.10583400 -1.94115800
S 1.69857400 -3.02165500 -0.00665000
O 0.01067300 -1.02413800 2.03194700
C -4.98755000 -0.13812100 -2.01888600
H -5.97082900 0.31641700 -1.99072400
C -4.72894100 -1.31415800 -2.72505200
H -5.53658700 -1.79107700 -3.28027600
C -2.39250200 -1.32241100 -2.00048000
C 6.85887600 4.16394600 -0.18193000
H 7.43135000 3.94537500 -1.08817700
H 7.51470500 3.95747300 0.66836300
H 6.59971400 5.23002000 -0.17912200
C 3.51450900 -0.93450500 -0.07395600
C -3.92774700 0.45897500 -1.32456700
C 4.45589900 -3.16282000 0.03313800
C -3.46284800 -1.89445100 -2.71364500
C -2.62918900 -0.10287600 -1.31142400
C 4.83023200 -0.41533200 -0.07487200
C 5.59022800 3.32089500 -0.11414300
C 5.94880400 -1.25313300 -0.02173700
H 6.94096500 -0.81802900 -0.01992500
C 4.82604700 3.65116100 1.17420700
H 4.58562700 4.72163700 1.20736500
H 5.42574200 3.41157000 2.05934600
H 3.88506000 3.09671300 1.24875500
C 4.70422600 3.63277000 -1.32614900
H 5.20740100 3.36560000 -2.26193200
H 4.47671100 4.70597800 -1.35933100
H 3.74957900 3.09700600 -1.30006300
C 5.74299800 -2.63251900 0.02813800
H 6.60408400 -3.29921200 0.06555600
C -4.80271300 3.54717600 0.72971700
C -6.05834000 4.37730900 0.97089600
H -6.86222300 3.76596000 1.39095000
H -6.43511200 4.80267900 0.03620600
H -5.83798200 5.19655100 1.66698500
C -4.32288700 2.94556600 2.05725200
H -3.38734700 2.38686600 1.94186500
H -5.07152400 2.26132500 2.47345000
H -4.14559800 3.74067600 2.79301200
C -3.70014900 4.44370800 0.15343000
H -3.99875100 4.86440000 -0.81315600
H -2.75876900 3.90421800 0.00491600
H -3.49826700 5.27827200 0.83730200
C 3.32733600 -2.32802200 -0.00739000
C -5.14356200 2.40450800 -0.26179600
O -6.28921300 2.24575300 -0.69746400
N -4.07179100 1.63625000 -0.55868800
H -3.17996000 1.87273000 -0.11844100
N 4.92489800 0.99075100 -0.12308900
C 5.99091300 1.82393100 -0.10636500
O 7.17502100 1.47289900 -0.07468400
H 3.99698300 1.41224600 -0.14395300
H -3.28037900 -2.82585700 -3.24694100
H 4.30160300 -4.24063800 0.07076300
N -2.69529600 -2.40406400 1.78208000
C -2.02997600 -2.97344200 2.99712300
H -1.79508000 -4.01234300 2.76266700
H -1.10850900 -2.40275600 3.13082500
H -2.69586300 -2.90272000 3.86736500
C -3.04395200 -0.96463700 2.02357200
H -2.10744700 -0.43372100 2.19506600

H -3.51521300 -0.59372900 1.11080800
H -3.72469800 -0.89194300 2.88074700
C -3.94873400 -3.15183600 1.48663900
H -4.37540500 -2.71121300 0.58418600
H -3.66433100 -4.18483700 1.28532200
H -4.64747100 -3.08715500 2.33054500
O -1.88114200 -2.56076400 0.68807100

Cis-TS2 NHCO (Cis Attack)

Mo -0.21626800 -1.67964200 -0.60224100
S 0.45685700 -1.52017200 2.05071100
S -1.87108100 0.09689000 -0.18905500
S 1.71991800 0.17953200 -0.47520400
S -2.06364300 -3.14517300 -0.11052700
O -0.07426700 -1.56724900 -2.31315000
C 3.54157000 0.49428900 3.71434300
H 3.97493900 0.57442600 4.71090700
C 4.09907000 1.22187200 2.66277300
H 4.95835800 1.86743300 2.79710600
C 2.38967900 0.27584200 1.15053400
C -3.43170000 -0.72446500 -0.09117500
C 2.44002300 -0.32778900 3.50448500
C -4.77698000 -2.74080700 0.05644700
H -4.82342500 -3.82859900 0.09072800
C 3.52009400 1.10359800 1.39595600
C 1.83360100 -0.46276000 2.23711800
C -4.63195700 0.02877900 -0.02065300
C -5.88312600 -0.58778800 0.07934200
H -6.77400900 0.02584000 0.12707200
C -5.94217000 -1.98028300 0.11776800
H -6.91021900 -2.47329600 0.19988600
C -3.51834100 -2.13235300 -0.04890000
H 2.00953200 -0.89012100 4.33101600
O 0.84242400 -3.50413300 -0.50920200
N 2.33579000 -3.65986800 -0.65148200
C 3.04872400 -3.02904300 0.47976700
C 2.72932500 -3.04887400 -1.93455100
C 2.53273800 -5.11466500 -0.65570700
H 4.11413400 -3.29078700 0.42144700
H 2.91560100 -1.95033600 0.40020000
H 2.58783500 -3.37142400 1.40675200
H 3.80705300 -3.18704800 -2.09383100
H 2.14201200 -3.51938300 -2.72350700
H 2.47576000 -1.98586100 -1.87873400
H 3.59483500 -5.35767000 -0.79412800
H 2.17018500 -5.49917600 0.29787400
H 1.92901800 -5.53037000 -1.46287400
C -5.46708200 4.60492200 -1.17805700
H -6.55556500 4.53235600 -1.09962500
H -5.16551400 4.17843200 -2.14142400
H -5.17903600 5.66381600 -1.17264700
C -4.79926100 3.86574800 -0.01511900
C -3.28173200 3.95001700 -0.16378500
H -2.96982900 5.00123500 -0.16819800
H -2.92905000 3.50022800 -1.09816700
H -2.75042800 3.45789500 0.65773900
C -5.21822100 4.52611800 1.30262100
H -6.30272100 4.46213900 1.43130900
H -4.92068300 5.58239400 1.31168500
H -4.74278600 4.03437700 2.15841600
N -4.46853900 1.43048700 -0.05373200
C -5.37665600 2.42944000 0.00337500
O -6.60300300 2.28058600 0.07860700
H -3.48185900 1.67688600 -0.11595600
C 5.21998200 3.10960000 -1.36378600
C 6.43453100 4.02716900 -1.44695300
H 7.34487100 3.50425900 -1.13959000

H 6.32260100 4.88930800 -0.78317800
 H 6.56245000 4.38762300 -2.47550100
 C 5.42019400 1.91231200 -2.30230900
 H 4.55243000 1.24357800 -2.31311400
 H 6.29312200 1.32031800 -2.00422000
 H 5.58389600 2.26077100 -3.33074500
 C 3.96452000 3.88113400 -1.78686800
 H 3.77210100 4.72104300 -1.11033900
 H 3.07058400 3.24942200 -1.79363500
 H 4.09293800 4.28533100 -2.79947900
 C 5.07436200 2.61329000 0.09836800
 O 5.87244400 2.95894300 0.97670500
 N 4.01431100 1.79185300 0.26970000
 H 3.44245800 1.57838700 -0.54920700

Dioxo_P NHCO (Cis/Trans) (Cis Attack)

Mo 0.37654700 1.66455600 -1.27158500
 S -1.86796300 0.64332900 -0.84087600
 S 1.30564700 -0.84170600 -0.78732300
 S 0.17756600 1.78636300 1.39313400
 S 2.79744000 2.05165700 -0.99761600
 O 0.02682900 1.17014200 -2.90351800
 C -3.61257300 -0.45356300 2.65695500
 H -4.51065100 -0.98598000 2.94252200
 C -2.71716900 0.04952500 3.60139500
 H -2.92638900 -0.09127800 4.66095100
 C -1.26120500 0.92567800 1.85120500
 C 2.84100000 -6.62457900 0.83643600
 H 3.33784600 -6.61260200 1.81095600
 H 3.58350100 -6.94967400 0.10194200
 H 2.02696800 -7.35941000 0.86636000
 C 3.00202400 -0.66567900 -0.43860100
 C -3.32593200 -0.26635900 1.30221900
 C 5.03806500 0.67325000 -0.32326900
 C -1.56369000 0.71685400 3.21187300
 C -2.16459800 0.42862500 0.88038400
 C 3.78126800 -1.78527600 -0.02998200
 C 2.28581900 -5.24907000 0.48445200
 C 5.15312800 -1.68419900 0.20407600
 H 5.70488900 -2.56775300 0.50077800
 C 1.58797400 -5.31345600 -0.88014100
 H 0.78842700 -6.06484800 -0.85817300
 H 2.29312400 -5.59327500 -1.67089300
 H 1.13566300 -4.35689200 -1.16209200
 C 1.27537000 -4.81396300 1.55267900
 H 1.75298700 -4.72225700 2.53423000
 H 0.47156300 -5.55609900 1.63679900
 H 0.81023600 -3.85048900 1.32035500
 C 5.77646700 -0.44561200 0.04770700
 H 6.84631800 -0.35499700 0.22729600
 C -5.88057300 -1.76933100 -1.09810400
 C -7.23464500 -2.45328100 -0.94559900
 H -7.95165600 -1.80023500 -0.43997700
 H -7.15293300 -3.36411400 -0.34581900
 H -7.63278800 -2.71697400 -1.93323900
 C -6.04190900 -0.50509800 -1.95131800
 H -5.09035400 0.00831700 -2.12458400
 H -6.72140400 0.20898400 -1.47308600
 H -6.45999400 -0.76403000 -2.93245200
 C -4.89895100 -2.72723100 -1.78423300
 H -4.73050600 -3.62241700 -1.17583100
 H -3.92427600 -2.26509900 -1.97026000
 H -5.30110700 -3.04829500 -2.75351600
 C 3.65820600 0.58090500 -0.56167100
 C -5.35560900 -1.39381000 0.31065700
 O -5.99740000 -1.65556500 1.33091800
 N -4.15356400 -0.76697700 0.27584000

H -3.74271100 -0.61094500 -0.64106900
 N 3.06314600 -2.98402700 0.12386000
 C 3.46147000 -4.24309700 0.42429800
 O 4.62762100 -4.59422000 0.62939800
 H 2.06765200 -2.82540400 -0.03538900
 H -0.86674300 1.09694000 3.9502300
 H 5.52038900 1.64269900 -0.42998500
 N 0.91462200 6.12615200 1.33522300
 C 1.94111900 5.21388700 0.84697900
 H 2.93183200 5.59507900 1.12376900
 H 1.80523500 4.22620000 1.29626500
 H 1.90436500 5.07313500 -0.24772900
 C -0.41035400 5.58722700 1.05891400
 H -0.49673600 4.58044300 1.48006200
 H -1.16971100 6.23741500 1.51216500
 H -0.61264800 5.49800000 -0.02365400
 C 1.06393700 7.42436900 0.72376900
 H 0.30622800 8.11507300 1.11573400
 H 2.05526300 7.83658400 0.95076800
 H 0.95548600 7.39770100 -0.38298500
 O 0.26962100 3.39896000 -1.34888700

Dioxo NHCO (Cis/Trans)

Mo -0.06413200 -2.38678500 -0.81560400
 S 1.95770500 -0.92170800 -0.59275500
 S -1.56995800 -0.08708900 -0.82995700
 S 0.05126900 -1.97372500 1.79980200
 S -2.34776700 -3.22572300 -0.38134300
 O 0.40584300 -4.04910600 -0.65170400
 C 3.68171800 0.65993500 2.72810000
 H 4.55002900 1.27167800 2.93565400
 C 2.82377400 0.22254200 3.73768900
 H 3.02988300 0.50211800 4.77000800
 C 1.41810400 -0.95125300 2.12384100
 C -4.30628200 5.41843000 -0.10108700
 H -4.74627500 5.49487600 0.89733300
 H -5.13290400 5.42314400 -0.81760800
 H -3.68192100 6.30295000 -0.27899900
 C -3.13681600 -0.56041000 -0.24089400
 C 3.39677600 0.29585700 1.40915300
 C -4.77898700 -2.26467500 0.35247400
 C 1.71465000 -0.56025500 3.44560200
 C 2.27400200 -0.50656200 1.08686600
 C -4.12544700 0.41744000 0.06894300
 C -3.46433800 4.15464800 -0.23725400
 C -5.40802300 0.06605200 0.49097200
 H -6.12585300 0.84924700 0.70365700
 C -2.88059100 4.08004100 -1.65375500
 H -2.27432200 4.97177400 -1.85845900
 H -3.67652700 4.03274300 -2.40547900
 H -2.23902800 3.20372200 -1.79461400
 C -2.32026900 4.19117800 0.78317100
 H -2.70531900 4.20500300 1.80867800
 H -1.71572700 5.09534500 0.63734500
 H -1.65151200 3.32939800 0.69270200
 C -5.72876400 -1.28512100 0.62512400
 H -6.72628900 -1.57198000 0.95375900
 C 5.85075300 1.62765100 -1.19008500
 C 7.13052000 2.45477800 -1.14520600
 H 7.90221500 1.95774500 -0.55046700
 H 6.95298800 3.43182400 -0.68715700
 H 7.51287200 2.60643500 -2.16228800
 C 6.14649400 0.26476500 -1.82861200
 H 5.24830400 -0.35313900 -1.93106200
 H 6.87178400 -0.30066900 -1.23313500
 H 6.56768300 0.40266200 -2.83264000
 C 4.79598400 2.36350300 -2.02531000
 H 4.54160100 3.33008100 -1.57687900
 H 3.86829000 1.79062600 -2.12509400

H 5.17919500 2.55039100 -3.03655400
 C -3.48636500 -1.92141500 -0.07256500
 C 5.33685200 1.43320300 0.25901500
 O 5.93647100 1.91127700 1.22572200
 N 4.19642100 0.70305600 0.32059600
 H 3.81579200 0.36965600 -0.56114800
 N -3.70391900 1.75056800 -0.07725700
 C -4.36916800 2.92481300 0.02401100
 O -5.56938200 3.04735000 0.29100200
 H -2.71364900 1.77965900 -0.32636100
 H 1.05127800 -0.89658100 4.23932300
 H -5.02344200 -3.31847600 0.47101000
 O 0.19200000 -2.06072600 -2.50910000

Trans-E NHCO

Mo-0.000001600 0.000000000 0.89625000
 S -2.30018800 -0.33753900 0.15913500
 S 2.30021100 0.33753900 0.15930800
 S -0.41967800 2.26186000 0.10667200
 S 0.41968900 -2.26187200 0.10673000
 O -0.000008100 0.000001400 2.60344800
 C -4.95307400 2.69259500 -0.53398000
 H -6.02345700 2.77626900 -0.67659200
 C -4.11341500 3.80678400 -0.56117700
 H -4.54182800 4.79351000 -0.73314600
 C -2.16645300 2.41195200 -0.13357500
 C 8.34604900 1.63021300 -0.46028000
 H 8.69350800 1.22437800 -1.41435000
 H 8.86740900 1.08140500 0.32944500
 H 8.63054100 2.68809000 -0.39958600
 C 2.99491500 -1.27470100 -0.10632900
 C -4.38579800 1.43375500 -0.31254200
 C 2.74146800 -3.67039600 -0.36881400
 C -2.74146200 3.67041500 -0.36880200
 C -2.99489600 1.27470500 -0.10646300
 C 4.38581600 -1.43374500 -0.31242900
 C 6.83430200 1.48961900 -0.32166300
 C 4.95308000 -2.69257400 -0.53396200
 H 6.02345800 -2.77624500 -0.67660900
 C 6.39211600 2.04681900 1.03676800
 H 6.71089400 3.09241300 1.13573000
 H 6.83783400 1.47916500 1.86098400
 H 5.30526200 2.02255900 1.16754800
 C 6.14156500 2.27361900 -1.44311400
 H 6.41988000 1.88075600 -2.42734500
 H 6.43689000 3.32994200 -1.40482000
 H 5.05049700 2.23123700 -1.36404000
 C 4.11341700 -3.80675800 -0.56121600
 H 4.54182400 -4.79347500 -0.73325800
 C -6.83428100 -1.48963700 -0.32158600
 C -8.34602500 -1.63025300 -0.46018300
 H -8.69347600 -1.22474100 -1.41439700
 H -8.86738600 -1.08118000 0.32935400
 H -8.63053000 -2.68810700 -0.39916200
 C -6.14156100 -2.27380600 -1.44291600
 H -5.05048700 -2.23142500 -1.36392600
 H -6.41991300 -1.88113400 -2.42721400
 H -6.43686500 -3.33012800 -1.40442400
 C -6.39211300 -2.04665700 1.03694900
 H -6.83776200 -1.47881100 1.86107100
 H -5.30525400 -2.02244600 1.16766400
 H -6.71097500 -3.09220600 1.13610800
 C 2.16646600 -2.41194400 -0.13351300
 C -6.46579100 0.01135600 -0.43661000
 O -7.32196500 0.87057600 -0.66883100
 N -5.14285500 0.24515500 -0.27063400
 H -4.54403100 -0.55726500 -0.08057700

N 5.14288400 -0.24514800 -0.27051500
 C 6.46579700 -0.01135900 -0.43666700
 O 7.32192600 -0.87055600 -0.66914000
 H 4.54409700 0.55726400 -0.08028400
 H -2.08936900 4.54214000 -0.39165000
 H 2.08937200 -4.54211600 -0.39171200

Trans-TS1 NHCO (Cis Attack)

Mo-0.27371700 -0.63690700 1.22673700
 S 1.42510200 0.12179000 -0.78452300
 S -2.42136500 -0.50223500 0.13774400
 S 0.24127300 -2.75340700 0.01251400
 S -0.55764300 1.79837700 1.38681900
 O -0.67152100 -1.14834900 2.81465200
 C 4.63287200 -2.34655600 -1.29404600
 H 5.67016900 -2.22567700 -1.58435900
 C 4.09166700 -3.59115500 -0.97256500
 H 4.72483100 -4.47725800 -1.00987500
 C 1.92006700 -2.58590100 -0.49690000
 C -8.11161600 -0.98093500 -2.25836500
 H -8.17967000 -0.24033600 -3.06036200
 H -8.84586500 -0.69840400 -1.49817900
 H -8.38489300 -1.96389500 -2.66220200
 C -3.03948500 1.15020700 0.36790500
 C 3.79998900 -1.22374200 -1.23647600
 C -2.74597300 3.45276200 1.07215500
 C 2.75794900 -3.70727800 -0.58225200
 C 2.43620400 -1.31276100 -0.85675500
 C -4.35889000 1.47978700 -0.02778200
 C -6.70364000 -1.03367100 -1.67559800
 C -4.87257500 2.77049700 0.13224600
 H -5.88870600 2.98163700 -0.17822600
 C -6.65770900 -2.06690800 -0.54340100
 H -6.96890700 -3.05042600 -0.91822900
 H -7.33250600 -1.78773600 0.27373400
 H -5.65339100 -2.17850300 -0.12202000
 C -5.71158200 -1.43779500 -2.77363700
 H -5.69689800 -0.69874600 -3.58221300
 H -6.00070500 -2.40478600 -3.20476000
 H -4.68838400 -1.53745600 -2.39691000
 C -4.04964900 3.75192500 0.68639900
 H -4.43574900 4.76261900 0.81490800
 C 5.42335900 2.11248300 -2.11188000
 C 6.84362800 2.58654200 -2.39953100
 H 7.26330400 2.06492700 -3.26412400
 H 7.50721000 2.38604800 -1.55269500
 H 6.84554200 3.66578600 -2.59794300
 C 4.52398500 2.43133800 -3.31275700
 H 3.48466300 2.13768400 -3.13281500
 H 4.86959100 1.90803400 -4.21145100
 H 4.53668900 3.50915600 -3.52186000
 C 4.88372700 2.83658700 -0.87222700
 H 5.46828300 2.58358700 0.02031500
 H 3.83482600 2.59232200 -0.66611400
 H 4.94278300 3.92341300 -1.01537500
 C -2.22853800 2.15715800 0.92426700
 O 1.98646500 -0.99518300 2.10178600
 N 2.59829000 -0.03393100 2.86359800
 C 3.84061000 -0.65598800 3.39962000
 C 2.96396200 1.15933300 2.03741400
 C 1.71175000 0.39570400 3.99139600
 H 3.48351400 1.89716800 2.66139100
 H 3.59197500 0.80220700 1.21981100
 H 2.03943300 1.56127500 1.61770700
 H 0.82987500 0.86885800 3.55090400
 H 1.39822600 -0.50903500 4.51135300
 H 2.25693000 1.08557200 4.64684300

H 4.40728300 0.06264400 4.00387100
 H 3.53667800 -1.51860000 3.99240300
 H 4.41750500 -0.99432700 2.53789300
 C 5.44843300 0.57746400 -1.88810900
 O 6.48393500 -0.08026800 -2.04991400
 N 4.24412700 0.08170500 -1.53212100
 H 3.46320300 0.73610000 -1.41707700
 N -5.10097700 0.42022700 -0.58685500
 C -6.33996900 0.37034100 -1.12911800
 O -7.12859200 1.31799700 -1.20428200
 H -4.54910000 -0.43690300 -0.59704800
 H 2.34886300 -4.67814600 -0.30713700
 H -2.10216200 4.22267700 1.49574400

Trans-ES_{NHCO} (Cis Attack)

Mo-0.26042200 -1.18277700 0.96299800
 S 1.33838500 0.43612100 -0.78388600
 S -2.37310400 -0.54440600 -0.06502000
 S 0.29893600 -2.60818700 -1.03145400
 S -0.55365600 0.96281500 2.12648300
 O -0.74815400 -2.29012600 2.17643600
 C 4.66951100 -1.56566700 -2.02639500
 H 5.69915800 -1.30168400 -2.23809100
 C 4.19483300 -2.87001700 -2.15604700
 H 4.87219200 -3.65909300 -2.48229700
 C 1.96885600 -2.19180100 -1.41264400
 C -8.01096400 0.10803300 -2.54919600
 H -8.06441900 1.11249800 -2.97882200
 H -8.75089200 0.06355800 -1.74474100
 H -8.28679700 -0.62038500 -3.32207400
 C -2.98814000 0.86458100 0.82475000
 C 3.77822500 -0.57107000 -1.60777100
 C -2.71576800 2.64482400 2.45284900
 C 2.86756300 -3.17527800 -1.85075700
 C 2.41576000 -0.84409100 -1.31125600
 C -4.29004100 1.36007000 0.56356000
 C -6.61033700 -0.19486700 -2.02883200
 C -4.80458100 2.47053100 1.23988800
 H -5.80770400 2.81185500 1.01485100
 C -6.58117800 -1.60795000 -1.43338300
 H -6.89252500 -2.34171100 -2.18806200
 H -7.26362800 -1.69113800 -0.58004400
 H -5.58186400 -1.89351000 -1.08887700
 C -5.60582100 -0.10895800 -3.18455200
 H -5.57794800 0.90130600 -3.60752100
 H -5.89227700 -0.80292000 -3.98529600
 H -4.58791400 -0.36595800 -2.87409000
 C -4.00121900 3.10763100 2.18584200
 H -4.38738600 3.97603000 2.71863800
 C 5.25897800 2.90904400 -1.14415300
 C 6.65134000 3.52134200 -1.24785500
 H 7.05470600 3.41721400 -2.25930700
 H 7.35276000 3.02397700 -0.57148700
 H 6.61137100 4.58791400 -0.99270200
 C 4.30981800 3.62526200 -2.11222000
 H 3.28497600 3.24651300 -2.03966100
 H 4.63972500 3.50220800 -3.15002200
 H 4.28374800 4.70033700 -1.89072000
 C 4.73397600 3.07126300 0.28820300
 H 5.36193100 2.52462400 1.00212800
 H 3.70557700 2.70672300 0.39716700
 H 4.74012200 4.13042900 0.57661200
 C -2.19931500 1.52347600 1.78718800
 O 1.83765400 -1.74138100 1.44969900
 N 2.56617500 -1.17913800 2.49259400
 C 3.80526900 -1.99491300 2.58179200
 C 2.92351600 0.24006900 2.19448800

C 1.79202700 -1.25881100 3.76707300
 H 3.51169300 0.64754000 3.02553600
 H 3.48620200 0.24227200 1.25935100
 H 1.99298800 0.79339000 2.04561200
 H 0.89956200 -0.63785600 3.64882600
 H 1.48375600 -2.29718300 3.88958100
 H 2.41735300 -0.91183400 4.59776800
 H 4.46327500 -1.60646300 3.36717100
 H 3.50164300 -3.02075600 2.78957200
 H 4.28446700 -1.95056800 1.60261800
 C 5.34925100 1.40321400 -1.50698200
 O 6.42570900 0.87954300 -1.82220600
 N 4.15678400 0.77565700 -1.43142100
 H 3.33326000 1.31286500 -1.13197100
 N -5.01618600 0.65519700 -0.41650500
 C -6.25043300 0.84482800 -0.93769800
 O -7.03903400 1.73749000 -0.60929500
 H -4.46436500 -0.12235500 -0.77963100
 H 2.50952700 -4.20078100 -1.92593100
 H -2.08708600 3.14741100 3.18693800

Trans-TS2_{NHCO} (Cis Attack)

Mo-0.61345100 0.59561600 1.09664100
 S 2.75478000 -0.98169400 -1.68359500
 S -2.69871100 -0.31737300 0.17456000
 S 0.24032500 -1.64504100 0.52998200
 S -1.45280700 2.64106900 0.04650500
 O -0.86171300 0.73491300 2.78165800
 C 4.66773300 -1.79619100 1.82132400
 H 5.70606900 -1.81142100 2.13301100
 C 3.62342000 -2.04700100 2.70967000
 H 3.83873200 -2.27755800 3.75214100
 C 1.97924200 -1.686662900 0.93240000
 C -5.65095600 -3.18023300 -0.06912500
 H -5.27313100 -2.78870300 0.88169700
 H -4.84025200 -3.10509700 -0.80165900
 H -5.85672500 -4.24687300 0.07895600
 C -3.69553900 1.06326800 -0.30304400
 C 4.36116700 -1.49256900 0.49532300
 C -3.95507400 3.43142800 -0.78147800
 C 2.30658000 -1.98673300 2.26344100
 C 3.01848300 -1.43216900 -0.00639600
 C -5.05863900 0.88365900 -0.64984800
 C -6.92295200 -2.47133800 -0.53014300
 C -5.85694200 1.95857400 -1.05272500
 H -6.89500700 1.78232400 -1.30472400
 C -7.40554600 -3.09397100 -1.84373000
 H -7.63130600 -4.15799300 -1.69958100
 H -6.64023100 -3.01490200 -2.62361200
 H -8.30666100 -2.58461400 -2.19725900
 C -8.01327500 -2.63881300 0.53308700
 H -7.69404200 -2.22228200 1.49499800
 H -8.23787600 -3.70220700 0.68385900
 H -8.92726300 -2.12291200 0.22500100
 C -5.29066500 3.23175900 -1.11729200
 H -5.90448000 4.07476700 -1.43078100
 C 7.27976500 -0.37120800 -1.66404300
 C 7.07388000 -1.40524000 -2.77624800
 H 6.01377500 -1.56720400 -2.99829600
 H 7.50951700 -2.37248500 -2.50063500
 H 7.56071800 -1.06731300 -3.70121100
 C 6.60709900 0.94780100 -2.06902400
 H 6.71203500 1.69908000 -1.27692000
 H 5.53571100 0.81306800 -2.26457600
 H 7.07100500 1.35041900 -2.97981600
 C 8.77184100 -0.14040800 -1.45225000
 H 9.27452000 -1.06450400 -1.15036100

H	8.94830900	0.59123300	-0.65885600	H	-3.74672100	-5.46385300	2.34279100
H	9.23203500	0.22331000	-2.38012000	C	-1.65890000	-3.80599700	1.75717300
C	-3.15301000	2.35926200	-0.37135100	H	-1.18773700	-2.81760400	1.74827300
O	1.36243100	0.93791300	0.83368400	H	-0.99404300	-4.49317100	1.22289800
N	2.09846400	2.22443700	0.47318400	H	-1.70849900	-4.13125000	2.80369800
C	3.51274000	1.83507800	0.65020500	C	-3.93844000	-2.77458400	1.87266800
C	1.82570800	2.53474300	-0.94520900	H	-4.94262000	-2.72767400	1.43509900
C	1.68469700	3.28733300	1.39744900	H	-3.51338600	-1.76468100	1.82596000
H	2.46819000	3.36737000	-1.25860100	H	-4.04091100	-3.04267800	2.93196600
H	2.05170700	1.62015900	-1.50705000	C	1.60442800	1.15537800	2.37897600
H	0.77138000	2.79700100	-1.04867700	O	-1.59579400	3.43773000	0.30095500
H	0.59456300	3.36824600	1.35348200	N	-4.92041800	1.60184100	1.10398300
H	1.98483500	2.99321000	2.40449600	C	-6.01858100	0.81395900	1.60715000
H	2.15401200	4.23570400	1.11085000	C	-4.47947700	1.09839400	-0.18602000
H	4.15408900	2.71482900	0.51871200	C	-3.81487600	1.60407800	2.04814800
H	3.62228900	1.40318300	1.64605700	H	-4.13925600	0.04358500	-0.13459300
H	3.73120200	1.07162800	-0.10257600	H	-5.30178000	1.15962700	-0.90916400
C	6.65545600	-0.86458500	-0.33234400	H	-3.63502000	1.69256800	-0.54703700
O	7.32649900	-0.92280200	0.70698200	H	-2.97856000	2.18124700	1.64389900
N	5.34953900	-1.17750000	-0.45515100	H	-4.14124500	2.05187400	2.99493800
H	4.87158800	-1.02485200	-1.36074900	H	-3.43956700	0.58108800	2.25694200
N	-5.54076300	-0.43823400	-0.54825000	H	-5.74650500	-0.25248900	1.77219100
C	-6.77115400	-0.95181100	-0.77937500	H	-6.36520800	1.21973300	2.56587200
O	-7.75338900	-0.30621800	-1.16212900	H	-6.85706400	0.83645800	0.89978900
H	-4.81068600	-1.07051000	-0.22787800	C	-3.00683100	-3.43411200	-0.35829800
H	1.48478800	-2.15148300	2.95740400	O	-3.49982600	-4.15821400	-1.22793200
H	-3.51152900	4.42471800	-0.83056400	N	-2.39020600	-2.24808000	-0.58283200

Dioxo_P NHCO (Trans/Trans) (Cis Attack)

Mo	-0.09709900	2.74894200	-0.25310500
S	-0.98389800	0.23105100	0.01116200
S	2.33909300	1.50669700	-0.25660700
S	-0.46971900	2.09173700	-2.60376700
S	0.35480500	2.37464900	2.16930700
O	0.77047300	4.10480000	-0.90780800
C	-2.62294900	-1.92836500	-3.01444500
H	-3.13608600	-2.87822000	-3.10268900
C	-2.39071600	-1.11009500	-4.12017100
H	-2.72725300	-1.42996100	-5.10478200
C	-1.29800100	0.54476100	-2.71327800
C	6.76436600	-2.72229900	-1.21074800
H	6.48184400	-3.69651500	-0.80180700
H	7.60068900	-2.35324000	-0.60950600
H	7.10647900	-2.85828800	-2.24431400
C	2.43749500	0.75031200	1.30898700
C	-2.18417000	-1.50641800	-1.75841100
C	1.76343700	0.57267100	3.64578700
C	-1.74023800	0.11099500	-3.97302900
C	-1.50890400	-0.26705700	-1.57670200
C	3.37812500	-0.28852400	1.55691600
C	5.59054900	-1.74982600	-1.17572500
C	3.52975400	-0.86056100	2.82071800
H	4.26706200	-1.64113900	2.96299200
C	6.03023700	-0.39693200	-1.74857200
H	6.40353000	-0.52647300	-2.77261900
H	6.83516400	0.04286000	-1.14905300
H	5.21065400	0.32877600	-1.78598100
C	4.43661800	-2.30823400	-2.01772700
H	4.07447100	-3.25886200	-1.61162900
H	4.77293700	-2.48697900	-3.04704700
H	3.58537500	-1.62165800	-2.06236300
C	2.72061800	-0.41319500	3.86527000
H	2.82875200	-0.85316200	4.85507600
C	-3.06446100	-3.80307900	1.14363700
C	-3.68354500	-5.18924200	1.28268100
H	-3.08556200	-5.94356400	0.76239100
H	-4.68722000	-5.21911700	0.84938400

Dioxo NHCO (Trans/Trans)

Mo	-3.38924400	-0.01373400	0.00908600
S	-1.27911300	-0.84234800	1.50232200
S	-1.31012300	0.84935600	-1.50705200
S	-2.85314300	-2.22847100	-0.98987800
S	-2.87789300	2.21062500	1.00184700
O	-4.46075100	0.21784200	-1.33843900
C	1.45666000	-3.42519800	-0.02571900
H	2.49898600	-3.65480800	0.16053400
C	0.70596500	-4.11999200	-0.97401100
H	1.16561900	-4.93478300	-1.53124700
C	-1.22315900	-2.70446500	-0.53705800
C	4.68751200	0.30859000	-3.05618500
H	5.25215900	0.24849300	-2.12087500
H	4.99363400	1.22997800	-3.56078800
H	4.96200800	-0.54860700	-3.68301700
C	-0.54701800	2.04489200	-0.49243700
C	0.85487100	-2.37829300	0.67532400
C	-0.64340100	3.75042800	1.24620000
C	-0.60852700	-3.74997600	-1.24378100
C	-0.51389100	-2.03820700	0.48947600
C	0.82052600	2.38869000	-0.67922400
C	3.18622400	0.29520700	-2.79049000
C	1.41922100	3.43865900	0.01996400
H	2.46078900	3.67138600	-0.16660500
C	2.42809400	0.36527400	-4.12251700
H	2.69931300	-0.48973300	-4.75481200
H	2.67258800	1.28325500	-4.67022300
H	1.34276900	0.33820000	-3.97867500
C	2.80582500	-0.99376700	-2.05198100
H	3.27786500	-1.04776000	-1.06446200
H	3.13569700	-1.87052600	-2.62309300
H	1.72594700	-1.10157300	-1.90051600
C	0.66777400	4.12857900	0.97128500

H	1.12491300	4.94509500	1.52804800
C	3.22163400	-0.27896400	2.77705100
C	4.70473800	-0.34231600	3.12516800
H	5.32007000	-0.35495400	2.22114700
H	4.94179600	-1.24915800	3.69026800
H	4.98377700	0.53203000	3.72576100
C	2.93388700	0.98869200	1.96256400
H	1.86911400	1.11267400	1.73536600
H	3.47326400	0.98863900	1.00800800
H	3.24785700	1.88064800	2.51898000
C	2.39276700	-0.25608000	4.06735100
H	2.56027200	-1.16158600	4.66234100
H	1.31838700	-0.17820500	3.86995100
H	2.67697500	0.60941700	4.67913100
C	-1.25532000	2.70340200	0.53953800
C	2.85858700	-1.52605300	1.93823500
O	3.69547300	-2.38768000	1.64884400
N	1.55524700	-1.54872400	1.56586300
H	0.95813600	-0.77929800	1.87380400
N	1.52280000	1.55683000	-1.56604200
C	2.82737400	1.53091100	-1.93260000
O	3.66561400	2.38915500	-1.63692500
H	0.92444000	0.78909000	-1.87601600
H	-1.17551700	-4.25614700	-2.02239300
H	-1.20918000	4.25085400	2.02935900
O	-4.44501800	-0.26171700	1.36613200

Table S5**Cis-ES NHCO (Trans attack)**

Mo -0.01659800 -1.43357100 -1.24229100
 S 1.74780700 0.19611500 -0.64045600
 S -1.83132000 0.18074900 -0.83990000
 S 1.71489300 -3.05456800 -0.60687400
 S -1.72827400 -3.08130500 -0.68108000
 O 0.03594400 -1.46643200 -2.94288000
 C 5.63815900 -0.76777400 0.15245600
 H 6.54886600 -0.21514400 0.34916900
 C 5.60407200 -2.16260700 0.14800300
 H 6.51851200 -2.72174300 0.34308200
 C 3.22055400 -2.14741400 -0.35574400
 C -5.93573300 4.66825800 0.19115600
 H -6.35162800 4.56538400 1.19745400
 H -6.75495100 4.49623500 -0.51306400
 H -5.57132800 5.69534200 0.06217700
 C -3.23846100 -0.76989000 -0.33808700
 C 4.45391500 -0.06846000 -0.09829900
 C -4.33439600 -2.87793500 0.15781300
 C 4.41344900 -2.84098000 -0.09824200
 C 3.23011300 -0.73643500 -0.36404800
 C -4.44111700 -0.11339800 0.02755500
 C -4.79705100 3.68040000 -0.03699600
 C -5.57304300 -0.81868600 0.44964300
 H -6.46905600 -0.27245200 0.71918400
 C -4.25359300 3.84618500 -1.46129800
 H -3.91349700 4.87823500 -1.61798700
 H -5.02730100 3.62906000 -2.20612200
 H -3.40488700 3.18417400 -1.66292700
 C -3.67324000 3.95478200 0.97009200
 H -4.02182400 3.80818900 1.99866100
 H -3.32576000 4.99191100 0.87537900
 H -2.80936100 3.30017500 0.81558700
 C -5.50533400 -2.21044800 0.50963800
 H -6.37745100 -2.77694600 0.83491800
 C 4.71589100 3.72841500 0.09111600
 C 5.82873800 4.72328600 0.40120700
 H 6.65789100 4.62001200 -0.30480000
 H 6.23841600 4.55919100 1.40188900
 H 5.44138100 5.74809000 0.34280200
 C 4.16993300 3.99371200 -1.31698400
 H 3.33241000 3.33518300 -1.56936300
 H 4.94726800 3.85022800 -2.07559900
 H 3.81041900 5.02795800 -1.39218500
 C 3.58331800 3.89141800 1.11315300
 H 3.93522100 3.67465300 2.12808900
 H 2.73671200 3.22831700 0.90544000
 H 3.20844500 4.92287000 1.09925300
 C -3.19244500 -2.17853500 -0.26422300
 C 5.29505200 2.29378200 0.17964900
 O 6.47301700 2.08942900 0.49102700
 N 4.38039100 1.33832200 -0.10666100
 H 3.43283300 1.64154000 -0.33577900
 N -4.40151300 1.29316200 -0.05152000
 C -5.33999300 2.24173100 0.16329600
 O -6.51415000 2.03400600 0.48982400
 H -3.46747800 1.60408300 -0.32248100
 H 4.38523000 -3.92989500 -0.09274500
 H -4.28322200 -3.96540500 0.20328400
 N 0.06493200 -1.63787900 2.56456400
 O -0.45303000 -0.99366800 1.48342100
 C -0.58998000 -1.07738200 3.78215000
 H -1.66289800 -1.22770200 3.65858300
 H -0.22079600 -1.56712800 4.69305900
 H -0.37357500 -0.00897500 3.79399600
 C -0.21304200 -3.10819800 2.49078400

H 0.28919000 -3.48028200 1.59509200
 H 0.15354800 -3.60663300 3.39795300
 H -1.29077000 -3.22082300 2.36771200
 C 1.54411600 -1.41307500 2.64539600
 H 1.70181700 -0.33467100 2.60430500
 H 1.95186200 -1.85267300 3.56448600
 H 1.98301200 -1.87265900 1.75973900

Cis-TS1' NHCO (Trans Attack)

Mo 0.01623100 -1.41240400 -1.08449000
 S 1.87551100 0.18756400 -0.53183200
 S -1.84599700 0.20955500 -0.73440100
 S 1.66549700 -3.06466100 -0.39846600
 S -1.78096200 -3.07975500 -0.78509900
 O 0.10624500 -1.35892000 -2.79221200
 C 5.69985700 -0.96319400 0.32008400
 H 6.64377400 -0.45709900 0.48375800
 C 5.58081800 -2.35093800 0.40201000
 H 6.45773900 -2.95163800 0.63972900
 C 3.20714700 -2.22054600 -0.12972400
 C -6.01549100 4.64517500 0.35251000
 H -6.43365300 4.47272500 1.34859100
 H -6.83272600 4.52256700 -0.36362200
 H -5.65114900 5.67873600 0.29941700
 C -3.29764600 -0.76422800 -0.41745100
 C 4.56224900 -0.20915600 0.01923900
 C -4.42815000 -2.88544000 -0.12206700
 C 4.35259300 -2.96867700 0.18130900
 C 3.29731300 -0.81396500 -0.20865900
 C -4.51749300 -0.11596200 -0.10125200
 C -4.87569500 3.67661700 0.05681200
 C -5.68134900 -0.83556500 0.18847800
 H -6.59367200 -0.30164100 0.42348500
 C -4.32339200 3.95115100 -1.34744100
 H -3.98045300 4.99112500 -1.42165800
 H -5.09323500 3.79378600 -2.11092400
 H -3.47475300 3.30411400 -1.59179800
 C -3.75861700 3.87202400 1.08919400
 H -4.11001900 3.63957400 2.10065100
 H -3.41878100 4.91553000 1.08162000
 H -2.88615500 3.24151200 0.88836000
 C -5.61787800 -2.22900900 0.17165500
 H -6.51382800 -2.80703700 0.39646300
 C 5.07584200 3.56433500 -0.11364200
 C 6.25657700 4.50538600 0.09758300
 H 7.06120400 4.29683800 -0.61365600
 H 6.67759900 4.39041400 1.10031800
 H 5.93354700 5.54581800 -0.03360600
 C 4.53347600 3.73555900 -1.53750000
 H 3.65112600 3.11495200 -1.72460300
 H 5.29091800 3.46890200 -2.28299200
 H 4.24514200 4.78092200 -1.70796400
 C 3.96949400 3.89730500 0.89529900
 H 4.32043000 3.75781900 1.92401600
 H 3.08220200 3.27026800 0.75861800
 H 3.65784900 4.94391300 0.78346700
 C -3.25049200 -2.17659000 -0.42483200
 C 5.55786300 2.10731700 0.10412900
 O 6.72253000 1.85324500 0.42940400
 N 4.57846000 1.19482000 -0.08991900
 H 3.65164500 1.53775800 -0.34897000
 N -4.46901000 1.29283100 -0.07696100
 C -5.42536900 2.22878600 0.12494600
 O -6.62136200 2.00138100 0.33332200
 H -3.51590700 1.61875200 -0.23875600
 H 4.25880900 -4.05210100 0.24325500
 H -4.38498800 -3.97365500 -0.12909400
 N -0.16225300 -1.39825400 2.54531300

O -0.77717100 -0.69183200 0.99692600
C -0.96497700 -0.61824200 3.46514700
H -2.01681500 -0.75180200 3.20226600
H -0.78953200 -0.93087300 4.51069500
H -0.70966100 0.43618600 3.34380300
C -0.52112100 -2.80661400 2.54154100
H 0.05433900 -3.31249300 1.76260200
H -0.31518000 -3.26276600 3.52811500
H -1.58240800 -2.89461300 2.29757200
C 1.26285700 -1.15009000 2.67740200
H 1.45794400 -0.09578700 2.46861100
H 1.61203100 -1.41352800 3.69268100
H 1.79735400 -1.74884300 1.93778600

Cis-INT1 NHCO (Trans Attack)

Mo 0.31779800 -1.56408900 -1.28856700
S 2.01586800 0.05499900 -0.59747200
S -2.53494200 -0.00545300 -1.79101400
S 1.55672500 -3.05200400 0.19061300
S -1.62867100 -3.07325400 -0.86112500
O 0.76581500 -1.95467900 -2.88323900
C 5.50601600 -0.94476500 1.27585500
H 6.43216500 -0.43817000 1.51897500
C 5.27104400 -2.27261500 1.63290100
H 6.03816000 -2.82287500 2.17645200
C 3.06771400 -2.21800500 0.59565700
C -6.06310500 4.40848500 0.81990400
H -5.97031400 4.32801300 1.90676700
H -7.10072200 4.17314400 0.56778500
H -5.85399700 5.44495800 0.52754700
C -3.39543800 -0.90657900 -0.55406400
C 4.50621000 -0.25382500 0.58430200
C -3.92759500 -2.98626900 0.57143000
C 4.07339200 -2.89894500 1.30035400
C 3.27960500 -0.87134700 0.23841600
C -4.44178200 -0.28088400 0.18547700
C -5.09625000 3.46526400 0.11276500
C -5.26227600 -1.01280300 1.04271300
H -6.06865700 -0.51501700 1.56625300
C -5.25414800 3.61637500 -1.40554800
H -5.05664700 4.65372200 -1.70480200
H -6.27130700 3.36092800 -1.72361600
H -4.55851500 2.97516500 -1.95764900
C -3.65637400 3.81274300 0.51192600
H -3.48554000 3.63840000 1.57989500
H -3.45516700 4.87142200 0.30505700
H -2.91296700 3.22544800 -0.03788200
C -5.00716100 -2.38113200 1.19608300
H -5.65330200 -2.97147700 1.84448800
C 5.34932100 3.34816900 -0.34062900
C 6.51923200 4.28672700 -0.06716400
H 7.45448800 3.87498200 -0.45643800
H 6.65996400 4.44055400 1.00674100
H 6.33626000 5.25977400 -0.53983800
C 5.18456200 3.16479200 -1.85460700
H 4.32659600 2.53240500 -2.10426800
H 6.07644300 2.70563800 -2.29540700
H 5.03149800 4.13853500 -2.33738300
C 4.06444200 3.94909600 0.24188900
H 4.13608600 4.05544000 1.32976100
H 3.18045000 3.33994200 0.02627600
H 3.88896300 4.94517500 -0.18408900
C -3.07162700 -2.26516800 -0.28862300
C 5.65122100 1.97861700 0.31920000
O 6.71983300 1.76228600 0.89898600
N 4.64147600 1.08838400 0.17619700
H 3.81130500 1.39446700 -0.33000000

N -4.57122200 1.10566400 0.00132000
C -5.43462100 2.01044500 0.52220600
O -6.40520500 1.74540400 1.23654600
H -3.82661900 1.44214400 -0.61622700
H 3.89517000 -3.93665500 1.57909000
H -3.69506100 -4.03323200 0.75704600
N -0.53830300 -0.56226600 1.89379500
O -0.91136300 0.07046400 -1.33672900
C -0.94107500 0.81232500 1.69866200
H -1.87034300 0.84427300 1.12094800
H -1.10466100 1.34684900 2.66313300
H -0.16970800 1.33588500 1.12377200
C -1.56887800 -1.33615100 2.54954900
H -1.31485600 -2.40118800 2.49890900
H -1.68847900 -1.04754100 3.61877200
H -2.53051600 -1.18920400 2.05186000
C 0.69470600 -0.63961100 2.64831500
H 1.47757100 -0.06284400 2.14849400
H 0.56410900 -0.24530400 3.68239400
H 1.02787500 -1.68054700 2.70544100

Cis-TS2' NHCO (Trans Attack)

Mo 0.30014900 -1.56252300 -1.30792400
S 2.02099700 0.04806600 -0.60399600
S -2.59490100 -0.02303300 -1.84882600
S 1.47698700 -3.02359500 0.27640000
S -1.66105600 -3.07757700 -0.96649800
O 0.81204200 -2.00203900 -2.87291500
C 5.44091600 -0.95990200 1.38220300
H 6.37208600 -0.46452200 1.62939100
C 5.16849000 -2.26886900 1.78006300
H 5.91013700 -2.81567500 2.36112300
C 2.99146600 -2.20548400 0.68827700
C -6.03333200 4.42153000 0.81638800
H -5.93599900 4.36080900 1.90400600
H -7.07058300 4.17562800 0.57225300
H -5.83266500 5.45399700 0.50432000
C -3.39687000 -0.90419800 -0.58190800
C 4.47395600 -0.27376100 0.64155400
C -3.88818800 -2.98137200 0.57937300
C 3.96596300 -2.88160400 1.44058500
C 3.24141100 -0.87658700 0.28850600
C -4.40311200 -0.27127700 0.21401900
C -5.06295000 3.47277400 0.12175300
C -5.18894800 -0.99886600 1.10307200
H -5.97049600 -0.49610300 1.65905800
C -5.23295600 3.59231300 -1.39796600
H -5.05037200 4.62639500 -1.71754500
H -6.24909000 3.31868100 -1.70385000
H -4.53427800 2.94962100 -1.94451600
C -3.62371300 3.84053700 0.50448700
H -3.45176600 3.70617000 1.57793800
H -3.42682000 4.89180400 0.25911000
H -2.87992400 3.23487800 -0.02444900
C -4.93914000 -2.37090600 1.24664200
H -5.56193000 -2.95634000 1.92149800
C 5.42808000 3.26800100 -0.39990500
C 6.60706800 4.19359000 -0.12089600
H 7.54650300 3.75010800 -0.46255400
H 6.71439200 4.38383200 0.95100300
H 6.46028700 5.15154100 -0.63523900
C 5.31812700 3.02133000 -1.90984500
H 4.45510700 2.39851500 -2.16591100
H 6.21477900 2.52219800 -2.29389400
H 5.20863200 3.97558300 -2.44105100
C 4.13509200 3.92009800 0.10488800
H 4.16599200 4.07026100 1.18958300

H	3.24660900	3.32113900	-0.12095300	H	6.44110800	3.50468300	-2.77469000
H	3.99876500	4.90124200	-0.36770800	C	5.26649100	1.04436300	-2.85726000
C	-3.06803100	-2.26517000	-0.31786100	H	4.38444700	0.39645400	-2.88603900
C	5.67351100	1.92354600	0.33022200	H	6.14794000	0.40095300	-2.75986500
O	6.71199600	1.71270100	0.96394200	H	5.32768000	1.55531000	-3.82653200
N	4.65259900	1.04656500	0.18224500	C	3.92739900	2.91359300	-1.86285800
H	3.84846900	1.34794500	-0.36655100	H	3.83984800	3.63779800	-1.04547700
N	-4.53287900	1.11387000	0.02930800	H	3.02293700	2.29569100	-1.85342000
C	-5.38003600	2.02365700	0.56759900	H	3.94007500	3.46913900	-2.80909600
O	-6.31903300	1.76635000	1.32581300	C	-3.55568100	-2.17101600	-0.11702100
H	-3.81782500	1.44244900	-0.62577400	C	5.21095700	1.37133700	-0.34561000
H	3.75967800	-3.90494400	1.75047200	O	6.06271000	1.62566500	0.50891900
H	-3.65185800	-4.02860200	0.75831500	N	4.19245100	0.48660300	-0.20226900
N	-0.58553000	-0.46373800	1.87251200	H	3.56266200	0.38099500	-0.99358000
O	-0.84022200	0.03661800	-1.42873000	N	-3.81187700	1.50259100	-0.13779300
C	-1.03093200	0.88542000	1.60788200	C	-4.52576500	2.65257500	-0.13034600
H	-1.96269600	0.85829400	1.03375600	O	-5.74348900	2.73367100	0.07001300
H	-1.20945100	1.46484700	2.54332000	H	-2.80805800	1.55381600	-0.30777000
H	-0.27906500	1.40328200	1.00239500	H	2.36025500	-2.39906900	3.81240800
C	-1.59291000	-1.23910800	2.56008000	H	-5.16129200	-3.58974500	0.01927700
H	-1.29709200	-2.29426200	2.57359600	N	0.70587700	2.44390400	2.33771700
H	-1.73732600	-0.89710000	3.61050200	O	-0.23685800	-2.00671300	-2.60144000
H	-2.55210200	-1.15802200	2.04418100	C	-0.68435500	2.84394700	2.38855200
C	0.64767400	-0.46849200	2.62907200	H	-0.79930100	3.84791500	1.95920400
H	1.40826000	0.11980000	2.10887400	H	-1.35418200	2.14950000	1.83917300
H	0.50228800	-0.04409000	3.64928700	H	-1.02396700	2.87789400	3.43112600
H	1.01927600	-1.49428900	2.72251400	C	1.18163000	2.43711000	0.96295100

Dioxo_P NHCO (Cis/Trans) (Trans Attack)

Mo	-0.16633200	-2.58014500	-0.95999800	C	0.86508200	1.11523800	2.91581500
S	1.83016500	-1.06049700	-0.89256200	H	0.53559600	1.12921600	3.96153500
S	-1.51551400	-0.31826700	-0.21840800	H	0.28509100	0.34218000	2.37721500
S	0.59746900	-2.72463700	1.59894000	H	1.92050600	0.82796900	2.89094400
S	-2.37516300	-3.46169200	-0.31717400				
O	0.29000500	-4.24343700	-1.14507700				
C	4.42867800	-0.27304400	2.12930900				
H	5.31415300	0.33740200	2.25189700				
C	3.91663800	-1.05631000	3.16509000				
H	4.42408600	-1.06153700	4.12883700				
C	2.07252200	-1.82565400	1.76233500				
C	-4.47913100	4.81365700	-1.34992200				
H	-5.51046800	4.95576300	-1.01675100				
H	-4.50525800	4.34572300	-2.34070100				
H	-3.99617500	5.79351400	-1.45188000				
C	-3.18503900	-0.80522100	-0.11033900				
C	3.76583400	-0.28459200	0.89822600				
C	-4.90388400	-2.53256000	0.02038900				
C	2.76422500	-1.81050200	2.99159500				
C	2.60062400	-1.06458100	0.69002000				
C	-4.22767200	0.16083900	-0.02458500				
C	-3.70873700	3.94771500	-0.35066300				
C	-5.56693400	-0.20933600	0.11189100				
H	-6.32260600	0.56318600	0.17835200				
C	-2.28818300	3.72676800	-0.86998400				
H	-1.79958100	4.69538200	-1.03313100				
H	-2.28138200	3.18557200	-1.82241100				
H	-1.65812100	3.16831300	-0.17003200				
C	-3.66154800	4.66646600	1.00306300				
H	-4.67546600	4.87176400	1.36117000				
H	-3.11978900	5.61704000	0.91460700				
H	-3.15108400	4.05757300	1.75657200				
C	-5.89535600	-1.56427300	0.14494600				
H	-6.93655300	-1.86310400	0.25328200				
C	5.20605400	2.07677500	-1.72475500				
C	6.42431600	2.98967700	-1.80623100				
H	7.35210600	2.42062500	-1.69521200				
H	6.41007600	3.73768500	-1.00898200				

Dioxo NHCO (Cis/Trans)

Mo	-0.06413200	-2.38678500	-0.81560400				
S	1.95770500	-0.92170800	-0.59275500				
S	-1.56995800	-0.08708900	-0.82995700				
S	0.05126900	-1.97372500	1.79980200				
S	-2.34776700	-3.22572300	-0.38134300				
O	0.40584300	-4.04910600	-0.65170400				
C	3.68171800	0.65993500	2.72810000				
H	4.55002900	1.27167800	2.93565400				
C	2.82377400	0.22254200	3.73768900				
H	3.02988300	0.50211800	4.77000800				
C	1.41810400	-0.95125300	2.12384100				
C	-4.30628200	5.41843000	-0.10108700				
H	-4.74627500	5.49487600	0.89733300				
H	-5.13290400	5.42314400	-0.81760800				
H	-3.68192100	6.30295000	-0.27899900				
C	-3.13681600	-0.56041000	-0.24089400				
C	3.39677600	0.29585700	1.40915300				
C	-4.77898700	-2.26467500	0.35247400				
C	1.71465000	-0.56025500	3.44560200				
C	2.27400200	-0.50656200	1.08686600				
C	-4.12544700	0.41744000	0.06894300				
C	-3.46433800	4.15464800	-0.23725400				
C	-5.40802300	0.06605200	0.49097200				
H	-6.12585300	0.84924700	0.70365700				
C	-2.88059100	4.08004100	-1.65375500				
H	-2.27432200	4.97177400	-1.85845900				
H	-3.67652700	4.03274300	-2.40547900				
H	-2.23902800	3.20372200	-1.79461400				
C	-2.32026900	4.19117800	0.78317100				
H	-2.70531900	4.20500300	1.80867800				
H	-1.71572700	5.09534500	0.63734500				

H	-1.65151200	3.32939800	0.69270200	H	8.69335600	-1.23070800	0.35062900
C	-5.72876400	-1.28512100	0.62512400	H	8.18634500	-2.91723300	0.61709400
H	-6.72628900	-1.57198000	0.95375900	C	5.50117300	-2.46401500	0.88097000
C	5.85075300	1.62765100	-1.19008500	H	4.50455000	-2.34203700	0.44169700
C	7.13052000	2.45477800	-1.14520600	H	5.42086600	-2.24889800	1.95288700
H	7.90221500	1.95774500	-0.55046700	H	5.78224900	-3.51925600	0.76905800
H	6.95298800	3.43182400	-0.68715700	C	6.56620900	-1.83724800	-1.29521100
H	7.51287200	2.60643500	-2.16228800	H	7.28452000	-1.18516200	-1.80477000
C	6.14649400	0.26476500	-1.82861200	H	5.58564200	-1.67625500	-1.75463300
H	5.24830400	-0.35313900	-1.93106200	H	6.85738500	-2.87787000	-1.48881100
H	6.87178400	-0.30066900	-1.23313500	C	-2.16219900	-2.37029700	-0.50234000
H	6.56768300	0.40266200	-2.83264000	C	6.21769700	-0.07151000	0.47371600
C	4.79598400	2.36350300	-2.02531000	O	7.01947100	0.68033900	1.03924900
H	4.54160100	3.33008100	-1.57687900	N	4.99507700	0.27788300	0.01551400
H	3.86829000	1.79062600	-2.12509400	H	4.42965000	-0.45183700	-0.42091700
H	5.17919500	2.55039100	-3.03655400	N	-5.12411700	-0.27398100	0.12690500
C	-3.48636500	-1.92141500	-0.07256500	C	-6.41088000	-0.07133600	0.49337100
C	5.33685200	1.43320300	0.25901500	O	-7.21859300	-0.95601600	0.79626700
O	5.93647100	1.91127700	1.22572200	H	-4.55781800	0.54641900	-0.09188200
N	4.19642100	0.70305600	0.32059600	H	2.02469500	4.62093900	0.21524100
H	3.81579200	0.36965600	-0.56114800	H	-2.03342200	-4.50927800	-0.39041000
N	-3.70391900	1.75056800	-0.07725700	N	0.47554400	-0.32520900	2.25124400
C	-4.36916800	2.92481300	0.02401100	O	0.31103500	0.53477600	1.20794100
O	-5.56938200	3.04735000	0.29100200	C	0.85696600	0.49625600	3.43691600
H	-2.71364900	1.77965900	-0.32636100	H	1.02445600	-0.13586900	4.31887300
H	1.05127800	-0.89658100	4.23932300	H	1.75994000	1.04294800	3.15940100
H	-5.02344200	-3.31847600	0.47101000	H	0.04580800	1.20485600	3.60536100
O	0.19200000	-2.06072600	-2.50910000	C	-0.80437500	-1.05292200	2.52857900

Trans-ES_{NHCO} (Trans Attack)

Mo	-0.07054400	0.19218400	-1.42758100
S	2.36302700	-0.10054500	-1.15980500
S	-2.38346700	0.40390000	-0.60569300
S	0.44193800	2.54203200	-0.89112600
S	-0.44599900	-2.18622000	-0.91570900
O	-0.23734700	0.25135300	-3.11989000
C	4.77726900	2.65503000	0.64762000
H	5.78322500	2.65664500	1.04997900
C	3.96167900	3.78651200	0.67305300
H	4.34307500	4.71175300	1.10452200
C	2.12754900	2.56296000	-0.37917400
C	-8.27147300	1.54051200	0.91373600
H	-8.44473900	1.10757000	1.90305900
H	-8.91686500	1.00413500	0.21196600
H	-8.57309800	2.59516700	0.93351900
C	-2.99896900	-1.24227800	-0.36510800
C	4.26301900	1.48297500	0.08067500
C	-2.69462200	-3.65035400	-0.28163100
C	2.66414500	3.74043300	0.17062400
C	2.95303200	1.41820000	-0.45337700
C	-4.35500000	-1.44726100	-0.00037100
C	-6.80532900	1.42718000	0.51063200
C	-4.87833500	-2.72673600	0.20931400
H	-5.92137600	-2.83509400	0.48156600
C	-6.60867300	2.04168300	-0.88038900
H	-6.94430600	3.08660400	-0.88058800
H	-7.18781000	1.50061900	-1.63690800
H	-5.56023300	2.03326100	-1.19526500
C	-5.93567200	2.18013600	1.52542400
H	-6.03141300	1.74341300	2.52583200
H	-6.24828600	3.23054600	1.58407000
H	-4.87461300	2.16600400	1.25532000
C	-4.03237300	-3.82635100	0.06380100
H	-4.42554100	-4.82968900	0.22369900
C	6.55007100	-1.56448000	0.21381900
C	7.92513700	-1.86714100	0.79897100
H	7.94605900	-1.68232800	1.87696600

Trans-TS1'_{NHCO} (Trans Attack)

Mo	0.00369400	-0.13628200	-1.20218400
S	2.41011400	-0.37704900	-0.66926700
S	-2.34623000	0.24388700	-0.66676700
S	0.49747100	2.28421100	-0.94341100
S	-0.58102300	-2.49167600	-0.62534900
O	0.05814600	-0.25665600	-2.90747600
C	4.95284800	2.71162200	0.13601400
H	6.00146000	2.80338200	0.39043400
C	4.11533100	3.82105700	0.01855800
H	4.52455000	4.81796600	0.18024200
C	2.20508200	2.40116700	-0.52918600
C	-5.76897400	2.37469800	1.20803800
H	-4.71655200	2.27955200	0.91931500
H	-5.87023100	1.98097100	2.22549400
H	-6.00768600	3.44555400	1.23471100
C	-3.09967900	-1.34498100	-0.35861200
C	4.40451500	1.44283200	-0.07770000
C	-2.96689400	-3.74882500	-0.10362700
C	2.76994000	3.66972400	-0.29794000
C	3.04162200	1.26709100	-0.42160600
C	-4.48425900	-1.42849800	-0.07754400
C	-6.71201700	1.64955400	0.23927200
C	-5.11250400	-2.65362900	0.17054000
H	-6.17476700	-2.67809600	0.37947600
C	-8.15738900	1.89855100	0.65594600
H	-8.37224600	2.97426700	0.63832600
H	-8.34763700	1.51806700	1.66365600
H	-8.85517400	1.38917700	-0.01489900
C	-6.49011900	2.18325700	-1.18122900
H	-5.45278500	2.06648300	-1.51167300

H	-6.73175900	3.25303500	-1.22455800	H	-6.06931000	-2.27531400	1.48571900
H	-7.13037700	1.66299300	-1.90227100	C	-6.40449600	2.22538000	-0.90638100
C	-4.33211500	-3.81088800	0.15166000	H	-6.62492100	3.27885800	-1.12112000
H	-4.80308700	-4.77471700	0.34333100	H	-7.12966800	1.61084700	-1.495143100
C	6.84737800	-1.45785400	0.31654700	H	-5.41125400	2.00673100	-1.31184000
C	8.32878800	-1.58545500	0.65364200	C	-5.42264800	2.80606500	1.32156400
H	8.55175200	-1.14521600	1.63007200	H	-5.42912400	2.61247200	2.39986700
H	8.94629300	-1.06235500	-0.08177800	H	-5.62032900	3.87480700	1.16915300
H	8.61852100	-2.64345400	0.67098300	H	-4.41287000	2.60387000	0.95377700
C	6.01804400	-2.19383500	1.37563300	C	-4.36511800	-3.57471700	1.12323700
H	4.94556800	-2.18042000	1.15552300	H	-4.84180200	-4.45819200	1.54657200
H	6.15904200	-1.74930500	2.36713300	C	6.72459900	-0.92334700	1.00531600
H	6.32771400	-3.24529100	1.43017300	C	7.96576100	-0.91116800	1.89042300
C	6.58115500	-2.07979000	-1.06029400	H	7.71780400	-0.61356200	2.91308300
H	7.13755800	-1.55379800	-1.84386400	H	8.70910100	-0.19935800	1.52018700
H	5.52000000	-2.05062200	-1.32889200	H	8.41684300	-1.91084200	1.91479000
H	6.89693200	-3.13087500	-1.06771600	C	5.70353500	-1.92228900	1.56529800
C	-2.32233100	-2.52408300	-0.36403100	H	4.82319300	-2.02652500	0.92205500
C	6.47598900	0.04659000	0.28251600	H	5.34969000	-1.61596800	2.55566000
O	7.32946300	0.92517000	0.44059200	H	6.16130500	-2.91503000	1.66059700
N	5.15962700	0.25913000	0.05048900	C	7.11531500	-1.33884900	-0.41809500
H	4.56613800	-0.56040800	-0.07464400	H	7.82560700	-0.62901600	-0.85665600
N	-5.17192300	-0.19699500	-0.05820300	H	6.24855000	-1.40139900	-1.08515200
C	-6.44319800	0.12354500	0.27876300	H	7.59055500	-2.32806100	-0.40480200
O	-7.32814100	-0.67922700	0.59054600	C	-2.43243800	-2.54088700	0.06230800
H	-4.54089500	0.57043800	-0.28551600	C	6.11254100	0.49918000	0.99175500
H	2.12181900	4.54067600	-0.38397100	O	6.62027100	1.43175700	1.62018300
H	-2.36362600	-4.65539000	-0.10764400	N	4.99402000	0.57970200	0.23093800
N	-0.08464200	0.11458600	2.44463900	H	4.69117900	-0.25609400	-0.27718700
O	0.92385900	-0.16386900	0.96363200	N	-5.04413200	0.02327700	0.48556600
C	-0.63330100	1.45633300	2.34869000	C	-6.25926300	0.46132600	0.89131100
H	-1.11886300	1.74957300	3.29885700	O	-7.12560700	-0.23120600	1.43429300
H	0.17880200	2.14596700	2.10696900	H	-4.41930200	0.70159400	0.05092000
H	-1.35750500	1.48167800	1.53100000	H	1.19534700	4.18032700	-0.37319000
C	-1.08158100	-0.93527800	2.55345000	H	-2.52714200	-4.60434800	0.64676100
H	-0.59258900	-1.89947800	2.39686800	N	0.53911400	-0.14909300	1.65362300
H	-1.57556200	-0.90673200	3.54209900	O	1.68246300	-1.10658300	-1.31846200
H	-1.82604000	-0.80242200	1.76703700	C	0.80665500	1.20294900	2.08928600
C	0.96410900	0.00917400	3.43800000	H	0.92303500	1.26993100	3.19506700
H	1.74312000	0.73583000	3.19654900	H	1.72579300	1.57601600	1.63099000
H	0.57072700	0.19576400	4.45432000	H	-0.01978000	1.85553900	1.78395100
H	1.39620100	-0.99179700	3.38345700	C	-0.58898600	-0.69234000	2.38034100

Trans-INT1 NHCO (Trans Attack)

Mo	-0.25495000	-0.58181300	-1.66604600
S	2.99958300	-0.15172400	-1.79491700
S	-2.34797500	0.14771800	-0.63790400
S	0.36039200	1.85438400	-1.69695000
S	-0.76851900	-2.67406800	-0.52874500
O	-0.60343500	-0.91151200	-3.29862200
C	4.15561200	2.84661700	0.68558100
H	5.00833300	3.05622400	1.31898000
C	3.13402500	3.78208400	0.47993600
H	3.20858300	4.76029900	0.95328900
C	1.88535900	2.22283000	-0.92377900
C	-7.86992300	2.35587700	1.11196100
H	-7.96094800	2.17409900	2.18675700
H	-8.65184400	1.76945000	0.62100600
H	-8.05310700	3.42006300	0.91783100
C	-3.11911600	-1.31149300	0.02481400
C	4.05836400	1.61100400	0.04759200
C	-3.07071400	-3.66091500	0.61857100
C	2.0125100	3.47172700	-0.27949500
C	2.97444200	1.31244000	-0.83015100
C	-4.43259200	-1.24451100	0.55053800
C	-6.48641900	1.96669100	0.60317100
C	-5.06295900	-2.36737300	1.09582200

Trans-TS2' NHCO (Trans Attack)

Mo	0.23489400	-0.61573800	1.69060100
S	-3.03644100	-0.11921300	1.84584200
S	2.32313100	0.14032300	0.62276100
S	-0.36634700	1.82190600	1.80253100
S	0.76521600	-2.69920400	0.52150800
O	0.62684000	-0.96804900	3.31016700
C	-4.06308700	2.84900900	-0.71175600
H	-4.89117000	3.06239700	-1.37623100
C	-3.03505600	3.77466900	-0.48490700
H	-3.08037700	4.74783300	-0.97202300
C	-1.85650400	2.21232700	0.97420300
C	7.83313900	2.38232500	-1.11547200
H	7.92121100	2.21522400	-2.19289400
H	8.61666000	1.78958100	-0.63479000
H	8.01646000	3.44376900	-0.90722000
C	3.09564800	-1.30971200	-0.04907400

C	-4.00759300	1.62129600	-0.05820400	C	-1.03859200	-1.74753100	2.33165200
C	3.06262400	-3.65793100	-0.65173200	C	1.67532700	5.28705000	2.02025900
C	-1.94467500	3.45403900	0.30984000	H	1.00290200	5.59365100	1.21337100
C	-2.96123200	1.31769700	0.86908700	H	2.60905600	5.84295700	1.89295700
C	4.40374200	-1.23006300	-0.58799900	H	1.22216000	5.56911400	2.97867500
C	6.45126600	1.98546300	-0.60823500	C	2.55429400	0.03864600	-0.74908200
C	5.03655500	-2.34434600	-1.14743100	C	-2.78368100	-0.42190300	1.28338100
H	6.03754700	-2.24139000	-1.54812300	C	3.40457800	-0.12581800	-3.02638700
C	6.37478700	2.21966900	0.90573000	C	-1.34116300	-1.12257000	3.55041300
H	6.59707000	3.26919300	1.13710700	C	-1.74933300	-1.39186600	1.15836100
H	7.10115000	1.59548200	1.43802600	C	3.04402500	1.37256600	-0.71155200
H	5.38277900	1.99525200	1.31116300	C	1.91668100	3.78169500	1.98449300
C	5.38553700	2.83680800	-1.30925100	C	3.73851900	1.92612100	-1.78709200
H	5.38891400	2.66163000	-2.39072800	H	4.09421600	2.94728900	-1.71731400
H	5.58379100	3.90276400	-1.13924000	C	2.86726100	3.38881000	3.12254000
H	4.37515000	2.62883100	-0.94205000	H	2.44028100	3.68738300	4.08855900
C	4.34909500	-3.55746600	-1.17298900	H	3.84103000	3.88132200	3.01522800
H	4.82802700	-4.43428700	-1.60714500	H	3.03812600	2.30805900	3.15558700
C	-6.69343900	-0.87953300	-1.04810800	C	0.57883500	3.04979800	2.15885200
C	-7.90994800	-0.85863600	-1.96672800	H	-0.09759800	3.27272100	1.32854500
H	-7.62729500	-0.59637100	-2.99003400	H	0.09806200	3.36928600	3.09176900
H	-8.64266800	-0.11680800	-1.63584900	H	0.67832400	1.95862100	2.20196400
H	-8.38764600	-1.84624900	-1.97597700	C	3.91493000	1.16630100	-2.94399500
C	-5.68310200	-1.91617500	-1.55671300	H	4.44546400	1.59419700	-3.79309200
H	-4.81823200	-2.01963000	-0.89264100	C	-5.00195700	0.77010700	-1.61428700
H	-5.30365500	-1.64621800	-2.54821100	C	-6.47833600	0.35943300	-1.58767900
H	-6.16049900	-2.90142800	-1.63331700	H	-7.03301400	0.98308200	-0.88035600
C	-7.13274700	-1.25061000	0.37336600	H	-6.59171800	-0.68707300	-1.28160800
H	-7.83531200	-0.51238200	0.77619500	H	-6.92411600	0.46993700	-2.58452400
H	-6.28616100	-1.31965200	1.06523700	C	-4.89607300	2.22796500	-2.07191700
H	-7.63375900	-2.22726100	0.36957700	H	-3.84940500	2.55047000	-2.12462400
C	2.42004200	-2.54627200	-0.08267200	H	-5.41792000	2.88495300	-1.37005400
C	-6.04586800	0.52710200	-1.05260100	H	-5.33767300	2.34838100	-3.06941900
O	-6.50380500	1.45177600	-1.72949300	C	-4.24515100	-0.12761800	-2.59114600
N	-4.95422400	0.60371900	-0.25357400	H	-4.30486900	-1.18661600	-2.31658400
H	-4.68940700	-0.22284400	0.28916000	H	-3.18358800	0.13574800	-2.66278600
N	5.00777700	0.04086400	-0.52059300	H	-4.67531200	-0.02307500	-3.59466800
C	6.22360600	0.48464500	-0.91872100	C	2.72058600	-0.69986100	-1.94210800
O	7.09096700	-0.20075800	-1.46887000	C	-4.50099500	0.71535800	-0.15138300
H	4.38310800	0.71246200	-0.07559600	O	-5.05928600	1.42221900	0.69685200
H	-1.11338100	4.14876900	0.41690200	N	-3.47938900	-0.13606400	0.09220200
H	2.52776100	-4.60611900	-0.67708000	H	-3.06864400	-0.64771700	-0.68964700
N	-0.55014600	-0.16863100	-1.64113200	N	2.77350500	2.08692600	0.46985300
O	-1.63574500	-1.14843400	1.37879800	C	2.57041000	3.42346900	0.62856000
C	-0.81175800	1.18300300	-2.07994100	O	2.90066800	4.28728700	-0.18570700
H	-0.95547900	1.24453000	-3.18283100	H	2.33636500	1.48020200	1.16130100
H	-1.71399000	1.57012300	-1.60127200	H	-0.76553500	-1.39830200	4.43137000
H	0.03043300	1.82722500	-1.80070200	H	3.52315500	-0.71040200	-3.93651100
C	0.55269100	-0.72983000	-2.39106200	N	-0.12596200	2.69057600	-1.27076100
H	0.74680500	-1.75379900	-2.06126200	O	0.51788100	-4.47989000	-0.92559300
H	0.33807700	-0.73917600	-3.48442200	C	-1.06662100	1.67658300	-0.83682000
H	1.45711300	-0.13712400	-2.21802700	H	-1.90247100	1.55553900	-1.55838000
C	-1.72310100	-1.00884300	-1.73509800	H	-0.56977700	0.70454600	-0.72307700
H	-2.54181600	-0.55919800	-1.16430300	H	-1.50195200	1.95042200	0.13150800
H	-2.05998800	-1.15039300	-2.78793400	C	-0.75010600	3.98933100	-1.33410600
H	-1.49934000	-1.98451100	-1.28988800	H	-0.00774200	4.74863900	-1.60598700

Dioxo_P NHCO (Trans/Trans) (Trans Attack)

Mo 1.16955300 -3.17442800 0.02180300
 S -1.38265400 -2.13044400 -0.37535100
 S 1.75302600 -0.64929000 0.63976800
 S 0.22249300 -2.97462400 2.32142200
 S 2.02175500 -2.30041100 -2.13049000
 O 2.54130200 -3.88415800 0.80924100
 C -3.07724100 0.19424500 2.50226900
 H -3.86548000 0.93565100 2.54283100
 C -2.34399300 -0.16191100 3.63385300
 H -2.55597800 0.32158200 4.58604300

Dioxo NHCO (Trans/Trans)

Mo-3.38924400 -0.01373400 0.00908600
 S -1.27911300 -0.84234800 1.50232200
 S -1.31012300 0.84935600 -1.50705200
 S -2.85314300 -2.22847100 -0.98987800
 S -2.87789300 2.21062500 1.00184700

O -4.46075100 0.21784200 -1.33843900
 C 1.45666000 -3.42519800 -0.02571900
 H 2.49898600 -3.65480800 0.16053400
 C 0.70596500 -4.11999200 -0.97401100
 H 1.16561900 -4.93478300 -1.53124700
 C -1.22315900 -2.70446500 -0.53705800
 C 4.68751200 0.30859000 -3.05618500
 H 5.25215900 0.24849300 -2.12087500
 H 4.99363400 1.22997800 -3.56078800
 H 4.96200800 -0.54860700 -3.68301700
 C -0.54701800 2.04489200 -0.49243700
 C 0.85487100 -2.37829300 0.67532400
 C -0.64340100 3.75042800 1.24620000
 C -0.60852700 -3.74997600 -1.24378100
 C -0.51389100 -2.03820700 0.48947600
 C 0.82052600 2.38869000 -0.67922400
 C 3.18622400 0.29520700 -2.79049000
 C 1.41922100 3.43865900 0.01996400
 H 2.46078900 3.67138600 -0.16660500
 C 2.42809400 0.36527400 -4.12251700
 H 2.69931300 -0.48973300 -4.75481200
 H 2.67258800 1.28325500 -4.67022300
 H 1.34276900 0.33820000 -3.97867500
 C 2.80582500 -0.99376700 -2.05198100
 H 3.27786500 -1.04776000 -1.06446200
 H 3.13569700 -1.87052600 -2.62309300
 H 1.72594700 -1.10157300 -1.90051600
 C 0.66777400 4.12857900 0.97128500
 H 1.12491300 4.94509500 1.52804800
 C 3.22163400 -0.27896400 2.77705100
 C 4.70473800 -0.34231600 3.12516800
 H 5.32007000 -0.35495400 2.22114700
 H 4.94179600 -1.24915800 3.69026800
 H 4.98377700 0.53203000 3.72576100
 C 2.93388700 0.98869200 1.96256400
 H 1.86911400 1.11267400 1.73536600
 H 3.47326400 0.98863900 1.00800800
 H 3.24785700 1.88064800 2.51898000
 C 2.39276700 -0.25608000 4.06735100
 H 2.56027200 -1.16158600 4.66234100
 H 1.31838700 -0.17820500 3.86995100
 H 2.67697500 0.60941700 4.67913100
 C -1.25532000 2.70340200 0.53953800
 C 2.85858700 -1.52605300 1.93823500
 O 3.69547300 -2.38768000 1.64884400
 N 1.55524700 -1.54872400 1.56586300
 H 0.95813600 -0.77929800 1.87380400
 N 1.52280000 1.55683000 -1.56604200
 C 2.82737400 1.53091100 -1.93260000
 O 3.66561400 2.38915500 -1.63692500
 H 0.92444400 0.78909000 -1.87601600
 H -1.17551700 -4.25614700 -2.02239300
 H -1.20918000 4.25085400 2.02935900
 O -4.44501800 -0.26171700 1.36613200

Figure S1

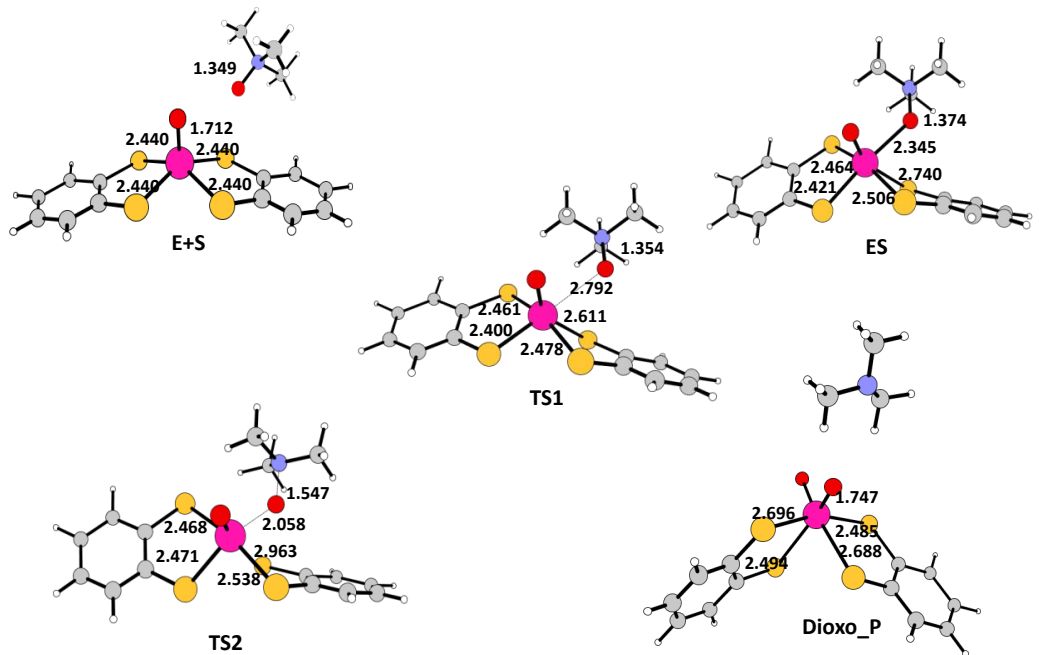


Figure S2

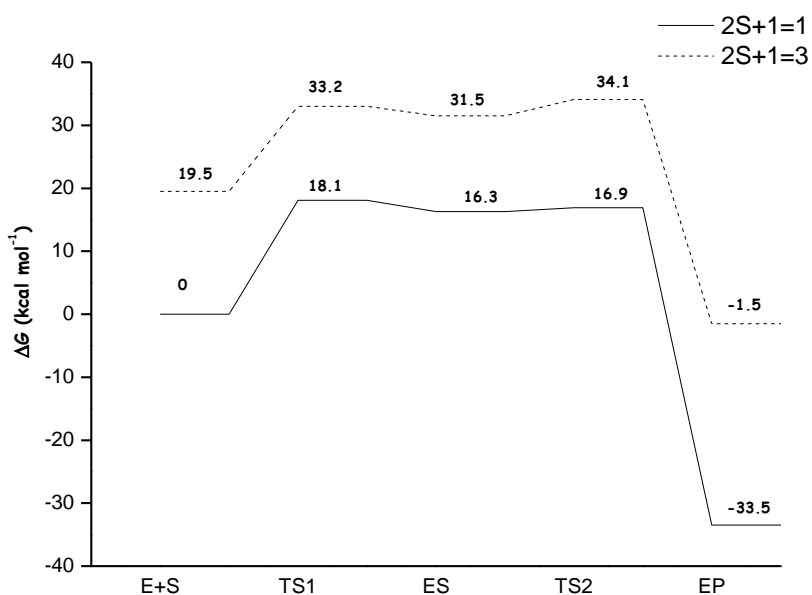


Figure S3

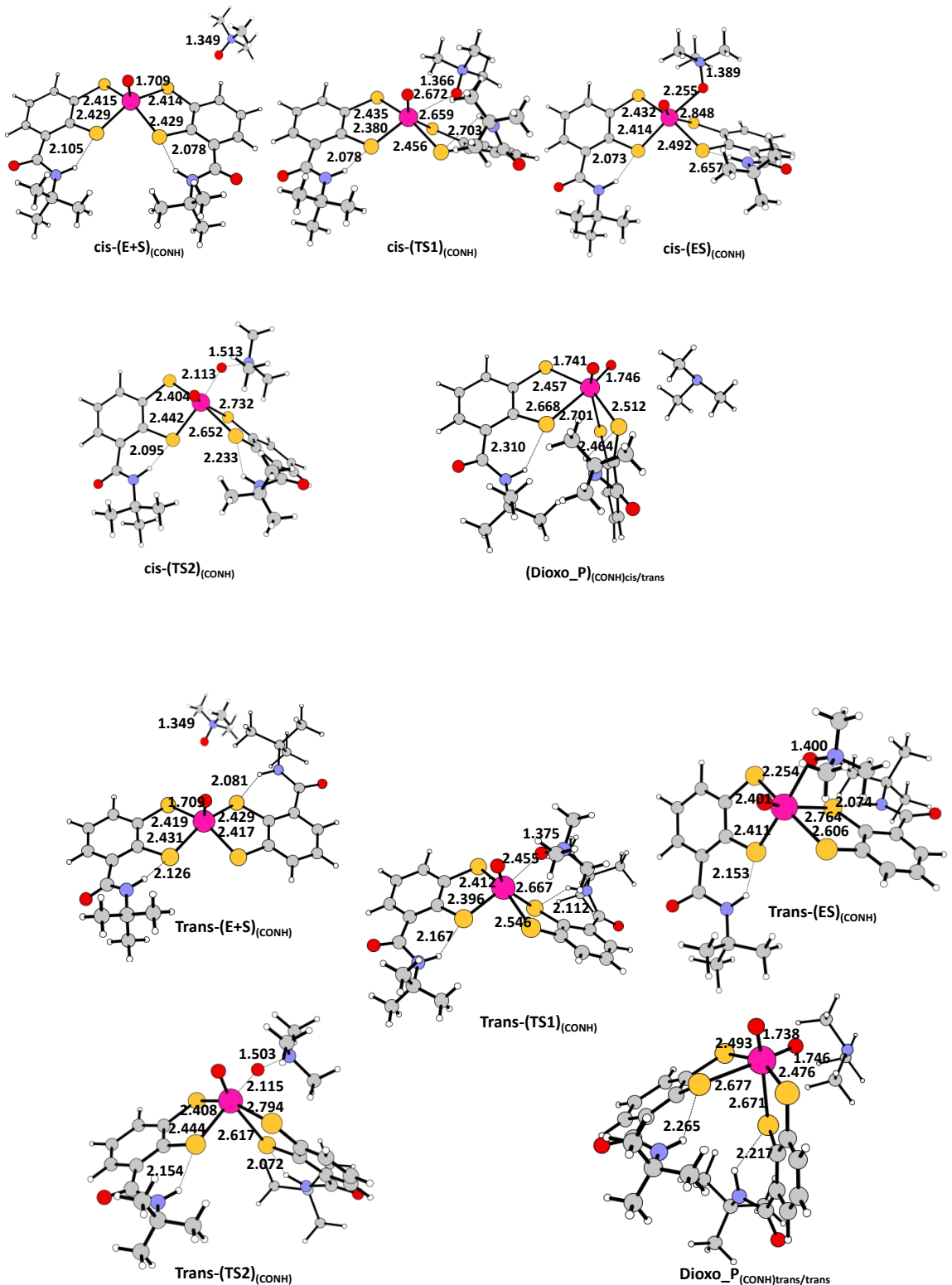


Figure S4

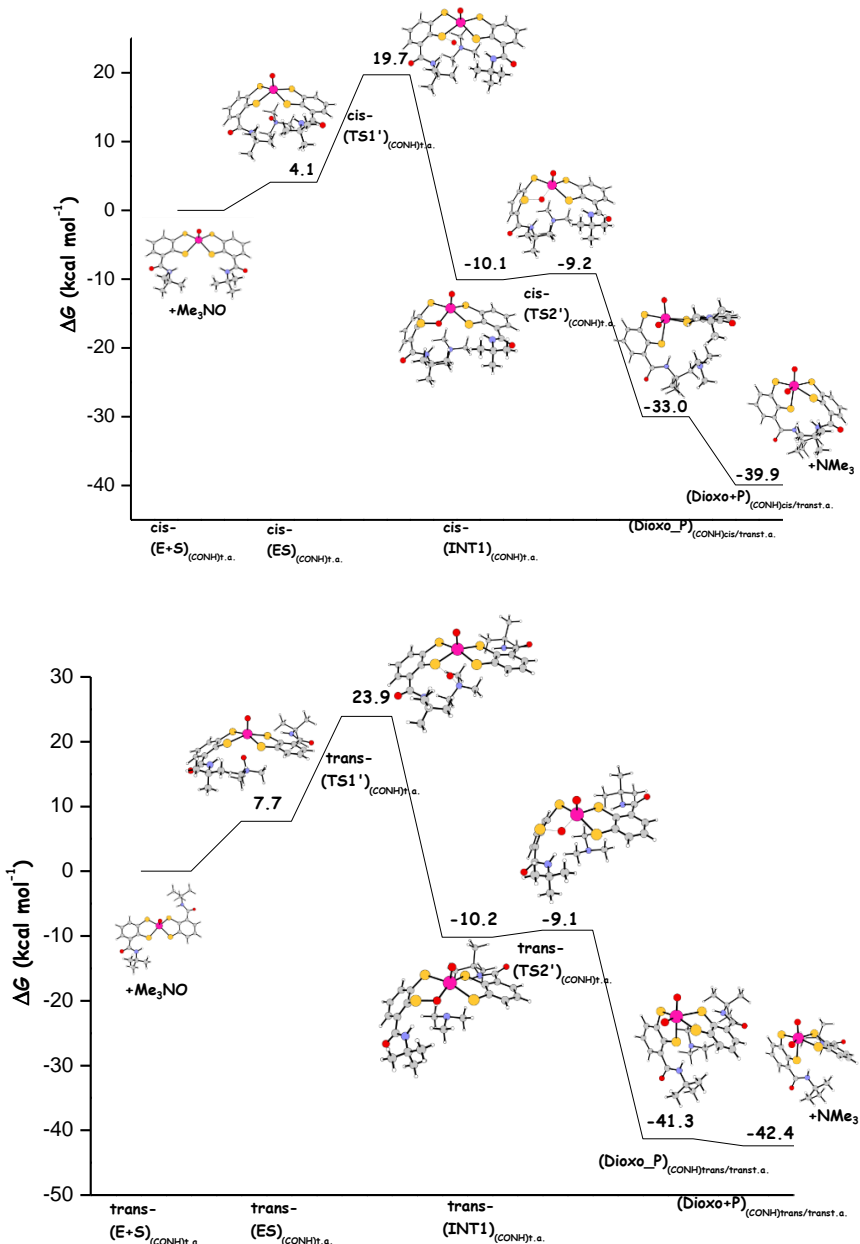


Figure S5

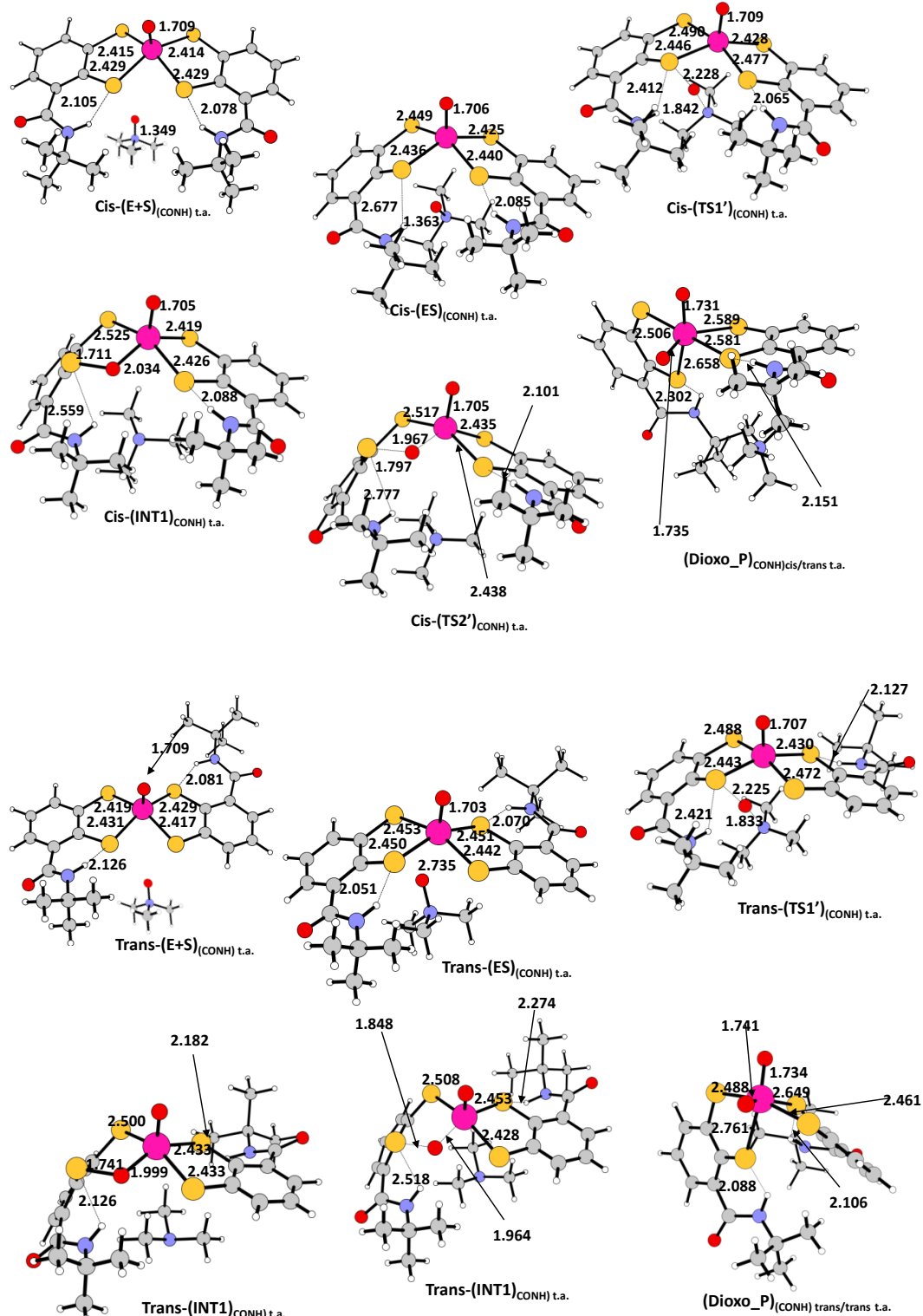


Figure S6

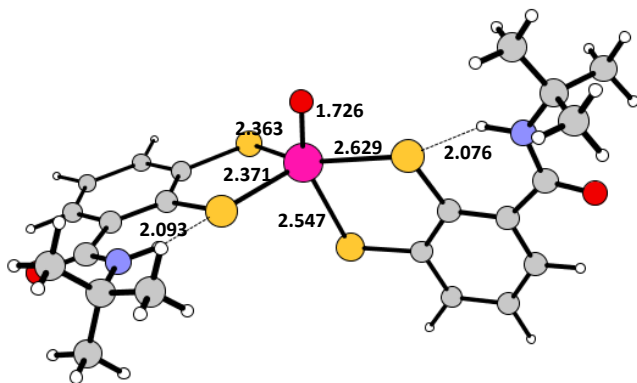


Figure S7

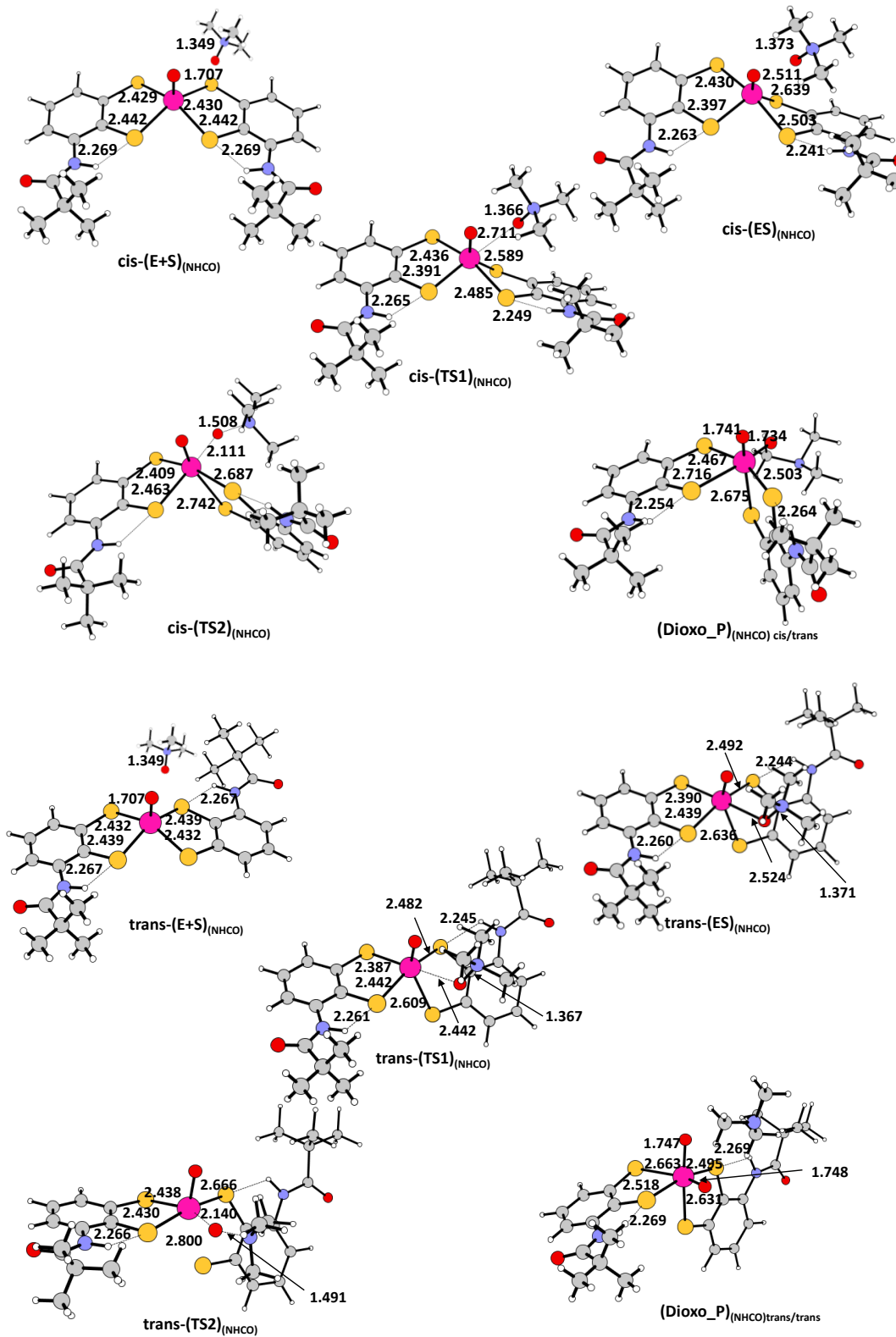


Figure S8

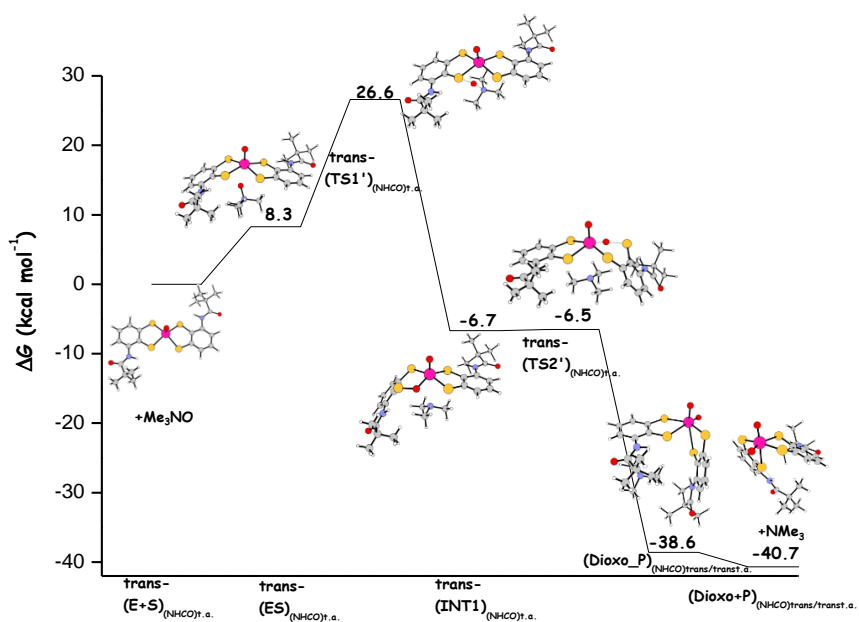
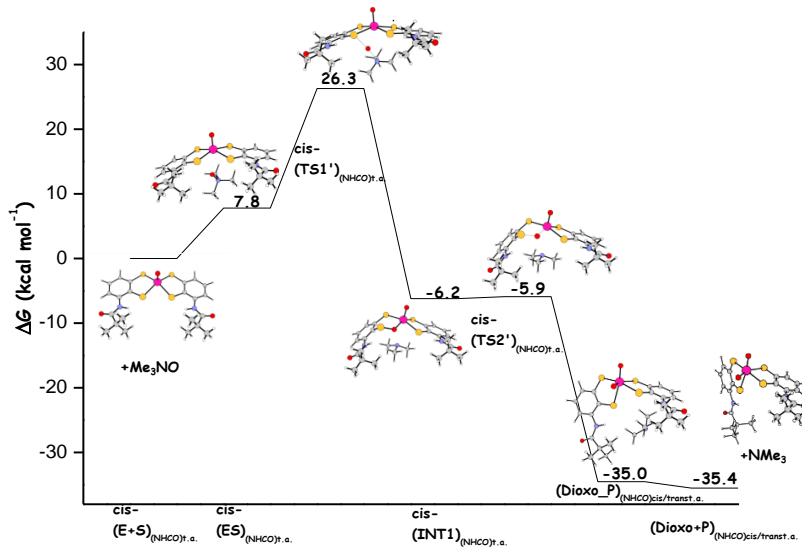
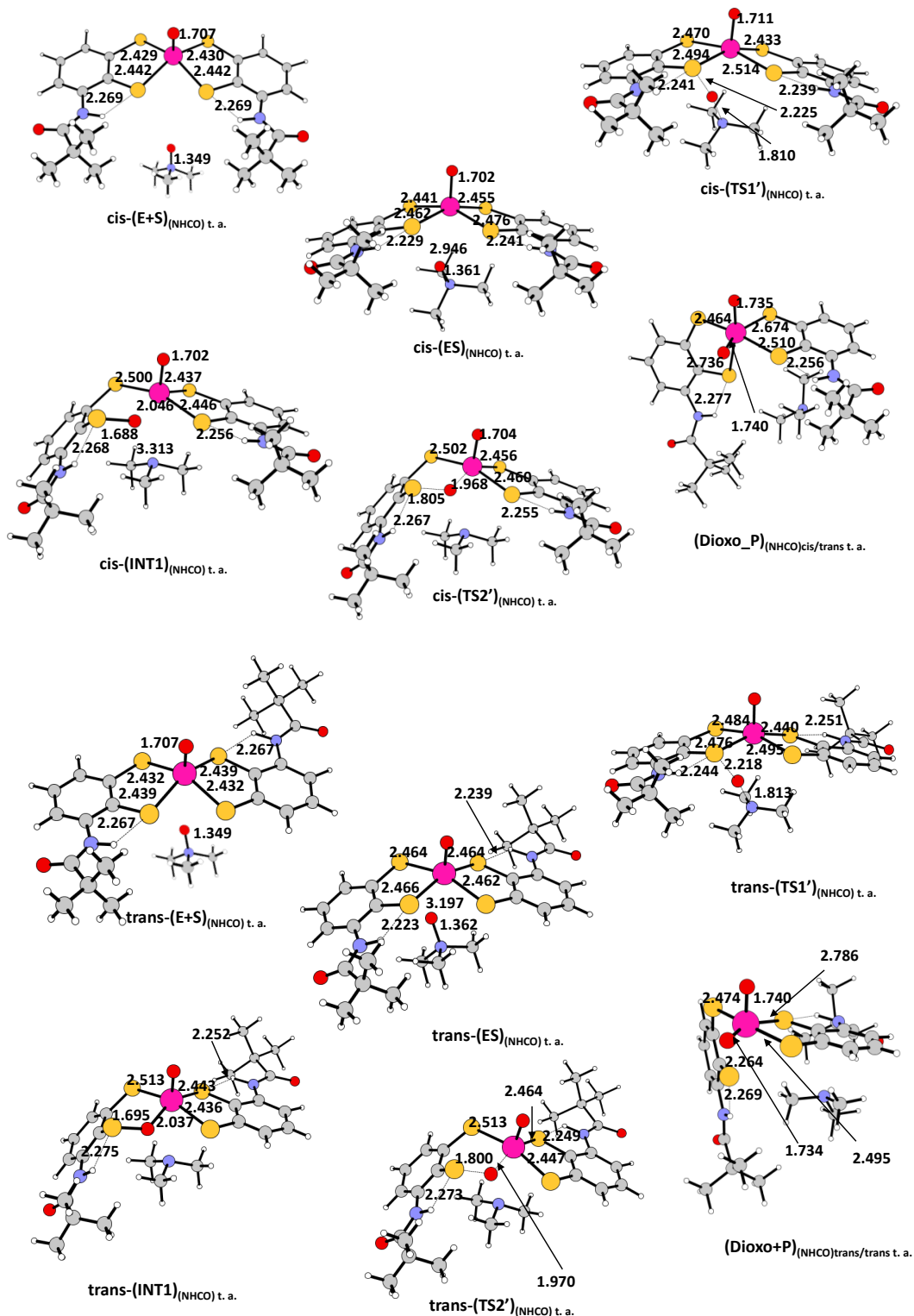


Figure S9



Chalcogen Substitution in a series of naphthyl-based iodothyronine deiodinase mimetics. A contribution of theoretical investigations to the elucidation of the role played by halogen bond

Mariagrazia Fortino, Tiziana Marino, Nino Russo and Emilia Sicilia

Dipartimento di Chimica e Tecnologie Chimiche, Università della Calabria, I-87030, Arcavacata di Rende, Italy

KEYWORDS: selenium- and tellurium-based compounds, deiodinase mechanism, regioselectivity, halogen bond, chalcogen, DFT

ABSTRACT

This paper deals with a systematic density functional theory (DFT) analysis of the mechanism of inner ring deiodination (IRD) of Thyroxine, T4, by a new series of naphthyl-based compounds having two tellurol groups and a tellurol-thiol pair in peri-position, as mimics of the seleno-containing iodothyronine deiodinase enzymes (IDs). This new series of naphthyl-based compounds having tellurium atoms showed a better deiodinase activity than that shown by the previous synthesized series of mimics of IDs, having selenol and thiol moieties.

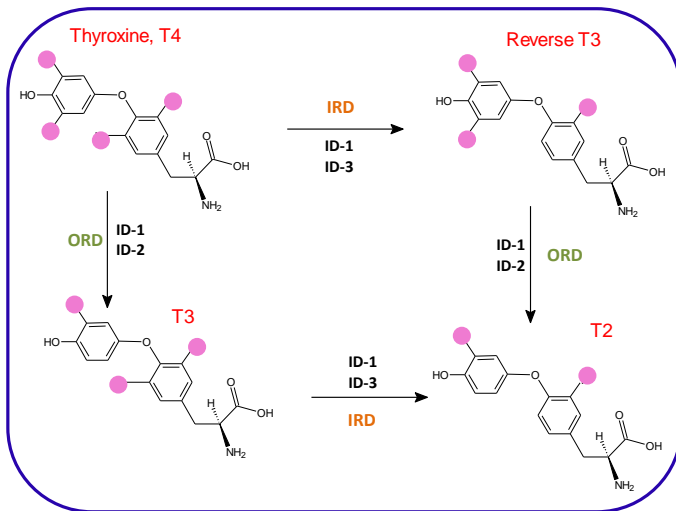
Our computational investigation allows to verify if this observed alteration of activity of thyroxine deiodination process, after chalcogen substitution is controlled by the nucleophilicity and the strength of halogen bond between the iodine atom and the chalcogen atom.

The examined herein mechanism arises from that proposed in our previous investigation: the first step is the proton abstraction by the imidazole moiety from one of the chalcogen-H groups to form the corresponding anions. The proton transfer from the imidazolium ion to the carbon, together with the heterolytic cleavage of C-I bond and the formation of chalcogen-I bond represents the rate-determining step of the whole process.

The calculated trend in the barrier heights of the corresponding transition states confirms the experimental results and the structural analysis of the first intermediates, INT1, allows us to rationalize this observed alteration of deiodinase activity after the chalcogen substitution.

1. INTRODUCTION

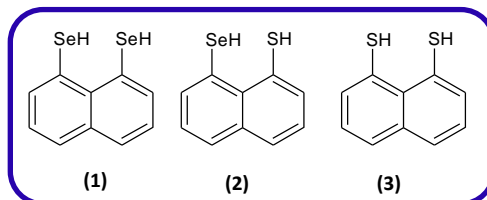
Gene expression in every vertebrate tissue such as the metabolism in the body are processes regulated by thyroid hormones released by the thyroid gland. Iodothyronine deiodinases, selenium-containing enzymes, are involved in the regulation of the thyroid hormone homeostasis by activating or inactivating thyroid hormones depending on whether they act on the phenolic or tyrosyl rings of the iodothyronines, respectively [1]. Thyroid hormones are singular example for humans of molecules containing iodine substituents on their aromatic rings. The iodine appears to be required by only two related compounds , the thyroid hormone L-thyroxine (T4) and its more active receptor-binding metabolite 3,5,3'-triiodothyronine (T3). Moreover these iodinated rings are connected by a diphenylether moiety whose presence in turns, is the alone case in human biochemistry. In fact the iodothyronine deiodinases types I, II, and III (ID-1, ID-2 and ID-3, respectively) regulate the activity of thyroid hormone removing specific iodine moieties from the precursor molecule T4. This prohormone is the main source of the circulating T3, the active thyroid hormone, via 5'-deiodination or outer-ring deiodination (ORD) of T4 catalyzed by the ID-1 and ID-2, that represents a key step in the activation of thyroid hormones (see Scheme 1). The deactivation of T3 is catalyzed by the ID-3 that is involved in a process that removes iodine selectively from the inner-ring deiodination (IRD) (see Scheme 1) for giving 3,3',5'-triiodothyronine (rT3). The triiodo derivatives T3 and rT3 are further metabolized by the three selenoenzymes to produce 3,3'-diiodothyronine (3,3'-T2), (Scheme 1) [2,4].



Scheme 1

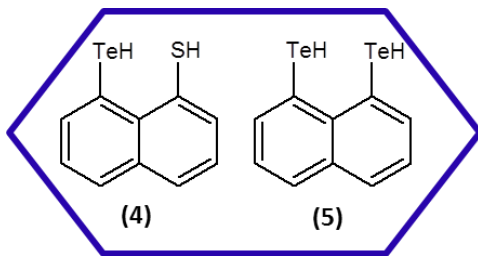
The high regioselectivity shown by different deiodinases in deiodination reactions of thyroid hormones has drawn attention so much that simple selenium compounds as mimics of these redox enzymes and able to mediate ORD [5] or IRD [6,7] have been developed. The synthesis of deiodinases biomimetics intends not only to understand the mechanism of enzyme catalysis but also to design new therapeutic agents aimed to control thyroid hormone levels regulating different essential processes. [6,7]

In particular, these naphthyl-based compounds bearing two selenol moieties in the peri-positions (1) of Scheme 2 exhibited major deiodinase activity on the inner-ring (mimicking ID-3 activity of Scheme 1, T4→rT3, T3→T2) than those having a thiol-selenol pair or two thiols, (2) and (3) of Scheme 2.



Scheme 2

All these compounds are unable to remove the second iodine atom from the phenyl ring of rT3 and 3,3'-T2 confirming their regioselective activity consisting in favoring the IRD over the ORD. Most recently the Mugesh's group has demonstrated as the replacement of sulfur/selenium atoms in a series of naphthalene derivatives including those sketched in Scheme 2 by tellurium, generates species (Scheme 3) mediating sequential deiodination of T4 to produce all the possible thyroid hormone derivatives under physiologically relevant conditions with a consequent remarkable change in the regioselectivity. Moreover this new series of compounds showed a better deiodinase activity, respect to that of the previous series, with an increased reaction rate for the conversion of T4 into rT3. [8]



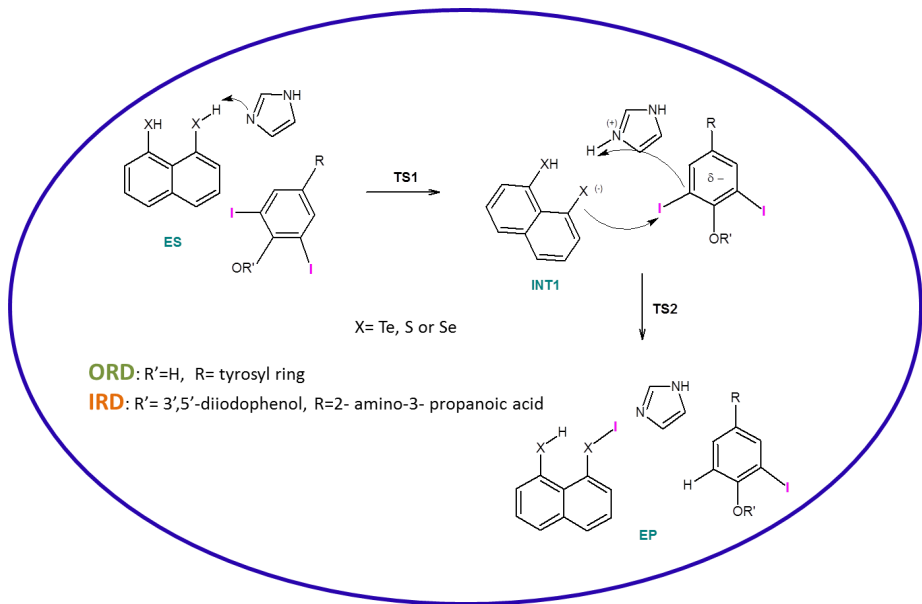
Scheme 3

While selenium represents an essential element closely related to thyroid function, [9] little is known about the Te biological activity, particularly with respect to potential chemical interactions with Se-containing components in the organism. Te showed properties similar to those elements known to be toxic to humans [10,11]. On the other hand, some organotelluric compounds are studied regarding possible antioxidative and anticancer effects [12-16]. In 2007 effects of selenium and tellurium on the activity of selenoenzymes involved in synthesis and activation of T4 have been observed [9].

In this scenario the tellurium compounds recently proposed as deiodinase mimetics [8] represent a novelty in the use and application of the tellurium compounds. The experimental works evidences as the regioselectivity of thyroid hormone deiodination process can be regulated by acting on the chalcogen nature that in turns, influences the nucleophilicity and strength of halogen bond between iodine and

chalcogen atoms. In fact during enzymatic deiodination the catalytic nucleophilic species (selonolate, thiolate and tellurate forms) performs the attack to the σ -hole of the iodine along the halogen bond with consequent weakening of the C3-I or C5-I or C3'-I or C5'-I bond depending if IRD or ORD occurs.

Back of our previous theoretical exploration on the T4 conversion into rT3 using the series of above mentioned naphtyl-based compounds [6,7] able to reproduce the catalytic functions of ID-3 including also an imidazole ring that mimicking the role of the His residue plays a crucial role as proton shuttle [17], we have undertaken a systematic density functional theory (DFT) study on the deiodinase mechanism of thyroid hormones by thiol-tellurol (**4**) and ditellurol (**5**) species of Scheme 3. A comparison of the calculated energy profiles for compounds (**4**) and (**5**) with those obtained for compound (**1**), having two selenol groups in our previous investigation will be done. In particular described in the present work is the sequential pathway of deiodination illustrated in the Scheme 4 taking into account the IRD mechanism until to the formation of deiodinated hormone excluding the step concerning the formation of the chalcogen-chalcogen bond because the role of the peri- interactions between chalcogen atoms appears emerged from our previous investigation [17] to be less prominent in determining the deiodination activity.



Scheme 4.

The role of the imidazole moiety as proton shuttle and the direct interaction of tellurol, thiol and selenol moieties with an iodine atom leading to the formation of a halogen bond have been considered in the considered mechanism (IRD). The dependence of the C3, C5, C3' and C5' carbons bonded to iodine from the different conformation of the hormone molecules in IRD/ORD deiodination of (1), (4) and (5) species has been also underlined.

2. RESULTS AND DISCUSSION

In the following sections we illustrate the outcomes of our computational analysis of the mechanism of enzymatic IRD process of thyroxine by naphthyl-based models, mimicking catalytic functions of the selenocysteine-containing iodothyronine deiodinases, having two tellurols and a tellurol-thiol pair in *peri*-position. The examined herein mechanism arises from that proposed in our previous investigation [17]. Such investigation showed that the mechanism of the process involves, first, proton abstraction by

the imidazole moiety from one of the chalcogen-H groups to form the corresponding anions. The subsequent heterolytic cleavage of the C-I bond leading to the formation of the chalcogen-I bond occurs simultaneously to the proton transfer from the formed imidazolium ion to the carbon atom. The sequence of steps is shown in Scheme 4.

For compound (**4**) of Scheme 3, as the initial proton transfer can occur either from the thiol SH or tellurol TeH groups, the two alternatives will be labeled **S_Te** in the former case and **TeS** in the latter. Compounds (**1**) of Scheme 2 and (**5**) of Scheme 3 will be indicated as **SeSe** and **TeTe**, respectively.

2.1 T4 IRD deiodination

B3LYP-D3 free energy profiles, calculated by including water solvent effects, for the deiodination reaction of T4 by compound all the compounds examined here in presence of an imidazole group, mimicking a histidine residue, is shown in Figure 1. Relative free energies are calculated with respect to the first formed adduct (**ES**) and expressed in kcal mol⁻¹. Schematic representations of the structures of stationary points intercepted along the reaction pathways are shown in the same Figure 1, whereas complete geometries of all minima and transition states can be found in the Supporting Information (SI).

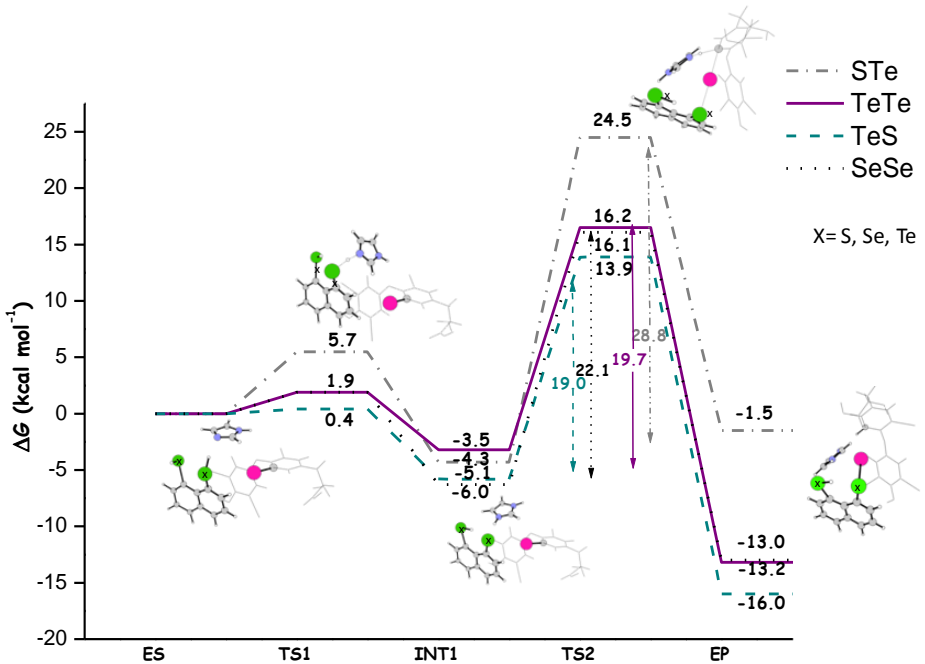


Figure 1. B3LYP-D3 free energy profiles for the inner ring deiodination of thyroxine by naphthyl-based compounds **TeTe** (solid line), **TeS** (dashed line), **STe** (dot-dashed line), and **SeSe** (dotted line). Energies are in $\text{kcal}\cdot\text{mol}^{-1}$ and relative to reactants' asymptote.

The most relevant geometrical parameters for **INT1** minima are reported and compared in Table 1 together with the estimated strength of the halogen bonding interaction, $E^{(2)}$, calculated by performing NBO second order energy analysis.

Deiodination begins with the proton abstraction from one of the X-H groups by the imidazole molecule to form the corresponding anions and the imidazolium ion. The proton transfer takes place by overcoming an energy barrier for the **TS1** transition state that is 1.9 kcal mol^{-1} for both **TeTe** and **SeSe** compounds, 5.7 kcal mol^{-1} for **STe** and only 0.4 kcal mol^{-1} for **TeS**. The formed **INT1** intermediate is stabilized by 3.5, 5.1, 6.0 and 4.3 kcal mol^{-1} for **TeTe**, **TeS**, **SeSe** and **TeS**, respectively with respect the

reference energy of the **ES** adduct. It is worth mentioning that in the case of the **INT1** intermediate formed from the **STe** compound, whose structure can be found in the SI (Figure S1), the remaining hydrogen atom is in an intermediate position between the two chalcogen S and Te atoms and, as confirmed by the NBO analysis, is bonded to the sulphur atom. The subsequent proton transfer from the formed imidazolium ion to the carbon atom gives rise to the concerted heterolytic cleavage of the C-I bond and formation of the new chalcogen-I bond. The corresponding **TS2** transition state for the **SeSe** compound lies 22.1 kcal mol⁻¹ higher in energy than the minimum leading to it. This value is larger than those calculated for **TeTe** and **TeS**, being 19.7 kcal mol⁻¹ the former and 19.0 kcal mol⁻¹ the latter. This trend confirms the experimental results showing that the replacement of sulphur/selenium atoms by tellurium in naphtyl-based deidinase mimetics increases the reactivity toward T4. The highest barrier, calculated to be 28.8 kcal mol⁻¹, is that for **STe**. IRC calculations [18] confirmed that the concerted heterolytic cleavage of the C-I bond and formation of the S-I bond is accompanied by the definitive transfer of the proton to the Te atom. The next connected minimum, labeled **INT2**, is stabilized with respect to the entrance channel energy by 16.0, 13.2, 13.0 and 1.5 kcal mol⁻¹ for **TeS**, **TeTe**, **TeS** and **TeS** compounds, respectively. Deiodination assisted by the **TeS** mimetic appears to be favored from both kinetic and thermodynamic points of view, even if the **TeTe** compound is calculated to be only slightly less active. On the contrary, the **STe** form of compound (**4**) is significantly less active in assisting deiodination of T4.

The previously explored superior catalytic activity of the naphthalyl compound having two selenol groups in the *peri*-positions with respect to the ones having two thiol groups or a thiol-selenol pair was explained invoking the formation of a chalcogen--I-C halogen bond (X-bond) in the **INT1** intermediate, in which the C-I bond is definitively broken and the chalcogen-I bond formed.

Compound	T e T e	T e S	S T e	S e S e
X-I	4.046(4.04)	3.830(4.04)	3.704(3.78)	3.457(3.80)
C-I	2.153[2.137]	2.162[2.138]	2.142[2.136]	2.163[2.137]
C-I-X	151.6	157.7	153.2	172.8
ΔE⁽²⁾	1.38	0.54	0.71	25.72

Table 1. The most relevant geometrical parameters and second order energy ($\Delta E^{(2)}$) for the **INT1** intermediates intercepted along the T4 IRD pathways assisted by synthetic deiodinase mimetics labeled **T**e**T**e, **T**e**S**, **S****T**e and **S****e****S**e. The data reported in parentheses and square brackets are ΣR_{vdW} and C-I bond length in the corresponding ES initial adducts, respectively. Bonds are in Å, angles in degrees and energies in kcal mol⁻¹.

The strongest halogen Se--I interaction for the naphthyl compound bearing two selenol groups facilitates the formation of the new Se-I bond, lowers the transition state barrier and, as a consequence, makes deiodination faster. Donation of electron density from lone pairs on the S/Se atom to C-I antibonding σ^* orbital causes an elongation of bond and this bond lengthening correlates with the strength of the interaction. The same kind of analysis was carried out here by performing NBO analysis of both charge and second order energy and by plotting the maps of the Molecular Electrostatic Potential (MEP) for all **INT1** intermediates formed by reaction of **T**e**T**e, **T**e**S**, **S****T**e and **S****e****S**e compounds with T4. The colors were chosen such that regions of attractive potential appear in red and those of repulsive potential appear in blue. The recently published IUPAC definition [19] describes the X-bond as due to a net attractive interaction between an electrophilic region associated with a halogen atom and a nucleophilic region. Currently, the term XB is used for defining any noncovalent interaction involving halogens very similar, in many respects, to the hydrogen bond (HB). The halogen atom X is shared between a donor D and an acceptor A, D···X···A, and like the HB such arrangement prefers a linear configuration, and the stronger the interaction is, the shorter the D···X distance is. The attraction between the two subunits results in a short contact distance between X and D, less than the van der Waals radii sum (ΣR_{vdW}). The main difference, instead, is the partial positive charge that is generally attributed to the H atom and the

electron richness of the covalently bonded halogens. As both the donor and especially the acceptor tend to be electronegative, or electron-withdrawing, it is somewhat counterintuitive that halogen atoms can interact with them. The explanation is found in the deformation of the spherically symmetric electron density of an atom as a consequence of bond formation, which results in regions with more or less electron density on the atom's equatorial or bond terminus, respectively. Therefore, the region of positive potential, called “ σ -hole”, can interact with the negative side of another molecule[20]. In The resulting electrostatic attraction to an incoming electron donor, is supplemented by other factors such as transfer from the D lone pair to the A–X σ^* antibonding orbital that causes a lengthening of the A–X bond. In light of this description of the halogen bond, it clearly appears that important differences exist in the behaviors of the synthetic deiodinase mimetics examined here. The data collected in Table 1 show that the geometrical requirements for a halogen bond formation are fulfilled only by the **SeSe** compound showing a Se-I bond distance and a C-I-Se bond angle of 3.457 Å and 172.8 degrees, respectively. That is, the distance between the iodine and the donor atom is shorter than the van der Waals radii sum, the C-I bond is elongated to a certain degree and the C-I-Te arrangement is almost linear. The chalcogen-I distance is 3.830 Å, that is shorter than the sum of the van der Waals radii, the C-I bond is as much elongated and the bond angle is 157.7 degrees for **TeS**. The values of 4.046 and 3.704 Å calculated for **TeTe** and **STe**, respectively are almost equal to van der Waals radii sum, the C-I bond elongation are less significant, mainly for **TeTe**, and the corresponding bond angles become 151.6 and 153.2 degrees. Since geometrical information gives a clear indication of a halogen bond formation only for the **SeSe** compound, let us examine the trend in NBO second order energies and MEPs reported in Table 1 and Figure 2, respectively. The strength of the halogen bonding interaction estimated through the donation of a chalcogen lone pair into the σ^* C-I orbital, is calculated to be 25.7 kcal mol⁻¹ for the **SeSe** compounds, whereas the values of 1.38, 0.54 and 0.71 kcal mol⁻¹ for **TeTe**, **TeS** and **STe**, respectively indicate that electron density donation into the antibonding orbital does not contribute to the interaction between X

and I atoms. The maps of the MEP show a region of positive potential, that is a σ hole, located on the iodine atom in the ES initial adduct for the compound with two selenols, SeSe.

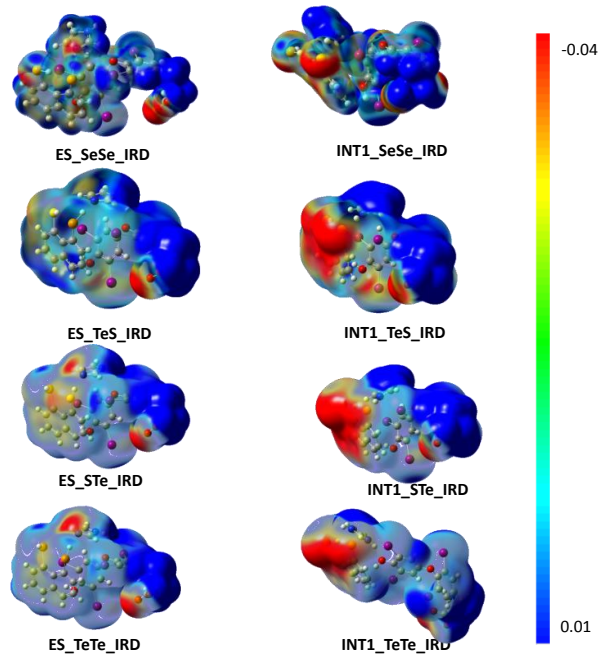


Figure 2. Maps of the Molecular Electrostatic Potential (MEP) for both ES and INT1 species formed by reaction of SeSe, TeS, STe and TeTe compounds with T4. The electrostatic potential is represented with a color scale going from red (-0.04 au) to blue (0.01 au).

A region of negative electrostatic potential, instead, corresponding to a dark red area is located on the chalcogen atom in the corresponding INT1 intermediate, while the electrostatic potential becomes significantly less positive on I atom confirming lone pair donation to the iodine σ hole and formation of a halogen bond. All the other examined compounds do not show any indication that in going from ES to INT1 a halogen bond is formed. Therefore, from our analysis results that only the SeSe naphthyl-based model having two selenols in *peri*-position forms in the INT1 intermediate a halogen bond. In contrast to our previous investigation [17] on the catalytic behavior of model systems mimicking deiodinase

enzymes, here the C-I bond breaking of and of the chalcogen-iodine bond formation in eth rate-determining step of the process is hampered by the formation of a halogen bond in the intermediate **INT1**. For example, the **TS2** energies for **TeTe** and **SeSe** calculated with respect to the reference zero energy of reactants are almost the same, about 16 kcal mol⁻¹, the barriers calculated with respect to the previous minimum, are different due to the different stabilization of the **INT1** intermediate, that is -6.0 and -3.5 kcal mol⁻¹ for **SeSe** and **TeTe**, respectively.

3. COMPUTATIONAL DETAILS

Molecular geometry optimizations, were carried out without symmetry constraints at the density functional level of theory, by using Gaussian 09 [21] code employing the B3-LYP functional with Grimme D3 correction[22]. The standard 6-31+G(d,p) basis set was used for the C, H, N, O, S and Se atoms, whereas the SDD pseudo-potential in connection with the relative orbital basis set was employed for the iodine and tellurium atoms [23]. All of the reported structures represent genuine minima or transition states on the respective potential energy surfaces, as confirmed by analysis of the corresponding Hessian matrices. For transition states, the vibrational mode associated with the imaginary frequencies was verified to be related to the correct movement of involved atoms.

Furthermore, the IRC method was used to asses that the localized TSs correctly connect to the corresponding minima along the imaginary mode of vibration [18]. The influence of water solvent effects on the energetic of the process was estimates in the framework of the CPCM model [24].

Single point calculations on all stationary points structures obtained from gas-phase calculations by using the same B3LYP-D3 and basis sets computational approach were performed.

Calculated reaction Gibbs free energies in solution, ΔG_{sol} , for each process were obtained as the sum of two contribution: a gas-phase reaction free energy ΔG_{gas} , and a salvation reaction free energy term

calculated with the CPCM approach, ΔG_{solv} . NBO analysis of the charge density and maps of MEP was performed for some key species intercepted along the reaction paths [25].

4. CONCLUSION

A systematic DFT study of the mechanistic details of the inner ring deiodination process of thyroxine, T4, was carried out by using several chalcogen-substituted naphthalenes mimicking of IDs.

Specifically the observed alteration of activity of thyroxine IRD process after replacement of selenium or sulphur atoms by tellurium atom has been investigated and rationalized.

The first step of the reaction is the proton abstraction by the imidazole moiety from one of the chalcogen-H groups, leading to the formation of the first intermediate, INT1. The subsequent proton transfer from the imidazolium ion to the carbon, together with the heterolytic cleavage of C-I bond and the formation of the chalcogen-I bond, represents the rate determining step of the whole process.

The calculated trend in the barrier heights of the corresponding second transitions states (22.1(**SeSe**)>19.7(**TeTe**)>19.0(**TeS**)) confirms the experimental results, showing that the replacement of sulphur/selenium atoms by tellurium atom increases the reactivity toward T4.

Moreover our results showed that the **STe** form of compound (**4**) is significantly less active in assisting deiodination of T4 (with a barrier of 28.8).

To rationalize this results the status of the halogen bond for all INT1 intermediates formed by reaction of compound (**1**), (**4**) and (**5**) with T4, has been investigated.

Our investigations revealed that the geometrical and charge distribution requirements for a halogen bond formation are fulfilled only by compound (**1**). Whereas for compound (**4**) and (**5**) not all the requirements are followed.

These results showed that, when the halogen bond is formed for each naphthalene-based compound reacting with T4, the strongest X-I halogen bond interaction corresponds to a lower barrier, and

the deiodination process is faster. Whereas, the comparison between species that may not form this non-covalent interaction revealed that, they undergo a minor stabilizing force facilitating the subsequent step of the deiodination process.

ASSOCIATED CONTENT

Supporting Information Available: Cartesian coordinates of intercepted stationary points. This material is available free of charge via the Internet at <http://pubs.acs.org>.

AUTHOR INFORMATION

Corresponding Author

*emilia.sicilia@unical.it

ACKNOWLEDGMENT.

This work has been financially supported by Universita` della Calabria and carried out within the FP7-PEOPLE-2011-IRSES, Project no. 295172. Mariagrazia Fortino gratefully acknowledges Commissione Europea, Fondo Sociale Europeo, Regione Calabria for the financial support.

REFERENCES:

- (1) a) Crabtree, G. W.; Dresselhaus, M. S.; Buchanan, M. V. *Phys. Today*, **2004**, 57, 39. b) Behne, D.; Kyriakopoulos, A.; Meinholt, H; . Köhrle, J. *Biochem. Biophys. Res. Commun.* **1990**, 173, 1143 – 1149. c) Leonard, J. L.; Visser, T. J.; *Biochemistry of Deiodination in Thyroid Hormone Metabolism* (Ed.: G. Hennemann), Marcel Dekker, New York, **1986**, p. 189. d). Berry, M. J; Banu, L.; Larsen, P. R.; *Nature*, **1991**, 349, 438 – 440. e) Larsen, P. R.; Berry, M. J.; *Annu. Rev. Nutr.*,

- 1995**, 15, 323. f) Leonard, J. L.; Köhrle, J. *Intracellular Pathways of Iodothyronine Metabolism in The Thyroid* (Eds.: L. E. Braverman, R. D. Utiger), Lippincott-Raven, Philadelphia, **1996**, p. 144. g) St. Germain, D. L.; Galton, V. A.; *Thyroid*, **1997**, 7, 655 – 668.
- (2) (a) Bianco, A. C., Salvatore, D.; Gereben, B.; Berry, M. J.; Larsen, P. R.; *Endocr. Rev.*, **2002**, 23, 38–89. (b) Köhrle, J. *Methods Enzymol.*, **2002**, 347, 125–167. (c) Kuiper, G. G. J.; Kester, M. H. A.; Peeters, R. P.; Visser, T. J. *Thyroid*, **2005**, 15, 787–798.
- (3) (a) Visser, T. J.; Schoenmakers, C. H. H. *Acta Med. Austriaca*, **1992**, 19, 18–21. (b) Köhrle, J. *J. Mol. Cell. Endocrinol.* **1999**, 151, 103–119. (c) Köhrle, J.; Jakob, F.; Contempré, B.; Dumont, J. E. *Endocr. Rev.* **2005**, 26, 944–984.
- (4) Bianco, A. C.; Kim, B. W. J.; *Clin. Invest.* **2006**, 116, 2571–2579.
- (5) Goto, K.; Sonoda, D.; Shimada, K.; Sase, S.; Kawahims, T. *Angew. Chem. Int. Ed.*, **2010**, 49, 545–547.
- (6) Manna, D.; Mugesh, G. *Angew. Chem. Int. Ed.*, **2010**, 49, 9246–9249.
- (7) Manna, D.; Mugesh, G. *J. Am. Chem. Soc.*, **2012**, 134, 4269–4279.
- (8) Raja, K.; Mugesh, G. *Angew. Chem. Int. Ed.*, **2015**, 54, 7674 –7678
- (9) Eybl, V.; Kotyzova, D.; Sykora, J.; Topolcan, O.; Pikner, R.; Mihaljevic, M.; Brtko, J.; Glattre, E. *Biol. Trace Elem. Res.*, **2007**, 117 (1-3), 105-114.
- (10) Larner, A. J. *Trace Elem. Electr.*, **1995**, 12, 26-31.
- (11) Taylor, A. *Biol. Trace Elem. Res.*, **1996**, 55, 231-239.
- (12) Brivida, K.; Tamler, R.; Klotz, L.O.; Engman, L.; Cotgrave, LA.; Sies, H. *Biochem. Pharmacol.*, **1998**, 55, 817-823.
- (13) Jacob, C.; Arteel, G. E.; Kanda, T.; Engman, L.; Sies, H. *Chem. Res. Toxicol.*, **2000**, 13, 3-9.
- (14) Klotz, L. O.; Kroncke, D.; Buchczyk, D. P.; Sies, H. *J. Nutr.*, **2003**, 133, 1448S-1451S.
- (15) Engman, L.; Al-Maharik, N.; McNaughton, M.; Birmingham, A.; Powis, G. *Bioorg. Med. Chem.*, **2003**, 11, 5091-5100.
- (16) Engman, L.; Al-Maharik, N.; McNaughton, M.; Birmingham, A.; Powis, G. *Antic. Drugs.*, **2003**, 14, 153-161.2003, 11, 5091-5100.
- (17) Fortino, M.; Marino, T.; Russo, N.; Sicilia, E. *Chem. Eur. J.*, **2015**, 21, 1 – 8.
- (18) a) Fukui, K. *J. Phys. Chem.*, **1970**, 74, 4161-4163. b) Gonzalez, C.; Schlegel, H. B. *J. Chem. Phys.*, 1989, 90, 2154-2161.

- (19) Desiraju, G. R.; Ho, P. S.; Kloo, L.; Legon, A. C.; Marquardt, R.; Metrangolo, P.; Politzer, P.; Resnati, G.; Rissanen, K. *Pure Appl. Chem.*, **2013**, *85*, 1711.
- (20) Gilday, L. C.; Robinson, S. W.; Berendt, T. A.; Langton, M. J.; Mullaney, B. R.; Beer, P. D. *Chem. Rev.*, **2015**, *115*(15) 7118-7195.
- (21) *Gaussian 09*, Revision **D.01**, Frisch, M. J.; Trucks, G. W.; Schlegel, H. B.; Scuseria, G. E.; Robb, M. A.; Cheeseman, J. R.; Scalmani, G.; Barone, V.; Mennucci, B.; Petersson, G. A.; Nakatsuji, H.; Caricato, M.; Li, X.; Hratchian, H. P.; Izmaylov, A. F.; Bloino, J.; Zheng, G.; Sonnenberg, J. L.; Hada, M.; Ehara, M.; Toyota, K.; Fukuda, R.; Hasegawa, J.; Ishida, M.; Nakajima, T.; Honda, Y.; Kitao, O.; Nakai, H.; Vreven, T.; Montgomery, J. A., Jr.; Peralta, J. E.; Ogliaro, F.; Bearpark, M.; Heyd, J. J.; Brothers, E.; Kudin, K. N.; Staroverov, V. N.; Kobayashi, R.; Normand, J.; Raghavachari, K.; Rendell, A.; Burant, J. C.; Iyengar, S. S.; Tomasi, J.; Cossi, M.; Rega, N.; Millam, J. M.; Klene, M.; Knox, J. E.; Cross, J. B.; Bakken, V.; Adamo, C.; Jaramillo, J.; Gomperts, R.; Stratmann, R. E.; Yazyev, O.; Austin, A. J.; Cammi, R.; Pomelli, C.; Ochterski, J. W.; Martin, R. L.; Morokuma, K.; Zakrzewski, V. G.; Voth, G. A.; Salvador, P.; Dannenberg, J. J.; Dapprich, S.; Daniels, A. D.; Farkas, Ö.; Foresman, J. B.; Ortiz, J. V.; Cioslowski, J.; Fox, D. J. *Gaussian, Inc.*, Wallingford CT, **2009**.
- (22) a) Becke, A.D *Phys. Rev. B*, **1988**, *38*, 3098. b) Lee, C.; Yang, W.; Parr, R. G. *Phys. Rev. B*, **1988**, *37*, 785. c) Grimme, J.; Ehrlich, A., S.; Krieg, H. *J. Chem. Phys.*, **2010**, *132*, 154104.
- (23) Andrae, D.; Haussermann, U.; Dolg, M.; Stoll, H.; Preuss, H *Theor. Chim. Acta*, **1990**, *77*, 123-141.
- (24) Barone, V.; Cossi, M. *J. Phys. Chem. A*, **102** (1998) 1995-2001.
- (25) Glendening, E. D.; Reed, J. E.; Carpenter, J. E.; Winhold, F. *NBO Program 3.1*; Madison, WI, **1988**.

Supporting Information

Cartesian Coordinates

IRD process of T4 using Te_Te

ES:

```
C -2.10311900 2.17292100 -2.76002500
C -3.33433000 1.80321900 -2.15491400
C -3.55043300 0.46120400 -1.63873900
C -2.48498500 -0.48658800 -1.87845400
C -1.29737800 -0.06011000 -2.45750200
C -1.08430400 1.26765400 -2.88208300
H -1.98160000 3.19580400 -3.10405800
H -0.49981200 -0.77431600 -2.61570200
H -0.13035400 1.55156500 -3.31405300
C -4.35032200 2.79456700 -2.07846100
C -5.56674800 2.51599800 -1.51278000
C -5.77242000 1.24527800 -0.93426300
C -4.80485000 0.24913200 -0.95165400
H -4.13892600 3.77807400 -2.49069200
H -6.35432600 3.26271700 -1.47386200
H -6.71350200 1.05801300 -0.42919200
H -5.66168200 -2.48204900 -0.62864500
H -2.41366200 -2.82973600 -0.17981000
C 5.55135900 -1.39747700 0.27646300
C 4.55866600 -1.93724300 -0.55201100
C 3.21028600 -1.74784800 -0.25560000
C 2.82632300 -1.00906000 0.87210000
C 3.82217500 -0.50507700 1.71900200
C 5.17216000 -0.68953700 1.42550400
C 7.01309600 -1.53413400 -0.08780600
C 7.52884200 -0.35512700 -0.96812300
C 6.77130000 -0.34344300 -2.31237400
N 7.42875300 0.89736700 -0.24075100
O 1.49732700 -0.85433500 1.17952200
O 5.93489800 0.47546600 -2.60168400
O 7.05675000 -1.35955300 -3.17470100
I 1.69161100 -2.61087100 -1.48638600
H 4.83762500 -2.49711900 -1.43866900
H 5.93392000 -0.28171500 2.08047600
H 7.17620400 -2.48560000 -0.60716500
H 7.63017700 -1.54299800 0.81493400
H 8.59139200 -0.54465800 -1.17341300
H 6.45607400 1.19628500 -0.20532200
H 7.93114700 1.63276600 -0.73037500
H 7.77767600 -1.91383800 -2.84142500
C -1.29052700 -2.00809500 3.87535300
C -2.32712700 -2.41888400 3.06919900
C -0.52150500 -2.96351700 2.03030600
N -0.14017200 -2.37281900 3.20028300
H 0.80377900 -2.10644900 3.44181400
H -1.26336700 -1.50598400 4.83010700
H -3.38872200 -2.31371300 3.23647000
H 0.18641300 -3.29603900 1.28631700
N -1.83561800 -3.01407900 1.92501200
I 3.25723500 0.52407000 3.51000100
C 0.85099300 0.32285300 0.80327800
C 1.43523700 1.27251600 -0.03117600
C 0.72635300 2.43426100 -0.33327100
C -0.55509000 2.67689900 0.18392000
C -1.10463100 1.68756600 1.01941300
C -0.42675000 0.51212500 1.32273500
O -1.18330100 3.83264400 -0.14373200
```

```
I 1.61719100 3.86370100 -1.64935100
I -3.03072500 2.01429800 1.91059600
H 2.42505500 1.11525800 -0.44165500
H -0.87201500 -0.24169400 1.95674100
H -2.09593000 3.82098500 0.18621000
Te -5.29221100 -1.30891800 0.46697600
Te -2.58426600 -2.64909000 -1.82028200
```

TS1:

```
C 1.65005400 1.68844300 2.41647400
C 2.95727500 1.69450200 1.86240800
C 3.57014600 0.46445800 1.39470300
C 2.88682900 -0.76455800 1.72826700
C 1.59509200 -0.70214500 2.23665000
C 0.95086500 0.51471500 2.54286600
H 1.21007800 2.63462100 2.71972800
H 1.08145400 -1.62745100 2.47723400
H -0.06552600 0.50886600 2.92396900
C 3.64784500 2.93541200 1.77112000
C 4.89956500 3.00094800 1.21238600
C 5.45176400 1.84151800 0.62506400
C 4.79824400 0.61641100 0.64840900
H 3.16155400 3.82461000 2.16446800
H 5.44620000 3.93890600 1.17259700
H 6.39908500 1.93032000 0.10116200
H 5.23706200 -2.07795500 0.07246400
H 2.85316700 -3.31192600 0.40020400
C -5.58801800 -1.64586500 -0.54178400
C -4.76530200 -1.89082800 0.56514400
C -3.39469500 -1.64666400 0.49555900
C -2.81935600 -1.15035700 -0.68130000
C -3.64115300 -0.94262600 -1.79682400
C -5.01259500 -1.17811000 -1.73133100
C -7.08508500 -1.83616800 -0.44156600
C -7.82320100 -0.55414800 0.05319100
C -7.36924800 -0.22367800 1.48998600
N -7.61573300 0.53647600 -0.88207900
O -1.46132200 -0.94927700 -0.76946000
O -6.62669000 0.68629000 1.76303100
O -7.80631300 -1.06374100 2.46979900
I -2.16104200 -2.05273400 2.19027100
H -5.19688700 -2.26025600 1.48940600
H -5.64049900 -0.99777600 -2.59669200
H -7.30644500 -2.67558800 0.22755600
H -7.50171700 -2.07835400 -1.42302600
H -8.89667300 -0.78631200 0.07322800
H -6.67489000 0.90953400 -0.77064000
H -8.24987100 1.30442500 -0.67964200
H -8.43706900 -1.71303000 2.12516500
C 1.41491000 -3.21371900 -2.90315100
C 2.42763200 -3.64396500 -2.08343000
C 0.85754600 -2.87872600 -0.78212700
N 0.42957400 -2.73537000 -2.05911100
H -0.44002300 -2.28771500 -2.32041200
H 1.30996400 -3.19823000 -3.97667100
H 3.38490300 -4.07041200 -2.34164000
H 0.29966600 -2.55022200 0.08042400
N 0.205687200 -3.43819100 -0.77121400
I -2.75801400 -0.31093600 -3.64365700
C -0.96017100 0.34668200 -0.57778800
C -1.60855300 1.28671900 0.21641800
C -1.01237300 2.53270400 0.40333300
C 0.21160600 2.86490800 -0.19888600
C 0.81364100 1.89403700 -1.02002400
C 0.24927100 0.63606800 -1.19942600
O 0.74986400 4.08206100 0.05088400
```

I	-1.94462700	3.92285300	1.72980300
I	2.64129400	2.34366200	-2.03902900
H	-2.54609700	1.05039900	0.70403200
H	0.73867700	-0.10939100	-1.81130600
H	1.64919100	4.12994300	-0.31247100
Te	5.57092300	-0.71942800	-0.84635900
Te	3.76017000	-2.74589300	1.93416800

I	2.86416600	-2.45195600	1.67797200
H	-2.50901100	-0.95746900	-0.56421400
H	0.60062500	-0.43683600	2.34594700
H	2.06803200	-3.58836000	-0.72955400
Te	5.60166400	1.21451500	0.44279800
Te	2.63760900	2.97608600	-1.18354900
H	2.23896800	2.35768600	1.05952000

INT1:

C	1.96492400	-1.58618000	-3.08813600
C	3.15792800	-1.45358600	-2.33051000
C	3.48852200	-0.21424000	-1.62844000
C	2.54402200	0.88135200	-1.79278500
C	1.38865100	0.66843900	-2.54089200
C	1.08153900	-0.54534300	-3.18026400
H	1.76242900	-2.53616100	-3.57332000
H	0.69084800	1.48651600	-2.66620000
H	0.15683800	-0.64253600	-3.74095200
C	4.01486700	-2.58815800	-2.29219700
C	5.20235300	-2.55114400	-1.60696600
C	5.54465800	-1.37847300	-0.91139400
C	4.73235000	-0.24855400	-0.88350600
H	3.71615600	-3.47470800	-2.84664500
H	5.87173600	-3.40670700	-1.59227800
H	6.48586100	-1.36865400	-0.36870500
H	4.49207000	2.41125700	-0.12159000
C	-5.52197300	1.55941300	0.35154000
C	-4.39049100	2.15628300	-0.22068100
C	-3.11002100	1.79005100	0.18969700
C	-2.93776600	0.81425200	1.18184100
C	-0.06999600	0.23541400	1.76772200
C	-5.35210700	0.60346700	1.36254700
C	-6.90743400	1.89107300	-0.15670700
C	-7.37830700	0.92812100	-1.28984800
C	-6.43927200	1.06728000	-2.50617700
N	-7.47086200	-0.43254100	-0.79045100
O	-1.67667500	0.46106000	1.61216500
O	-5.61858600	0.23915400	2.81363300
O	-6.53797900	2.22594700	-3.21625300
I	-1.36901700	2.70378700	-0.68739900
H	-4.50818900	2.89790500	-1.00441600
H	-6.22193600	0.13900000	1.81324000
H	-6.93195100	2.92665800	-0.51511800
H	-7.64001300	1.80452100	0.65060000
H	-8.38515400	1.24889700	-1.59011100
H	-6.53684800	-0.82963300	-0.70789100
H	-7.96788400	-1.02004400	-1.45438700
H	-7.26775500	2.77610200	-2.89576400
C	1.80423800	1.15864200	4.05638800
C	2.63525600	1.34519800	2.98697900
C	0.70041700	2.30475800	2.49880800
N	0.60294900	1.77154400	3.72727200
H	-0.24797300	1.75093600	4.27320200
H	1.95166700	0.64573500	4.99297000
H	3.64835600	1.02365000	2.78839900
H	-0.08446500	2.80028900	1.95004500
N	1.92420600	2.06063100	2.04540200
I	-3.83004800	-1.23784200	3.30444100
C	-1.02073300	-0.58103800	0.95284500
C	-1.54743500	-1.24034400	-0.15475900
C	-0.80673700	-2.26461800	-0.74431600
C	0.45645400	-2.64632500	-0.26189500
C	0.94682800	-1.95445100	0.85998500
C	0.22013500	-0.93641000	1.46819200
O	1.11003300	-3.66526300	-0.86998300
I	-1.62431300	-3.26102900	-2.44746900

TS2:

C	3.75260700	2.54760500	-0.04563100
C	4.26313500	1.38877900	-0.68993600
C	3.96068400	0.04456000	-0.20264300
C	3.14209900	-0.01355600	0.99805500
C	2.68113300	1.16499100	1.57836700
C	2.97368100	2.44550800	1.07362400
H	3.99073600	3.52058400	-0.46594800
H	2.05252800	1.10328300	2.46003400
H	2.56586200	3.32316100	1.56227300
C	5.08051900	1.60892300	-1.83094300
C	5.62376700	0.55293100	-2.52182100
C	5.33245600	-0.75576500	-2.09143100
C	4.52576800	-1.03831700	-0.98743200
H	5.27651700	2.63380500	-2.13377100
H	6.27103600	0.711134300	-3.37974000
H	5.76661000	-1.57777900	-2.65468700
H	3.44742800	-3.05862100	0.60107100
H	-0.54508800	-1.03617300	-2.43966900
C	-4.03327600	-2.73335000	-1.45772400
C	-2.63338100	-2.66958000	-1.52957900
C	-1.93124000	-1.45534200	-1.57490200
C	-2.69403300	-0.27968700	-1.55029500
C	-4.08887700	-0.31206400	-1.48964300
C	-4.76158500	-1.53449800	-1.43593500
C	-4.74974600	-4.06066600	-1.33145300
C	-4.95704400	-4.50627400	0.14572000
C	-3.60454700	-4.71916200	0.86229000
N	-5.82535900	-3.56901200	0.83680000
O	-2.05724000	0.95267200	-1.73769700
O	-3.23835000	-4.07477400	1.81306500
O	-2.811159100	-5.71295800	0.36849100
I	0.06483500	-1.80170400	0.28302600
H	-2.06997100	-3.60133300	-1.52364200
H	-5.84427600	-1.56050800	-1.37327200
H	-4.19179600	-4.82973700	-1.87978700
H	-5.74562000	-4.00488300	-1.78105100
H	-5.46537600	-5.48127200	0.12276200
H	-5.33596800	-2.68581400	0.96807300
H	-6.03330200	-3.91052200	1.77143500
H	-3.23343600	-6.15570800	-0.38207700
C	1.50596300	1.05998900	-3.92926700
C	0.22837000	0.63809000	-3.68651900
C	1.58962500	-0.84440700	-2.78934800
N	2.33866000	0.111153300	-3.36158400
H	3.35156700	0.15889800	-3.29149900
H	1.88868900	1.93574300	-4.42774900
H	-0.72285200	1.08759900	-3.91849700
H	1.97569800	-1.69570200	-2.24898100
N	0.30725400	-0.54810800	-2.98522200
I	-5.23100200	1.51534500	-1.48130800
C	-1.53155000	1.64105600	-0.67039800
C	-0.80676800	2.79297700	-0.98382100
C	-0.22557700	3.53941600	0.03473500
C	-0.33152500	3.15627400	1.38187600
C	-1.06556400	1.99146500	1.65512900
C	-1.68393900	1.24433800	0.65588400
O	0.29291800	3.90985100	2.32929200

I	0.85874800	5.31198000	-0.48412900	I	-4.90479400	-4.49689600	-0.47722900
I	-1.17966200	1.26673700	3.67542900	I	0.47642100	-1.78530900	0.71167300
H	-0.71299800	3.09118500	-2.02033300	H	-5.53112900	-1.67661200	0.75565700
H	-2.24129800	0.34973600	0.89766600	H	-1.75975000	0.18458100	1.61552300
H	0.08310600	3.57047500	3.21399500	H	-0.80115300	-3.88241600	-0.25433200
Te	2.38432600	-1.69289700	2.14090100	Te	4.19001600	0.07099100	-2.51699800
Te	4.30203500	-3.17839800	-0.84173700	Te	5.52700700	0.76211100	1.06667900

EP:

C	3.19253500	-4.32065200	-0.51758500
C	3.69188600	-3.37523000	0.41981000
C	4.07172000	-2.02527600	0.01447800
C	3.81667800	-1.71012200	-1.38170200
C	3.29535800	-2.67589500	-2.24200500
C	3.00296600	-3.99025500	-1.83185200
H	2.93976500	-5.31286800	-0.15390900
H	3.07803800	-2.40614700	-3.26935000
H	2.60736200	-4.70634000	-2.54504100
C	3.77366100	-3.80342400	1.76878800
C	4.22834700	-2.95501800	2.74510300
C	4.65329800	-1.66994200	2.37444500
C	4.61412100	-1.19472400	1.06547000
H	3.45562200	-4.81325500	2.01030700
H	4.27589700	-3.26423200	3.78442300
H	5.05512000	-1.03366700	3.15956700
H	5.47688900	0.95974200	-0.57181300
H	-2.69808700	1.82800800	3.10482000
C	-3.21074200	4.34508100	0.85928700
C	-2.70291700	3.65917100	1.96995900
C	-3.12098200	2.36256300	2.26220900
C	-4.03719300	1.71709200	1.43017200
C	-4.56174000	2.39889300	0.32454700
C	-4.16089800	3.70642100	0.04767400
C	-2.69847700	5.72058200	0.49267900
C	-1.57375700	5.68613800	-0.58796900
C	-0.39826900	4.83113900	-0.07909000
N	-2.09839900	5.22704900	-1.86129700
O	-4.45628200	0.43430900	1.73071900
O	-0.14059800	3.73130200	-0.51269900
O	0.34809000	5.34422400	0.93139100
I	2.09722200	1.76628400	-1.55231600
H	-1.95892800	4.12546400	2.60990100
H	-4.57434500	4.23123800	-0.80718300
H	-2.32880800	6.22654200	1.39262200
H	-3.50078600	6.33796400	0.07783500
H	-1.21435400	6.71616000	-0.72064500
H	-2.29501800	4.22927100	-1.81226600
H	-1.40259200	5.34137800	-2.59335300
H	0.03960100	6.22671500	1.18509800
C	2.00097700	0.72303500	3.43943700
C	0.73156900	0.65889300	3.96578700
C	0.55375400	1.74240800	2.11298900
N	1.86929900	1.42179400	2.25863700
H	2.61078400	1.61869900	1.59732800
H	2.95132700	0.34043800	3.77510900
H	0.41125800	0.18745000	4.88418000
H	0.18393700	2.28757200	1.25701200
N	-0.16404500	1.29914500	3.13353100
I	-5.98110500	1.44145600	-0.96033600
C	-3.72138400	-0.62915400	1.21574600
C	-4.44927000	-1.72163300	0.74567800
C	-3.771155200	-2.83436800	0.25640700
C	-2.36776500	-2.88418500	0.21746600
C	-1.67304700	-1.76502300	0.70743100
C	-2.32760400	-0.64272600	1.20898500
O	-1.76520000	-3.99470200	-0.28217200

IRD process of T4 using Te_S

ES:

C	2.61527200	-1.16550600	-3.05171500
C	3.77987900	-0.92615400	-2.27368500
C	3.91998400	0.28742700	-1.48445400
C	2.84560700	1.24948300	-1.60324500
C	1.72609400	0.94838500	-2.36642600
C	1.59042900	-0.25972500	-3.08042000
H	2.54568600	-2.09813700	-3.60314100
H	0.91982200	1.66808700	-2.43427300
H	0.68669200	-0.45414700	-3.64856900
C	4.79492500	-1.92121600	-2.29418300
C	5.95457700	-1.75662600	-1.57910600
C	6.10696100	-0.60847700	-0.78187800
C	5.12525800	0.37164800	-0.68418100
H	4.63598300	-2.80549400	-2.90571500
H	6.74440800	-2.50123200	-1.61200500
H	7.01359900	-0.49141600	-0.19599900
H	4.88165200	2.62337100	0.13221300
H	2.42097600	3.01336600	0.61931300
C	-5.28807100	1.08910200	0.40680800
C	-4.26266900	1.87231900	-0.13931200
C	-2.93521600	1.65053800	0.22283100
C	-2.60416400	0.64013500	1.13697300
C	-3.63590400	-0.12383500	1.69916000
C	-4.96484200	0.09394700	1.33912600
C	-6.72007200	1.27146500	-0.04507500
C	-7.08746000	0.37191000	-1.26483300
C	-6.22676100	0.77228900	-2.48138200
N	-6.96565700	-1.03077500	-0.91110200
O	-1.29943900	0.44719700	1.51661700
O	-5.32115400	0.10167500	-2.91020700
O	-6.50678300	1.98048400	-3.04691000
I	-1.37159100	2.85345300	-0.60222700
H	-4.49838900	2.64699700	-0.86167500
H	-5.75330600	-0.51347300	1.76923200
H	-6.89876400	2.32447000	-0.29171200
H	-7.40876200	1.00191300	0.76047200
H	-8.14025900	0.57064900	-1.50841700
H	-5.98162000	-1.28851800	-0.86715600
H	-7.37727600	-1.61556800	-1.63329700
H	-7.28425600	2.38976200	-2.63940200
C	1.85556600	1.12285700	4.29785600
C	2.68536000	1.63739600	3.32968800
C	0.711738700	2.41639100	2.90116200
N	0.60110800	1.63517100	4.01258400
H	-0.26123900	1.40110600	4.48256200
H	2.03121400	0.45949300	5.13038000
H	3.73973500	1.46075200	3.17613700
H	-0.12394300	2.90460200	2.43328800
N	1.96408600	2.44197600	2.47101500
I	-3.16897400	-1.63668300	3.13933400
C	-0.54688100	-0.52047000	0.85358500
C	-1.00724000	-1.21378300	-0.26307100

C	-0.18247400	-2.17541800	-0.84591200	C	-0.21928100	-2.16216500	-0.83562600
C	1.09577800	-2.46241500	-0.34313800	C	1.05488900	-2.46841700	-0.33173500
C	1.51825300	-1.73279700	0.78351200	C	1.46989800	-1.77402500	0.81919700
C	0.71632500	-0.76777800	1.38063900	C	0.66429400	-0.82349000	1.43594200
O	1.83962700	-3.41786200	-0.95306100	O	1.79596700	-3.41496300	-0.95743700
I	-0.89408900	-3.22326500	-2.56882800	I	-0.92314900	-3.16014000	-2.58955900
I	3.44669300	-2.12464600	1.63747200	I	3.39618100	-2.17691900	1.67101800
H	-1.98646100	-1.01064000	-0.67831000	H	-2.01614600	-0.98887200	-0.65682800
H	1.05071600	-0.21216800	2.24411900	H	0.99475100	-0.30885700	2.32575900
H	2.75400500	-3.38721500	-0.62828500	H	2.72910500	-3.33775000	-0.70069000
S	5.48549100	1.52219800	0.64276400	S	5.61143600	1.51065000	0.54007100
Te	2.79757200	3.33318500	-0.98276300	Te	2.82804300	3.30975300	-0.88251300

TS1:

C	2.57346200	-1.16994900	-3.04545300
C	3.73432600	-0.97152200	-2.25166700
C	3.92002300	0.24875800	-1.47785500
C	2.88186200	1.25332000	-1.60379600
C	1.76582200	0.98475700	-2.38692500
C	1.59309100	-0.21710400	-3.10069500
H	2.47059500	-2.10561300	-3.58635000
H	0.98964700	1.73471600	-2.47099300
H	0.69273600	-0.37384800	-3.68629900
C	4.69983400	-2.01545200	-2.24442700
C	5.86030500	-1.89529700	-1.52127800
C	6.06754400	-0.73598200	-0.75538200
C	5.13665700	0.29615300	-0.68943200
H	4.50527900	-2.89910100	-2.84688200
H	6.61192600	-2.67927200	-1.53142200
H	6.98138300	-0.64630600	-0.17520500
H	4.85992700	2.55794600	0.08494600
H	2.41575900	2.79630300	0.87589800
C	-5.28301500	1.16779400	0.37657100
C	-4.22404800	1.90888400	-0.16408800
C	-2.91023600	1.65438800	0.22520500
C	-2.62812400	0.65189300	1.16440100
C	-3.69189200	-0.07211600	1.71845500
C	-5.00742300	0.18074300	1.33247400
C	-6.69948700	1.38565300	-0.10735000
C	-7.07639400	0.46066800	-1.30510000
C	-6.16275100	0.77593000	-2.50766400
N	-7.03150600	-0.93284000	-0.89930900
O	-1.33634800	0.41992600	1.57470400
O	-5.27160000	0.05316200	-2.87793900
O	-6.37482200	1.97042700	-3.12892100
I	-1.29450400	2.79074500	-0.60324000
H	-4.42311500	2.67593100	-0.90546700
H	-5.82173900	-0.39441400	1.75867000
H	-6.83526200	2.43569800	-0.39108600
H	-7.41240300	1.16627700	0.69239600
H	-8.11150300	0.69946500	-1.58560500
H	-6.06257500	-1.23696000	-0.82493900
H	-7.45713100	-1.52248200	-1.60934000
H	-7.14978100	2.42386500	-2.76595600
C	2.05996300	1.26241000	4.13438600
C	2.84118400	1.61175400	3.06255400
C	0.85380800	2.42734000	2.67752500
N	0.80574400	1.79196300	3.87316600
H	-0.02620200	1.66271900	4.43174800
H	2.27000700	0.69319700	5.02617700
H	3.87327200	1.38021600	2.84475300
H	0.00822400	2.89520300	2.19883600
N	2.07337100	2.33702700	2.17513900
I	-3.29575600	-1.58092200	3.18428400
C	-0.58958000	-0.54798800	0.90201900
C	-1.04368000	-1.21087400	-0.23550300

INT1:

C	-2.54279600	-0.62508600	3.21482900
C	-3.66908700	-0.54895600	2.35477100
C	-3.83181300	0.55750500	1.41843500
C	-2.80789000	1.58855700	1.44349100
C	-1.73500000	1.44428600	2.31940200
C	-1.58298300	0.35140500	3.19159700
H	-2.45183500	-1.48132000	3.87601400
H	-0.97707400	2.21751800	2.34823200
H	-0.71197900	0.29313800	3.83734900
C	-4.62918300	-1.59480000	2.45346100
C	-5.76197800	-1.58730500	1.67753300
C	-5.94820900	-0.54226100	0.75839700
C	-5.02640000	0.48852500	0.59764400
H	-4.45832900	-2.38092700	3.18517500
H	-6.50824000	-2.37173900	1.76531800
H	-6.84327600	-0.53798700	0.14277000
H	-4.64255000	2.61728900	-0.47553200
C	5.19496100	1.23971000	-0.51295700
C	4.05966700	1.98520900	-0.16711900
C	2.78782300	1.56873800	-0.55554700
C	2.63025000	0.39058300	-1.29856500
C	3.76554500	-0.34614400	-1.65641200
C	5.03922800	0.07281700	-1.27365200
C	6.56485800	1.65253900	-0.02163900
C	6.94627400	0.98618900	1.33558400
C	5.94567500	1.42230500	2.42644700
N	7.03440300	-0.45543400	1.18258000
O	1.38029900	-0.01465000	-1.71971500
O	5.10121700	0.69561400	2.88737100
O	6.02336200	2.72079700	2.83261100
I	1.03234400	2.70958400	-0.01717800
H	4.16728400	2.88948400	0.42378700
H	5.91163300	-0.50971100	-1.54777900
H	6.60797400	2.74354900	0.07518500
H	7.33335300	1.35587300	-0.74101000
H	7.94213900	1.35938500	1.61161600
H	6.09764600	-0.84950600	1.11905400
H	7.45847100	-0.87293900	2.00656000
H	6.77305500	3.17535100	2.42121400
C	-2.24855200	0.42867500	-4.23321100
C	-2.91914400	0.94472800	-3.15977700
C	-0.87293000	1.78818500	-3.12748500
N	-0.97266300	0.97427900	-4.19220100
H	-0.20858000	0.75337000	-4.81646000
H	-2.55107500	-0.27273600	-4.99367200
H	-3.91961400	0.78676700	-2.78128100
H	0.00874000	2.32063200	-2.80955600
N	-2.04338100	1.78170800	-2.50094800
I	3.546334400	-2.14587400	-2.79858200
C	0.62044400	-0.81754400	-0.87093000
C	1.05534500	-1.23823800	0.38319800
C	0.21104800	-2.03135700	1.15958400

C	-1.06747400	-2.41448900	0.72036800	C	1.35013300	2.99871000	0.24554500
C	-1.45856100	-1.97704000	-0.55785100	C	1.13097100	2.56097700	1.56192200
C	-0.63001800	-1.19001000	-1.35070700	C	0.01229300	1.74188100	1.78100600
O	-1.82841600	-3.20191000	1.51944400	C	-0.86345400	1.38202000	0.75995800
I	0.89606200	-2.66605200	3.08045000	O	2.01293500	2.93049700	2.53192000
I	-3.37773600	-2.52908500	-1.33977300	I	3.01800800	4.27079000	-0.18728200
H	2.02744300	-0.94583200	0.75958900	I	-0.32635300	0.92250800	3.73908800
H	-0.93697900	-0.88193300	-2.33904000	H	0.68863700	2.98464000	-1.81011900
H	-2.77183400	-3.07059100	1.32946000	H	-1.71547000	0.74606700	0.95765500
S	-5.51629700	1.58007800	-0.73880600	H	1.70578100	2.61375400	3.39637100
Te	-2.69322800	3.49650900	0.39247600	Te	1.82046800	-3.04883200	1.70583700
H	-2.25380000	2.34578700	-1.60259000	S	2.97088700	-4.37367000	-1.44319600

TS2:

C	4.64143600	0.60879700	-0.12065500
C	4.63859600	-0.56951500	-0.91437900
C	3.84664300	-1.73223900	-0.53458700
C	3.10408900	-1.61997500	0.70683100
C	3.15668600	-0.43595100	1.43539200
C	3.91390100	0.68192300	1.03632500
H	5.22923300	1.45786600	-0.45719700
H	2.58072100	-0.35881200	2.35135500
H	3.89581500	1.58567300	1.63531300
C	5.43993700	-0.55733200	-2.08830600
C	5.50027800	-1.65843800	-2.91020300
C	4.73018900	-2.79067700	-2.58707600
C	3.90702200	-2.84937400	-1.46088200
H	6.01609500	0.33643200	-2.31033300
H	6.13367300	-1.66833200	-3.79258200
H	4.77419400	-3.65769900	-3.24039300
H	2.42796300	-4.25660900	-0.18980700
H	-0.80404500	-0.85692700	-2.55394000
C	-4.64627600	-1.12568800	-1.49224400
C	-3.34029600	-1.61557200	-1.64519400
C	-2.21304900	-0.77928200	-1.64815700
C	-2.44201000	0.59433600	-1.48899300
C	-3.73091300	1.11202900	-1.34452800
C	-4.83384300	0.25625400	-1.33906000
C	-5.83129600	-2.06434300	-1.42125900
C	-6.16794700	-2.51494900	0.03051800
C	-4.99016500	-3.29639700	0.65431000
N	-6.58072100	-1.37407900	0.82944300
O	-1.37060100	1.48414700	-1.62325200
O	-4.36138900	-2.91587800	1.60985200
O	-4.67701800	-4.48533100	0.06358400
I	-0.44678000	-2.07068000	0.04384200
H	-3.19726900	-2.69068900	-1.74198400
H	-5.83466400	0.65488100	-1.21227200
H	-5.63978600	-2.94263900	-2.04984200
H	-6.73068800	-1.57896200	-1.81191700
H	-7.01997700	-3.20728600	-0.03277800
H	-5.77814900	-0.77129200	1.00048800
H	-6.89280200	-1.68460700	1.74572800
H	-5.26967800	-4.67306400	-0.67858200
C	1.79066100	0.46062600	-4.09984900
C	0.45745900	0.49490600	-3.79832100
C	1.25923900	-1.39691000	3.00342200
N	2.26812100	-0.73641200	-3.59484100
H	3.23579100	-1.04709300	-3.58083600
H	2.42984100	1.16829700	-4.60255200
H	-0.28735600	1.25411400	-3.97075800
H	1.34767600	-2.34928300	-2.50301800
N	0.15133200	-0.67021000	-3.12497900
I	-4.04837600	3.23329400	-1.13283700
C	-0.59705800	1.81509200	-0.53666600
C	0.50826600	2.62803400	-0.79696000

EP:

C	3.77664500	-4.03035400	-0.46870100
C	4.23970400	-3.13755200	0.53657500
C	4.52378200	-1.74227900	0.23169300
C	4.29769000	-1.34330000	-1.14547600
C	3.811151300	-2.26133500	-2.07444300
C	3.55684300	-3.60852600	-1.75269000
H	3.58118100	-5.06060300	-0.18432900
H	3.61350700	-1.93210600	-3.08835000
H	3.18421900	-4.28631900	-2.51407800
C	4.37959800	-3.66040800	1.84759200
C	4.80577800	-2.86094400	2.87852400
C	5.11084900	-1.51768900	2.61300500
C	4.98151400	-0.94660900	1.34952500
H	4.13456000	-4.70467500	2.01676600
H	4.91407200	-3.25196900	3.88517900
H	5.47385400	-0.89494800	3.42583300
H	5.60401300	1.01557600	0.09617100
H	-2.53801500	1.65038800	3.11646700
C	-3.09535300	4.20718300	0.92811200
C	-2.59259600	3.51191400	2.03514900
C	-2.95783600	2.18883000	2.27487100
C	-3.81172800	1.52666300	1.39161000
C	-4.33064800	2.21633500	0.28839400
C	-3.98662200	3.55005000	0.06566400
C	-2.63642200	5.61571400	0.62059900
C	-1.48394200	5.66864600	-0.42945600
C	-0.28439000	4.84597400	0.07697600
N	-1.95623300	5.23596800	-1.73239900
O	-4.17647200	0.21574200	1.63681600
O	0.03380000	3.77732400	-0.39365700
O	0.41378600	5.34995800	1.12516200
I	2.50806100	2.07828300	-1.34592200
H	-1.89259800	3.99158500	2.71365700
H	-4.39876300	4.08130800	-0.78580000
H	-2.31384700	6.10659200	1.54667700
H	-3.45440000	6.21099000	0.20403700
H	-1.16596000	6.71712100	-0.51488600
H	-2.10608300	4.22895500	-1.72544700
H	-1.24904100	5.41038100	-2.44134500
H	0.05992400	6.20662000	1.40665300
C	2.17864500	0.72386700	3.58435600
C	0.89807400	0.64897300	4.08179700
C	0.75958900	1.76685900	2.24618600
N	2.07210900	1.44648500	2.41546800
H	2.82781600	1.64104000	1.76946900
H	3.12196200	0.33438200	3.93285600
H	0.55848900	0.16039100	4.98419400
H	0.40699400	2.32497400	1.39118600
N	0.01965200	1.30324600	3.24195900
I	-5.65119400	1.22848300	-1.07641200
C	-3.36653200	-0.79276500	1.12515800
C	-4.01602600	-1.91528500	0.61241400

C	-3.26145300	-2.97724500	0.12266100	H	3.80323700	-1.95896100	-2.40998600
C	-1.85652600	-2.94622600	0.12509700	H	-0.08212600	-3.37843800	-1.73399700
C	-1.24253200	-1.79964700	0.65677600	N	1.97435400	-2.79255700	-1.65967900
C	-1.97469600	-0.72699400	1.15918900	I	-3.39027100	0.94114800	-3.39858200
O	-1.17589600	-4.00912200	-0.37797600	C	-0.66222400	0.31839200	-0.98547300
I	-4.27493400	-4.68630800	-0.67652200	C	-1.13232300	1.20491700	-0.01981300
I	0.90267400	-1.69332600	0.72761600	C	-0.30774400	2.24999100	0.39549900
H	-5.09849800	-1.93209800	0.59030100	C	0.98009600	2.43513000	-0.13003500
H	-1.46635800	0.12369000	1.59431000	C	1.41349200	1.50998800	-1.09808900
H	-0.22134300	-3.84280200	-0.31583300	C	0.61112100	0.45939900	-1.52754200
Te	4.76244500	0.49788200	-2.14073200	O	1.71824000	3.48654600	0.30419200
S	5.36531500	0.80496600	1.41282300	I	-1.04146700	3.59679800	1.88542100
				I	3.36085300	1.72110500	-1.97319200
				H	-2.12002700	1.08694900	0.40785800
				H	0.95840800	-0.23951900	-2.27452600
				H	2.64286600	3.38524600	0.02613000

IRD process of T4 using Se_Se

ES:

C	2.39161900	1.74779100	2.87757300
C	3.55380300	1.36694800	2.15404900
C	3.73981000	0.00244800	1.68242000
C	2.66931800	-0.91904100	2.00309600
C	1.56024700	-0.48689300	2.71367000
C	1.40393500	0.84217400	3.15235100
H	2.29580900	2.78369200	3.18739300
H	0.77633600	-1.19901300	2.93813300
H	0.50703300	1.13449400	3.68849900
C	4.52662500	2.37530700	1.91917400
C	5.69187100	2.08499500	1.25485300
C	5.90114700	0.77535400	0.79311200
C	4.97119300	-0.24362300	0.96540200
H	4.33201500	3.37547700	2.29691900
H	6.44763200	2.84633100	1.08570300
H	6.82883700	0.55195400	0.27404800
Se	2.59107300	-2.84961400	1.69260400
Se	5.57845600	-1.84981500	0.07677200
H	4.67775900	-2.78199600	0.78436100
H	2.32924600	-2.80806400	0.21507700
C	-5.35262600	-1.31387600	-0.16344300
C	-4.28558500	-1.93197100	0.50183400
C	-2.97425500	-1.73008900	0.07557700
C	-2.70172900	-0.90764900	-1.02741000
C	-3.77317000	-0.30372700	-1.69869400
C	-5.08648100	-0.50362500	-1.27528000
C	-6.76920200	-1.47015900	0.34409800
C	-7.16505500	-0.37296600	1.37880700
C	-6.26934600	-0.49081400	2.62969600
N	-7.12141000	0.94028200	0.76131000
O	-1.41467700	-0.74604600	-1.47664600
O	-5.39752400	0.29492600	2.90567500
O	-6.47678900	-1.58275100	3.41906100
I	-1.34822200	-2.66390500	1.10115900
H	-4.47645300	-2.56047300	1.36562500
H	-5.90629500	-0.02152100	-1.79601400
H	-6.89441800	-2.46417800	0.78887700
H	-7.47955400	-1.38944500	-0.48333800
H	-8.20277600	-0.57138300	1.68071700
H	-6.15297700	1.22830200	0.63530300
H	-7.54353100	1.63368100	1.37283400
H	-7.23519400	-2.10119300	3.11246800
C	2.07447000	-2.08934000	-3.79857100
C	2.78177900	-2.23304400	-2.62913000
C	0.79627700	-2.98527900	-2.22207900
N	0.80834100	-2.57770700	-3.52271400
H	0.01652600	-2.57724800	-4.14893100
H	2.34096900	-1.69286400	-4.76589000

TS1:

C	3.58705700	1.10915600	2.82852500
C	4.65005100	0.77160300	1.94816600
C	4.69397500	-0.52836500	1.29788200
C	3.52641100	-1.36238100	1.47224000
C	2.53422000	-0.99465200	2.36817200
C	2.56715000	0.22400400	3.07504400
H	3.60552100	2.08480100	3.30674400
H	1.67743600	-1.64829600	2.49248600
H	1.76385000	0.47233000	3.76253300
C	5.67054900	1.73649900	1.73089200
C	6.73616300	1.45862700	0.91092700
C	6.85173400	0.17198400	0.35154400
C	5.90113400	-0.81844600	0.55814200
H	5.58262900	2.69934900	2.22669800
H	7.50820100	2.19964900	0.72477600
H	7.73895300	-0.06675600	-0.22875400
Se	3.07884900	-2.96608600	0.46144000
Se	6.55329600	-2.53968600	-0.03917100
H	5.26383400	-3.26405800	0.11814800
H	3.18904300	-2.26527400	-1.02598300
C	-4.80242600	-2.52823000	-0.69571000
C	-3.47183600	-2.81023700	-0.36002000
C	-2.45167900	-1.90392500	-0.64880000
C	-2.74615900	-0.68470200	-1.27711100
C	-4.07470800	-0.41340000	-1.63127500
C	-5.09283200	-1.32095800	-1.34570400
C	-5.91175400	-3.50815500	-0.37200300
C	-6.62583400	-3.25403900	0.99079700
C	-5.65344800	-3.46857100	2.17007300
N	-7.25727000	-1.94614800	0.99817800
O	-1.73977300	0.18601500	-1.63405200
O	-5.22613100	-2.57597500	2.85993600
O	-5.26584700	-4.75426800	2.40495100
I	-0.41857700	-2.40398200	-0.15686400
H	-3.22413400	-3.74781800	0.12829800
H	-6.11496100	-1.09429800	-1.62703000
H	-5.51157300	-4.52873500	-0.39425300
H	-6.68989500	-3.44969800	-1.13831700
H	-7.42108400	-4.00801800	1.07349100
H	-6.55228000	-1.22395100	1.13054400
H	-7.89470000	-1.86508500	1.78574700
H	-5.71761600	-5.37193800	1.81149500
C	4.03435000	-0.85286600	-4.34552600
C	4.39715700	-1.38247500	-3.13452600
C	2.22534800	-1.26775200	-3.12805300
N	2.65169700	-0.78642900	-4.32417100
H	2.05917500	-0.44255400	-5.06638700
H	4.61318300	-0.52390800	-5.19427700

H	5.37883400	-1.59987300	-2.73818600	H	4.57847800	-1.57983200	-3.51833600
H	1.18763200	-1.33529200	-2.83317000	H	1.67624900	-0.08081400	-0.84655000
N	3.26146800	-1.63300300	-2.39380700	N	2.96827800	-1.20217800	-2.14247400
I	-4.56135400	1.39727300	-2.66379400	I	-4.09919300	2.20343400	-2.31970200
C	-1.32949500	1.17568000	-0.75182200	C	-0.95396500	1.15815900	-0.74533200
C	-1.80674900	1.30060400	0.55253900	C	0.00458700	2.11416300	-1.08549300
C	-1.31030300	2.32091000	1.36288500	C	0.59685800	2.87420700	-0.08225100
C	-0.34513300	3.23053900	0.90466900	C	0.23874800	2.73047100	1.26846200
C	0.09973800	3.07466700	-0.41839600	C	-0.75643800	1.78399300	1.56413700
C	-0.37771400	2.06564000	-1.24751800	C	-1.34644500	0.99094100	0.58176700
O	0.09780200	4.19488900	1.74987300	O	0.86412700	3.50310700	2.19234900
I	-2.03336000	2.48954900	3.36550200	I	2.07486100	4.32792500	-0.62919500
I	1.56971700	4.43763700	-1.19886400	I	-1.41875300	1.54553100	3.59201100
H	-2.54339900	0.60896500	0.94083900	H	0.25581400	2.25083200	-2.13060400
H	-0.02852700	1.95755800	-2.26698300	H	-2.09689300	0.25621100	0.84497300
H	0.77747100	4.73308300	1.31424500	H	0.49243700	3.33795900	3.07372300

INT1:

C	2.10236500	0.10286000	2.71118000
C	3.19273000	0.18177500	1.80640100
C	3.63356600	-0.99366000	1.07795300
C	2.77618800	-2.16100300	1.14373300
C	1.75452200	-2.19045000	2.08918500
C	1.42959100	-1.08200500	2.89216500
H	1.82161300	0.99578300	3.26083600
H	1.14353200	-3.08407600	2.15696100
H	0.60992000	-1.15211100	3.60097000
C	3.83610200	1.43848000	1.62710200
C	4.93461500	1.55232800	0.80991300
C	5.46331200	0.39672200	0.19917400
C	4.87170700	-0.85217900	0.34251300
H	3.43556700	2.30354900	2.14796500
H	5.41923700	2.51335600	0.66093500
H	6.37900200	0.47951900	-0.37974900
Se	2.73523600	-3.63979600	-0.11063900
Se	5.96924600	-2.28607100	-0.33254000
H	4.82148700	-3.27216900	-0.38197700
H	2.81690900	-2.16456500	-1.69569000
C	-4.84474100	-1.96065300	-1.10501900
C	-3.55936300	-2.49457600	-0.95473800
C	-2.42474600	-1.71442000	-1.17940800
C	-2.56945500	-0.37471600	-1.55831600
C	-3.85396500	0.15666300	-1.73223100
C	-4.98534700	-0.62788100	-1.51638100
C	-6.06250300	-2.78329300	-0.74832300
C	-6.54416700	-2.53684300	0.71481300
C	-5.40448300	-2.87445900	1.69963600
N	-7.04098000	-1.17942300	0.86453200
O	-1.45824700	0.41347200	-1.79168600
O	-4.78050600	-2.04121000	2.30982300
O	-5.08743100	-4.19185000	1.82959300
I	-0.46543200	-2.58014400	-0.87589500
H	-3.43831800	-3.52495300	-0.63455000
H	-5.97595700	-0.20712600	-1.64747700
H	-5.84349400	-3.84751800	-0.89332900
H	-6.90485000	-2.53032800	-1.39855100
H	-7.37951800	-3.22513200	0.90288200
H	-6.25619000	-0.53174200	0.90254900
H	-7.52902700	-1.07915400	1.75048500
H	-5.68758300	-4.75185800	1.31561300
C	4.04298100	0.52063800	-3.01171700
C	3.97900000	-0.84354800	-3.00971700
C	2.44693700	-0.10547300	-1.59854800
N	3.06749500	0.95605900	-2.12824500
H	2.91824100	1.91422600	-1.82707400
H	4.68611300	1.20511500	-3.53983400

TS2:

C	4.53370900	1.01866400	0.11114200
C	4.63181200	-0.24364000	-0.53435300
C	3.88531200	-1.39769100	-0.05422600
C	3.06209400	-1.16909300	1.11825900
C	3.02643500	0.08590900	1.71400900
C	3.75008800	1.18687900	1.22174400
H	5.09032100	1.85534000	-0.30087800
H	2.38920600	0.22470600	2.58067200
H	3.65788200	2.15279000	1.70555800
C	5.49099900	-0.32768700	-1.66315900
C	5.65433600	-1.51659300	-2.33542700
C	4.93462100	-2.64625300	-1.90307300
C	4.06383400	-2.61799900	-0.81400200
H	6.03079500	0.56408000	-1.96878800
H	6.33179200	-1.59682000	-3.18087700
H	5.06727400	-3.58229600	-2.43859600
Se	1.89474100	-2.41485200	2.04573100
Se	3.20589400	-4.32987000	-0.58237200
H	2.48782100	-3.92735600	0.67282500
H	-0.64800400	-1.15288500	-2.34650400
C	-4.44317600	-1.72744200	-1.36553200
C	-3.08113500	-2.06355500	-1.40245300
C	-2.06278200	-1.10049700	-1.47438900
C	-2.46330700	0.24275600	-1.51080500
C	-3.81060700	0.60788100	-1.48210100
C	-4.80224800	-0.37206300	-1.40352100
C	-5.50882300	-2.79206000	-1.22014600
C	-5.86232300	-3.10552700	0.26353600
C	-4.63318500	-3.65983000	1.01706400
N	-6.44230500	-1.93612800	0.90044400
O	-1.50334900	1.23832800	-1.72667400
O	-4.09067300	-3.09050100	1.93069200
O	-4.16403900	-4.86913700	0.59478200
I	-0.21861800	-1.91639700	0.38764000
H	-2.80426500	-3.11577500	-1.35506800
H	-5.84877000	-0.08828000	-1.36880100
H	-5.18122800	-3.70784700	-1.72730900
H	-6.43889800	-2.47328700	-1.70011900
H	-6.62491700	-3.89775300	0.25615900
H	-5.72435400	-1.22457300	1.02263600
H	-6.76180500	-2.17041000	1.83661700
H	-4.70292400	-5.21942500	-0.12928200
C	1.92225100	0.19786100	-3.90796300
C	0.57874700	0.17568000	-3.65507600
C	1.44873300	-1.62038300	-2.72263200
N	2.44278800	-0.94051000	-3.31742400
H	3.42540600	-1.18847600	-3.23867200
H	2.54224500	0.91057900	-4.42727600

H	-0.19902000	0.88056300	-3.89811300	H	0.34224500	-0.40099100	4.55884500
H	1.57293200	-2.53292200	-2.15776100	H	0.91291600	2.31557900	1.41122100
N	0.30851400	-0.96449700	-2.92528200	N	0.18575900	1.10284600	3.02694100
I	-4.38684400	2.68218000	-1.56499100	I	-5.64054700	1.59705600	-0.90869000
C	-0.79201500	1.76369500	-0.67443400	C	-3.43647500	-0.53379900	1.18781100
C	0.26910100	2.60625900	-1.01224200	C	-4.23222200	-1.60454500	0.78293700
C	1.04622100	3.17246000	-0.00805800	C	-3.63143700	-2.72985600	0.22715200
C	0.80330300	2.90681400	1.34946700	C	-2.23923000	-2.81239800	0.05473600
C	-0.27042800	2.05307500	1.64758200	C	-1.47420500	-1.71428900	0.48401400
C	-1.08207200	1.49774100	0.66174500	C	-2.04971000	-0.58103700	1.05357600
O	1.62080300	3.46660900	2.28395900	O	-1.71484500	-3.93209800	-0.50855400
I	2.64980000	4.47718200	-0.56573900	I	-4.87096000	-4.35718400	-0.40660600
I	-0.64345900	1.50610900	3.69286800	I	0.66552800	-1.78397800	0.27720400
H	0.46853500	2.80970100	-2.05666400	H	-5.30699900	-1.53218000	0.89270700
H	-1.89882800	0.83788600	0.92100200	H	-1.42773600	0.22762800	1.41840000
H	1.29872600	3.25542800	3.17480900	H	-0.74986100	-3.84420000	-0.56881100

EP:

C	3.40545500	-4.01987700	-1.22179000
C	3.93801100	-3.31250800	-0.10835200
C	4.39621200	-1.93742600	-0.23705500
C	4.24286900	-1.35842500	-1.55845100
C	3.69508900	-2.09553900	-2.60334300
C	3.28583300	-3.43314900	-2.45415800
H	3.08020000	-5.04455200	-1.06458200
H	3.57231200	-1.61338100	-3.56659700
H	2.86863900	-3.97212100	-3.29852000
C	3.99310900	-4.00334900	1.12885900
C	4.49647600	-3.39130300	2.24952900
C	4.97024800	-2.07455300	2.14711500
C	4.93544400	-1.34519000	0.96287800
H	3.62439300	-5.02385000	1.16927500
H	4.54018100	-3.91017900	3.20192300
H	5.39137100	-1.60860900	3.03417900
Se	4.76677900	0.39589000	-2.17224900
Se	5.68560100	0.41500400	1.25232200
H	5.68722500	0.82175900	-0.16650700
H	-2.26560100	1.88283300	3.08850400
C	-2.71667500	4.39800500	0.82730200
C	-2.22191400	3.70697300	1.94068500
C	-2.68575300	2.43132100	2.25379200
C	-3.64053600	1.81480900	1.44403000
C	-4.15716800	2.50443200	0.33962500
C	-3.70503600	3.78984700	0.03861600
C	-2.14696800	5.74154200	0.42931000
C	-1.01133700	5.62959900	-0.63426400
C	0.13444400	4.76200300	-0.08006600
N	-1.53667400	5.13983200	-1.89510500
O	-4.09288600	0.54804000	1.76575400
O	0.37669000	3.64481100	-0.47813200
O	0.87732600	5.28756900	0.92610200
I	2.74401300	1.86280000	-1.39899100
H	-1.44996300	4.15177600	2.562266800
H	-4.10833900	4.32026100	-0.81763400
H	-1.76958600	6.26004300	1.31891500
H	-2.91922100	6.37665600	-0.01461400
H	-0.61694900	6.64182200	-0.80152800
H	-1.78895900	4.15753100	-1.80614100
H	-0.82475700	5.18527600	-2.61904200
H	0.58677500	6.18433900	1.14929900
C	2.15610400	0.04985000	3.37244300
C	0.84675800	0.15422600	3.78063700
C	1.08365300	1.56653500	2.17114300
N	2.29103600	0.96045300	2.34676300
H	3.13592800	1.12437700	1.80952700
H	2.97169900	-0.58086300	3.68763100

IRD process of T4 using S_Te

ES:

C	-2.21041800	2.94549000	-1.87938200
C	-3.42136300	2.32146100	-1.47521000
C	-3.61776000	0.88782100	-1.61097500
C	-2.51486400	0.15570900	-2.19772400
C	-1.35227300	0.82004300	-2.56218800
C	-1.18348900	2.20897400	-2.40656000
H	-2.11132600	4.01802900	-1.74225000
H	-0.54523800	0.24142500	-2.99272700
H	-0.24919300	2.67834400	-2.69688000
C	-4.44028300	3.15737900	-0.94275200
C	-5.65325600	2.63915300	-0.57139800
C	-5.86733600	1.25033200	-0.69044300
C	-4.89126500	0.37739900	-1.15628000
H	-4.23809200	4.22198900	-0.85709200
H	-6.44402000	3.27705000	-0.18756100
H	-6.83159700	0.85467800	-0.38950500
H	-5.33860600	-2.24659800	-2.30094700
H	-2.47900000	-2.21040600	-1.54064000
C	5.46289600	-1.31097500	-0.21577400
C	4.54699200	-1.47931700	-1.26232400
C	3.17738000	-1.49402200	-1.00509400
C	2.69239500	-1.33653600	0.30070400
C	3.61484600	-1.20536500	1.34809300
C	4.98563400	-1.18793000	1.09644800
C	6.94455100	-1.20541700	-0.50082300
C	7.40906700	0.26484100	-0.73538700
C	6.70388800	0.83562400	-1.98334500
N	7.19268300	1.05857400	0.46093600
O	1.34335800	-1.38189800	0.54698000
O	5.81927900	1.65359000	-1.93639500
O	7.09713200	0.32558700	-3.18461800
I	1.78372800	-1.77707300	-2.59823000
H	4.90150300	-1.58230600	-2.28268200
H	5.68855800	-1.07021500	1.91362100
H	7.19826200	-1.81929300	-1.37275100
H	7.52238800	-1.58418100	0.34680800
H	8.48947800	0.23556300	-0.93275300
H	6.20102700	1.26762500	0.55945900
H	7.66282300	1.95608800	0.38112100
H	7.84597900	-0.28019300	-3.08322700
C	-1.52167200	-3.71792500	2.24716600
C	-2.52215600	-3.45768200	1.33976700
C	-0.70278700	-3.59886500	0.19113300
N	-0.36473800	-3.81240900	1.49496100
H	0.57540000	-3.89730800	1.85295900
H	-1.52332200	-3.83758800	3.31950700

H	-3.57509800	-3.30269600	1.52156900	H	-3.98520200	-0.71323700	2.35503700
H	0.02432800	-3.56589000	-0.60595200	H	-0.07071800	-2.23140900	2.63996800
N	-1.99909100	-3.38656300	0.06448800	N	-2.07871800	-1.67339400	2.14630600
I	2.90858800	-1.06073000	3.36383000	I	3.60237700	1.94832400	2.86393200
C	0.65106700	-0.18053800	0.69974400	C	0.81811500	0.68133700	0.82708500
C	1.19163000	1.05319300	0.34613500	C	1.28816900	1.03554100	-0.43452900
C	0.43126500	2.20464500	0.54470600	C	0.52722700	1.90030900	-1.22004600
C	-0.86247700	2.15532100	1.08599300	C	-0.70497700	2.41330800	-0.78272000
C	-1.36756700	0.88551800	1.42067800	C	-1.13014700	2.04355900	0.50689000
C	-0.63017400	-0.27777800	1.23240000	C	-0.38188800	1.19047100	1.31088000
O	-1.54081700	3.31577600	1.26186500	O	-1.39272600	3.24820400	-1.59903300
I	1.26078900	4.09024300	-0.02533500	I	1.27495700	2.44413300	-3.14627800
I	-3.32101100	0.71723100	2.29321900	I	-2.96304200	2.82493600	1.30035000
H	2.18643100	1.12125300	-0.07675500	H	2.22456400	0.64116100	-0.80836600
H	-1.03264700	-1.24287800	1.50454900	H	-0.71186200	0.93269200	2.30673200
H	-2.46242400	3.13139600	1.50370300	H	-2.33177300	3.26218800	-1.35211200
Te	-5.50571600	-1.65915900	-0.77557800	S	-2.57042500	-3.08328400	-0.51446100
S	-2.53360800	-1.56657000	-2.74221200	Te	-5.74197700	-2.20050100	0.20111500

TS1:

C -2.15629100 0.57026500 -3.27709700
C -3.29143100 0.55893400 -2.42288200
C -3.57635600 -0.57985100 -1.56727500
C -2.59654200 -1.64337500 -1.60388900
C -1.52163300 -1.59892900 -2.47906600
C -1.29480200 -0.49606800 -3.32418000
H -1.97340400 1.45396500 -3.88066700
H -0.82049200 -2.42587600 -2.49202100
H -0.42818700 -0.48377700 -3.97750300
C -4.15048600 1.69111200 -2.43321900
C -5.26451400 1.72706400 -1.62800000
C -5.57947100 0.61441000 -0.82599300
C -4.80676200 -0.54523300 -0.80471500
H -3.91947000 2.51032900 -3.10996400
H -5.91916200 2.59464600 -1.62463700
H -6.49061900 0.64573000 -0.23582300
H -4.05084400 -2.99438000 -0.14091600
H -2.25233100 -2.30009900 0.94717500
C 5.37408400 -1.44836600 0.69521800
C 4.26213900 -2.19733600 0.28908700
C 2.97226400 -1.77333500 0.60176800
C 2.76513500 -0.59325100 1.33043700
C 3.88082800 0.14652400 1.74456600
C 5.17326000 -0.27464300 1.43366400
C 6.76993500 -1.86648700 0.28933600
C 7.20990200 -1.25348300 -1.07580500
C 6.28295800 -1.77199800 -2.19497700
N 7.24949800 0.19508400 -0.98690200
O 1.49431600 -0.19630000 1.67613300
O 5.43428300 -1.09942100 -2.72522900
O 6.42631100 -3.08323800 -2.53825700
I 1.28456700 -2.911115000 -0.05994600
H 4.40218900 -3.10417900 -0.29006700
H 6.02852700 0.31199700 1.74988400
H 6.82888500 -2.95999700 0.24198000
H 7.49789100 -1.52969300 1.03250600
H 8.22922800 -1.61007600 -1.27769900
H 6.30083600 0.56477600 -0.99618800
H 7.71313000 0.58828500 -1.80139300
H 7.17436600 -3.48981700 -2.07654700
C -2.45936800 -0.44558300 3.96276100
C -3.00979100 -0.88389400 2.78763600
C -0.98837400 -1.72661700 2.89440700
N -1.18476800 -0.99103400 4.01219100
H -0.49713500 -0.83965700 4.73656000
H -2.84498100 0.18922600 4.74419700

INT1:

C -2.15122300 -0.04084500 -3.27335100
C -3.24122100 0.08779300 -2.37193900
C -3.52769600 -0.93814400 -1.38209600
C -2.58805500 -2.03980100 -1.33655400
C -1.56392800 -2.13815600 -2.27059600
C -1.33809100 -1.14601200 -3.24196600
H -1.96484700 0.76425000 -3.97757300
H -0.89984800 -2.99519800 -2.22767200
H -0.50783200 -1.24571300 -3.93433300
C -4.05078000 1.25228100 -2.46607000
C -5.10704200 1.43780900 -1.60673800
C -5.42589300 0.43516600 -0.67189100
C -4.72056000 -0.76551700 -0.57292700
H -3.82690300 1.97514900 -3.24713000
H -5.71890500 2.33453600 -1.66279700
H -6.30438400 0.57443700 -0.04858400
H -3.95260800 -3.20991100 0.34578400
C 5.28709500 -1.42582500 0.99988700
C 4.15148200 -2.19214700 0.70679500
C 2.87488600 -1.67600700 0.92084200
C 2.70785000 -0.38189300 1.43284700
C 3.84521100 0.37551900 1.74015700
C 5.12403400 -0.13836500 1.52920700
C 6.66997600 -1.95123900 0.68427700
C 7.14760100 -1.56166100 -0.74863300
C 6.20445000 -2.19312400 -1.79362200
N 7.25411600 -0.11855600 -0.86951100
O 1.44778700 0.11829000 1.67933300
O 5.39149800 -1.56516400 -2.42503700
O 6.28775700 -3.54487700 -1.94357900
I 1.14291400 -2.83754900 0.43048500
H 4.26277900 -3.18734100 0.28870800
H 5.99789000 0.46143000 1.75808500
H 6.68645100 -3.04121600 0.79867500
H 7.40274900 -1.53577300 1.38154700
H 8.15060200 -1.98918800 -0.88323700
H 6.32442000 0.28666900 -0.96081500
H 7.75410000 0.13023900 -1.71864400
H 7.01479900 -3.91451900 -1.42129100
C -2.63490400 0.43034300 3.67025000
C -3.14958700 -0.22493500 2.58750100
C -1.16250400 -1.10830300 3.01608000
N -1.39453900 -0.14326500 3.92120000
H -0.74139800 0.13610900 4.63997500
H -3.02803100 1.23667500 4.26713500
H -4.08802500 -0.13002700 2.06125800

H	-0.26805700	-1.70354300	2.93066300	H	-0.40021400	0.57425900	-4.01709400
N	-2.21594500	-1.16767900	2.21006100	H	1.99413600	-2.18997700	-1.91557100
I	3.61998900	2.34675500	2.54278900	N	0.45010100	-1.01920000	-2.85402900
C	0.81651800	0.85338700	0.67518600	I	-4.77163000	1.86797300	-1.68834700
C	1.27111200	0.90240000	-0.63972300	C	-1.10097100	1.64151400	-0.73144100
C	0.55304900	1.64550300	-1.57556400	C	-0.16152500	2.60571100	-1.10079600
C	-0.62566200	2.33143600	-1.23478900	C	0.46313500	3.36859000	-0.12062300
C	-1.03100400	2.27715000	0.11105400	C	0.18359100	3.18759300	1.24379300
C	-0.32263300	1.54982000	1.06204200	C	-0.75862000	2.20054600	1.57418500
O	-1.27794900	3.02679100	-2.19705500	C	-1.41747100	1.44199400	0.61003100
I	1.29206600	1.74152700	-3.57628800	O	0.84298100	3.95365700	2.15548800
I	-2.75091800	3.38240700	0.76742200	I	1.88512100	4.85023600	-0.72624100
H	2.16383000	0.36770300	-0.93844200	I	-1.15753100	1.77753800	3.64402900
H	-0.62695800	1.54084300	2.09874000	H	0.06659800	2.74472100	-2.14984600
H	-2.19413600	3.19537900	-1.92595900	H	-2.13161400	0.68104100	0.89488500
H	-2.31220400	-1.87916400	1.42095300	H	0.50607700	3.77084600	3.04704400
Te	-5.74632300	-2.25343700	0.60865400	S	2.09322400	-1.79984400	2.20480700
S	-2.50015200	-3.29769900	-0.05301700	Te	3.92722000	-3.90722400	-0.01682100

TS2:

C	4.17053700	1.85399900	0.34146600
C	4.47661100	0.60762700	-0.26887900
C	3.93794600	-0.64436300	0.24557400
C	3.05470500	-0.51871300	1.39674700
C	2.81398100	0.73358700	1.95719900
C	3.36713800	1.92145200	1.44935300
H	4.58080500	2.75913000	-0.09618600
H	2.13648800	0.78781500	2.80291000
H	3.11773200	2.87327900	1.90538200
C	5.33846500	0.63802200	-1.39817000
C	5.70103100	-0.52400000	-2.03801000
C	5.20290700	-1.75010700	-1.55433800
C	4.35614200	-1.84426400	-0.44930500
H	5.71639700	1.59993700	-1.73330100
H	6.37773400	-0.51085100	-2.88818300
H	5.51461400	-2.65954100	-2.06212000
H	2.93258200	-3.42259500	1.24334600
H	-0.48693100	-1.33767200	-2.23132400
C	-4.06990600	-2.46995400	-1.27068100
C	-2.67084200	-2.57065900	-1.28642300
C	-1.83338600	-1.44941500	-1.40033100
C	-2.45574000	-0.19511500	-1.50038800
C	-3.84565200	-0.06535500	-1.49597900
C	-4.65353200	-1.19856300	-1.37470300
C	-4.94197700	-3.69299000	-1.08438500
C	-5.24355300	-4.00791600	0.41020200
C	-3.94366200	-4.33540500	1.17825100
N	-6.00239900	-2.92393500	1.00879900
O	-1.66930700	0.92809800	-1.76136200
O	-3.50430900	-3.65977300	2.07460000
O	-3.28333100	-5.46386100	0.78985700
I	0.04858000	-1.77946400	0.52051000
H	-2.21742800	-3.55553600	-1.18654900
H	-5.73352100	-1.09870400	-1.35849700
H	-4.46357000	-4.55824100	-1.55928600
H	-5.90997000	-3.55142500	-1.57401300
H	-5.87101400	-4.91076800	0.43203000
H	-5.40545200	-2.10487100	1.10621500
H	-6.28437200	-3.17439000	1.95280100
H	-3.75763700	-5.91947000	0.07930600
C	1.81483200	0.37831800	-3.91386400
C	0.49923800	0.08065600	-3.68747300
C	1.69746600	-1.38151000	-2.56585700
N	2.54634100	-0.55725900	-3.20273000
H	3.55434500	-0.57468600	-3.07373400
H	2.28461200	1.15791200	-4.49158700

EP:

C	3.33800400	-4.17083400	-1.11955900
C	3.88248400	-3.29546200	-0.13898500
C	4.30848500	-1.94776400	-0.48358800
C	4.03950900	-1.54967200	-1.85503200
C	3.48720800	-2.44860300	-2.76542800
C	3.16071800	-3.77160300	-2.41950500
H	3.04823700	-5.16972200	-0.80496300
H	3.28374400	-2.09720600	-3.77108100
H	2.74133900	-4.44186100	-3.16283500
C	3.97768800	-3.78570300	1.18847600
C	4.49784000	-3.00028600	2.18615100
C	4.98129800	-1.72233200	1.86062200
C	4.92936000	-1.19152100	0.57447700
H	3.62365300	-4.79081600	1.39735300
H	4.55649600	-3.35732200	3.20948300
H	5.44114400	-1.14361200	2.65848700
H	5.75919000	0.98287400	-1.03253900
H	-2.08178400	1.88970600	3.07501100
C	-2.55947700	4.39848900	0.81374300
C	-2.02245200	3.69172900	1.89699300
C	-2.52750600	2.44459600	2.25810200
C	-3.56103000	1.86594700	1.52058800
C	-4.12512000	2.57677800	0.45301100
C	-3.63706900	3.83843800	0.11045400
C	-1.94183200	5.70143200	0.35620300
C	-0.96436100	5.52351800	-0.84751600
C	0.13711900	4.51403200	-0.47453400
N	-1.68918700	5.14960700	-2.04861000
O	-4.04348100	0.61937800	1.87532200
O	0.18748600	3.39066500	-0.92487800
O	1.06674500	4.91281500	0.42777900
I	2.42522600	1.49896000	-1.82473700
H	-1.18625700	4.09943600	2.45826700
H	-4.08194700	4.38595700	-0.71374600
H	-1.41156200	6.16972900	1.19406600
H	-2.70917600	6.40542600	0.02076400
H	-0.48692200	6.49646800	-1.02919900
H	-2.00127600	4.18337800	-1.97514000
H	-1.07728800	5.18804000	-2.85930000
H	0.91803800	5.82773100	0.70925900
C	2.53810600	0.61224300	3.19688600
C	1.28180400	0.56596100	3.75504500
C	1.05703600	1.57222700	1.86416300
N	2.37663800	1.26107300	1.99137200
H	3.10232900	1.43680800	1.30677100
H	3.49853900	0.25403500	3.53011400

```

H 0.98506300 0.13396800 4.70034300
H 0.66212800 2.07495600 0.99358200
N 0.36537000 1.16946500 2.91843500
I -5.73417300 1.73494000 -0.68002700
C -3.43079600 -0.49201700 1.30099600
C -4.27071600 -1.50650300 0.84454700
C -3.71520000 -2.65578600 0.28994700
C -2.32445600 -2.81880300 0.17167500
C -1.51358400 -1.77791500 0.65683600
C -2.04469200 -0.62244300 1.22413600
O -1.84560900 -3.95736400 -0.39304600
I -5.02248400 -4.19381400 -0.42559900
I 0.62702800 -1.97837100 0.54690300
H -5.34281900 -1.37419600 0.91601500
H -1.38868400 0.13947300 1.62691400
H -0.87558500 -3.92654300 -0.41805400
Te 5.99356800 0.68585600 0.56653600
S 4.34563600 0.03900600 -2.59933000

```

Figure S1

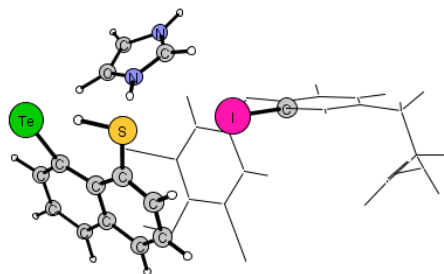


Figure S1. INT1 of IRD process of T4 using STe compound.